5-2007

Kinetics and Mechanism of Oxygen Delignification

Yun Ji

KINETICS AND MECHANISM OF OXYGEN DELIGNIFICATION

By

Yun Ji

B.E. Northwest University of Light Industry, 1999

M.S. Asian Institute of Technology, 2002

A THESIS

Submitted in Partial Fulfillment of the

Requirements for the Degree of

Doctor of Philosophy

(in Chemical Engineering)

The Graduate School

The University of Maine

May, 2007

Advisory Committee:

Adriaan R.P. Van Heiningen, Professor of Chemical Engineering, Advisor

Joseph M. Genco, Professor of Chemical Engineering

M. Clayton Wheeler, Professor of Chemical Engineering

Barbara J. W. Cole, Professor of Chemistry

Raymond C. Fort Jr., Professor of Chemistry

LIBRARY RIGHTS STATEMENT

In presenting this thesis in partial fulfillment of the requirements for an advanced degree at The University of Maine, I agree that the Library shall make it freely available for inspection. I further agree that permission for "fair use" copying of this thesis for scholarly purpose may be granted by Librarian. It is understood that any copying or publication of this thesis for financial gain shall not be allowed without my written permission.

Signature:

Date:

KINETICS AND MECHANISM OF OXYGEN DELIGNIFICATION

By

Yun Ji

Thesis Advisor: Dr. Adriaan R.P. Van Heiningen

An Abstract of the Thesis Presented
in Partial Fulfillment of the Requirements for the
Degree of Doctor of Philosophy
(in Chemical Engineering)
May, 2007

Considerable research has been conducted into the kinetics and selectivity of the oxygen delignification process to overcome limitation in its use. However most studies were performed in a batch reactor whereby the hydroxide and dissolved oxygen concentrations are changing during the reaction time in an effort to simulate tower performance in pulp mills. This makes it difficult to determine the reaction order of the different reactants in the rate expressions. Also the lignin content and cellulose degradation of the pulp are only established at the end of the experiment when the sample is removed from the batch reactor. To overcome these deficiencies, we have adopted a differential reactor system used frequently for fluid-solid rate studies (so-called Berty reactor) for measurement of oxygen delignification kinetics. In this reactor, the dissolved oxygen concentration and the alkali concentration in the feed are kept constant, and the rate of lignin removal is determined from the dissolved lignin content in the outflow stream measured by UV absorption. The mass of lignin removed is verified by analyzing

the pulp at several time intervals. Experiments were performed at different temperatures, oxygen pressures and caustic concentrations.

The delignification rate was found to be first order in HexA-free residual lignin content. The delignification rate reaction order in caustic concentration and oxygen pressure were determined to be 0.42 and 0.44 respectively. The activation energy was found to be 53kJ/mol. The carbohydrate degradation during oxygen delignification can be described by two contributions: one due to radicals produced by phenolic delignification, and a much smaller contribution due to alkaline hydrolysis.

From the first order of the reaction and the pKa of the active lignin site, a new oxygen delignification mechanism is proposed. The number 3 carbon atom in the aromatic ring with the attached methoxyl group forms the lignin active site for oxygen adsorption and subsequent electrophic reaction to form a hydroperoxide with a pKa value similar to that of the present delignification kinetics. The uniform presence of the aromatic methoxyl groups in residual lignin further support the first order in lignin kinetics.

ACKNOWLWDGEMENTS

I would like to acknowledge my advisor Dr. Adriaan R.P Van Heiningen for his excellent guidance and enthusiastic encouragement through this study.

I am grateful to all my committee members, Dr. Adriaan R.P Van Heiningen, Dr. Joseph M. Genco, Dr. Clayton M. Wheeler, Dr. Barbara J. W. Cole and Dr. Raymond C. Fort Jr. for their valuable suggestions and guidance during the process of proposal development.

I wish to express my utmost appreciation to the technical association of Finland VTT and TEKES for their financial help.

I wish to thank the members of Ober Research Group for their friendship and encouragement to help me complete the study at the University of Maine.

I wish to thank all the staff in the Chemical Engineering Department, especially Mr. Amos E. Cline for their warm-hearted help.

I also would like to thank my parents for their sincere support and encouragement. Last but not the least, I wish to give my special thanks my husband, Xuefei Zhang, for his love and encouragement.

TABLE OF CONTENT

LIST OF TABLES

LIST OF FIGURES

LIST OF EQUATIONS

Equation 4.1

$$\left[PhOH^{-}\right]=\frac{0.25\times\left[A_{300}(Alk)-A_{300}(Neu)\right]+0.107\left[A_{350}(Alk)-A_{350}(Neu)\right]}{\text{Lignin Concentration(g/liter)}} \quad \text{..... 63}$$

Equation 4.2 PhOH Content of Lignin Monomer $=\frac{mmoles}{g}\times\frac{185g}{mol}\times\frac{1mole}{1000mmoles}$ 63

Equation 4.3

$$\text{Carbohydrate Rate} = (\text{TOC Rate} - \text{MeOH Rate}\times\frac{12}{32} - \text{Delig Rate}\times\frac{108}{185})\times\frac{162}{72} \quad \text{..... 53}$$

Equation 5.1 $0-\phi_v C(t)dt+r(t)m_p dt=V_r dC(t)$ 63

Equation 5.2 $r(t)=\left[\phi_v C(t)+V_r\frac{dC(t)}{dt}\right]\frac{1}{m_p}$ 63

Equation 5.3 $t_d=\frac{96}{\phi_v}\ \frac{\text{(ml)}}{\text{(ml/min)}}$ 63

Equation 5.4 $C(t)=C_L(t+t_d)$ 64

Equation 5.5 $r(t)=\frac{\phi_v}{m_p}C_L(t+t_d)+\frac{V_r}{m_p}\left.\frac{dC_L}{dt}\right|_{t+t_d}$ 64

Equation 5.6 $m_L(t)=\phi_v\int_0^{t+t_d}C_L(t)dt+V_r C_L(t+t_d)$ 64

Equation 5.7 $L_c=\left(Kappa-\frac{HexA}{10}\right)\times 1.5 \quad \left(\frac{\text{mg lignin}}{\text{g pulp}}\right)$ 65

Equation 5.8 $\text{Final Kappa} = \text{Initial Kappa} - \frac{\text{Removed Lignin}}{0.18\%}$ 69

Equation 6.1 $\text{Kappa} = \text{Initial Kappa} - \frac{\phi_v\int_0^{t+t_d}C_L(t)dt+V_r C_L(t+t_d)}{1.5}$ 83

Equation 10.13 $$[O_2]_{ads} = \frac{K_e C_t [O_2]_{dis}}{1 + K_e [O_2]_{dis}}$$ 137

Equation 10.14 $$[O_2]_{dis} = 4.4 \times 10^{-5} \times P_{O2}$$ 138

Equation 10.15

$$-\frac{dL_C}{dt} = k \cdot K_{HL*} C \cdot K_e C_t \frac{[OH^-]}{K_{water} + K_{HL*}[OH^-]} \cdot \frac{[O_2]_{dis}}{1 + K_e [O_2]_{dis}} \cdot L_C$$ 138

Equation 10.16 $$-\frac{dL_C}{dt} = C_1 \frac{[OH^-]}{K_{water} + K_{HL*}[OH^-]} \cdot \frac{P_{O2}}{1 + K_e P_{O2}} \cdot L_C$$ 139

Equation 10.17 $$-\frac{dL_C}{dt} = C_2 \frac{P_{O2}}{1 + K_e P_{O2}} \cdot L_C$$ 139

Equation 10.18 $$slope = C_2 \frac{P_{O2}}{1 + K_e P_{O2}} \text{ or } \frac{1}{slope} = \frac{K_e}{C_2} + \frac{1}{C_2 P_{O2}}$$ 139

Equation 10.19 $$-\frac{dL_C}{dt} = 1.18 \times 10^{-3} \frac{[OH^-]}{0.111 + [OH^-]} \cdot \frac{P_{O2}}{1 + 2.26 \times 10^{-2} P_{O2}} \cdot L_C$$ 140

Equation 10.20 $$K_L = 1.18 \times 10^{-3} \frac{[OH^-]}{0.111 + [OH^-]} \cdot \frac{P_{O2}}{1 + 2.26 \times 10^{-2} P_{O2}}$$ 141

Equation 10.21 $$L_{ct} = L_{c0} \cdot e^{-K_L \cdot t}$$ 142

Equation 10.22 $$K_t = (K_0 - \frac{HexA}{10}) \cdot e^{-K_L \cdot t} + \frac{HexA}{10}$$ 142

Equation10.23

$$[\text{Ph - OH}^-] = \frac{0.25 \times [\text{A}_{300}(\text{Alk}) - \text{A}_{300}(\text{Neu})] + 0.107[\text{A}_{350}(\text{Alk}) - \text{A}_{350}(\text{Neu})]}{\text{Lignin Concentration(g/liter)}}$$ 144

Equation 10.24 $$\text{Phenolic Fraction} = [\text{Ph} - \text{OH}^-] \times \frac{185g}{mol} \times \frac{1mole}{1000mmoles}$$ 144

CHAPTER 1

INTRODUCTION

1.1 Wood Pulping

Wood is a natural composite material consisting of hollow, flexible tubes of cellulose bonded together and rigidified by glue called lignin. Wood has four major components: cellulose, hemicelluloses, lignin and extractives. The proportions of those four components vary between different types of softwood and hardwood species. Wood is the most important fiber source of the pulp and paper industry and can be converted into pulps by two processes: mechanical and chemical pulping. In mechanical pulping, wood fibers are separated from each other through mechanical abrasion. The mechanical force is transformed into heat which softens the lignin that holds the fibers together in the wood. Steam is usually fed to the process to accelerate the softening and breaking of bonds between lignin and fibers. Therefore, the drawback of mechanical pulping is that it is energy intensive. Mechanical pulping produces high yields pulps (Yield is about twice as high as that of chemical pulps) because lignin still remains in the pulp. Mechanical pulps are commonly used for printing paper because of its good printability.

Alternatively, pulp can be produced from wood chips by chemical pulping, whereby the lignin is degraded and dissolved thus free fibers are obtained. Two types of technologies are commonly used in chemical pulping: sulfite and sulfate pulping. Sulfite pulping uses sulfurous acid and an alkali to produce pulps of lower physical strength and bulk, but exhibits better sheet formation properties. The yield on the basis of wood is about 45 percent for sulfite pulping. These pulps are usually blended with ground wood pulps for newsprint, bond papers, and tissue. Sulfate pulping is also referred as the “kraft” or

"alkaline process". It produces pulps of high physical strength and bulk, but relatively poor sheet formation. The kraft process has a recovery system that can recycle the pulping chemicals, and also supplies a big portion of the steam generation for the industrial mill. The yield of pulp is about 45 percent for kraft pulping. Kraft pulping is the most popular pulping process in the world because of its high pulp strength and wide adaptability.

Figure 1.1 shows how the fiber composition depends on extent of pulping and bleaching.

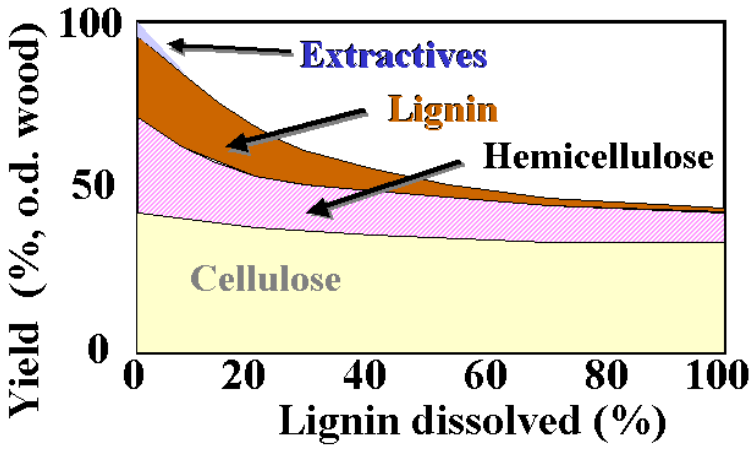

Figure 1.1 Fiber Composition Depends on Extent of Pulping & Bleaching
(Tappi Kraft Pulping Short Course, 1997)

It can be seen that the cellulose content does not change much with the dissolved lignin amount. However, the hemicellulose decreases with the amount of the dissolved lignin. The extractives are only a small portion of the wood which can be removed by the pulping process. The residual lignin content depends on the condition of the pulping process. The fiber components of pulps after pulping have important effect on oxygen

delignification and bleaching processes such as chemical charges, retention time, temperature etc.

1.2 Cellulose

Cellulose is a long chain of glucose molecules, linked to one another through $\beta^{(1-4)}$ glycosidic bonds. It forms the skeleton of the plant wall and has the most desired properties for making paper because of the high molecular weight. Cellulose is very stable chemically and extremely insoluble. The structure of cellulose is shown in Figure 1.2.

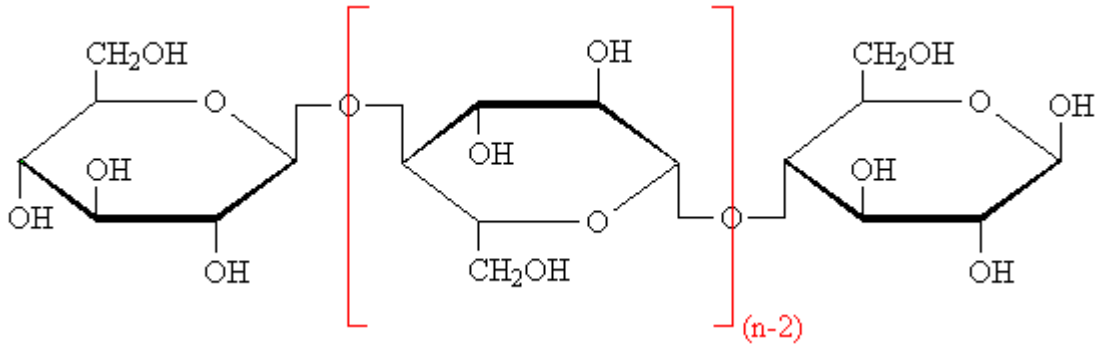

Figure 1.2 Structure of Cellulose (Sjöström, 1993)

As Figure 1.2 shows, cellulose is a linear polymer glucan with uniform chain structure whereby one water molecule is eliminated by two adjacent glucose units. The –OH groups at both ends of the cellulose chain have different chemical properties. The –OH group at the C1 is a reducing end and the –OH group on C4 is a non-reducing end. The molecular weight of cellulose is in a large range between 50000 and 2.5 million depending on different samples (Wegener, 1984). Because cellulose is a long chain with

uniform glucose units, one can use Degree of Polymerization (DP) to describe the size of cellulose. Table 1.1 shows the various DPs of cellulose from various materials.

$$DP = \frac{\text{molecular weight of cellulose}}{\text{molecular weight of one glucose unit}} \qquad \text{(Equation 1.1)}$$

Table 1.1 Summary of DP of Celluloses from Various Materials (Goring, Timell, 1962)

Material	DP	Mode of Solution
White Birch Wood	9400	Nitrate
White Birch Bark	7500	Nitrate
Jack Pine Wood	7900	Nitrate
Engelmann Spruce Wood	8000	Nitrate
Engelmann Spruce Bark	7100	Nitrate
Kapok	9500	Nitrate
California Cotton, opened	8100	Nitrate
California Cotton, unopened	15300	Nitrate
Trembling Aspen Wood	10300	Nitrate

Table 1.1 shows that DPs are from 7000 to 15000 for cellulose from plants. However, DP can decrease even under the influence of atmospheric oxygen. The unopened cotton has a much higher DP than opened cotton. It should be noted that chemical processes such as pulping, bleaching, delignification and extraction decrease DP values.

1.3 Hemicelluloses

Hemicelluloses are low molecular weight, branched chains of xylose, arabinose, galactose, mannose, and glucose molecules. The hemicellulose polymer fills in space in the plant wall and intimately associated with lignin. The hemicelluloses are non-crystalline and thus more soluble in water and are thus often removed during the pulping process. The hemicellulose monomer structures are shown in Figure 1.3.

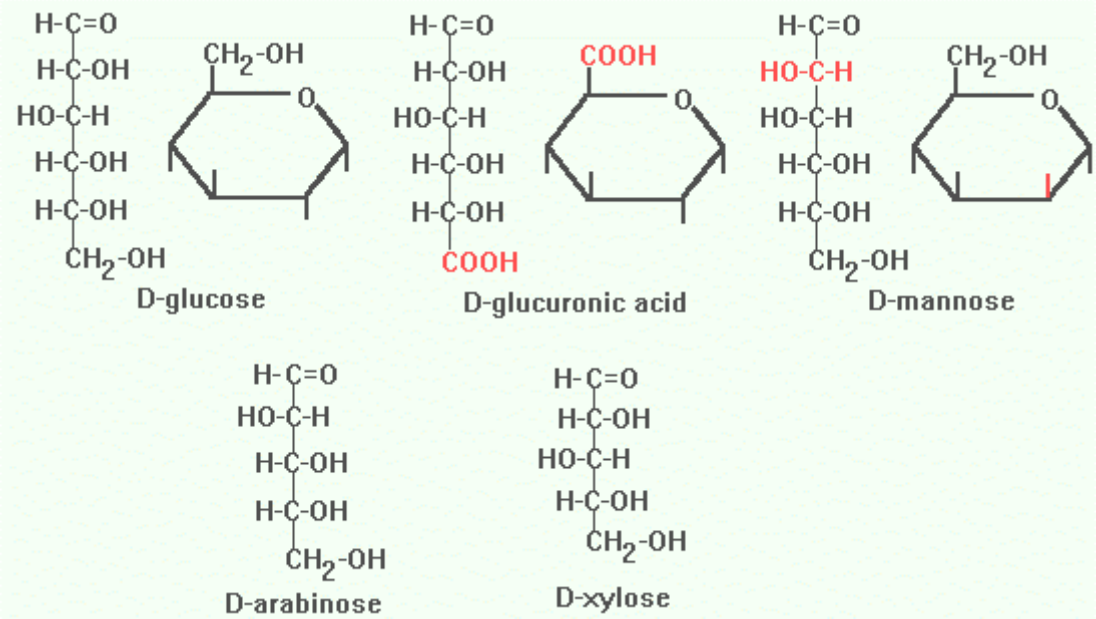

Figure 1.3 Structures of Hemicellulose Monomers (Sjöström, 1993)

Table 1.2 summarizes the main structural features of hemicelluloses appearing in both softwood and hardwood. Unlike glucomannan, xylan contains acidic groups (glucuronic acid) and has a molecular structure similar to cellulose when their branches are removed from xylan, which may make xylan combine with cellulose in a more ordered structure after kraft pulping. Glucomannan is very sensitive to kraft cooking conditions and is already dissolved to a large extent at the beginning of kraft cooking, whereas xylan is more resistant (Wagberg and Annergren, 1997). Therefore, the content of xylan in chemical softwood kraft pulp becomes almost as important as that of glucomannan in spite of considerably higher content of glucomannan in softwood.

Table 1.2 Major Hemicellulose Components in Softwood and Hardwood(Sjöström, 1993)

Wood	Hemicellulose type	Amount (% on wood)	Composition			DP
			Units	Molar ratios	Linkage	
SW	Galacto-glucomannan	5-8	β-D-Man*p* β-D-Glc*p* α-D-Gal*p* Acetyl	3 1 1 1	1 → 4 1 → 4 1 → 6	100
	(Galacto)-glucomannan	10-15	β-D-Man*p* β-D-Glc*p* α-D-Gal*p* Acetyl	4 1 0.1 1	1 → 4 1 → 4 1 → 6	100
	Arabino-glucuronoxylan	7-10	β-D-Xyl*p* 4-O-Me-α-D-Glc*pA* α-L-Araf	10 2 1.3	1 → 4 1 → 2 1 → 3	100
HW	Glucuronoxylan	15-30	β-D-Xyl*p* 4-O-Me-α-D-Glc*pA* Acetyl	10 1 7	1 → 4 1 → 2	200
	Glucomannan	2-5	β-D-Man*p* β-D-Glc*p*	1-2 1	1→ 4 1→ 4	200

Table 1.3 shows the cellulose and hemicelluloses content in pine and birch before and after kraft pulping. The data show that hemicelluloses in birch are dominated by xylan while pine has mostly glucomannan. After kraft pulping, cellulose is left for papermaking purpose, but most of the hemicelluloses are dissolved in the pulping process for pine. It should be noted that the birch kraft pulp has more xylose than pine kraft pulp. Relocation of xylan in fibers may occur during kraft cooking due to the sorption of xylan from the cooking liquor.

Table 1.3 Change of Chemical Composition before and after Kraft Pulping of Birch and Pine (Sjöström, 1993)

Constituents	Pine	Birch	Pine kraft pulp	Birch kraft pulp
Cellulose (%)	40	41	35	34
Glucomannan (%)	16	2.3	4	1
Glucuronoxylan (%)	8.9	27.5	5	16
Other polysaccharides (%)	3.6	2.6	-	-
Lignin (%)	27.7	22	3	2
Extractives (%)	3.5	3	0.5	0.5

In addition, all sugar components can take part in the formation of lignin carbohydrate complexes by covalent linkages between lignin and carbohydrates in both wood and pulp. The most frequently suggested LCC-linkages in native wood are benzyl ester, benzyl ether, and glycosidic linkages (Fujimoto, 1998). However, the benzyl ester linkage is alkali-labile and may therefore be hydrolyzed during kraft pulping process. The latter two linkages are alkali-stable and would survive hydrolysis during the kraft pulping process.

1.4 Lignin

Lignin is a very complex polymer of phenylpropane units, which are randomly cross-linked to each other by a variety of different chemical bonds. This complexity has proven as resistant to detailed chemical characterization as it is to microbial degradation, which greatly impedes our understanding of its effects. Lignin has the following characteristics:

- Made of basic phenylpropane units
- No repeating structure
- Amorphous
- Concentrated in middle lamella

- Formed last during cell development
- Covalently bonded to polyoses

Sometimes lignin can be isolated as a brown powder, but more often it is a gummy mixture of polymers with a wide range of molecular weights. Lignin resists attack by most microorganisms, and anaerobic biological processes tend not to attack the aromatic rings at all. Aerobic breakdown of lignin is slow and may take many days. Lignin is nature's cement along with hemicellulose to exploit the strength of cellulose while conferring flexibility. In softwoods, coniferyl alcohol is the predominant lignin monomer. However, coniferyl and sinapyl alcohol are lignin monomers found in hardwood. The exact lignin structure is not fully understood because of the random nature of the linkages between the phenyl-propane units. These reactions are irreversible. There are many possible monomers of lignin, and the types and proportions depend on the source in nature. The three most common lignin monomers or precursors are shown in Figure 1.4.

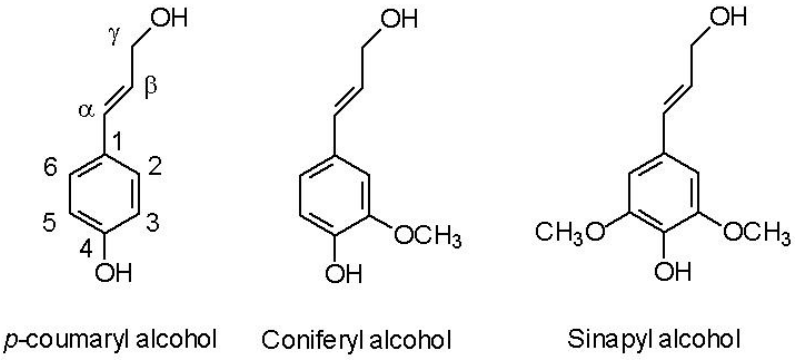

Figure 1.4 Common Lignin Monomers (Wegener, 1984)

The hydroxyl groups (either the alcoholic hydroxyls on the side chains or the phenolic hydroxyl groups on the aromatic rings) can react with each other or with aldehyde or

ketone groups. When a hydroxyl group reacts with another, an ether linkage is formed. A hydroxyl group reacts with an aldehyde or ketone and forms a hemiacetal and ketal respectively.

It is rather difficult to study the polymerization of the monomeric precursors by random coupling reactions. The first step in polymerization is the formation of dimeric structures. Figure 1.5 shows the major types of linkages (also called dilignols) between phenypropane units in lignin.

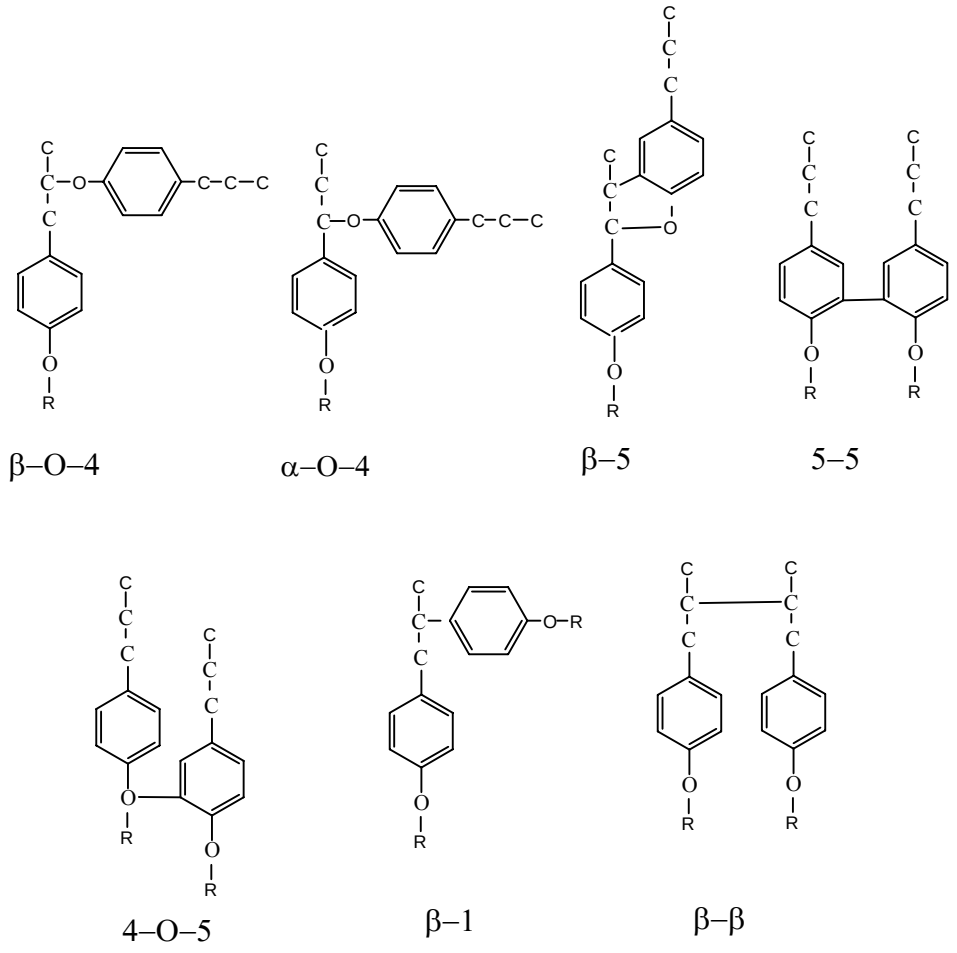

Figure 1.5 Major Types of Linkages between Phenylpropane Units in Lignin

The further polymerization of lignin involves monolignols with phenolic end groups or radicals, which forms a branched large polymer by tri-, tetra-, penta and oligolignols (Wegener, 1984). Figure 1.6 shows the designed structural scheme of lignin model.

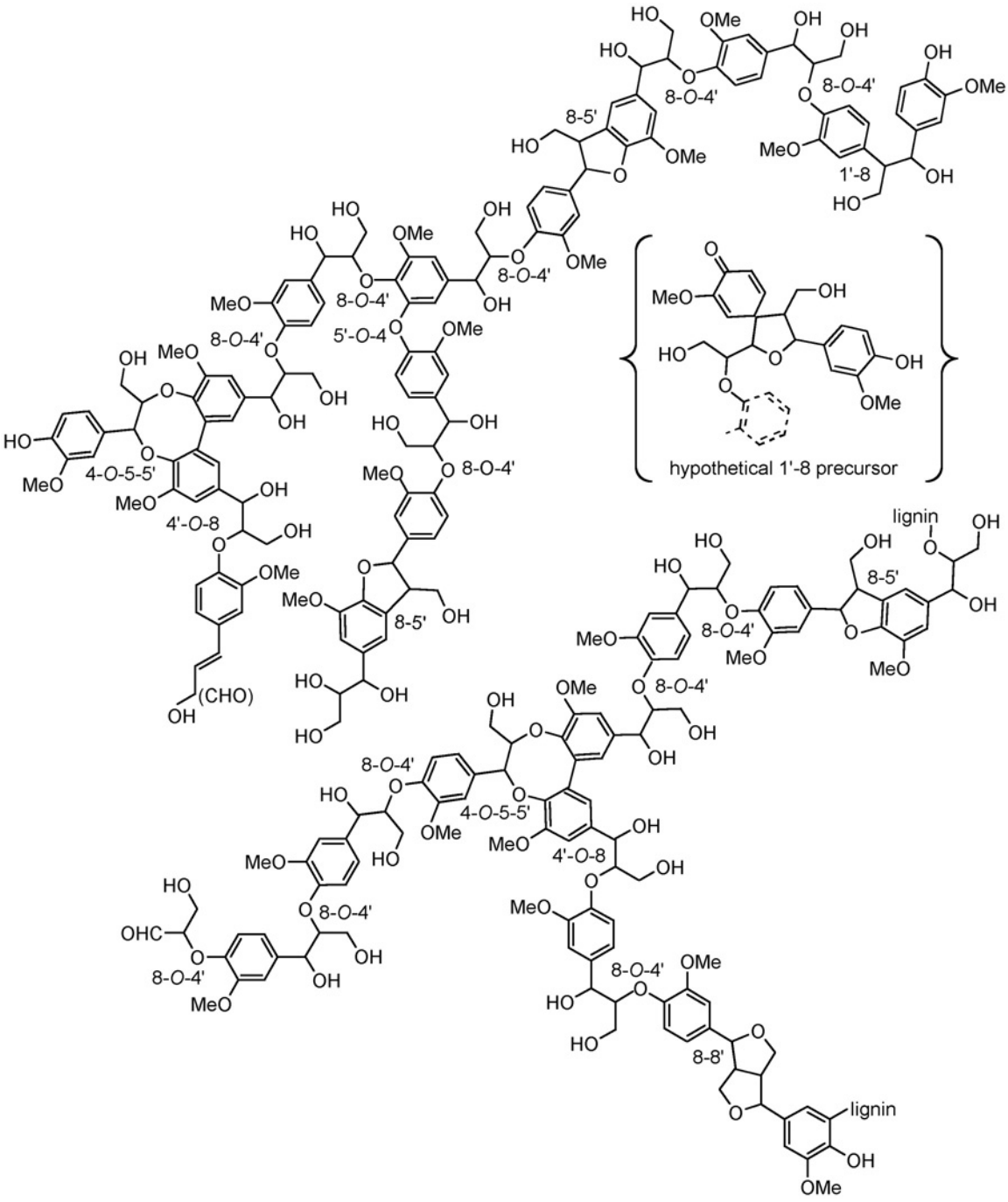

Figure 1.6 Model of Lignin Structure (Theory Proposed by Brunow, 1998)

1.5 Lignin Carbohydrates Complex (LCC)

Lawoko et al (2003) recently reported that 90% of the residual lignin in softwood kraft pulp was linked to various carbohydrates in kraft pulp, and mainly to xylan and glucomannan forming network structures. The study has demonstrated that lignin is linked through covalent bonds to all the major polysaccharides in the woody cell wall, arabinoglucuronoxylan (Xyl), galactoglucomannan, glucomannan (GlcMan) and cellulose. Such a network structure may play an important mechanical role for the "woody" properties of the secondary xylem in contrast to non-lignified plant cells as for instance the seed hairs of cotton. Furthermore, the progressive degradation of lignin-carbohydrate networks may be important in technical processes involving wood, such as chemical pulping. In kraft pulps, 85-90% of the residual lignin was somewhere linked to carbohydrates, and mainly to glucomannan and xylan in network structures. During the end of a kraft cook and oxygen delignification, LCC structures were observed to be degraded at different rates. Thioacidolysis of the various LCCs showed that the predominant inter-lignin linkage, the ß-O-4 linkage, was always present in a large amount although a large decrease in the absolute amount was found when going from wood to kraft pulp and further to oxygen-delignified pulp. Thioacidolysis in combination with size exclusion chromatography of the various LCCs from wood revealed pronounced differences in the lignin structure between the GlcMan-L-Xyl and the Xyl-L-GlcMan fractions. The latter type of lignin was found to have a rather linear coupling mode of ß-O-4 structures whereas the former gave a chromatographic pattern indicating a more complex polymeric structure with a larger variability of inter-unit coupling modes. As a result of these analyses and with reference to literature data, a softwood fiber cell wall

comprising two different types of lignin has therefore been suggested as shown in Figure 1.7. The delignification rates of the LCC types were different, with the xylan and cellulose rich LCCs being delignified faster than the glucomannan rich LCC toward the end of a kraft cook and during oxygen delignification (Lawoko et al. 2004), so that after a kraft cook and subsequent oxygen delignification, nearly all the residual lignin was found in the glucomannan fraction. Therefore, it is unlikely that the delignification process during oxygen delignification is limited to reactions taking place in the lignin skeleton only. The effect of the reactions taking place in the carbohydrate skeleton on oxygen delignification of pulp also needs to be investigated.

Figure 1.7 illustrates a segment of the secondary wall in a softwood fiber (Lawoko, 2005).

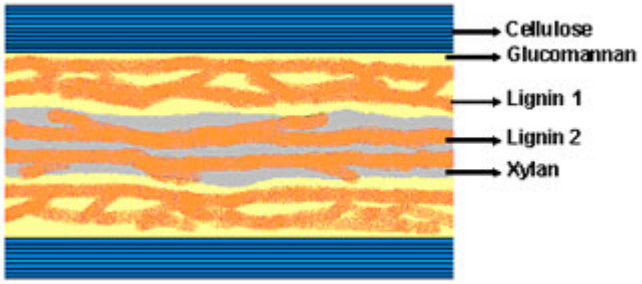

Figure 1.7 LCC in softwoods (Lawoko, 2005)

It can be seen that the arrangement of the various wood polymers is indicated with a more branched and cross-linked lignin attached to glucomannan (Lignin 1) and a more linear to xylan (Lignin 2). The result suggests that the two major types of LCC from wood contain glucomannan and xylan respectively as the predominant polysaccharide, in both cases combined with substantial amounts of lignin. The large difference in the lignin structure of these two types of LCC demonstrates that the fiber wall must have a more complex

pattern than previously thought with one lignin type only surrounded by xylan and one only by glucomannan.

1.6 Oxygen Delignification Process

Oxygen delignification is a process which uses oxygen and alkali to remove a substantial fraction of the lignin remaining in the pulp after cooking. This process is operated at relatively high temperature and pressure and high or medium consistencies in single or multiple stages. The process is very flexible, and is best viewed as a "bridging strategy" between cooking and final bleaching (Berry, 2002). Medium consistency is the most common industrial application. Table 1.4 lists some typical process conditions for oxygen delignification of SW kraft pulps.

Table 1.4 Typical Process Conditions for Oxygen Delignification of SW Kraft Pulps (McDonough, 1996; Reid et al, 1998)

Operating Conditions	Medium Consistency	High consistency
Pulp consistency (%)	10-14	25-34
Retention time (min)	50-60	30-45
Initial temperature (^{o}C)	70-105	100-115
Inlet pressure (kPa)	610-800	415-600
Outlet pressure (kPa)	260-550	415-600
Alkali (kg/t)	18-28	18-23
Oxygen consumption (kg/t)	20-24	15-24
$MgSO_4$ (kg/t)	0~2.5	0~1.5

However, the effectiveness of an oxygen delignification stage is limited because severe cellulose degradation takes place after a certain point of delignification, resulting in the

deterioration of pulp viscosity and strength properties. Therefore, the lack of selectivity is a drawback of oxygen delignification. With a single stage, the delignification is normally in the range of 30%-50%. A number of new oxygen delignification installations involve two reaction stages, and extend the range of delignification to 65%-70% while preserving the pulp quality. Although a higher delignification limit of 70% can be reached by double oxygen stages, a significant fraction of residual lignin remains even after four-stage oxygen delignification.

One of the themes in oxygen delignification research is to achieve a more fundamental understanding of chemical factors governing delignification and carbohydrate damage during the process. Figure 1.8 shows the location of oxygen delignification in the kraft pulping process.

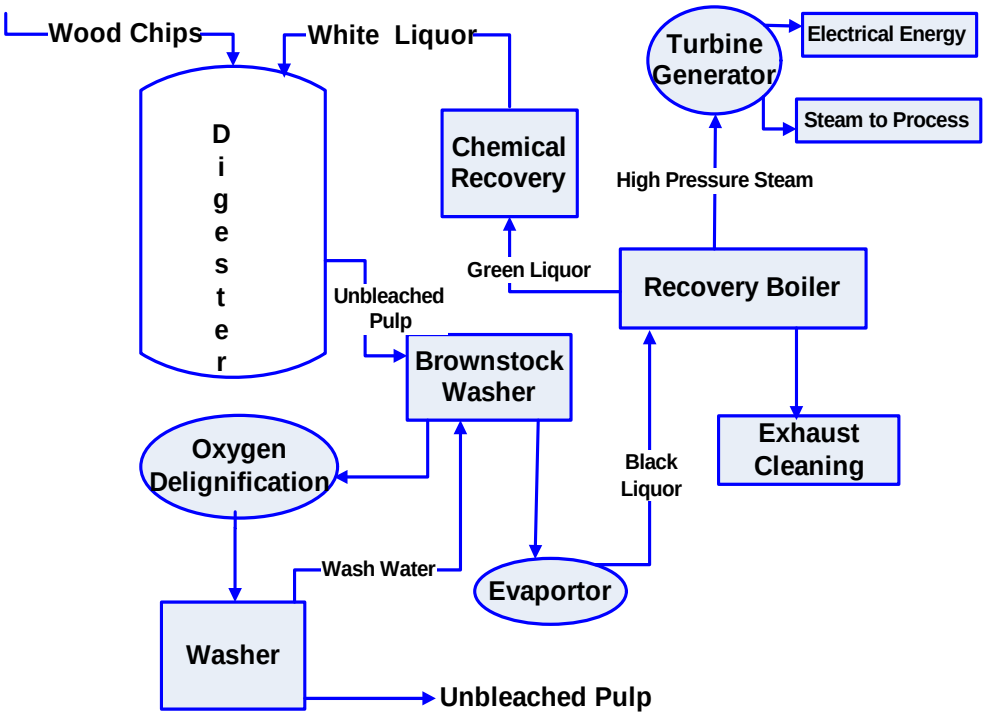

Figure 1.8 Oxygen Delignification within Kraft Pulping

The process in Figure 1.8 shows that the pulp is washed after it leaves the tower where it has reacted with oxygen. The waste water or filtrate can either be used in the brownstock washers or it can be routed directly to the evaporator where it will be combined with the black liquor. The degraded lignin products will be burned for energy in the recovery boiler, so less organic waste will be discharged in the waste water from the bleach plant.

Today, a well designed oxygen system can reduce up to 70% of the kappa number from unbleached pulp. Kappa number is a measurement to indicate the lignin amount in pulps. Historically the lignin content was calculated from the kappa number by multiplying it by a factor of 0.15%. However, the kappa number measurement includes the HexA groups in the pulps, and can thus the former calculation gives the wrong lignin content.

Oxygen delignification is a proven technology that can remove as much as 70% of the lignin before before the bleaching process removes the remaining lignin and colored substances. Mills will have to install oxygen delignification, extended delignification or both in order to minimize the use of chemicals in the bleach plant and allow more organic waste to be burned in the recovery boiler rather than these being released to the environment and also to produce high quality, totally chlorine-free pulp (TCF). A major drawback of oxygen delignification is its high capital cost. However, oxygen delignification is environmentally and economically attractive because oxygen (O_2) is cheap.

The spent chemicals and reaction products of the oxygen stage are removed by washing and sent to the chemical recovery process. The decrease in effluent properties such as content of chlorinated organics, Biological Oxygen Demand (BOD), Chemical Oxygen Demand (COD), and color in the bleach plant effluent is proportional to the degree of delignification achieved in oxygen delignification. Therefore, the installation of oxygen delignification will lead to substantial environmental benefits. Moreover, the oxygen stage provides a significant reduction in bleaching chemical cost. However, because capital costs are relatively high, this has lead to slow adoption of the technology in North America.

Oxygen delignification also raises the pulp yield (Zou, 2003) compared to kraft pulping. The improvement in pulp yield when using oxygen delignification compared to extending delignification by cooking is shown in Figure 1.9.

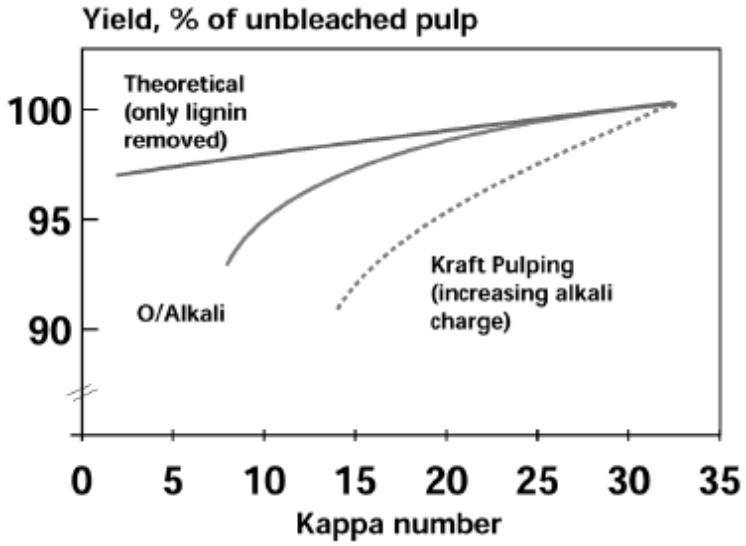

Figure 1.9 Yield Selectivity of Extended Cooking and O_2 Delignification
(Sunds Defibrator, 1999)

Oxygen delignification is a bridging step between cooking and bleaching. A pulp mill wants to operate at its optimal production level, operating costs, pulp quality, and environmental requirements. In another words, the goal of a pulp mill is to deliver pulp at the lowest kappa number to the bleach plant, and still maintain the required pulp strength and avoid the sharply dropping ranges of the cooking yield curve (see Figure 1.9). The oxygen bleaching curve provides a better yield compared to the extended cooking curve. Therefore, bleaching costs and level of the effluent parameters are the major considerations in determining the kappa number at which to start bleaching. If only cooking and bleaching processes are available, bleaching process must start at a relatively high kappa number for production reasons. Consequently, an oxygen delignification step is the preferred method to extend the cooking resulting in a rather small yield loss, but a significant reduction of the kappa number to the bleach plant. However, an unacceptable loss of yield and pulp strength will occur if the oxygen step is extended too far by

employing high temperatures and high alkali charges. This may be alleviated to some degree by applying oxygen delignification in two stages where the process conditions can be more closely controlled. As with any series of sequential steps, the addition of a new step such as the second oxygen stage provides the possibility to find a new and better total optimum for the entire sequence. The selection of the optimum will be aided by understanding the mechanism of oxygen delignification and a detailed description of the effect of operating conditions on the kinetics of oxygen delignification.

CHAPTER 2

DESCRIPTION OF PROBLEM AND OBJECTIVES

2.1 Description of Problem

Many studies have been performed to determine the kinetics of oxygen delignification (Edwards and Nordberg, 1973; Teder and Olm, 1981; Kovasin et al, 1987). All the delignification kinetics equations were obtained using laboratory batch reactors. When performing experiments at medium consistency conditions, it is difficult to determine the real kinetics because the alkali and the dissolved lignin concentrations are changing with time. Another problem is the transfer of oxygen from the gas to the liquid phase, which must be fast enough so that the oxygen concentration in the liquid phase is close to that of saturation. Another limitation in the batch reactor oxygen delignification studies is that the pulp properties can only be determined from the samples taken at the end of an experiment. In order to obtain multiple data points, the experiments must be performed at different reaction times which increases the number of experiments required and experimental error for the kinetics calculation.

In the present study, medium consistency conditions and a constant NaOH concentration at a level commonly used in industry (e.g 3.3g/l NaOH) are realized by adoption of continuous flow of an oxygenated caustic solution through a medium consistency pulp bed. The whole bed is contained inside a reactor in which the caustic solution is rapidly circulated through the pulp bed, while fresh oxygenated caustic solution is added and spent liquor is removed simultaneously. Thus, this novel medium consistency kinetic system is similar to a differential continuous stirred tank reactor (CSTR) with the dissolved oxygen and sodium hydroxide concentrations close to that of the feed.

Furthermore in this thesis, the experimental data of the rate of oxygen delignification are fitted for a kinetic equation which is based on plausible elementary reactions and fundamental physical phenomena. The oxygen delignification kinetics reported in literature have mathematical forms which were mostly chosen to obtain a good fit with the experimental data rather than based on fundamental chemical mechanisms. This leads to equations for the rate of delignification with high reaction orders in lignin content or to arbitrary identification of so called “fast reacting” and “slow reacting” lignin. Also the reaction orders in NaOH concentration and oxygen pressure do not have a mechanistic basis.

2.2 Objectives

- To measure the kinetics of lignin removal during alkaline oxygen treatment using the Berty Continuous Stirred Tank Reactor (CSTR);
- To measure the kinetics of cellulose degradation during alkaline oxygen treatment in the Berty CSTR;
- To determine the relationship between carbohydrate and lignin removal during oxygen delignification in the Berty CSTR;
- To understand the mechanism of delignification and carbohydrate removal from pulp during alkali oxygen treatment;
- To describe the rates of delignification and cellulose degradation by kinetic equations which are based on plausible elementary reactions and fundamental physical phenomena.

CHAPTER 3

LITERATURE REVIEW

3.1 Introduction

A review of oxygen delignification can be organized under the concepts of the chemistry of oxygen, lignin and carbohydrates, kinetics of delignification and carbohydrate degradation, and finally mass transfer of oxygen from the gas to the fiber phase. McDonough (1996) stated that the chemistry was complicated due to the complexity of the lignin structure and different oxygen species formed during the free radical reactions between oxygen, lignin and water.

3.1.1 Oxygen Chemistry

Many researchers have studied the mechanism of oxygen bleaching (Singh, 1987; Ljunggren & Johansson; 1987 Gratzl, 1992). In the oxygen delignification process, there are several oxygen species present as shown in Figure 3.1.

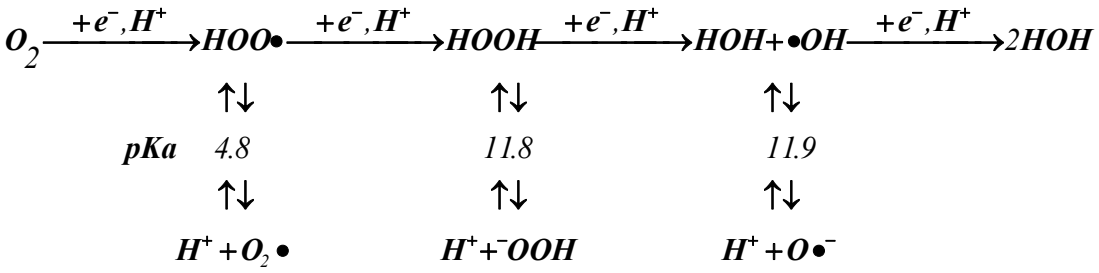

Figure 3.1 Oxygen Chemistry in Aqueous Solution (McDonough, 1996)

Oxygen is a molecule with the triplet state as its normal configuration (low energy). It contains two electrons that are unpaired. Therefore each of these electrons has an affinity for other electrons of opposite spin, and thus oxygen behaves as a free radical. Consequently, oxygen has a strong tendency to react with organic substances, and radical

chain reactions are initiated which liberate hydroperoxy radicals $HOO^{\cdot}$ (McDonough, 1996). At alkaline conditions, the hydroperoxy radical is converted into the superoxide anion radical. By subsequent one electron reduction reactions, the hydroperoxy radical is transformed to hydrogen peroxide, subsequently the hydroxyl radical and finally water. McDonough (1996) proposed that oxygen delignification can be described by the following chain reactions.

Initiation	$RO^{-} + O_2 \rightarrow RO\cdot + O_2^{\cdot -}$	
	$RH + O_2 \rightarrow R\cdot + HO_2^{\cdot}$	
Propagation	$R\cdot + O_2 \rightarrow RO_2\cdot$	Peroxyradical
	$RO_2\cdot + RH \rightarrow RO_2H + R\cdot$	Hydroperoxide
Termination	$RO\cdot + R\cdot \rightarrow ROR$	

The reactions show possible initiation, propagation and termination steps in the oxygen delignification process. In more detail, the mechanism of oxygen delignification can be described as the following reactions: the free phenolic hydroxyl groups in the residual lignin are ionized at alkali conditions, and then attacked by oxygen to form a superoxide anion and a phenoxy radical. An electron also can be abstracted from a non-phenolic group or another functional group to give the corresponding organic radical. Propagation of the chain reaction regenerates a new organic radical. The chain can be terminated by coupling reactions which are also called condensation reactions.

3.1.2 Lignin Chemistry

A large amount of research has been done to learn about the mechanisms of lignin removal during oxygen delignification. Many researchers (Ljunggren & Johansson, 1987; Gierer & Imsgard, 1977; Gierer & Reitberger, 2001) used model compounds to study the

reaction of lignin during oxygen alkaline treatment. Moreover, many experimental studies (Gellerstedt & Lindfors, 1991; Yang & Lucia, 2003) have been conducted in laboratory batch reactors to study the effects of process parameters, on the structural features of both residual and dissolved lignins.

Figure 3.2 shows how a phenolic hydroxyl group in lignin reacts with alkali to generate a phenolate ion, which is considered to be the initiation of the lignin reactions. The anion then reacts with oxygen to form a reactive intermediate called a hydroperoxide. The primary reaction of oxygen with lignin under alkaline conditions proceeds via a resonance stabilized phenoxy radical.

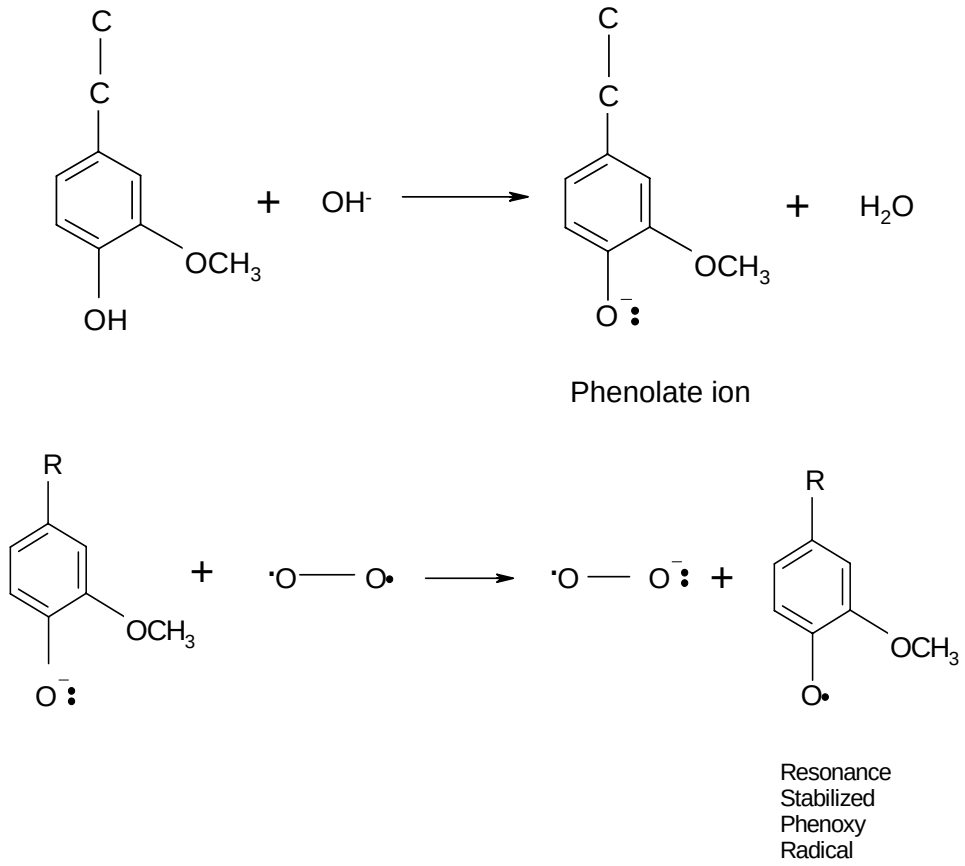

Figure 3.2 Initial Attack of Oxygen on Phenolic Nuclei (Ljunggren, 1997)

The resonance stabilized intermediates then undergo reaction with themselves (lignin condensation) or with oxygen species such as hydroxyl (HO·), hydroperoxy (HOO·) and superoxide ($O_2^{\cdot -}$) radicals to form organic acids, carbon dioxide and other small molecular weight organic products via side chain elimination, ring opening and demethoxylation reactions (Ljunggren, 1987). Figure 3.3 illustrates these reactions pathways.

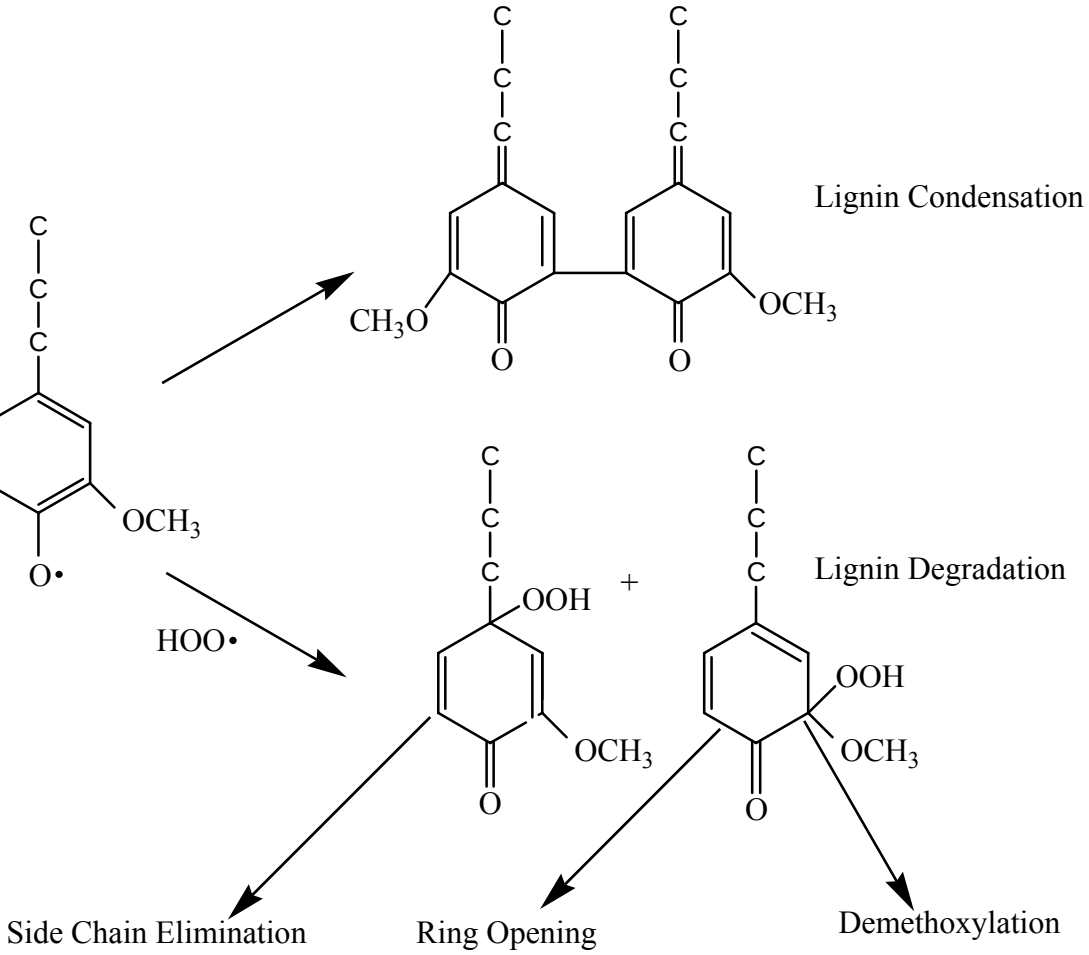

Figure 3.3 Possible Reactions of Lignin via Phenoxyradical
(Johansson and Ljunggren, 1994)

Johansson and Ljunggren (1994) found that phenolic structures with a conjugated side chain, like stilbene and enol ethers, react very rapidly, whereas diphenylmethane-type

condensed structures are particularly resistant to oxygen bleaching. The p-hydroxylphenyl and 5,5'- biphenolic units in the residual lignin are quite stable and tend to accumulate during oxygen delignification (Fu and Lucia,2003; Akim et al, 2001). During oxygen delignification, the number of phenolic hydroxyl groups in the pulp decrease and the number of carboxylic acid groups increase, which is expected since the degradation products from oxygen delignification are predominately organic acids and carbon dioxide (Zou, 2002).

There are many papers in the literature on the lignin structure after cooking and oxygen delignification. However, it is very difficult to determine the structure of the residual lignin in pulp without changing the lignin chemically during isolation, especially when lignin is only a small portion of the pulp such as oxygen delignified pulps. Also, the yield of residual lignin is only 30-80% (Gustavsson et al, 1999). However, all these studies generally suggest that the lignin structures, before and after oxygen delignification, are not very much different (Van Tran, 2001). Recently, many researchers have suggested (Backa et al, 2004; Lawoko, 2004) that the residual lignin is covalently bound to hemicellulose through so-called LCC (Lignin Carbodydrate Complexes) linkages. Backa et al. (2004) proposed that after cooking the residual lignin consists mostly of oligolignin structures bound to hemicellulose through LCC bonds. Therefore, the decreasing efficiency of oxygen delignification at increased lignin removal may be explained by the lack of phenolic groups and by the presence of LCC bonds (Gellerstedt and Lindfors, 1991).

A modified oxygen delignification mechanism proposed by Backa et al. is shown in Figure 3.4.

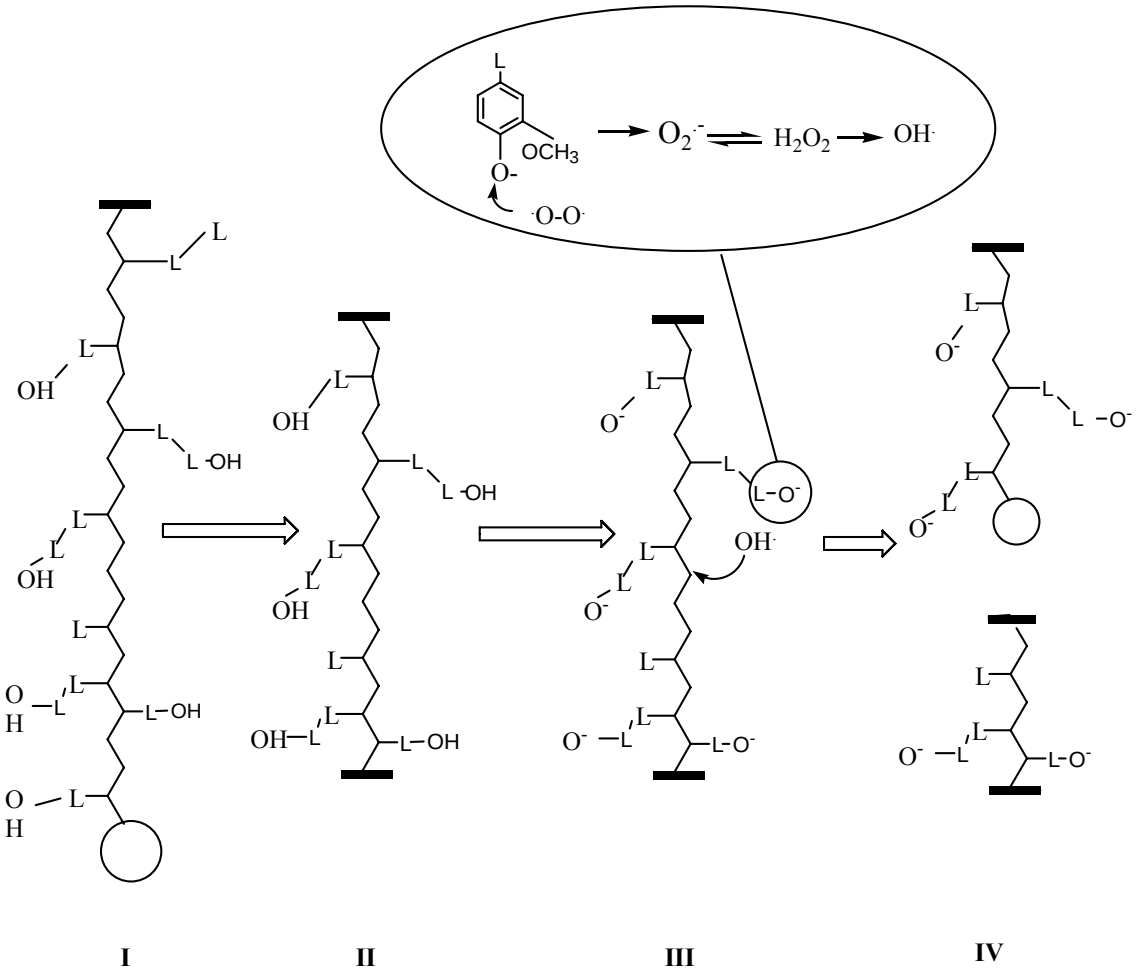

Figure 3.4 Modified Oxygen Delignification Mechanism
(adapted from Backa et al, 2004)

In Figure 3.4, the chain represents a part of a hemicellulose chain with two end groups. The circle at one end in structure I represents a labile reducing end, while the bar at the other end is a non-reducing end. The reducing end of the chain is subject to endwise peeling and finally the stopping reaction so that in structure II both ends of the chain are alkali stable. The residual lignin (in the form of low molecular weight oligolignins) is bound to the hemicellulose chain through LCC bonds. The formation of structure II after

the peeling leads to loss of lignin, and is called "endwise peeling delignification". Furthermore, the phenolic end of one of the oligolignins in structure II dissociates to phenolate (structure III) where it reacts with oxygen according to the earlier described "phenolate delignification". Since a radical species (shown as hydroxyl radical in Figure 3.4) is formed at a location close to the hemicellulose chain, it may cleave the chain and form two new end groups, one reducing and one non-reducing (structure IV). One of our present objectives is to test the validity of this proposed mechanism by using the Berty CSTR reactor which allows the analysis of dissolved lignin and carbohydrate products at any time during the delignification process.

3.1.3 Carbohydrate Chemistry

In industrial practice, delignification is usually stopped when the kappa number of the pulp entering the oxygen delignification system is reduced by about 50%. This is because carbohydrate reactions also take place during oxygen delignification, which result in the loss of the pulp yield and strength. Carbohydrate degradation reactions are described in terms of the decrease in intrinsic viscosity, "$\Delta\eta$", of the pulp. The reactions of the cellulose and hemicellulose polymers have been studied by many researchers (Guay et al, 2001; Sjostrom, 1981). Usually, the reactions can be divided into two categories: one is random chain cleavage and the other is carbohydrate peeling reactions. Random chain cleavage means that cleavage occurs at any glycosidic linkage along the carbohydrate chain, while peeling reactions occur on the sugar units at the reducing end of the chain, leading to successive removal of one sugar unit at a time (Sjostrom, 1981). Both types of reactions may occur during oxygen delignification, but random chain cleavage is thought to be more relevant to the viscosity drop. In random chain cleavage, metals such as iron

and copper play an important role because it accelerates the chain cleavage reactions. They catalyze the formation of reactive radicals that randomly attack the cellulose chain, ultimately resulting in chain breakage at the point of attack. A decrease in the average length of the cellulose chains results in a decrease in pulp viscosity, which causes pulp strength loss. Experimental and computational methods were used to determine the mechanism of the attack of a hydroxyl radical on cellulose (Guay et al, 2001). Their research results presented an alternative degradation mechanism. Methyl β-D-cellulose was used as a model compound to represent cellulose as shown in Figures 3.5 and 3.6.

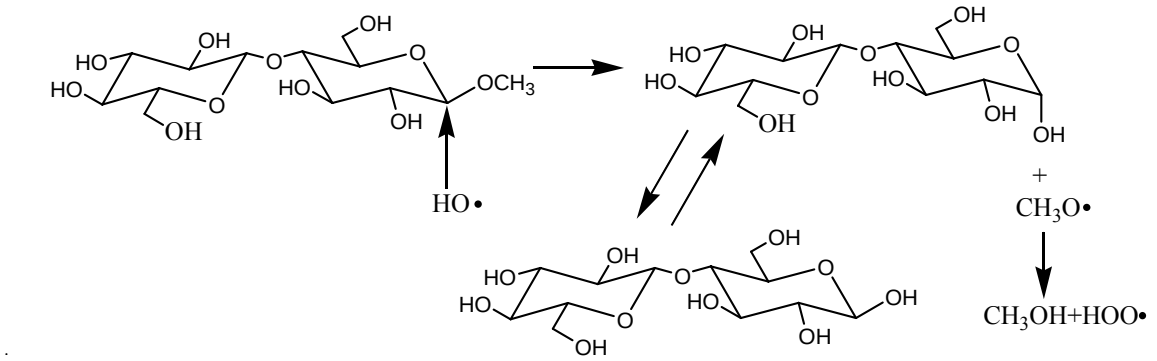

Figure 3.5 Proposed Mechanism for Cellobiose Formation (Guay et al, 2001)

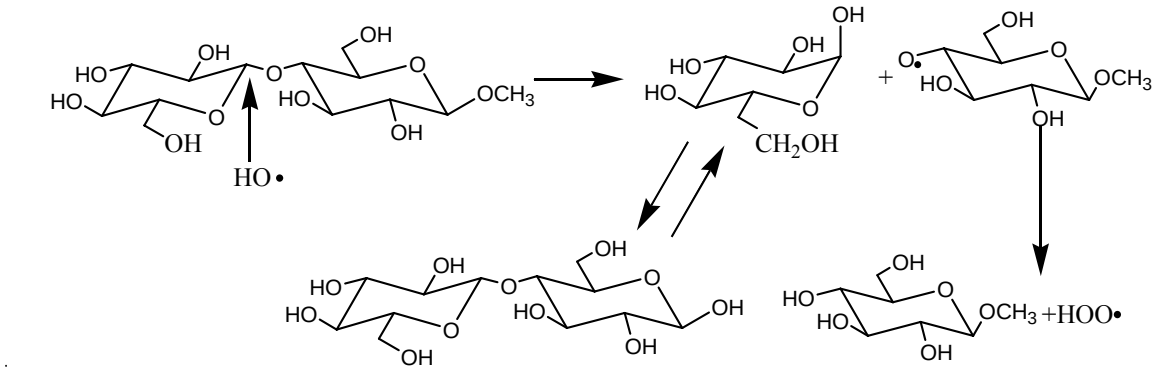

Figure 3.6 Proposed Mechanism for Formation of Methyl β-D-glucoside and D-glucose (Guay et al, 2001)

Figure 3.5 indicates that one pathway of cellulose degradation by hydroxyl radicals is a hydroxyl radical substitution reaction at the anomeric carbon forming cellobiose and methanol. The other pathway in Figure 3.6 shows a hydroxyl radical substitution reaction at the glycosidic linkage between the two pyranose rings forming methyl β-D-glucoside and D-glucose (Guay et al., 2001).

The peeling reaction is responsible for the decrease in pulp yield. Primary and secondary peeling reactions are possible in the oxygen delignification process. Primary peeling occurs at reducing end of the carbohydrate chain and terminates with a stopping reaction or oxidation by oxygen. Secondary peeling is initiated on the reducing end of the new chain immediately following random hydrolysis. However, it is believed that the peeling reaction is less important in oxygen delignification because the reducing ends are oxidized by oxygen, preventing the peeling reaction.

3.1.4 Limitations in Oxygen Delignification

Hydroxyl radicals formed during oxygen delignification can react with both lignin and pulp polysaccharides. Reaction of hydroxyl radicals with lignin leads to hydroxylation of aromatic rings and thus making lignin more reactive for further attack by oxygen. However, the random chain cleavage of cellulose and hemicellulose by hydroxyl radicals limits the extent of delignification which can be achieved without serious pulp degradation. Oxygen is a rather weak reactive oxidant because it requires high temperature and/or the ionization of the reacting functional groups to get a reasonable reaction rate. That's why oxygen delignification is performed at alkali conditions, and fairly high temperature and high pressure. However, the temperature increase is limited because severe carbohydrate degradation takes place when the temperature is above 120

°C (Gratzl, 1992). Limitation in the mass transfer of oxygen from the gas phase to the liquid phase is also a quite important issue in oxygen delignification. The following shows the radical formation and radical attack reactions.

Radical Formation

$$O_2 + \text{R-Ph - } O^- \rightarrow \text{R-Ph - } O\bullet + \bullet O_2^-$$

$$H_2O + \bullet O_2^- \rightarrow HO\bullet + \text{- OOH}$$

Radical Attack

$$\text{Lignin} + (1\text{-x})\ HO\bullet \rightarrow (1\text{-x})\ \text{Hydroxylated Lignin}$$

$$\text{Cellulose} + x\ HO\bullet \rightarrow \text{Cleaved or Oxidized Cellulose}$$

Where x is number much smaller than 1

3.1.5 Mass Transfer of Oxygen

Oxygen delignification involves three phases: solid (fiber), liquid (aqueous alkali solution), and gas (oxygen). Therefore, mass transfer between the multiple phases must be considered. Oxygen must cross the gas-liquid interface, diffuse through the liquid film surrounding the fiber, and finally diffuse into the fiber wall before oxygen delignification reactions occur. The rate of oxygen transport is important to the rate of the overall process (Ljunggren & Johansson, 1987, Krothapalli, 2004). Transport effects on the overall reaction rate can be divided into inter-phase and intra-phase factors. Hsu et al (1985) measured the concentration change as a function of time at different mixing speeds and gas flow rates. Their results show that the mass transfer resistance inside the fibers does not have a significant influence on the delignification kinetics compared to the resistance in the liquid phase during a 30 minutes reaction period. Rewatkar and Bennington (2002) reported that the mass transfer coefficient is dependent on the

superficial velocity of oxygen in the reaction tower. Mass transfer effects are aggravated by the low solubility of oxygen in aqueous sodium hydroxide (Broden & Simonson, 1979).

Agarwal and co-workers(1999) reported that there was no improvement in the oxygen delignification rate after southern hardwood kraft pulp was heavily refined, which confirmed that intra-fiber mass transfer effects did not influence the delignification rate. Krothapalli, Genco and van Heiningen (2004) investigated the effect of mass transfer on the kinetics of oxygen delignification for northeast hardwood kraft pulp at relatively low kappa numbers. They concluded that mass transfer did not affect the observed delignification rates in the University of Maine oxygen delignification reactors.

3.2 Kinetics of Oxygen Delignification

Lignin and carbohydrate degradation occur simultaneously during oxygen delignification. Therefore, a kinetic study of oxygen delignification should include the kinetics of both delignification and carbohydrate degradation. The kinetics of oxygen delignification are influenced by reaction temperature, oxygen pressure, and alkali concentration as well as mixing of oxygen and alkali with fibers. Most of the kinetic models are empirical and neglect mass transfer effects in the mathematical representation of the data. The degree of delignification is normally measured by determining the kappa number of the pulp which is an indirect measure of the lignin content of the pulp. Carbohydrate degradation is monitored by measuring the decrease in intrinsic viscosity [η]. However, recent studies show that kappa number does not represent the amount of residual lignin in the pulp. The hexenuronic acid (HexA) and other non-lignin structures also consume $KMnO_4$ in the kappa number measurement. It is generally believed that the HexA content is relatively

small in softwood kraft pulp (Li, 1999). Also, HexA is not degraded during oxygen delignification (Rööst et al, 2003).

3.2.1 Kinetic Models of Oxygen Delignification

3.2.1.1 Single Equation Model

Usually, the kinetics of oxygen delignification is presented by a single rate equation which describes the influence of the process variables. The most widely used model for lignin removal reactions is the power law equation (Iribarne and Schroeder,1997)

$$-r_l = -\frac{dK}{dt} = k[OH^-]^m[P_{O_2}]^n K^q \qquad \text{(Equation 3.1)}$$

where (K) is the kappa number; [OH^-] is the sodium hydroxide concentration and (P_{O2}) represents the oxygen pressure. The constants m, n, and q in Equation 3.1 and 3.3 are determined empirically from the experimental data. The reaction rate coefficient k depends on the temperature and is given by the Arrhenius equation:

$$k = A\exp(-\frac{E_A}{RT}) \qquad \text{(Equation 3.2)}$$

where (E_A) is the activation energy, (R) is the gas constant and (T) is the absolute temperature. A summary of power law equations reported in the literature is given in Table 3.1.

Table 3.1 Summary of Power Law Equations

Reference	$[OH^-]$ exponent (m)	$[O_2]$ or P_{O2} exponent (n)	Kappa Number exponent (q)	Active Energy (kJ/mol)	Frequency Factor
Agarwal (1998)	0.92	0.53	7.7	107.2	2.368×10^6
Perng (1997)	0.4	0.5	4.8	60	1.8
Teder (1981)	0.6	0.5	3.2	70	-
Kovasin (1987)	0.13	0.5	1	18.6	-
Iribane (1997)	0.7	0.7	2.0	51	3×10^6
Evans (1979)	1	1.23	1	49.1	10^5

It can be seen that the reaction orders of the different studies very over a wide range, expecially for the lignin reaction order. The activation energy is 50±10 kJ/mol except for the studies of Kovasin (1987) and Teder (1981). Based on the comparison in Table 3.1, it is very difficult to make a choice regarding the appropriate kinetics for pulp delignification during alkaline oxygen treatment.

3.2.1.2 Two Region Model

The kinetics of oxygen delignification has also been described by using the so called two region kinetic model. The first two region model was presented by Olm et al (1979).

$$-r_l = -\frac{dK}{dt} = k_1[OH^-]^{m1}[P_{O_2}]^{n1}K_1{}^{q1} + k_2[OH^-]^{m2}[P_{O_2}]^{n2}K_2{}^{q2} \quad \text{(Equation 3.3)}$$

$$K = K_1 + K_2$$

In the two region models, the basic equation is the same as that of single power law equation kinetics except that the model is now composed of two parts, one describing a fast reaction and the other a slow reaction. Two region kinetics models appear widely in the literature (see Table 3.2). It should be noted that in most studies that use a two region

kinetics model, the lignin reaction order was assumed to be 1.0, although this was not experimentally verified.

Table 3.2 Summary of Kinetics Studies for Two Region Model

Reference	Phase	[OH-] exponent (m)	[O_2] or PO_2 exponent (n)	Kappa Number exponent (q)	Active Energy (kJ/mol)	Frenquency Factor
Iribane et al, 1997	Fast	1.2	1.3	1	67	36×10^{11}
	Slow	0.3	0.2	1	40	6×10^{4}
Vincent et al, 1997	Fast	0	0.4	1	24.2	27.5
	Slow	0.39	0.38	1	46.3	7667
Myers et al, 1989	Fast	0	0.4	1	31.6	1.51×10^{5}
	Slow	0.875	0.43	1	61.4	1.68×10^{-5}
Hsu et al, 1986	Fast	0.78	0.35	3.1	36	2.46
	Slow	0.70	0.74	3.1	71	143.49
Olm et al, 1979	Fast	0.1	0.1	1	10	-
	Slow	0.3	0.2	1	45	-

Again, it is clear from the comparison in Table 3.2 that there is a wide range of the reaction orders and activation energies, making it difficult, if not impossible to decide which kinetic equation to choose.

3.2.2 Kinetics of Carbohydrate Degradation

Similar empirical power law models have also been proposed for cellulose degradation. One such model is given by Equation 3.4

$$-r_C = -\frac{dM}{dt} = k[OH^-]^m[P_{O_2}]^n M^q \qquad \text{(Equation 3.4)}$$

where (M) is number average molecular weight of cellulose. Inherent in Equation 3.4 is the assumption that the hemicellulose polymers in the pulp do not contribute appreciably to the number average molecular weight of the carbohydrates comprising the pulp.

3.3 Interpretation of the High Rate Orders

The reaction order in kappa number is very important for the delignification kinetics. Some studies showed that the exponent of the kappa number was greater than one (Hsu and Hsieh, 1988; Perng and Oloman, 1994, Olm, Agarwal et al., 1999; Teder, 1981). Olm and Teder (1999) determined from their experimental data on softwood pulp that a one region kinetic model resulted in a lignin the reaction order of 3.2. This result agreed with the reaction order of 3.1 determined by Hsu and Hsieh (1988) for Southern Pine softwood. On the contrary, Agarwal and coworkers (1999) determined that the exponent on the kappa number was 7.7 for southern hardwood at low kappa numbers. The proposed explanation for these high rate orders is that delignification consists of a large number of parallel first-order reactions corresponding to the different lignin moieties in the pulp which take place simultaneously (Axegard et al., 1979). Schoon (1982) reported that very high reaction orders with respect to lignin were found for several pulping and bleaching reactions for hardwood pulps. His work showed that the decomposition of lignin (L) in pulping and bleaching processes can be expressed as a power law model when assuming that the decomposition occurs by an infinite number of first-order parallel reactions.

$$-\frac{dL}{dt} = k_{\alpha} L^{m} \qquad \text{(Equation 3.5)}$$

In Schoon's model, the assumption is made that the activation energy (E_A) for each of the reactions pathways is the same. The assumption of a large number of parallel first-order reactions with different rate constants can explain the observed high delignification rate orders. Some lignin fractions have a high rate constant which determines the initial phase of the delignification reaction, and other fractions have a low rate constant which dominates the final slow reaction phase. This explanation is supported by the fact that

lignin exists several different moieties, some of which are formed during pulping (Zou, 2002) and some during oxygen delignification (Argyropoulos and Liu, 1998).

3.4 Demand of Oxygen in Oxygen Delignification Process

Literature shows that the primary mechanism for delignification is oxygen attack on the aryl groups. Studies show that one C_9 structure reacts with one oxygen molecule. (Vuorenvirta, 2001). In the industry, oxygen also can be consumed by carry-over of organic materials. It has been found that the carry over also has a negative effect on the lignin-cellulose selectivity. There are a few investigations which have quantified the oxygen demand in an industrial situation and in laboratory reactors. These results are summarized in Table 3.3.

Table 3.3 Summary of Oxygen Consumption in Oxygen Delignification Process

Reference	Reaction Conditions	Oxygen Consumption per Unit Kappa Number (%)
Thompson, 1976	Laboratory: 100°C, 25% consistency	0.05-0.06
Evans,1979	Industrial: 100-116°C, 30% Consistency	0.08-0.09
McDonough, 1996	Industrial: Medium Consistency	0.14
Berry et al, 2002	Laboratory: 95-110°C, 10% Consistency	0.055-0.064
Seifert et al, 2002	Industrial: 15-28% Consistency	0.12-0.19
Ragnar et al 2004	Industrial Mill A and Mill B	0.06-0.10
Salmela M., 2004	Industrial:90°C, 6.9 bar, 5.5 kg/ADt NaOH, 2.5 kg/ADt MgSO4, Medium Consistency	0.103-0.152

It shows that the oxygen consumption in percentage on oven dried pulp per unit kappa number ranges from 0.05-0.15 for medium consistency operation. This is equivalent to about 2-6 moles of O_2 consumed per lignin monomer unit removal.

3.5 Treatment of Experimental Data

3.5.1 Power Law Model

With the assumption of a constant alkali concentration during delignification reaction, the oxygen delignification data may be fitted to the general power law model proposed by Schoon (1982).

$$-\frac{dK}{dt} = k_q K^q \qquad \text{(Equation 3.6)}$$

In the kinetics study, the rate constant (k_q) incorporates the absolute temperature (T), the initial sodium hydroxide concentration (OH^-) and the pressure (P_{O2}) into one single process parameter that describes the oxygen delignification kinetics (Equation 3.7).

$$k_q = A_q \exp(-E_A / RT)(OH^-)^m (P_{O_2})^n \qquad \text{(Equation 3.7)}$$

where K is Kappa Number (unitless)

t is time (min)

k_q is reaction rate constant (min^{-1})

q is reaction order

E_A = activation energy (J/gmol)

R = gas constant (8.314J/gmol K)

T = temperature (K)

OH^- = initial sodium hydroxide concentration (g/L)

P_{O2} = oxygen pressure (psig)

m = parameter showing alkali dependence (unitless)

n = parameter showing oxygen pressure dependence (unitless)

A_q = frequency factor (min^{-1}) $(g/l)^{-m}$ $(psig)^{-n}$

The advantage of incorporating all of the variables into a single process parameter (k_q) is that Equation 3.6 can be integrated between the limits (K_0), the initial kappa number at time (t) equal to zero, and any kappa number (K) present at time (t) provided the reaction coefficient (k_q) and reaction order (q) are approximately constant.

$$-\int_{K_o}^{K} \frac{dK}{K^q} = k\int_{t=0}^{t} dt \qquad \text{(Equation 3.8)}$$

Equation (3.8) can be solved to give an analytical expression for the kappa number (K)

$$\left(\frac{1}{K^{q-1}}\right)-\left(\frac{1}{K_0^{q-1}}\right) = k(q-1)t \quad for \quad q \neq 1 \qquad \text{(Equation 3.9)}$$

which is a linear function of time (t) in terms of variable y

$$y \;=\; \left(\frac{1}{K^{q-1}}\right)-\left(\frac{1}{K_0^{q-1}}\right) \qquad \text{(Equation 3.10)}$$

Equation (3.11) can be rearranged further to estimate the kappa number (K) as a function of time (t).

$$K(t) = \left[\left(\frac{1}{K_0^{q-1}}\right) + k_q\,(q-1)t\right]^{-\left(\frac{1}{(q-1)}\right)} \quad q \neq 1 \qquad \text{(Equation 3.11)}$$

Equation 3.12 can also be solved for the special case where the reaction order is equal to one (q =1).

$$\ln\left(\frac{K}{K_0}\right) = -k_q t \quad q = 1 \qquad \text{(Equation 3.12)}$$

3.5.2 Two Region Kinetic Model

Olm and Teder (1979) applied Equation 3.6 to two regions and the data were divided into two regions corresponding to the “fast” and “slow” periods. Delignification is assumed to

occur by two parallel first order reactions where the kappa number in the fast region is (K_1) and that in the slow region is (K_2), so that the total kappa number K is:

$$K = K_1 + K_2 \qquad \text{(Equation 3.13)}$$

The reduction in the kappa number for the two regions is

$$-\frac{dK_1}{dt} = k_1 K_1 \qquad \text{(Equation 3.14)}$$

and

$$-\frac{dK_2}{dt} = k_2 K_2 \qquad \text{(Equation 3.15)}$$

which can be integrated to give the reduction in kappa number for the two regions

and

$$K_1 = K_{01} \exp(-k_1 t) \qquad \text{(Equation 3.16)}$$

$$K_2 = K_{02} \exp(-k_2 t) \qquad \text{(Equation 3.17)}$$

where K_{01} is the difference between the initial kappa number (K_0) and the extrapolated value for the second region (K_{02}) as shown in Figure 3.7.

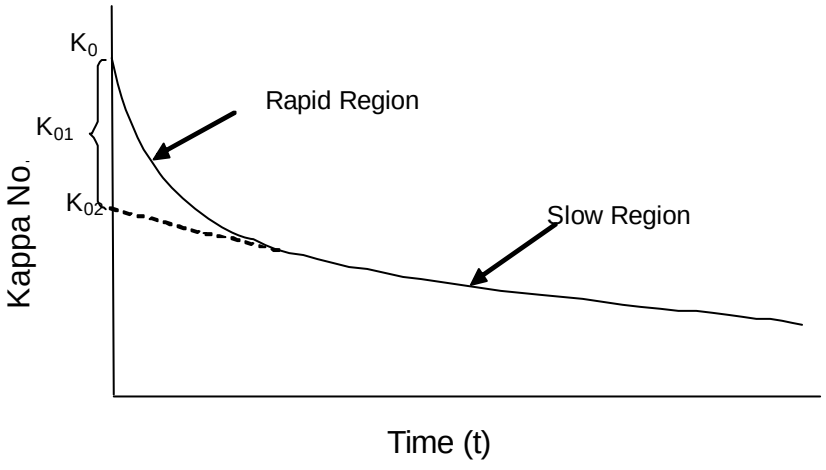

Figure 3.7 Olm and Teder Two Region Model

The initial lignin content in the fast region can be described in terms of the kappa number (K_{01}).

$$K_{01} = K_0 - K_{02} \qquad \text{(Equation 3.18)}$$

The kappa number K(t) at any time (t) is the sum of Equation 3.16 and 3.17.

$$K = K_{01}\exp(-k_1 t) + K_{02}\exp(-k_2 t) \qquad \text{(Equation 3.19)}$$

3.5.3 Cellulose Degradation

3.5.3.1 Degree of Polymerization of Cellulose

The intrinsic viscosity [η] of the pulp may be used to estimate the degree of polymerization (DP) of the cellulose in pulp. The average degree of polymerization is estimated from the intrinsic viscosity and hemicelluose content of pulps (van Heiningen et al, 2003) and the weight of glucose (G) and hemicellulose content (H).

$$DP = \left(\frac{1.65[\eta] - 116H}{G}\right)^{1.111} \qquad \text{(Equation 3.20)}$$

3.5.3.2 Number of Moles of Cellulose per Ton of Pulp

The number of moles of cellulose per ton of pulp may be determined by following the procedure presented by Irabarne and Schroeder (1999). The number of moles of cellulose per ton of pulp is related to the number average degree of polymerization (DP_n) by the simple equation

$$m_n = \frac{Grams\ Per\ Ton}{Molecular\ Wt\ (Grams/mole)} = \frac{10^6}{162DP_n + 18} \cong \frac{10^6}{162DP_n} = \frac{Gram\ Moles}{Ton\ Pulp} \qquad \text{(Equation 3.21)}$$

In Equation (3.21), the factor of 162 is the molecular weight of the anhydro glucose unit and 18 is the molecular weight of water.

3.5.3.3 Power Law Model for Cellulose Degradation

The cleavage of polysaccharide chains was monitored by Irabarne and Schroeder (1999) using the increase in the number-average moles of cellulose per ton of pulp (m_n) as a parameter. They describe the kinetics for the apparent polysaccharide cleavage using a power law mathematical model similar to Equation 3.22.

$$\frac{dm_n}{dt} = k_\lambda m_n^{\ \lambda} \qquad \text{(Equation 3.22)}$$

The reaction rate constant (k_λ) in Equation 3.22 is given by an equation analogous to Equation 3.23 for the kappa number.

$$k_\lambda = A_m \exp(-E_m / RT)(OH^-)^\chi (P_{O_2})^\beta \qquad \text{(Equation 3.23)}$$

The units to be used in Equation 3.23 are:

m_n = number of average moles of cellulose (moles/ton)

λ = parameter showing dependence on m_n (unitless)

k_λ = reaction rate coefficient [$(\text{mole/ton})^{1-\lambda}$/min]

E_m = activation energy (J/gmol)

R = gas constant (8.314J/gmol K)

T = temperature (K)

OH^- = initial sodium hydroxide concentration (g/L)

P_{O2} = oxygen pressure (psig)

χ = parameter showing alkali dependence (dimensionless)

β = parameter showing oxygen pressure dependence (dimensionless)

A_m = Frequency Factor = $[(\text{moles/ton})^{1-\lambda}/\text{min}]$ $(\text{g/L})^{-\chi}$ $[\text{psig}]^{-\beta}$

Assuming a constant hydroxyl concentration, equation 3.23 can be integrated between the initial number of moles of cellulose present at time equal to zero (m_0) and any value for the moles of cellulose (m_n) present at time (t). Similar to the kappa number, the integration can be performed provided the reaction coefficient (k_λ) and reaction order (λ) are approximately constant.

$$\left(\frac{1}{m_n^{\lambda-1}}\right)-\left(\frac{1}{m_{n0}^{\lambda-1}}\right)=k_\lambda\,(1-\lambda)t \quad for \quad \lambda \neq 1 \qquad \text{(Equation 3.24)}$$

The treatment of experimental data for the number of moles of cellulose is the same as that used for the kappa number. Equation 3.24 is used to fit experimental data and used to estimate the rate constant (k_λ) and the reaction order (λ) for each delignification curve. A trial and error method may be used with the integral method to estimate the "best" values for both the rate constant (k_λ) and the reaction order (λ).

3.6 Selectivity of the Oxygen Delignification Process

Selectivity is commonly calculated as the ratio of the change in kappa number to the change in viscosity of the pulp. However, it is scientifically more correct to determine the intrinsic viscosity and then convert it to degree of polymerization (DP). The lignin-cellulose degradation selectivity is dependent upon the pulping process and the process variables used in the delignification process. Violette (2001) performed an investigation that focused on the selectivity during the oxygen delignification process. It was found that increasing the temperature over the range from 90°C to 120°C had almost no effect on the selectivity. However, increasing the alkali charge had a significant negative effect

on selectivity. The selectivity coefficient (α) is defined as the slope of a curve when [1/ $DP_t - 1/DP_0$] is plotted versus the change in kappa number (ΔK). The value ($1/DP_t$-$1/DP_0$) represents the number of chain scissions per polymer unit of cellulose. The definition of the selectivity coefficient, α, is based on the following analysis. Equation 3.25 can be obtained by taking the ratio of the rate equations for the kappa number and the moles of cellulose.

$$\frac{dm_n / dt}{dK / dt} = \frac{k_\lambda m_n^{\ \lambda}}{-k_q K^q} = \frac{dm_n}{dK} \qquad \text{(Equation 3.25)}$$

Because the degree of polymerization of cellulose is high, the rate order λ can be taken to be zero. Because the attack on cellulose is by radicals, the rate constant k_λ will be proportional to the number of radicals generated during delignification. Since the latter is proportional to the rate of attack of oxygen on phenolic lignin, the rate constant k_λ is likely proportional to the rate of delignification, i.e. $k_\lambda = Ck_qK^q$. Insertion in equation 3.25 and integration between the initial values (m_0 and K_0) at time zero to any value (m and K) at time (t) gives

$$m_n - m_0 = -C(K - K_0) \qquad \text{(Equation 3.26)}$$

The moles of cellulose (m) can be converted to the degree of polymerization by using the definition for the moles of cellulose.

$$(K_0 - K_t) = \frac{10^6}{C \cdot 162}\left(\frac{1}{DP_t} - \frac{1}{DP_0}\right) \qquad \text{(Equation 3.27)}$$

CHAPTER 4

EXPERIMENTAL EQUIPMENT AND PROCEDURES

4.1 Testing Standards

Kappa number: T236 cm-85 (or SCAN-C 1:77)

Intrinsic viscosity: D1795-62 (re-approved 1985)

4.2 Raw Materials

A commercial unbleached Southern Pine kraft pulp with an initial Kappa number of 26 and intrinsic viscosity of 1,189 ml/g was used. No $MgSO_4$ was added to the caustic solution.

4.3 Equipment

4.3.1 Parr Reactor

The Parr reactor is a 2-liter continuously stirred horizontal batch reactor obtained from Parr Instruments with an anchor rotating device which wipes the inside of the reactor with Teflon blades. Figure 4.1 shows a schematic diagram of the Parr reactor set-up.

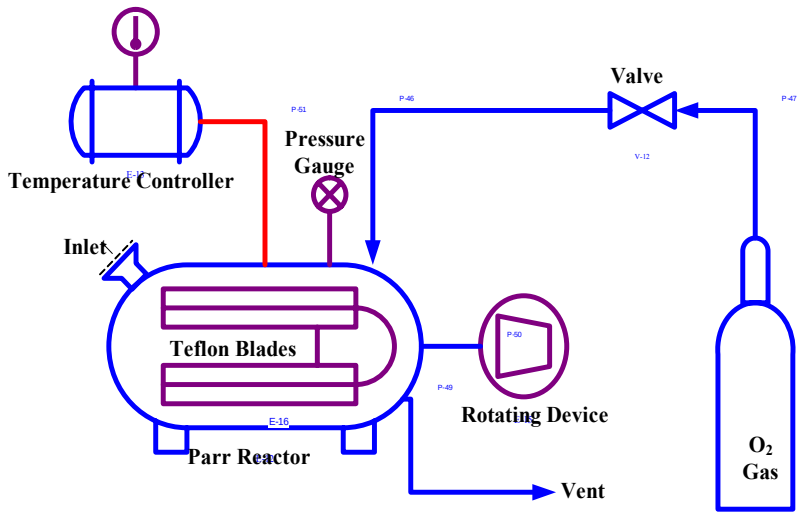

Figure 4.1 Schematic Diagram of the Horizontal Parr Reactor Set-up

4.3.2 Flow through Differential Continuous Flow Stirred Tank Reactor (CSTR)

The flow diagram of the reactor setup is shown in Figure 4.2. Oxygen from a gas cylinder is bubbled into a caustic solution held in a pressurized (130 psig max.) 3 gallon stainless steel container. The container is kept at the desired temperature by an external heating blanket. The actual reactor is a Berty reactor (Appendix Figure) manufactured by Autoclave Engineers with a stationary basket which holds the pulp bed. The nominal volume of the reactor is a 280 ml. It contains a 100 ml basket with a rotor underneath which induces flow through the pulp mat inside the basket (Figure 4.3). The entire reactor is filled with liquid at the operating pressure and any gas inside the reactor is vented at the top of the reactor. Oxygen is bubbled overnight through the NaOH solution to obtain a saturated oxygen concentration at the set oxygen pressure. Then the reaction is started by feeding the oxygenated caustic solution at constant flow rate and oxygen pressure. The reactor pressure, temperature and outflow rate are recorded every 5 seconds. The UV-VIS absorption of the outflow stream is monitored every 15 seconds. The UV-VIS data are

converted into dissolved lignin concentration using a calibration curve prepared with Indulin AT lignin of MeadWestvaco.

An experiment with the differential CSTR consists of the following steps:

1. Fill the reactor with water; heat the reactor, the liquor tank and the stainless steel tubing to the desired temperature;
2. Use by-pass to measure blank UV absorption;
3. Let the NaOH solution go into the reactor, at the same time start the UV-VIS spectrophotometer (collect 1 data every 15 seconds). The pressure and the temperature inside the reactor are monitored every 5 seconds;
4. During the reaction, collect liquid samples at 2, 7, 12, 10, 20, 30, 40, 50 and 60 minutes for 60 seconds to test the Methanol, TOC and TC concentration at different reaction time. In addition, the flow rates can be calculated from the weight of collected samples at the different reaction times.
5. Stop the reaction at the desired time by using a cold water flush so that the reactor will cool down to 20 ºC in one minute. All the NaOH is also removed so the reaction is stopped immediately;
6. Open the reactor; wash and dry the pulp sample;
7. Measure yield, kappa number and intrinsic viscosity of the pulp sample.

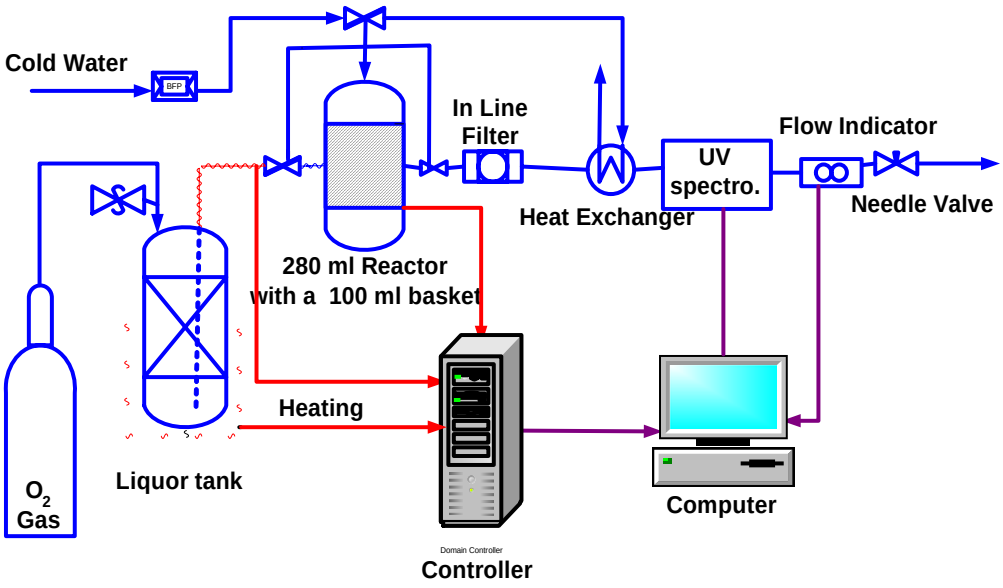

Figure 4.2 Diagram of CSTR Reactor Setup

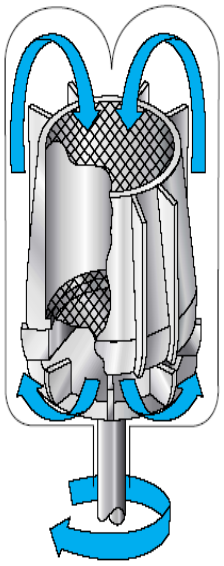

Figure 4.3 Berty Stationary Basket Inside the Reactor

4.4 Experiments

4.4.1 Experiments in Batch Reactor

All the batch delignification experiments were done in the 2-liter Parr batch reactor. The controller can control the temperature within 2 ºC. 20 g o.d. pulp (10% consistency) was added to the reactor and the oxygen pressure raised to the desired value to start the delignification. After the delignification, the pulp was washed three times at about 1% consistency.

Part A: Instead of using oxygen, the procedures were performed with nitrogen gas. The objective of these tests was to determine the small decrease in kappa number and viscosity drop which occur because of alkali extraction. Nitrogen extraction was done at the same conditions as the regular oxygen delignification experiments.

Part B: Commercial unbleached softwood pulp sheets were disintegrated and homogenized. Oxygen delifnication were done at 90ºC, 75 psi, 3.0% NaOH, and 10% consistency. Reaction times were 10, 20, 40, 60 and 180 minutes. To study the effects of different reaction pressures and stirring speeds, the pressure was varied from 20, 75, 140 and 190 psi; and the stirring speeds were 45, 225, 500 and 1000 rpm.

4.4.2 Experiments in CSTR

Part A: Effect of reaction time (10, 20, 40, 60, 180 and 360 minutes) at standard conditions (90ºC, 75 psig, 3.3 g/l NaOH).

Part B: Effect of operating conditions to study the kinetics:

-Temperature (80, 90, 100, 110 and 115ºC)

-Pressure (35, 55, 75 and 95 psig)

-NaOH (1.1, 3.3, 5.5, 7.7, 20 and 50 g/l)

4.5 Measurements

- *Pulp Yield*

Yield% = (total weight after O_2 delignification) / (original pulp weight) ×100%

- *Modified Kappa Number Measurement*

The kappa number was measured according to a modification of the TAPPI standard T236-cm-85. Due to the small amount of the pulp sample, all the chemical dosages were reduced to one tenth of the amount in the standard TAPPI method.

Table 4.1 Modified Method for Kappa Number Measurement

Chemical Dosages	**TAPPI Method**	**Modified Method**
Oven-dried pulp (g)	2-10	0.2-1
Volume of 0.1N $KMnO_4$ (ml)	100	10
Volume of 4N H_2SO_4 (ml)	100	10
Total Volume (ml)	1000	100
Volume of 1.0N KI (ml)	20	2
Total reaction Time (min)	10	10

- *Intrinsic Viscosity*

The intrinsic viscosity was determined according to the A.S.T.M. designation D1795-62 (re-approved 1985).

- *Selectivity Coefficient α*

Selectivity is defined as reduction in kappa number is divided by number of chain scissions of cellulose ($1/DP_t$-$1/DP_0$).

$$Selectivit\ y = \frac{\Delta K}{1/DP_t - 1/DP_0}$$

- *Flow Rate*

The flow rate was measured every 5 seconds by FLR-1000 Liquid Flow Measurement Meter (Appendix Figure B.5) and recorded by SOFTWIRE.

- *Dissolved Lignin Concentration*

A HP 8453 UV-VIS from Agilent Technology is used for measurement of the dissolved lignin concentration. During pulping, lignin structures are changed because of degradation reactions. A part of the lignin is dissolved and a part remains in the pulp (so called residual lignin). The composition of the dissolved and residual lignin is different from that of the native lignin in wood. The terms “kraft lignin”, “alkali lignin” and “sulfide lignin” usually refer to the soluble lignin degradation products in spent liquors after pulping. Their compositions markedly differ from the composition of the residual pulp lignin. To determine the dissolved lignin concentration, a UV spectrophotometer is usually used. For lignin dissolved during sulfite and Kraft pulping, it is feasible to quantify the lignin concentration by UV absorption at 205nm or 280nm since the aromatic structure of lignin is still intact. In this study, the dissolved lignin concentration was measured by UV absorption at 280nm.

- *TOC Concentration of the Liquor Samples*

Liquor samples of the oxygen delignification tests are collected at different time intervals for TOC analysis. All the tests are performed in the Maine Soil Testing Service Analytical Lab at the Plant, Soil and Environment Science Department of the University of Maine. Total Organic carbon (TOC) is determined by high temperature combustion and infrared detection of CO_2 using a Shimadzu TOC-5000A Analyzer with autosampler.

- *Methanol Concentration of the Liquor Samples*

Liquor samples of the oxygen delignification are collected at different intervals. The samples are sent to the Institute of Paper Science and Technology at the Georgia Institute of Technology and tested for methanol content by headspace gas chromatography (HS-GC) according to the method by Xinsheng Chai (Chai et al, 2001).

- *Klason Lignin and Acid Soluble Lignin*

Klason lignin and Acid Soluble Lignin are measured according to the LAB MANUAL (Analytical Testing) of the Chemical and Biological Engineering Department at the University of Maine. The lignin content was measured gravimetrically after two steps of hydrolysis. The primary hydrolysis was performed with 72% H_2SO_4 at 30°C for 1 hour and the secondary hydrolysis with 4% H_2SO_4 at 120°C for 1 hour.

- *Mono Sugar Analysis*

Monomeric sugars were measured by HPAEC (High Performance Anion Exchange Chromatography) in the Chemical and Biological Engineering Department at the University of Maine. The pulp after oxygen delignification was converted into monosugars using a two step acid hydrolysis (primary hydrolysis with 72% H_2SO_4 at

30°C and secondary hydrolysis with 4% H_2SO_4 at 120°C). The sugar monomers were then analyzed by HPAEC. Fucose was used as an internal standard.

- *Isolation of Residual Lignin*

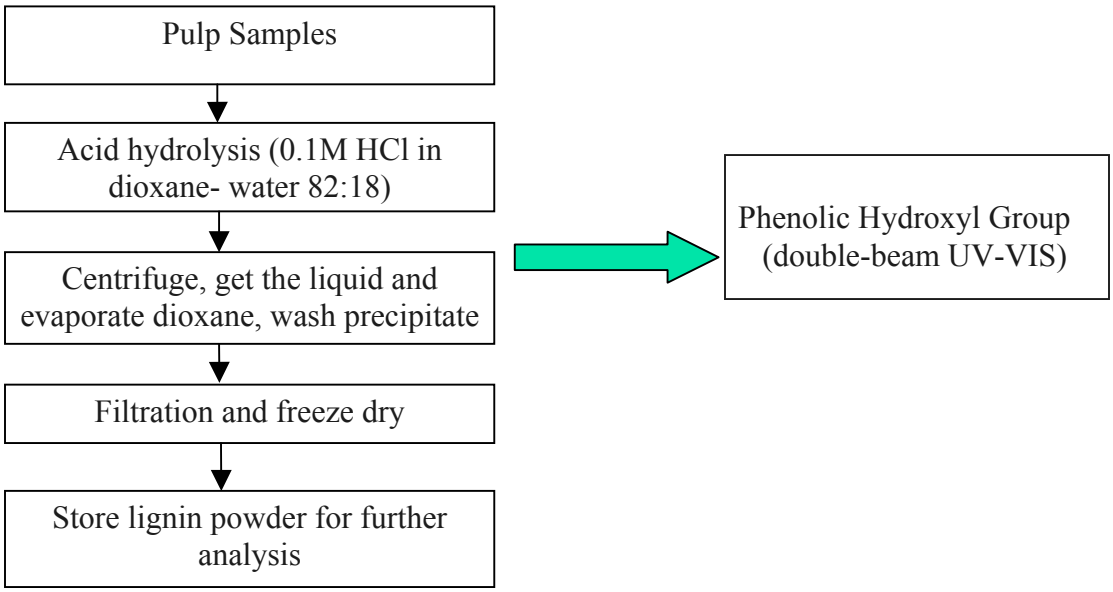

Figure 4.4 Isolation and Analysis Procedure of Residual Lignin of Pulps

Residual lignin of pulps is separated by the procedure described in Figure 4.4 (Gellerstedt, 1994). The phenolic hydroxyl group content of lignin is measured by double-beam UV-VIS.

- *Phenolic Hydroxyl Groups of Residual Lignin and Dissolved Lignin*

Phenolic hydroxyl groups in the lignin are very important because these groups are thought to be the initial site for the oxygen delignification reactions. The phenolic hydroxyl group contents in the liquor samples and the pulp are measured by a double-beam UV-VIS spectrophotometer. This method is based on difference of the spectroscopic absorbance of the ionized and the non-ionized phenols in the lignin

structure, e.g., the differences in the maximum absorption close to 300nm and 350nm of the same sample dissolved in neutral and alkaline solutions.

$$\left[PhOH^{-}\right]=\frac{0.25\times\left[A_{300}(Alk)-A_{300}(Neu)\right]+0.107\left[A_{350}(Alk)-A_{350}(Neu)\right]}{\text{Lignin Concentration(g/liter)}}\ \frac{\text{mmol}}{\text{g Lignin}}$$

(Equation 4.1)

$$\text{PhOH Content of Lignin Monomer}=\frac{mmoles}{g}\times\frac{185g}{mol}\times\frac{1mole}{1000mmoles}$$ (Equation 4.2)

- *Carbohydrate Removal Rate with the Waste Liquor*

The carbohydrate removal rate in the waste liquor was calculated from the delignification rate and the formation rate of TOC and methanol using equation (4.1).

$$\text{Carbohydrate Rate} = (\text{TOC Rate} - \text{MeOH Rate}\times\frac{12}{32} - \text{Delig Rate}\times\frac{108}{185})\times\frac{162}{72}$$

(Equation 4.3)

- *Hexenuronic Acid (HexA)*

A UV-VIS spectrophotometer was used to quantify the HexA groups in the pulps by a method obtained from HUT (Helsinki University of Technology). The pulps are hydrolyzed under weak acidic conditions (0.01M sodium formiate buffer in an autoclave at 120°C). The HexA content is proportional to the hydrolysis products (2-furnic and 5-carboxyl-2-furaldehyde) which have a clear absorption peak at 245nm. The HexA content can be calculated by Concentration = A_{245}/(87×Pulp Weight). In this equation, the absorption coefficient includes the effect from both 2-furnic and 5-carboxyl-2-furaldehyde.

- *Sugar Reducing End Content of Carbohydrates in Pulp (colorimetric method)*

The chemical reagent contains 1% dinitrosalicylic acid, 0.2% phenol, 0.05% sodium sulfite and 1% sodium hydroxide. This method tests for the presence of free carbonyl group (C=O) in so called reducing sugars. This involves the oxidation of the aldehyde functional group such as in glucose and the ketone functional group in fructose. Simultaneously, 3,5-dinitrosalicylic acid (DNS) is reduced to 3-amino,5-nitrosalicylic acid under alkaline conditions:

oxidation
aldehyde group ----------> carboxyl group

reduction
3,5-dinitrosalicylic acid ----------> 3-amino,5-nitrosalicylic acid

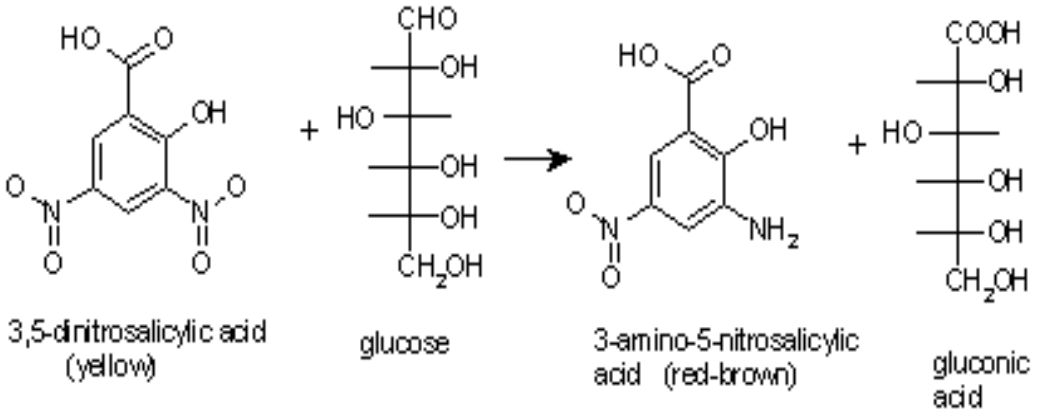

Figure 4.5 Reaction of Reducing Ends Measurement

3-amino-5-nitrosalicylic acid is an aromatic compound that reflects light strongly at 575nm (red). It is produced when 3,5-dinitrosalicylic acid reacts with a reducing sugar. Sulfite is present in the reagent to absorb any dissolved oxygen because dissolved oxygen can interfere with the sugar oxidation. The above reaction scheme in Figure 4.5 shows that one mole of sugar will react with one mole of 3,5-dinitrosalicylic acid. However, it is suspected that there are many side reactions, and the actual reaction stoichiometry is more complicated than described in Figure 4.5. The type of side reaction depends on the

exact nature of the reducing sugars. Different reducing sugars generally yield different color intensities; thus, it is necessary to make a calibration curve for each sugar. In addition to the oxidation of the carbonyl groups in the sugar, other side reactions such as the decomposition of the sugar also competes for the availability of 3,5-dinitrosalicylic acid. As a consequence, carboxymethyl cellulose can affect the calibration curve by enhancing the intensity of the developed color.

4.6 Study Kinetics of Oxygen Delignification

To study the kinetics of oxygen delignification, experiments were done at different temperatures, different alkali charges and different pressures according to Taguchi's Design.

Table 4.2 Experiment Plan Conditions for Kinetics Study

Runs	Temperature (°C)	Pressure (psig)	NaOH (g/liter)
1	80	75	3.3
2	90	75	3.3
3	100	75	3.3
4	110	75	3.3
5	115	75	3.3
6	90	35	3.3
7	90	55	3.3
8	90	75	3.3
9	90	95	3.3
10	90	75	1.1
11	90	75	3.3
12	90	75	5.5
13	90	75	7.7
14	90	75	20
15	90	75	50

4.7 Study the Effect of Hydroxyl Radical Attack

Instead of using an oxygenated NaOH-water solution for oxygen delignification experiment, a mixture of water and ethylene glycol (water:ethylene glycol = 50:50) was used as the reaction solution. The intrinsic viscosity and kappa number of the final pulp is compared with control pulps obtained at standard conditions.

4.8 Effect of Reducing Ends (Sodium Borohydride $NaBH_4$ Treatment)

Two sets of experiments were done to study the importance of reducing ends on oxygen delignification of softwood kraft pulp.

1. A reference experiment of oxygen delignification was performed directly on the kraft pulp,
2. Kraft pulp is first reduced with sodium borohydride and then oxygen delignified at similar conditions to the reference pulp. The idea here is to stabilize the carbohydrates against alkaline peeling reactions.

CHAPTER 5

DATA COLLECTION AND TREATMENT

5.1 Determination of the Residence Time Distribution of the Reaction System

Because there is tubing to connect the Berty CSTR and the UV detector, the dead volume of the tubing and the residence time distribution (RTD) of the reactor system should be determined for the kinetics study. To measure the RTD, step tracer experiments were done with methyl red as tracer at 4 different flow rates 61ml/min, 73ml/min, 91ml/min and 141ml/min. The RTD measurement procedure is as follows:

1. Initially, the reactor is filled with water.
2. At t = 0, the feed is switched to the liquor tank which contained a constant concentration methyl red.
3. The effluent tracer concentration is then monitored by UV-VIS for t>0.

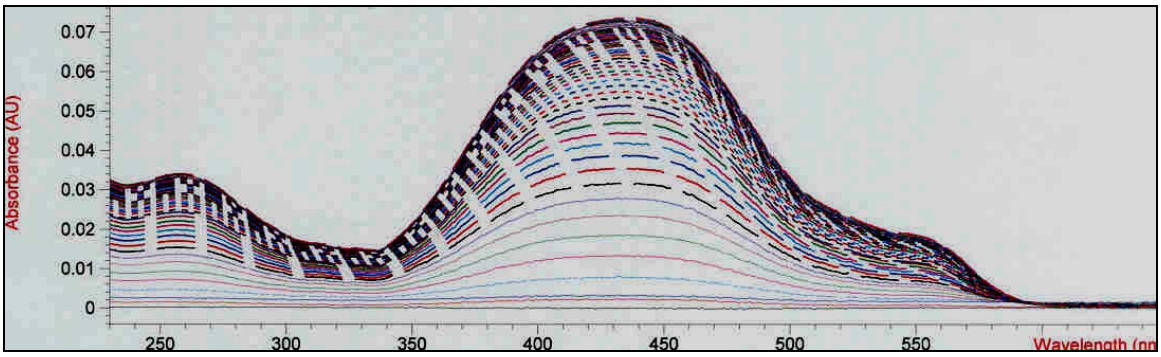

Figure 5.1 UV Absorption of Methyl Red at Different Concentrations

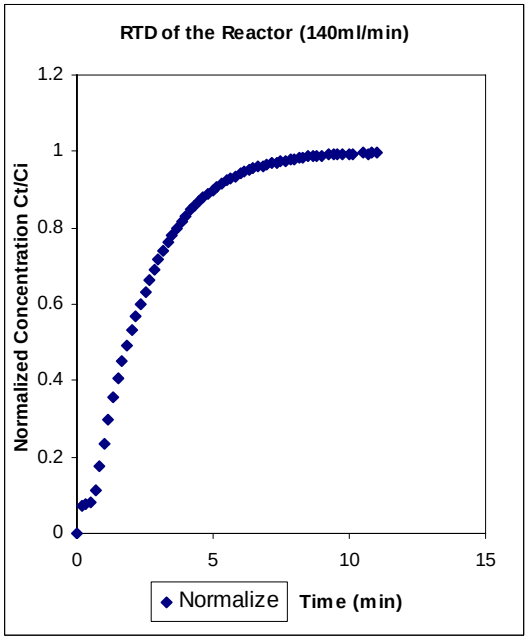

Figure 5.2 RTD Response (140ml/min)

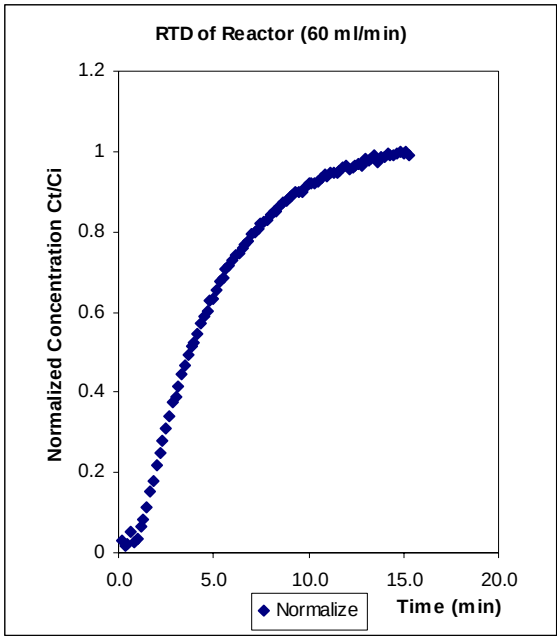

Figure 5.3 RTD Response (60ml/min)

Table 5.1 Reactor Volume and Dead Volume Results

Flowrate(ml/min)	Space time(min)	Delay(min)	Reactor Volume(ml)	Dead Volume (ml)
61.0	4.01	1.73	244.61	105.29
73.0	3.67	1.31	267.60	95.27
91.0	2.85	1.16	259.79	105.57
141.0	2.04	0.55	287.08	77.55
		Average	**264.77**	**95.92**

The results of the VisSim program (Appendix) show that the CSTR reactor volume is 265 ml and the tubing dead volume is 96 ml. These results agree with the real reactor design data. The reactor volume is specified as 280 ml by the manufacturer. However, the 4 g pulp sample and the metal basket also take up some volume of the reactor. The dead volume of the tubing is calculated as follows: The total length of the tubing is 542 cm. The outer diameter of the tubing is 0.25 inch, and the wall thickness is 0.035 inch. Based on these dimensions, a volume of 89 ml is obtained, which is 7% less than the VisSim

program calculation of 96 ml. Because of the difficulty of measuring the length of heat exchanger, the VisSim result was considered to be the more precise result. So the CSTR volume used was 265 ml, and the plug flow dead volume after the reactor was 96 ml.

5.2 UV-VIS Absorption Calibration by Indulin C and Indulin AT

Indulin C and Indulin AT were obtained from MeadWestvaco. The chemical name of Indulin C is sodium lignate, which is a sodium salt of heterogeneous guaiacylpropane polyether. Its chemical formula is $\{(CH_3O)(ONa)Ar(C_3H_4O)\}_x$. Indulin AT is the protonated form of Indulin C, i.e. its chemical formula is $\{(CH_3O)(OH)Ar(C_3H_4O)\}_x$. Indulin C is complete soluble in water while Indulin AT is insoluble in water. However, Indulin AT is soluble in a caustic solution.

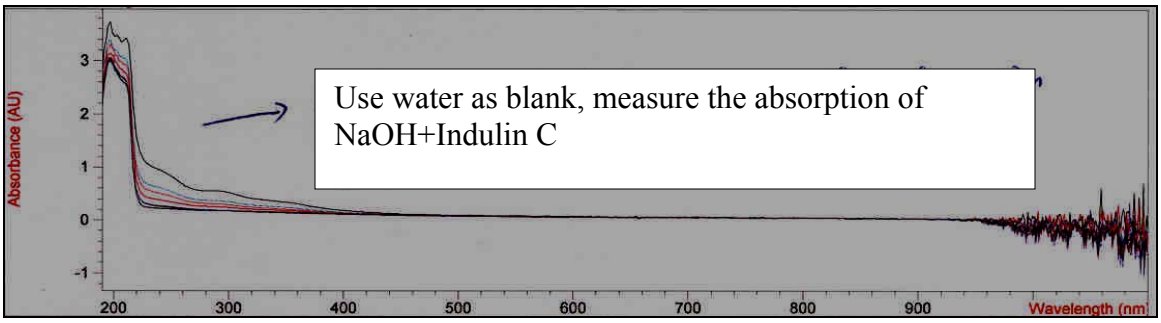

Figure 5.4 UV Absorption of Indulin C with Water as Blank

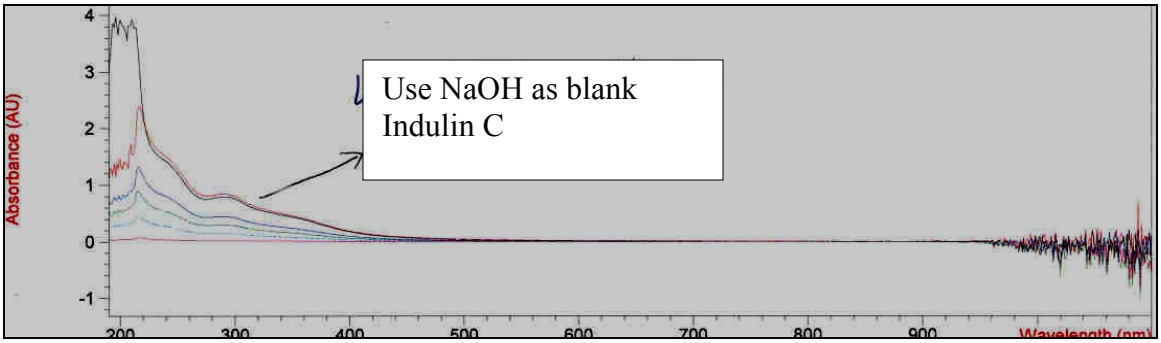

Figure 5.5 UV Absorption of Indulin C with NaOH (3.3 g/liter) as Blank

Figures 5.4 and Figure 5.5 show that the UV absorptions of Indulin C are very different when different reference blank samples (NaOH or Water) are used. It clearly shows that NaOH solution has absorption in the 190-210 nm wavelength range. Therefore, 280nm is a good wavelength to measure the lignin concentration because it is not affected by NaOH.

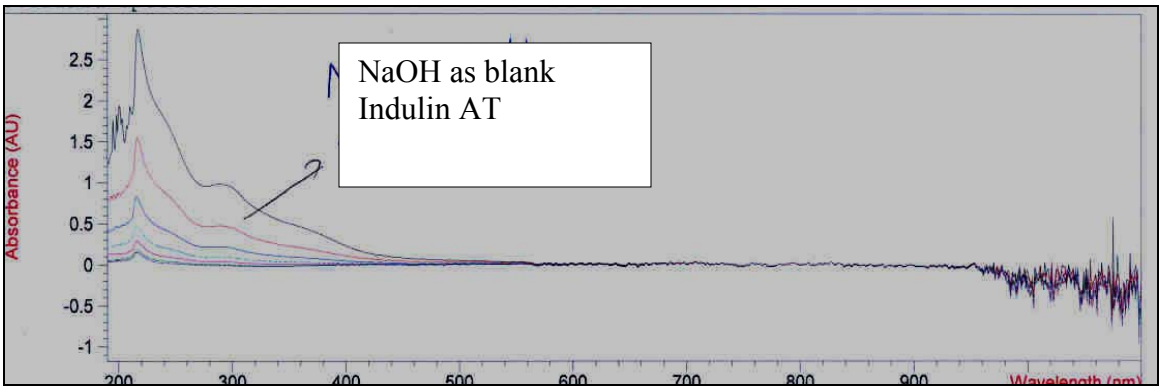

Figure 5.6 UV Absorption of Indulin AT with NaOH as Blank

Figure 5.6 shows Indulin AT has the same absorption curve as Indulin C. Indulin C is the sodium salt of kraft pine lignin, and Indulin AT is the almost sodium-free form of kraft pine lignin. Indulin AT is also completely free of all hemicelluloses. Therefore, it is ideal to be used as a lignin calibration standard. The ash content was measured to get an estimation of the sodium content in Indulin C and Indulin AT. The average ash content of Indulin C is 18.7%, and of Indulin AT only 3.3% (see Table 5.2). This shows that Indulin C contains about 81% lignin while Indulin AT is almost pure. When preparing the UV calibration curves with Indulin AT and Indulin C, all lignin concentrations were corrected for the ash content and the moisture content of the original samples.

Table 5.2 Ash Content of Indulin C and Indulin AT

Test	1	2	3	4	Average
Indulin C Ash (%) at 700 ºC	18.4	17.4	19.9	19.3	**18.7**
Indulin AT Ash (%) at 700 ºC	3.49	3.34	3.22	3.24	**3.32**

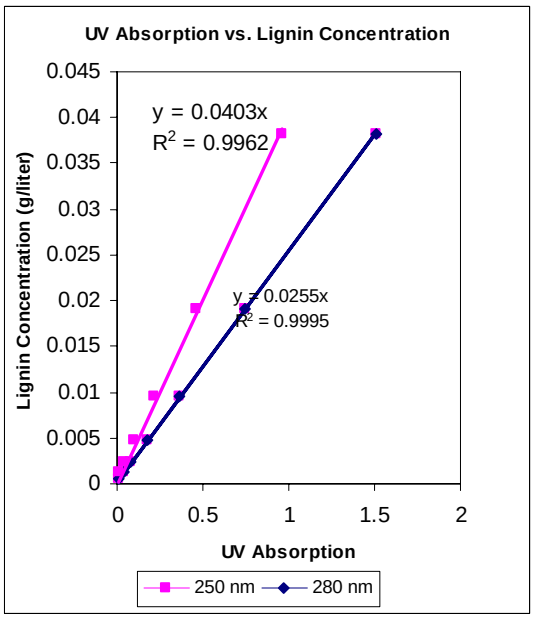

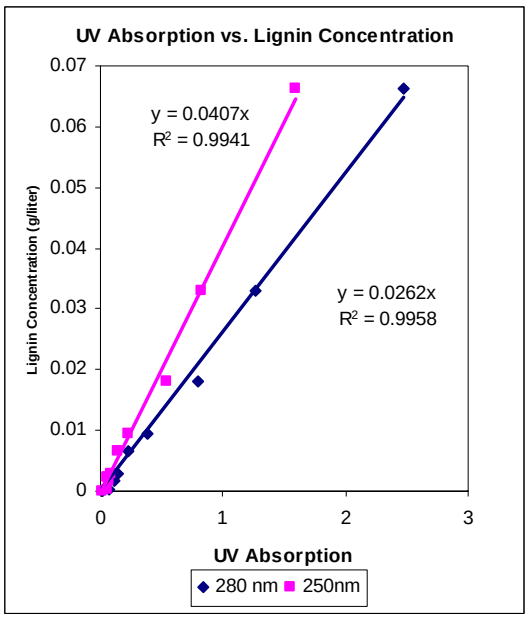

Figure 5.7 Calibration Curve of Indulin AT Figure 5.8 Calibration Curve of Indulin C

Comparison of the calibration curves for Indulin C and Indulin AT with this correction in Figure 5.7 and Figure 5.8 shows that exactly the same calibration curves are obtained. In the present kinetic study, the Indulin AT calibration curve is used to calculate the dissolved lignin concentration during the oxygen delignification experiments.

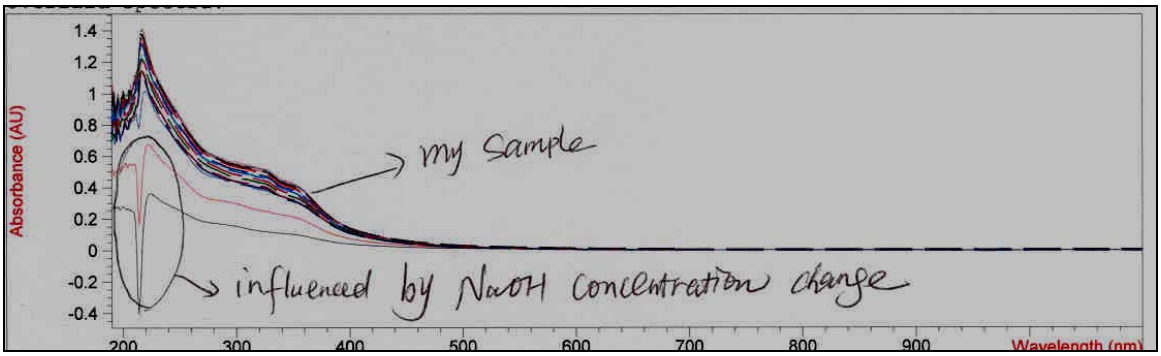

Figure 5.9 The UV Absorption of the Solutions from CSTR

Figure 5.9 shows that the UV-VIS absorption of alkali-soluble lignin in samples taken from a typical CSTR oxygen delignification experiment is similar as that of Indulin AT in Figure 5.6. So, Indulin AT is the proper calibration chemical for this project. Also, seen in Figure 5.9 there are negative absorption values at about 205 nm. These negative peaks are the result of the NaOH concentration change in the first few CSTR samples due to NaOH absorption at 190nm-210nm, when the water in the reactor is being replaced by the NaOH solution. After the reactor is filled with a constant NaOH solution, the negative values disappear. However, since the UV absorption of 280nm is used for this study, the lignin concentrations will not be influenced by the NaOH change. According to the Beer-Lambert Law, the concentration of an unknown compound can be calculated as

$$\text{absorbance} \times k$$

where k is the calibration coefficient of 0.0403 (g/liter)

Thus, the extinction coefficient Ed = 1/k = 24.81. So, the extinction coefficient is 24.81 for Indulin AT.

5.3 Data Reduction Procedure

The dissolved lignin mass balance for the well mixed reactor during time interval, dt, is:

Inflow - Outflow + Dissolved by Reaction = Accumulated in Reactor

or $$0 - \phi_v C(t)dt + r(t)m_p dt = V_r dC(t) \qquad \text{(Equation 5.1)}$$

or $$r(t) = \left[\phi_v C(t) + V_r \frac{dC(t)}{dt} \right] \frac{1}{m_p} \qquad \text{(Equation 5.2)}$$

where r(t) is the rate of delignification (mg lignin/g pulp/min)

Φ_v is the liquid flow rate (ml/min)

C(t) is the dissolved lignin concentration (mg lignin/ml)

V_r is the reactor volume (ml)

m_p is the pulp weight (o.d pulp)

In the previous section, it was shown that the Berty reactor and piping up to the UV-VIS detector could be described by a CSTR of 265 ml and a plug flow volume of 96 ml. This closely agrees with the free volume in the reactor and piping respectively. Therefore, the reactor volume V_r is taken as 265 ml, and the residence time between the Berty reactor and UV detector, t_d, is

$$t_d = \frac{96}{\phi_v} \quad \frac{(\text{ml})}{(\text{ml/min})} \qquad \text{(Equation 5.3)}$$

Thus the dissolved lignin concentration inside the Berty reactor at time t, C(t), is equal to the concentration measured by UV at time $t+t_d$, $C_L(t+t_d)$:

$$C(t) = C_L(t + t_d) \qquad \text{(Equation 5.4)}$$

and

$$r(t) = \frac{\phi_v}{m_p} C_L(t + t_d) + \frac{V_r}{m_p} \frac{dC_L}{dt}\bigg|_{t+t_d} \qquad \text{(Equation 5.5)}$$

The amount of lignin removed from the pulp at time t is:

$$m_L(t) = \phi_v \int_0^{t+t_d} C_L(t)dt + V_r C_L(t + t_d) \qquad \text{(Equation 5.6)}$$

A typical dissolved lignin concentration profile is displayed in Figure 5.1. Application of equation (5) leads to the rate of delignification versus time shown in Figure 5.2.

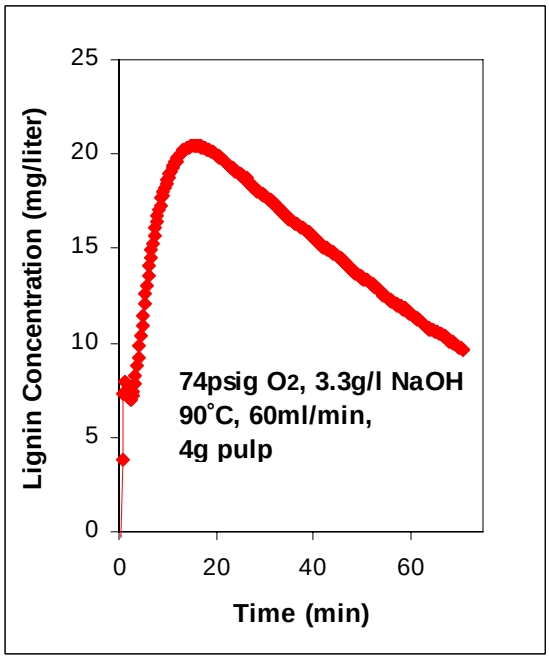

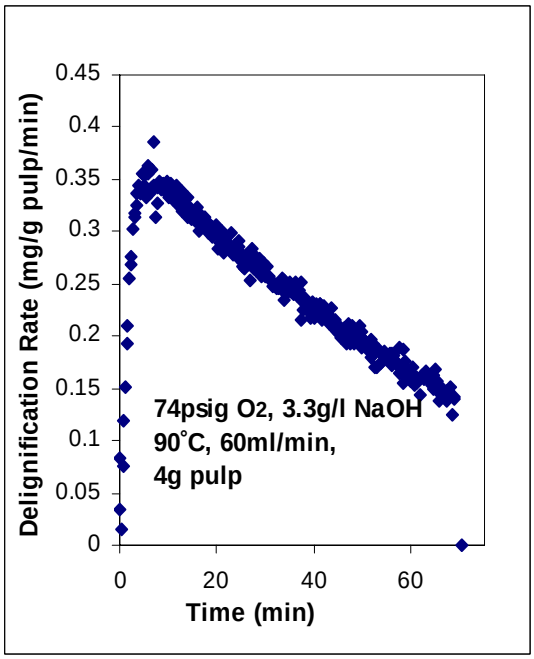

Figure 5.10 Lignin Concentration vs. Time Figure 5.11 Delignification Rate vs. Time

Figure 5.10 shows a finite dissolved lignin concentration at time t = 0 because lignin is leached from the pulp by hot water extraction before the start of the experiment. The

results in Figure 5.11 show a rapid initial increase in delignification rate due to the fact that it takes a few minutes before the water in the reactor is replaced by the oxygenated caustic solution (residence time in Berty reactor is 265/60 = 4 minutes and 25 seconds).

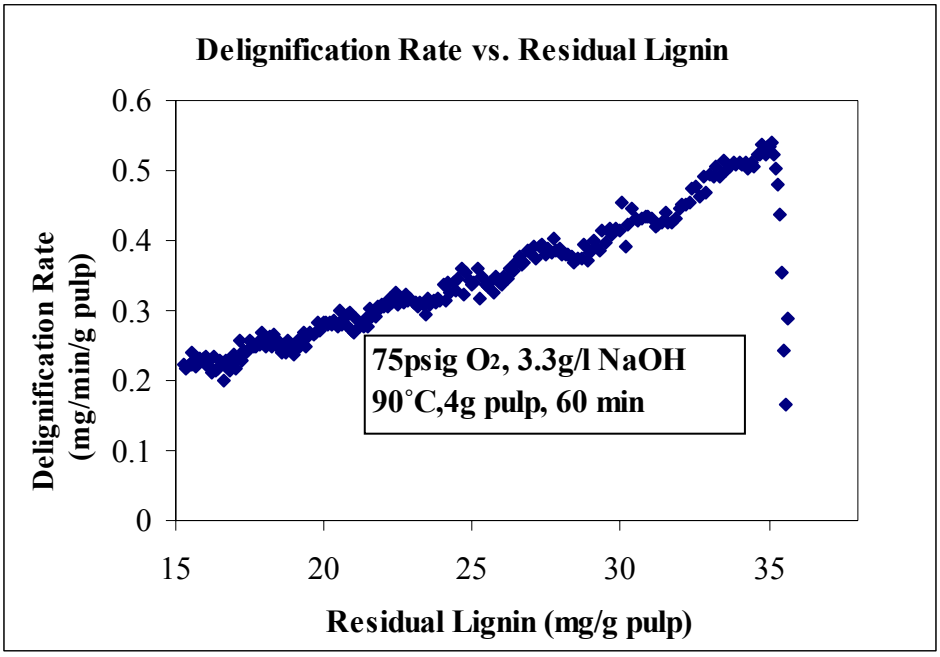

Figure 5.12 Delignification Rate vs. Residual Lignin Amount

Figure 5.12 shows that the delignification rate decreases with the residual lignin amount in a linear fashion. The Residual lignin amount can be calculated by equation 5.7.

$$L_c = \left(Kappa - \frac{HexA}{10} \right) \times 1.5 \qquad \left(\frac{\text{mg lignin}}{\text{g pulp}} \right) \qquad \text{(Equation 5.7)}$$

5.4 Lignin Mass Balance

A lignin mass balance was made by comparison of the lignin removed with the effluent from the reactor with that of the difference in lignin content between the original pulp and that of the pulp after oxygen delignification. For the calculation of lignin removed with the effluent, a correction must be made for the dead time in the tubing. The results

showed that some lignin was extracted from the pulp before the oxygen enters the reactor. Therefore, a hot water extraction was done to determine how much lignin was extracted before the oxygen delignification reaction started. Figure 5.13 shows the UV absorption when the pulp is contacted with hot water.

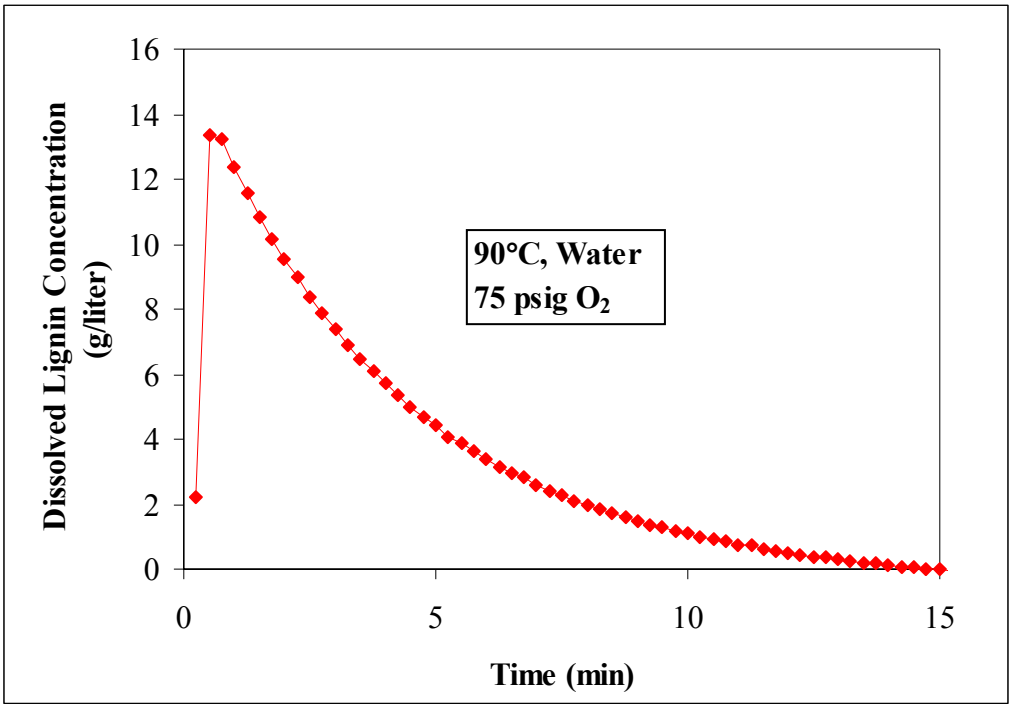

Figure 5.13 Lignin Concentration vs. Time in Hot Water Extration

The area under the curve times the flow rate is equal to the total amount of lignin extracted.

In order to know the total residual lignin amount in the pulp sample, kappa number, Klason lignin and the acid- soluble lignin amount of different oxygen delignified samples were measured. The results in Figure 5.14 show that Klason lignin amount can be represented by 0.16%×kappa number. This is close to the relation of Klason lignin (g) = ΔKappa × 0.15% reported in literature for softwood pulp. The absorption of acid-soluble

lignin was measured by UV-VIS. However, the absorption spectrum is totally different from that of alkaline-soluble lignin showing in Figure 5.15.

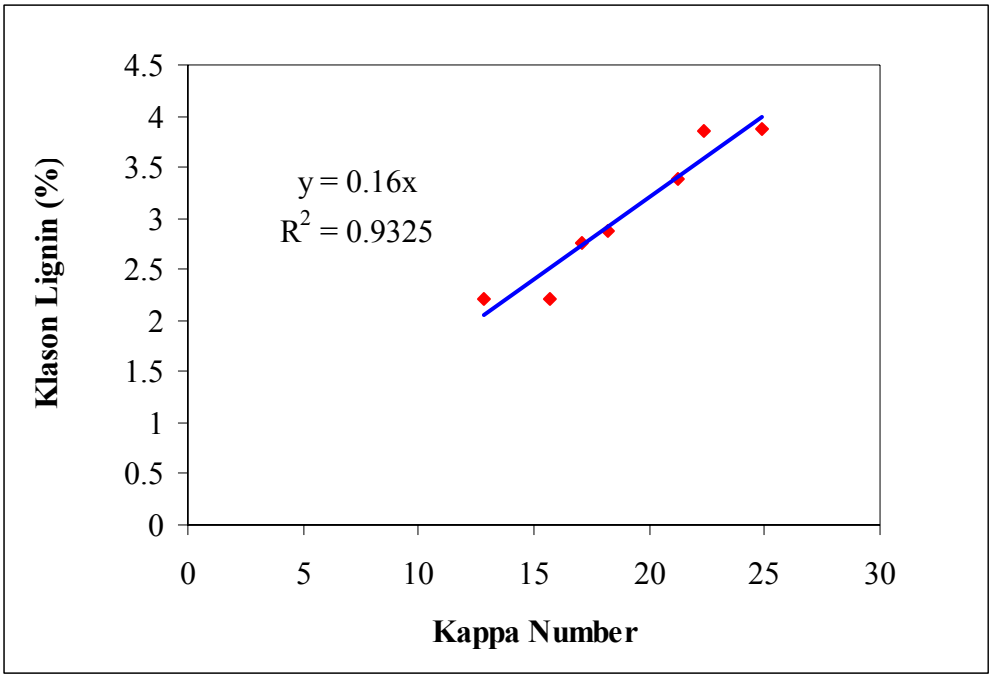

Figure 5.14 Klason Lignin vs. Kappa Number

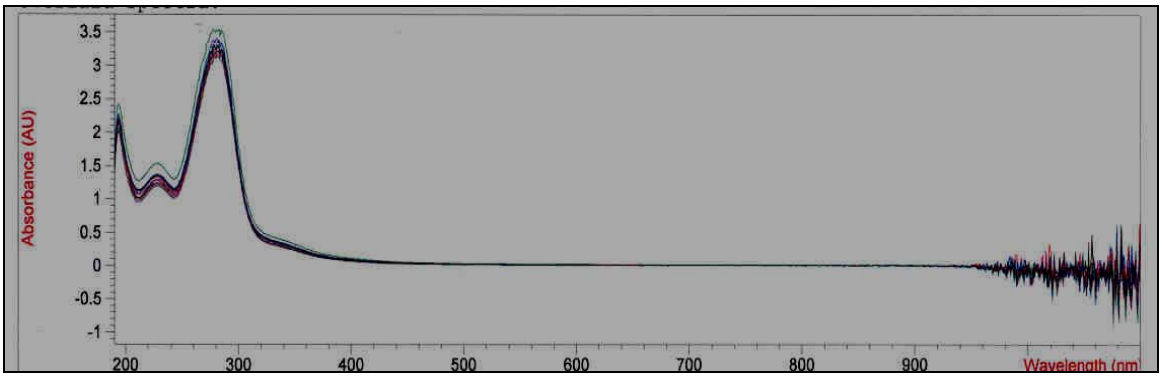

Figure 5.15 UV-Absorption of Acid-Soluble Lignin of Different Samples

According to the laboratory procedure of the University of Maine, the acid soluble lignin is determined from the absorption at 205nm with an extinction coefficient of 110 l/g.cm.

Table 5.3 shows the measured Klason lignin, acid soluble lignin and the UV lignin calculated from the Indulin AT calibration curve based on the presence of 4 grams pulps.

Table 5.3 Measured and Calculated Lignin Results

Kappa	Δkappa	Klason Lignin (%)	Acid-soluble Lignin (%)	Total lignin (%)	Lignin Change (g)	Calculated from Indulin AT (g)
22.41	0	3.873	0.533	4.406	0	0
21.26	1.15	3.383	0.495	3.878	0.021	0.017
18.19	4.22	2.871	0.555	3.426	0.039	0.031
17.12	5.29	2.762	0.462	3.224	0.047	0.040
15.66	6.75	2.214	0.467	2.681	0.069	0.059
12.83	9.58	2.211	0.454	2.665	0.070	0.067

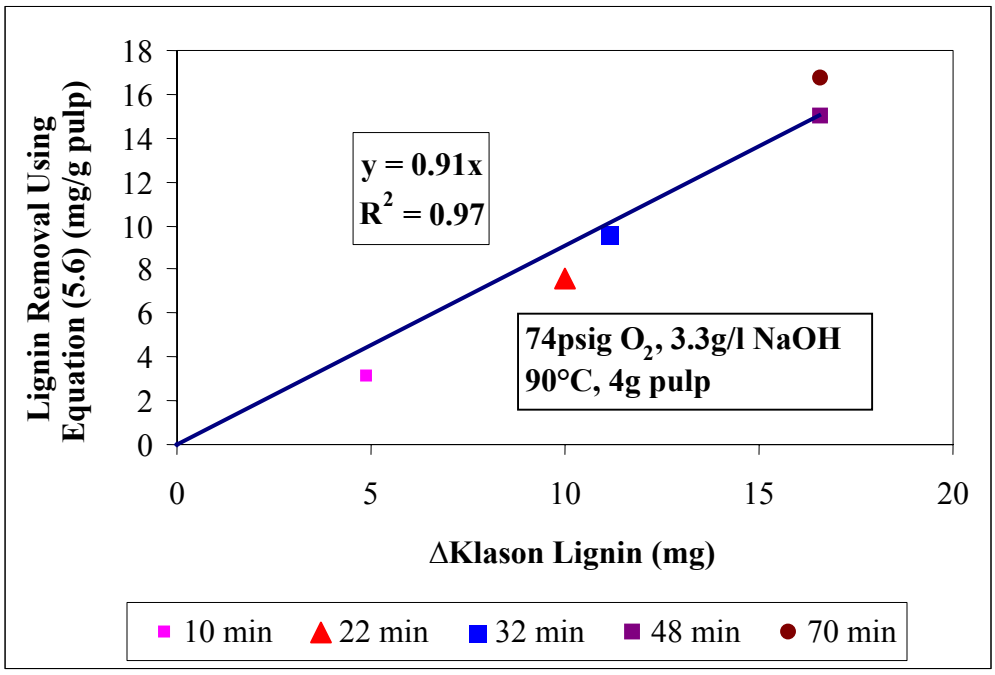

Figure 5.16 Lignin Mass Balance

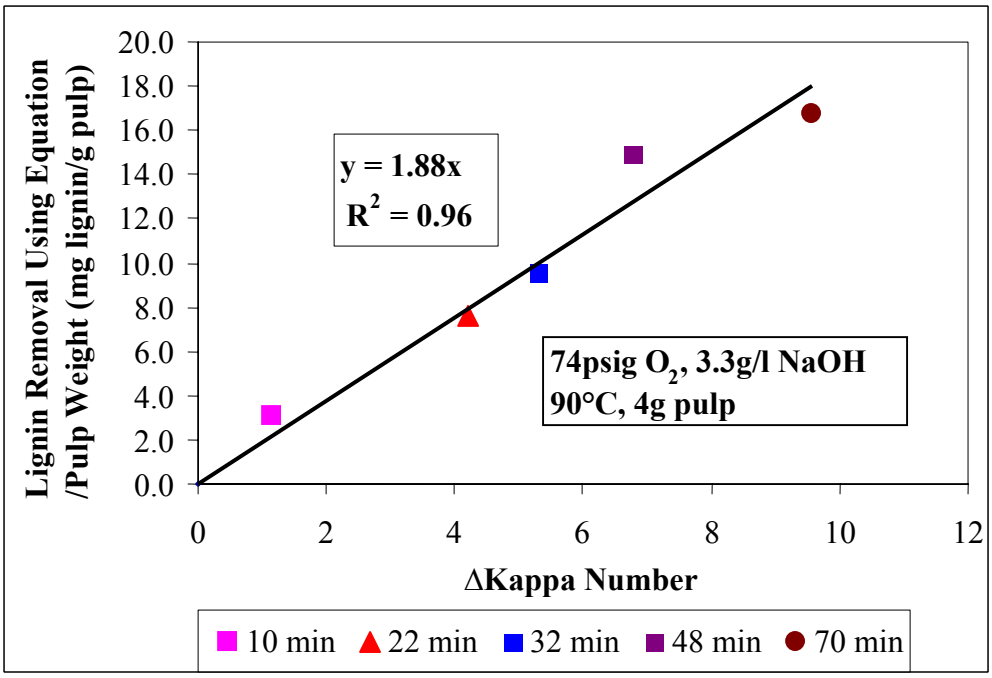

Figure 5.17 Removed Lignin vs. ΔKappa

In Figure 5.16 the amount of lignin removed calculated by equation (5.6) was compared with the difference in Klason lignin content between the original and delignified pulps obtained after different reaction times. The slope of the straight line in Figure 5.16 is 0.91, which is slightly less than 1.0, the value expected if all lignin is represented by Klason lignin. The small difference shows that the lignin mass balance is reasonably closed. Plotted in Figure 5.17 is the amount of removed lignin calculated by equation 5.6 versus change in Kappa number. This figure shows that the removed lignin expressed in % on oven dried pulp is equal to 0.18 × ΔKappa.

Based on those results, the kappa number of the pulps can be calculated by equation 5.8.

$$\text{Final Kappa} = \text{Initial Kappa} - \frac{\text{Removed Lignin}}{0.18\%} \qquad \text{(Equation 5.8)}$$

Table 5.4 Comparison of Measured Kappa and Calculated Kappa

Experiment #1 (24min, 67ml/min)			**Experiment #2 (50min, 50.5ml/min)**		
Mini Kappa	**Mini Kappa**	**Calculated Kappa**	**Mini Kappa**	**Mini Kappa**	**Calculated Kappa**
18.50	18.03	18.53	15.38	14.84	14.96

(The experiments were performed at 90ºC, 76 psig, 3.3g/liter NaOH)

Two experiments were done and the final kappa number was measured and calculated by equation 5.8. The calculated kappa number and the measured kappa number (modified TAPPI method) are very close (see Table 5.4). Thus, it may be concluded that the mass balance is good and equation 5.8 is accurate enough to determine the kappa number during oxygen delignification.

CHAPTER 6

VALIDATION OF BATCH REACTOR AND DIFFERENTIAL CSTR

6.1 Validation of Batch Reactor

The batch reactor operation was validated by showing reproducibility of the results, and by comparison of the data with those obtained in reference studies.

6.1.1 Effect of Stirring Speed on Kappa Number

The influence of stirring speed on this particular unbleached softwood pulp was studied to validate that the batch reactor results were reproducible and free of oxygen mass transfer limitations.

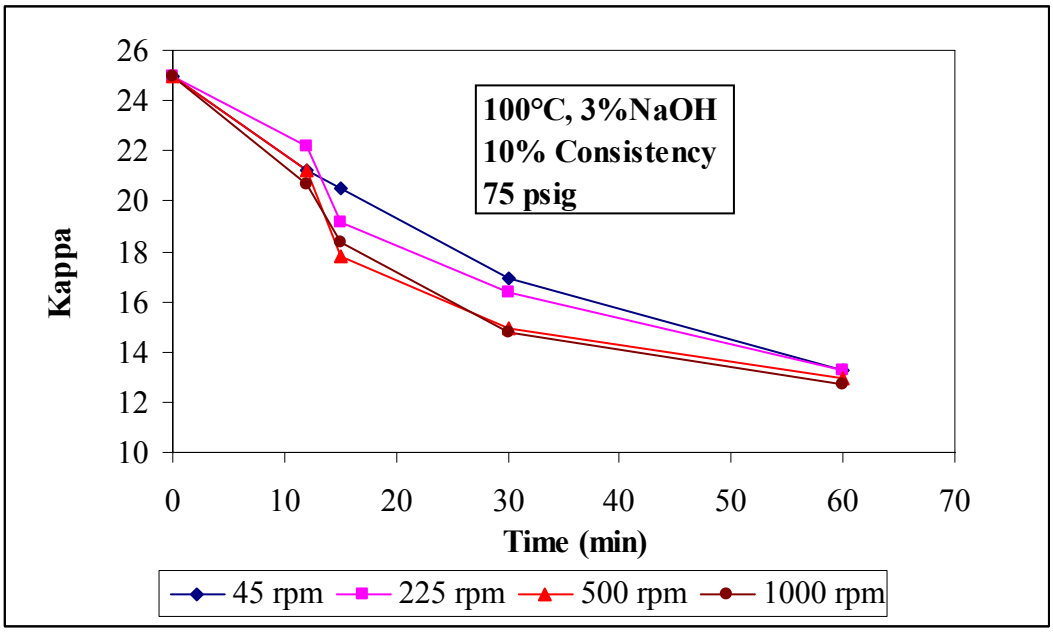

Figure 6.1 Kappa Number vs. Time at Different Stirring Speeds in Batch Reactor

Figure 6.1 shows that when the stirring speed increases from 45 rpm to 225 rpm, the kappa number decreases slightly because of improved mixing. However, the kappa number is not much further reduced when the stirring speed was increased from 225rpm

to 1000rpm, which shows that at this speed, the data is free of oxygen mass transfer limitations, and that the data are reproducible.

6.1.2 Effect of Stirring Speed on Intrinsic Viscosity

Figure 6.2 shows the intrinsic viscosity of oxygen delignified pulps at different stirring speeds. Similar to the kappa number results, the intrinsic viscosity vs. time profiles of the pulps do not change much with different stirring speeds.

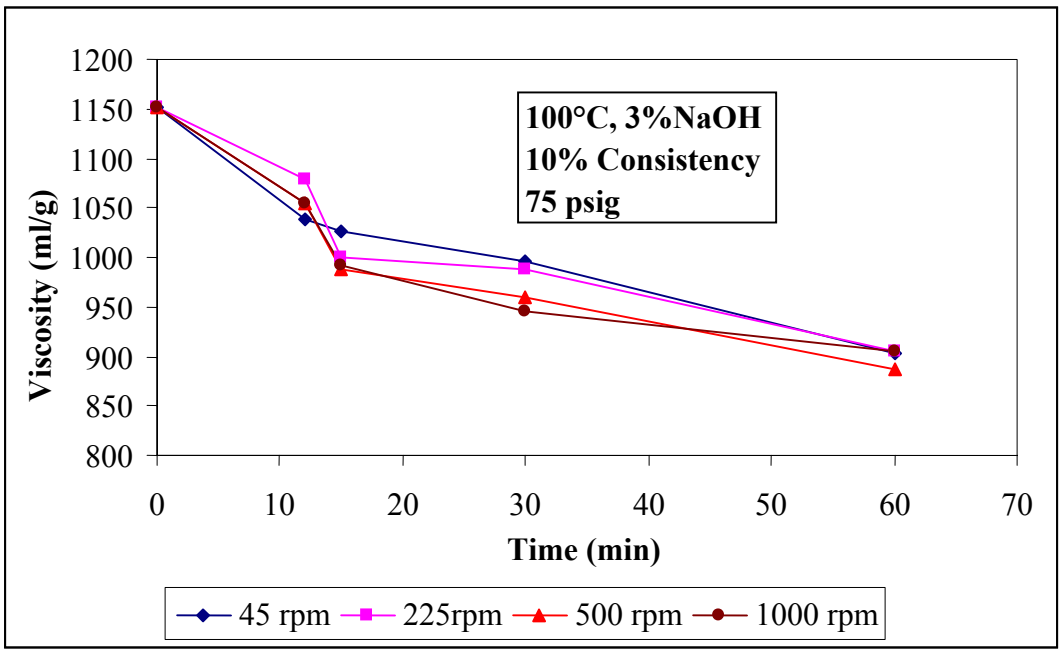

Figure 6.2 Intrinsic Viscosity vs. Time at Different Stirring Speeds in Batch Reactor

6.1.3 Effect of Stirring Speed on Selectivity

Figure 6.3 shows the selectivity of the oxygen delignified pulps at different stirring speeds.

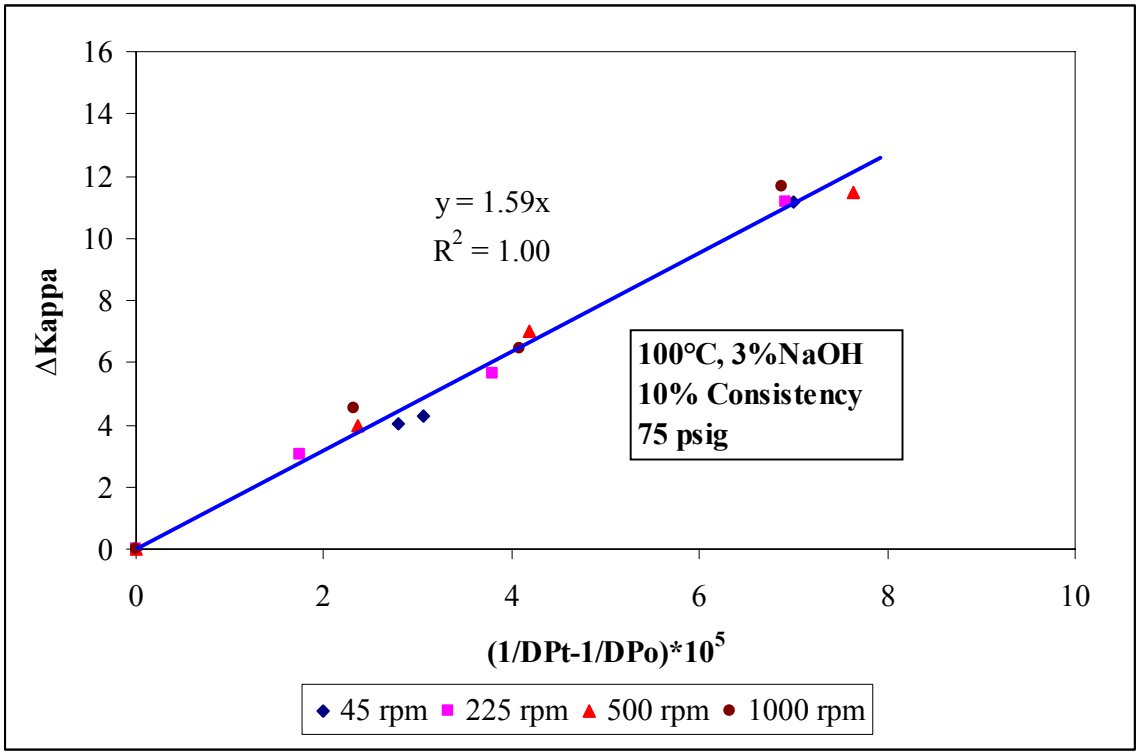

Figure 6.3 Selectivity at Different Stirring Speeds in Batch Reactor

Figure 6.3 clearly shows that the stirring speed does not have a significant effect on the selectivity. Based on these results, all subsequent experiments were performed at a stirring speed of 225rpm.

6.1.4 Effect of Oxygen Pressure on Kappa Number

Figure 6.4 shows the trend of kappa number versus time at different oxygen pressures. A higher pressure results in a larger reduction in kappa number. Most of the kappa number drop occurs during the first 5 minutes, followed by a slower decrease at longer reaction times.

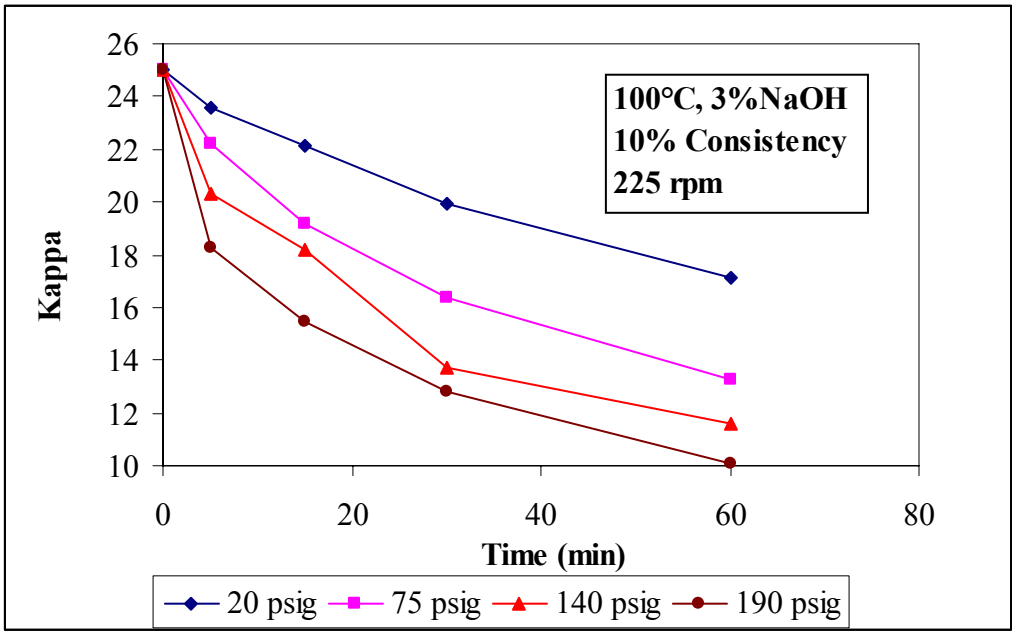

Figure 6.4 Kappa vs. Reaction Time at Different O_2 pressures in Batch Reactor

6.1.5 Effect of Oxygen Pressure on Intrinsic Viscosity

Figure 6.5 shows the trend of intrinsic viscosity versus time at different oxygen pressures.

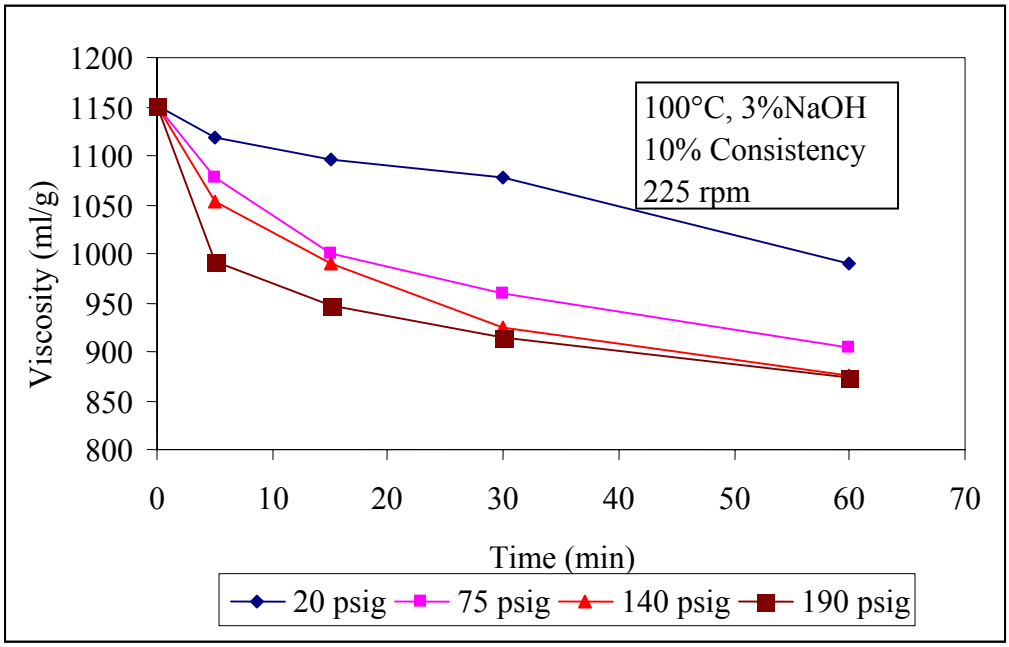

Figure 6.5 Intrinsic Viscosity vs. Time at Different O_2 pressures in Batch Reactor

The intrinsic viscosity decreases more at higher oxygen pressures. The differences in intrinsic viscosity become smaller when the oxygen pressure is higher than 75 psig at longer reaction times.

6.1.6 Effect of Oxygen Pressure on Selectivity

Figure 6.6 shows the selectivity of the softwood oxygen delignification pulps at different pressures.

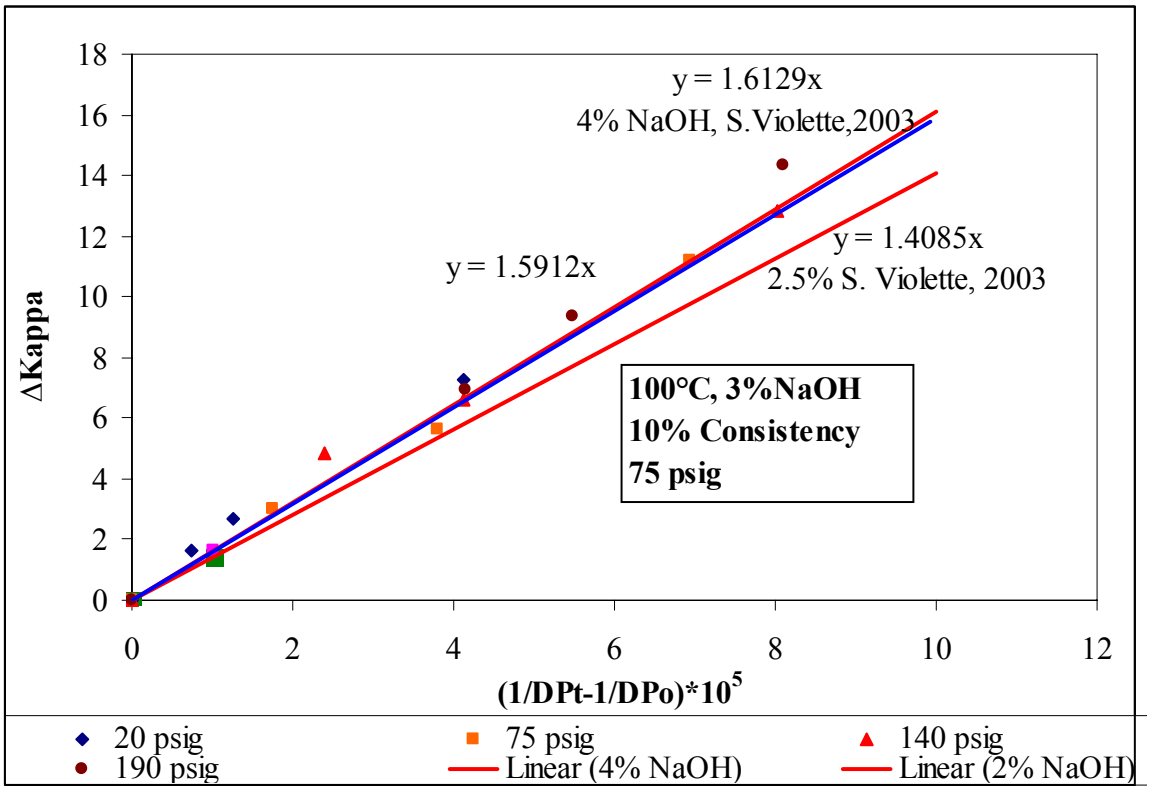

Figure 6.6 Selectivity at Different O_2 Pressures in Batch Reactor

This figure indicates that pressure does not affect the selectivity of oxygen delignification. The two red lines are data published by Violette (2003) obtained from the same reactor but with 2.5% and 4% NaOH. The data at 3% NaOH charge have almost the same selectivity with 4% NaOH showed in Violette's dissertation.

6.1.7 Repeatability of Experiments in Batch Reactor

Several experiments were performed under the same operating conditions (100°C, 75psig, 3% NaOH, 60minutes) to study the repeatability. 30 g of oven dried pulp was used for all the experiments. The kappa number and intrinsic viscosities of the oxygen delignified pulps are shown in Table 6.1. The data show that the repeatability of oxygen delignification experiments in the batch reactor is very good.

Table 6.1 Kappa Number and Intrinsic Viscosity of Pulps for Repeatability

Initial kappa: 30.8, Initial viscosity:1056 (100 °C, 75 psig, 3% NaOH, 60 minutes)	
Kappa	**Viscosity (ml/g)**
16.0	853
15.4	840
15.8	844
16.0	833
16.6	840
16.1	850
16.0 (Average)	**843**
0.3 (Standard Derivation)	**6.7**

6.2 Validation of Differential CSTR

The CSTR operation was validated by showing that the oxygen delignification kinetics were not influenced by the amount of pulp in the reactor, feed flow rate, and rotor speed under the basket.

6.2.1 Effect of Different Stirring Speeds

The results in Figure 6.7 show that at stirring speeds of 200 rpm or higher, the oxygen delignification profile is independent of rotor speed. A rotor speed of 400 rpm was adopted as the normal operating condition.

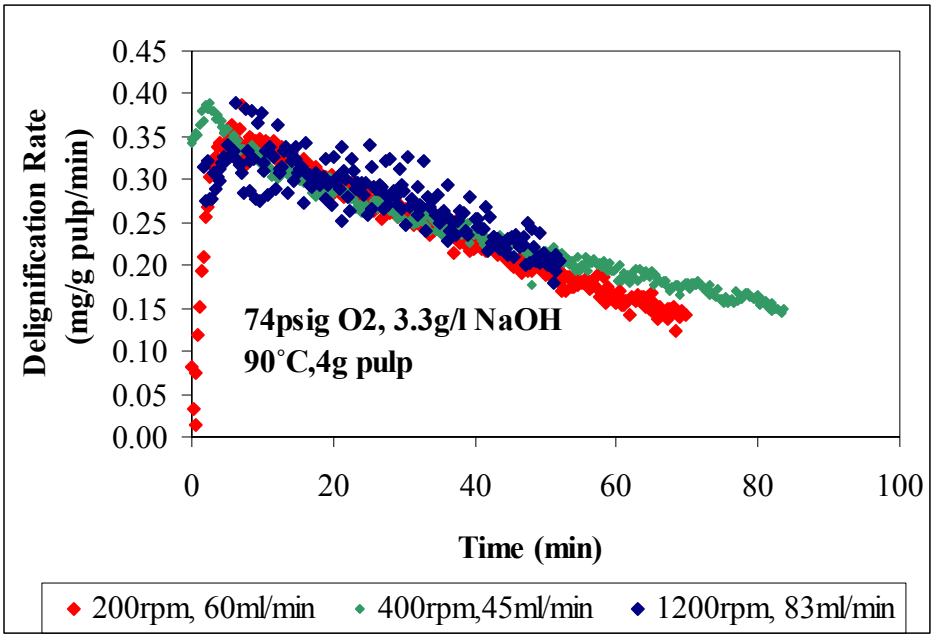

Figure 6.7 Effect of Different Stirring Speeds

6.2.2 Effect of Different Flow Rates

The effect of flow rate is seen in Figure 6.8. It shows that the delignification rate is not affected by the flow rate. Because of the size of the feed tank (3 gallon total volume), a flow rate of 75 ml/min was adopted for the rest of the experiments.

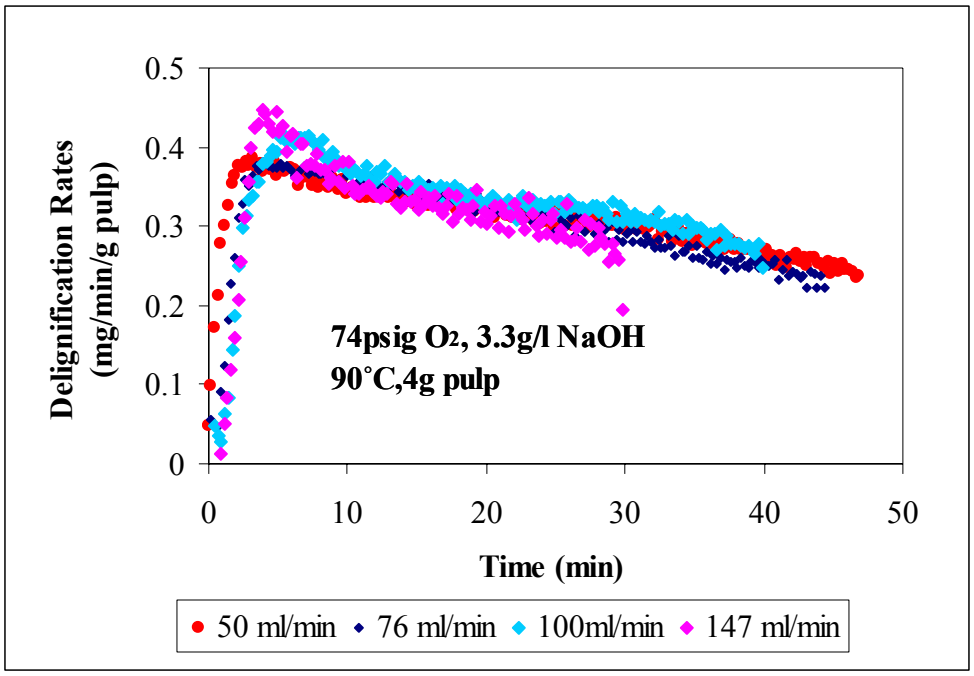

Figure 6.8 Effect of Different Flow Rates

6.2.3 Effect of Different Pulp Sample Weights in the Berty Basket

Shown in Figure 6.9 is the effect of pulp weight on the delignification rate. The close agreement of the three results confirms that the experimental method and procedures are sound and reproducible. Because of analysis requirements most experiments were performed with 4 grams (oven dry basis) of pulp.

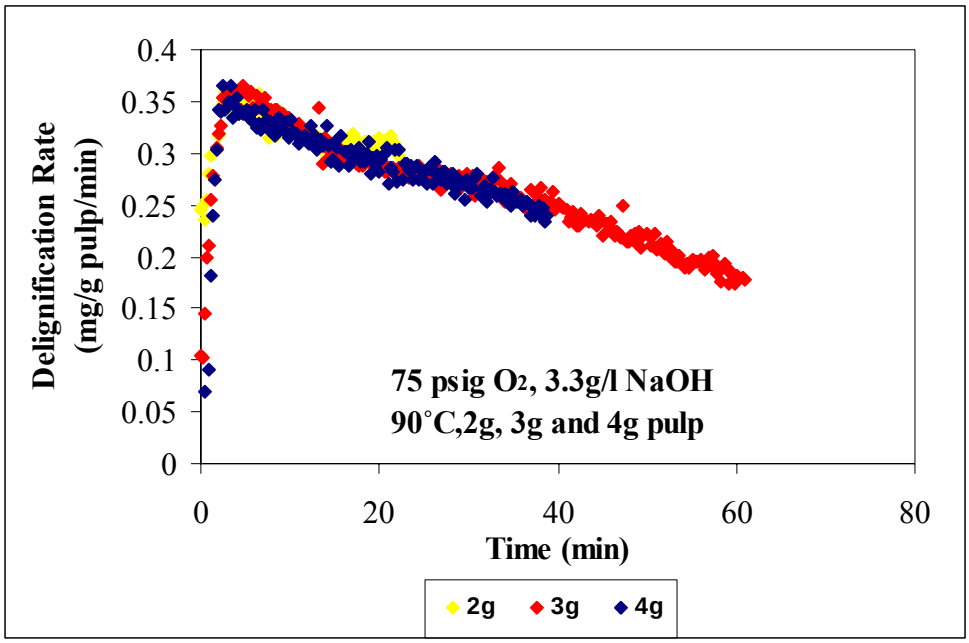

Figure 6.9 Effect of Pulp Sample Weight on Delignification Rate

6.2.4 Effect of Different Initial Conditions

If the reactor is initially filled with caustic of the same concentration as that of the feed, then there would be no initial transient in the NaOH concentration. However, some lignin would be extracted from the pulp by NaOH during the heating period prior to starting the actual experiment. Therefore, it was tested how the delignification rate was affected by the initital conditions in the reactor, i.e. filled with pure water or NaOH solution.

Three experiments were performed with the reactor initially filled with non-oxygenated NaOH or filled with water. In two experiments, the heating time of the reactor to the desired temperature was about 2 hours. The third experiment was performed with water in the reactor, but the preheating time increased to 10 hours.

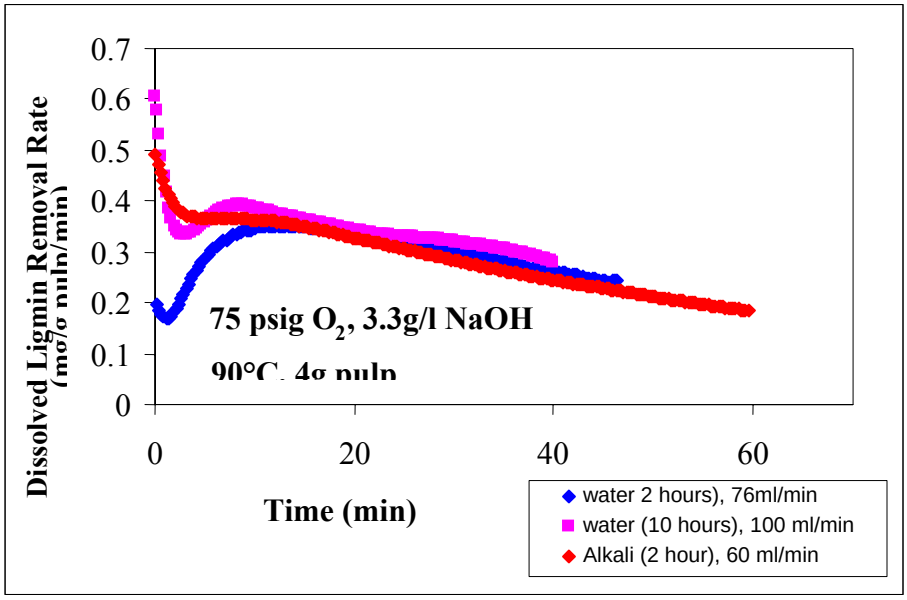

Figure 6.10 Effect of Initial Condition; Dissolved Lignin Removal Rate versus Time

Shown in Figure 6.10 is the dissolved lignin removal rate versus time. The dissolved lignin removal rate is calculated as the product of the measured lignin concentration in the CSTR effluent and the flow rate divided by the amount of pulp in the basket. The dissolved lignin removal rate is different from the delignification rate because it does not correct for the accumulation of dissolved lignin in the reactor. It can be seen in Figure 6.10 that the experiments with NaOH at 2 hours preheating and with water at 10 hours preheating lead to a similar pre-extraction behavior of lignin from the pulp. In contrast, only a small amount of lignin is pre-extracted with water after 2 hours preheating.

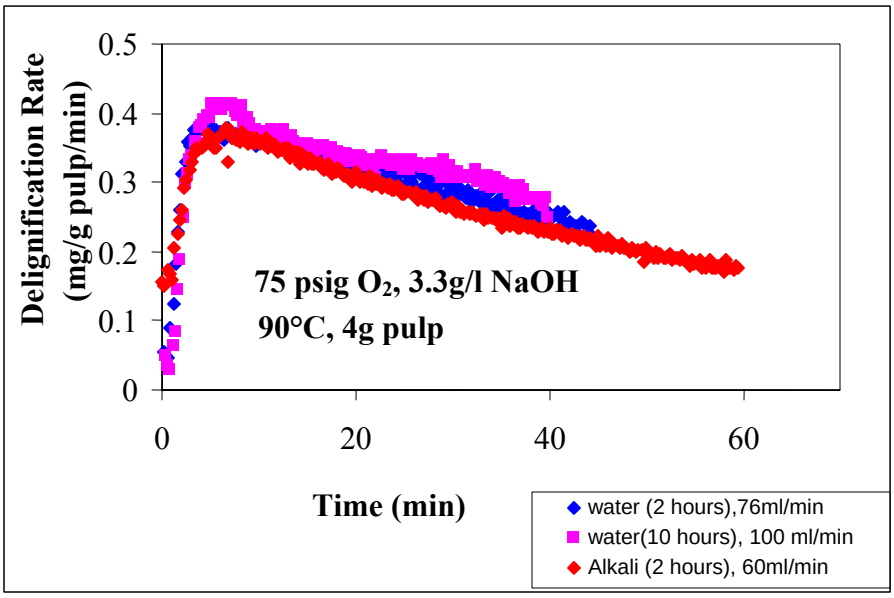

Figure 6.11 Effect of Initial Condition; Delignification Rate versus. Time

Figure 6.11 shows the oxygen delignification rates as calculated using equation (5.5), which corrects for the lignin accumulation in the reactor and the residence time distribution in the reactor and piping. Contrary to the results in Figure 6.10, it can be seen that the delignification rate for the three different initial conditions are very similar. This implies that the pre-extraction has no significant effect on the delignification rate. It can also be seen that the maximum delignification rate is reached at about 7 minutes. This shows that oxygen is needed for the delignification to proceed, irrespectively whether the reactor is initially filled with water or caustic. For this reason, as well as experimental simplicity, the reactor was filled with water in all other kinetic experiments. The pre-extraction of lignin from pulp at alkaline conditions or at high temperature in water after 10 hours may be the result of "peeling delignification" or just lignin leaching.

6.3 Data Repeatability of CSTR

Experiments were performed at the same operating conditions, but different reaction times to test the reproducibility of the system. The results in figure 6.12 show that the reproducibility is acceptable.

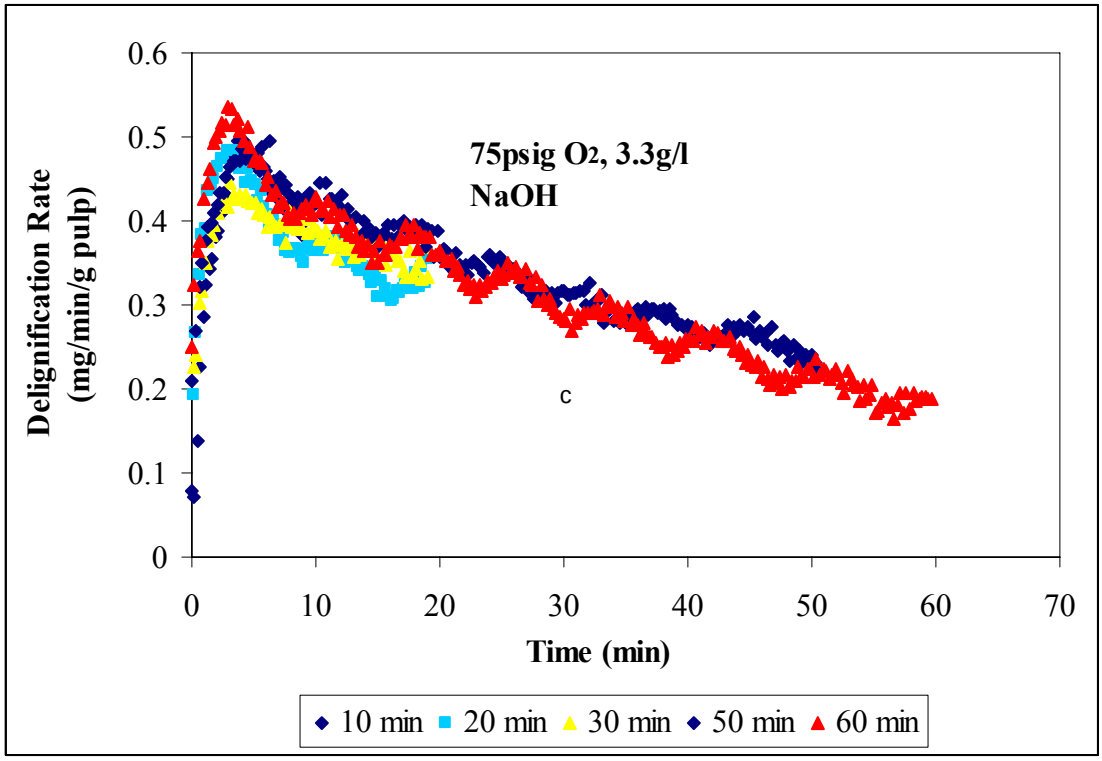

Figure 6.12 Experiment Reproducibility

In addition, two sets experiments were done at exactly the same conditions: 75 psig, 3.3 g/l NaOH, 90ºC, 4 g pulp and 60 minutes reaction time. Figure 6.13 shows that the delignification rates obtained in the two sets of experiments are very close. Some of the differences are due to the characteristics of the temperature controller. The temperature controller can control temperature within ±2 ºC. As will be shown later the activation energy of oxygen delignification is 46.5 KJ/mol. At 90°C, this activation energy leads to a change of ±8% in the delignification rate when the temperature is changed by ±2 ºC.

This explains the "wavy" character of the delignification rate which closely follows the temperature in the CSTR. It also means that small differences in the final reactor temperature lead to significant changes in delignification rate. However, from the results in Figure 6.14, it may be concluded that the CSTR produces reproducible data and is well suited to study the kinetics of oxygen delignification.

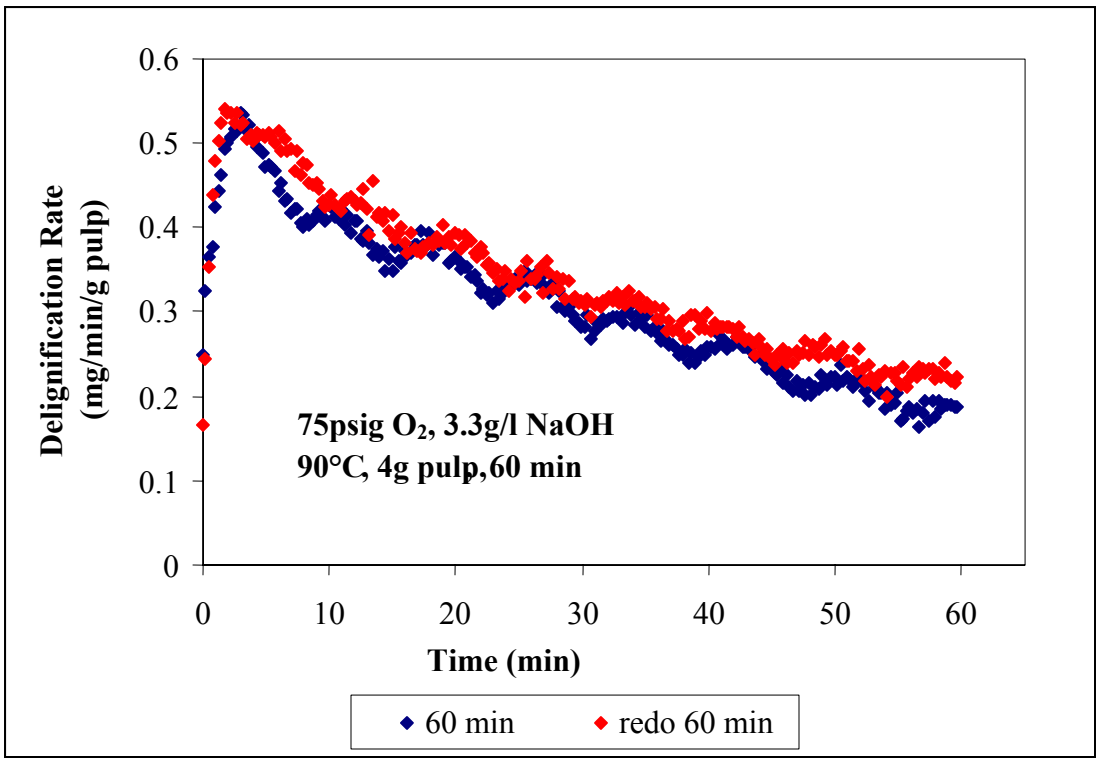

Figure 6.13 Experiment Repeatability

6.4 Comparison of Kappa Number Predicted from Dissolved Lignin Concentration with Measured Kappa Number

$$\text{Kappa} = \text{Initial Kappa} - \frac{\phi_v \int_0^{t+t_d} C_L(t)dt + V_r C_L(t+t_d)}{1.5} \qquad \text{(Equation 6.1)}$$

The kappa numbers calculated by equation 6.1 and the corresponding experimentally measured values for the different operating conditions of the CSTR are listed in Table 6.2.

Table 6.2 Measured Kappa Number and Calculated Kappa

Temperature (°C)	Total Pressure (psig)	NaOH (g/liter)	Measured Kappa	Calculated Kappa (by equation 6.1)
81	75	3.3	14.9	14.8
91	75	3.3	12.5	12.5
100	75	3.3	10.8	9.2
112	75	3.3	6.7	4.0
117	75	3.3	5.5	2.6
90	35	3.3	14.4	14.7
90	55	3.3	13.1	15.2
93	95	3.3	11.0	11.1
89	75	1.1	16.3	17.0
93	75	5.5	10.9	10.1
93	75	7.7	9.4	7.7
90	75	20	8.1	5.0
89	75	50	5.1	4.8

It can be seen that the calculated kappa numbers are very close to the measured kappa numbers for the experiments similar to industrial operating conditions. However, the calculated kappa numbers are lower than the experimental data at 110°C, 115°C, 20g/l and 50g/l. This may be explained by severe carbohydrate degradation at those operating conditions, which produces products which contribute to UV absorption at 280nm. For example, furfural has a very strong absorption peak at 280nm. To test the effect of carbohydrate degradation on the dissolved lignin concentration measurement, an experiment was performed at the relatively severe operating conditions of 100°C, 7.7g/l NaOH, 90 psig total pressure, for an extended reaction time of 6 hours. The delignification rate versus HexA-free residual lignin is plotted in Figure 6.14.

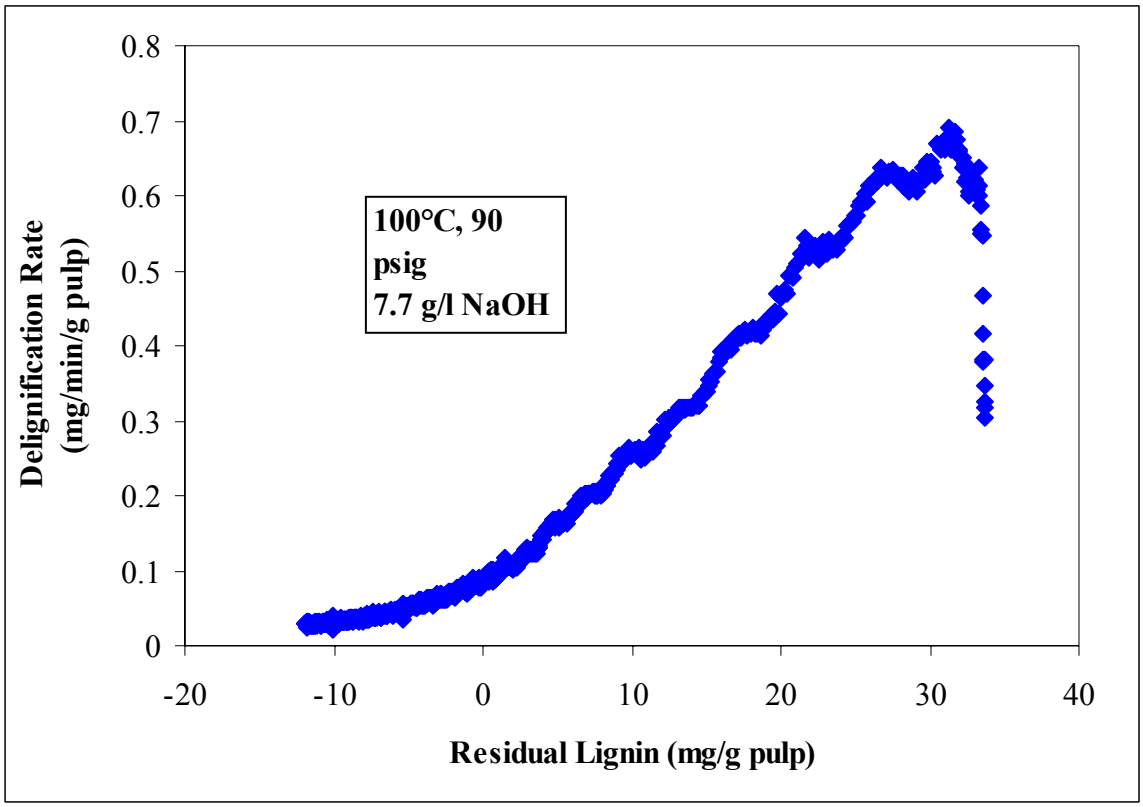

Figure 6.14 Delignification Rate vs. Residual Lignin of 6 Hours O_2 Delignification

Figure 6.14 shows that the HexA-free residual lignin calculated using equation (9.7) goes to negative numbers after 6 hours reaction which shows that the lignin concentration determined from UV absorption at 280nm wavelength leads to an overprediction of the amount of lignin removed after 6 hours. Initially the delignification rate decreases linearly with residual lignin content. However, below a residual lignin content of about 5mg/g pulp, the rate derates from the linear behavior indicating that the UV absorption-lignin concentration calibration curve was not valid. The carbohydrate loss of the final pulp sample is very large; (100-84.5)-(24.4-3.7)×0.15=12.4%. This gives further support that at low kappa numbers the carbohydrate losses contributes significantly to UV absorption relative to that of the low dissolved lignin concentration.

Table 6.3 Pulp Properties of 6 Hours O_2 Delignification Compared with Original Pulp

Samples	Kappa Number	Intrinsic Viscosity (g/ml)	Yield (%)	HexA (µmol/g pulp)
Original Pulp	24.4±0.5	1089±20	100	25.1±1
6 hours O_2 delig.	3.7±0.5	215±20	84.5	20.2±1

In Table 6.3, the pulp properties of the 6 hour O_2 delignified pulp compared with the original pulp are listed. The kappa number drops to 3.7 from 24.4 where 2 kappa units represent the contribution from HexA in the pulp. The intrinsic viscosity is only 215 after 6 hours reaction. The data also indicates that it is very hard to remove all residual lignin from the softwood pulp, even after 6 hours reaction under 100°C, 90psig and 7.7g/l NaOH.

6.5 Conclusion

Both the batch reactor and differentially operated CSTR reactor were shown to give reproducible oxygen delignification data representing pure chemical kinetics. The data obtained in the batch reactor compared well with reference studies. The differentially operated CSTR set-up is well suited to measure rate data of oxygen delignification.

CHAPTER 7

COMPARISON OF OXYGEN DELIGNIFIED PULPS IN THE BATCH AND CSTR REACTORS

7.1 Introduction

Many researchers have performed kinetics studies of oxygen delignification in batch reactors (see chapter 3). Since the NaOH concentration is changing in a batch reactor due to acid products formed in the reaction process, it is difficult to obtain real kinetic data. To investigate the difference between the kinetic data obtained in a CSTR and batch reactor, a few oxygen delignification experiments were performed in both reactors at similar operating conditions. The conditions for the batch reactor are: 90°C, 75 psig, 10% consistency, 3% NaOH and 20 g o.d pulp. The similar conditions for the CSTR are: 90°C, 75 psig and a flow of 3.3 g/l NaOH fed continuously to 4 g o.d pulp in the Berty basket. In the previous chapter it was shown that the pulp mass in the CSTR does not affect the rate of the delignification. The concentration of 3.3g/l NaOH was chosen to obtain the same initial NaOH concentration as in the batch reactor, i.e. $0.03\times20/(0.9\times0.2)\times1000=3.3$g/l.

7.2 Results and Discussion

7.2.1 Extraction by NaOH under an Atmosphere of Nitrogen

Table 7.1 shows the kappa number and intrinsic viscosity after alkali extraction under an atmosphere of N_2 gas for both batch reactor and CSTR. The data show that the kappa number drop 2.5 units during alkali extraction under nitrogen in the batch reactor after 60 minutes. The biggest drop in kappa number occurs during the first 5 minutes. The kappa

number change is very small after 15 minutes reaction. A similar kappa number drop of about 2.3 units is obtained after 40 minutes in the CSTR. However, the kappa number drop increases to almost 4 at 75 minutes and remains the same at 140 minutes. The intrinsic viscosity of the CSTR samples is slightly lower than that of batch reactor samples. The results show that alkali by itself can remove a small fraction of the residual lignin, especially in the beginning of oxygen delignification. However, at the same time it shows that oxygen is necessary to achieve significant delignification. The slightly larger drop in intrinsic viscosity and kappa number in the CSTR suggests that the constant high NaOH concentration in the CSTR is responsible for this behavior. The increased lignin removal may be explained by increased peeling delignification. However, peeling delignification does not explain the decrease in intrinsic viscosity.

Table 7.1 Kappa Number and Viscosity after Alkali Extraction

Batch Reactor (3% NaOH, 90°C, 75 psig, 10%Consistency)			**CSTR (3.3g/l NaOH, 75psig, 90°C, 4g pulp)**		
Sample	**Kappa**	**Viscosity (ml/g)**	**Sample**	**Kappa**	**Viscosity (ml/g)**
original	24.4	1189	**original**	24.4	1189
5 min	22.7	1152	**40 min**	22.1	1130
15 min	22.3	1150	**75 min**	20.5	1096
60 min	21.9	1149	**140 min**	20.5	1093

7.2.2 Kappa Number vs. Time

Table 7.2 shows the kappa number, intrinsic viscosity and yield of oxygen delignified pulps obtained in both CSTR and batch reactor under the same reaction conditions.

Table 7.2 Kappa Number, Viscosity and Yield of Oxygen Delignified Pulps

Sample	Batch Reactor(3% NaOH, 90°C, 75 psig, 10%Consistency)			CSTR (3.3g/l NaOH, 75psig, 90°C, 4g pulp)		
O_2 Delig time, t (min)	Kappa	Intrinsic Viscosity, η (ml/g)	Yield (%)	Kappa	Intrinsic Viscosity, η (ml/g)	Yield (%)
0	24.4	1189	100	24.4	1189	100
10	20.8	1058	98.1	20.1	1079	98
20	18.5	1011	97.6	18.5	1033	96.5
40	15.0	924	96.6	14.3	877	96.0
60	13.5	898	96.0	12.7	828	95.4
180	10.1	829	95.8	7.6	592	92.5

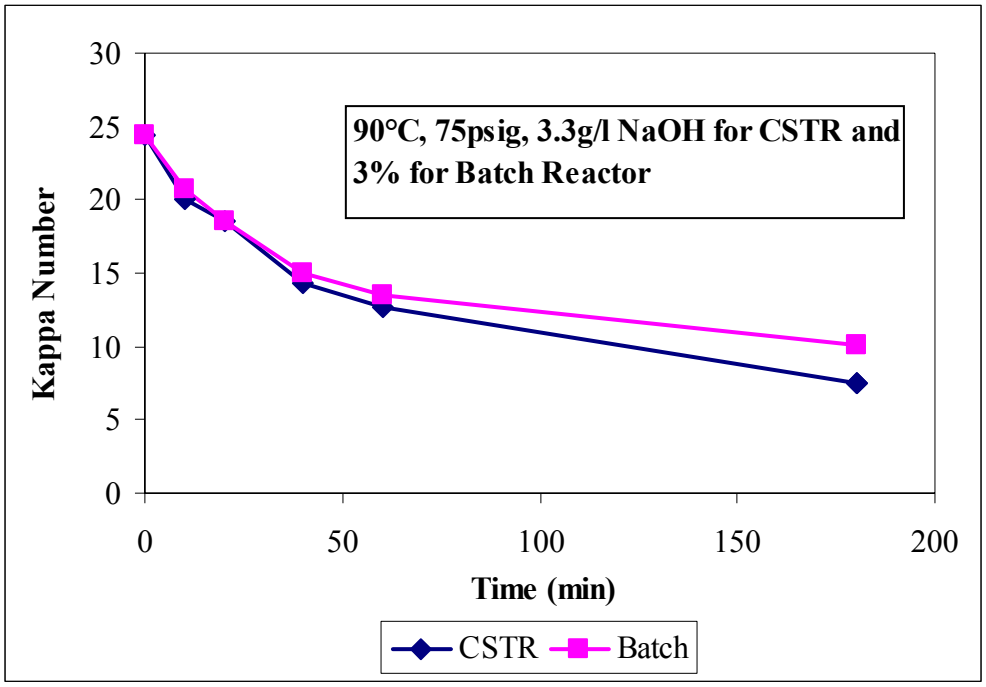

Figure 7.1 Kappa Number vs. Time in CSTR and Batch Reactor

Figure 7.1 shows the kappa number vs. time for the CSTR and batch reactor samples. The kappa numbers of the CSTR and batch reactor samples are almost the same during the first 30 minutes. The CSTR kappa numbers are lower than that of the batch reactor after 40 minutes. At 180 minutes reaction, the CSTR sample has a 3 points lower kappa

number. The main difference between these two sets of experiments is the caustic concentration; it decreases rapidly in the batch reactor and remains unchanged in the CSTR.

7.2.3 Viscosity vs. Time

In Figure 7.2, the intrinsic viscosity vs. reaction time of CSTR and batch reactor samples is shown.

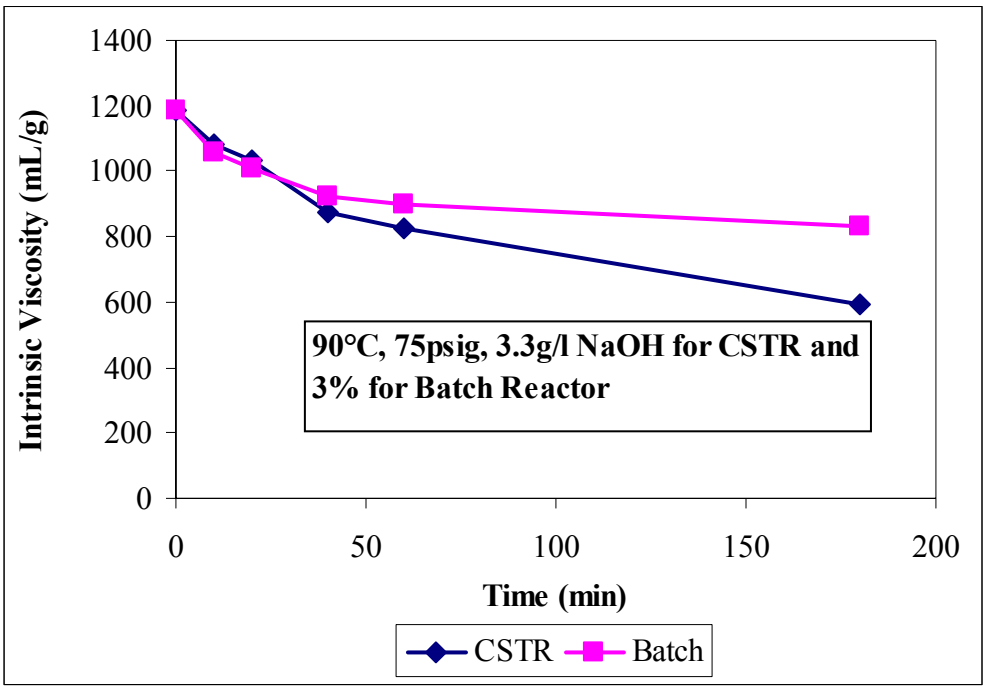

Figure 7.2 Intrinsic Viscosity vs. Time in CSTR and Batch Reactor

Similar to the kappa number result, the intrinsic viscosities of the CSTR and batch reactor samples are almost the same during the first 30 minutes. However, the CSTR samples have a lower viscosity after 40 minutes reaction. The difference after 180 minutes of reaction is 230 ml/g.

7.2.4 Selectivity Coefficient of Oxygen Delignification

Shown in Figure 7.3 is the kappa number change plotted versus cellulose cleavages per glucose unit calculated as $1/DP_t$-$1/DP_0$.

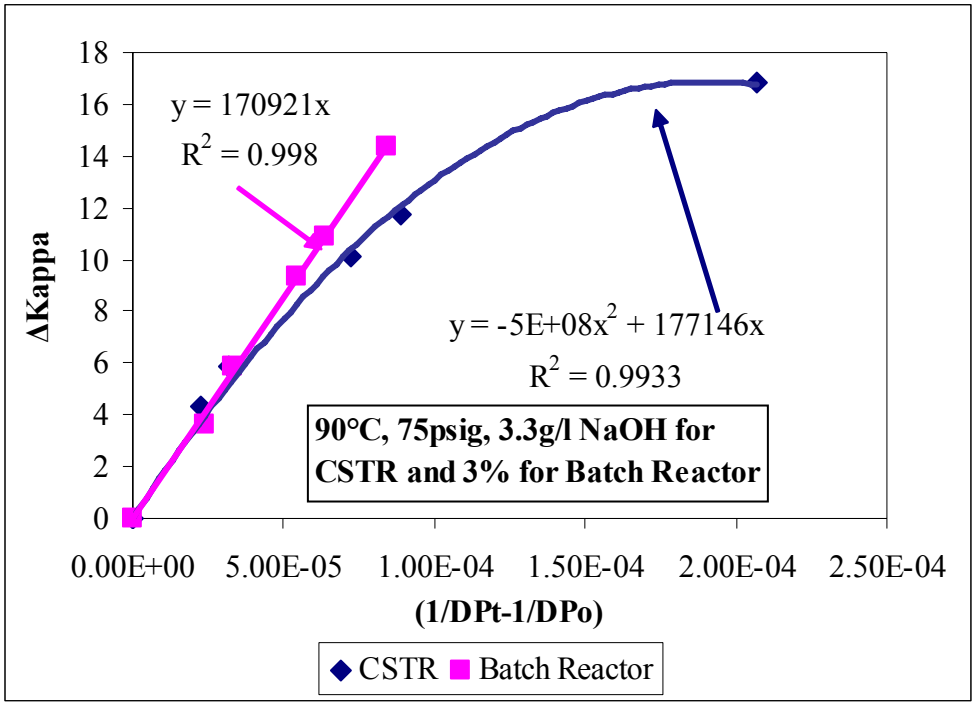

Figure 7.3 ΔKappa vs. (1/DP-1/DP0) of CSTR and Batch Reactor

The DP of cellulose is calculated using equation (7.1). This formula considers the actual weight of cellulose rather than the pulp weight being responsible for the viscosity, and makes a correction for the small contribution of the hemicelluloses to the pulp intrinsic viscosity (Da Silva Perez, 2002).

$$\text{DP of Cellulose} = \left(\frac{1.65[\eta] - 116H}{G} \right)^{1.111} \qquad \text{(Equation 7.1)}$$

where [η] is intrinsic viscosity of the pulp in cm^3/g

G and H are the mass fractions of cellulose and hemicelulose in the pulp (see Table 7.3)

It can be seen that a linear relationship is obtained for the batch reactor data, while the change in kappa number decreases with increasing number of cellulose cleavages for the pulps in the CSTR. This indicates that the delignification-cellulose selectivity remains constant in the batch reactor while it decreases in the CSTR. The explanation for this behavior is that the cellulose degradation is caused by radical species, the formation of which are proportional to the degree of delignification (Violette, 2003). However, the decrease in selectivity in the CSTR suggests that there is an additional cellulose degradation mechanism which becomes important when the caustic concentration remains high for a long period of time. This suggests that alkaline hydrolysis of cellulose may be significant in the CSTR where the fibers are continuously exposed to a constant high alkaline concentration. This will be further addressed in Chapter 9.

7.2.5 Reducing Ends Content of Pulps

Figure 7.4 shows the reducing ends content of pulps in CSTR and batch reactors.

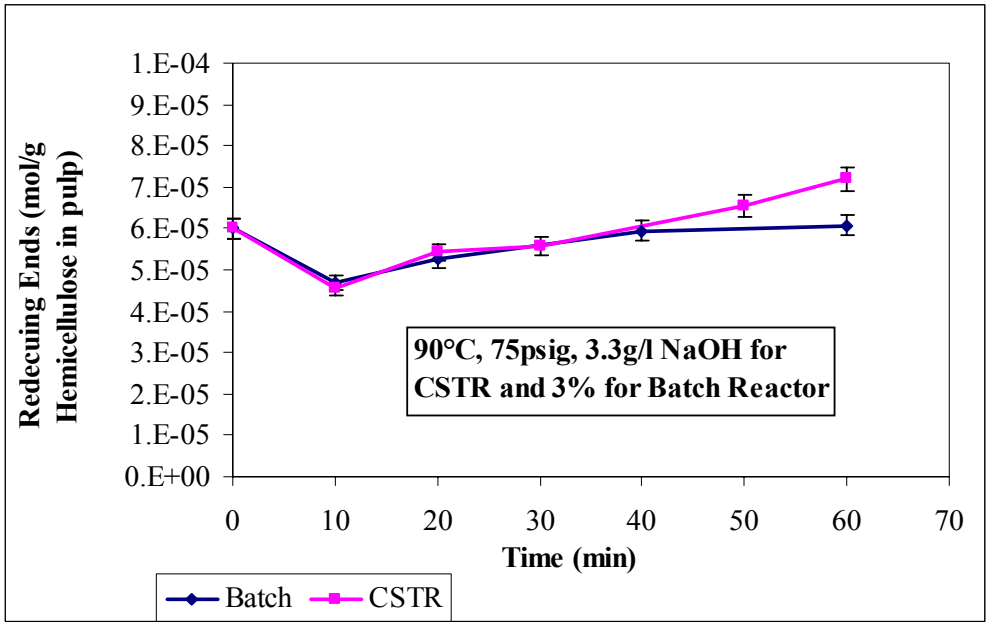

Figure 7.4 Reducing Ends Content of Pulps vs. Time in CSTR and Batch Reactor

The content of reducing ends of the pulps in Figure 7.4 show no difference between CSTR and batch reactor during the first 40 minutes of reaction. The reducing end content initially decreases, and then it increases with reaction time. The initial decrease in reducing end content may be explained by "peeling" and/or oxidation of the carbohydrates. The subsequent increase in content of reducing ends may be caused by radical attack which leads to the formation of new reducing ends. Theoretically, reducing ends may be present in hemicelluloses, as well as cellulose. If we assume that the contribution of reducing ends associated with cellulose are negligible due to cellulose's much higher DP , it is possible to calculate the DP of hemicelluloses in the pulps by equation 7.2. Table 7.3 shows the calculated DP of hemicelluloses in different oxygen delignified pulps. The DP of cellulose calculated using equation (7.1) is also included in Table 7.3.

$$\text{DP of Hemicellulose} = \frac{1}{C_{\text{Recucing End}} \times H \times 162} \qquad \text{(Equation 7.2)}$$

where, H is the mass fraction of hemicelulose in the pulp and $C_{\text{reducing end}}$ is the reducing end content of the pulps in mol/g pulp.

Table 7.3 Cellulose and Hemicelulose Content, and Their DP

O_2 Delig time, t (min)	**Cellulose, G (g/g od pulp)**		**Hemicellulose, H (g/g od pulp)**		**DP of Cellulose**		**DP of Hemicellulose**	
	Batch	CSTR	Batch	CSTR	Batch	CSTR	Batch	CSTR
0	0.714	0.714	0.142	0.142	6561	6561	103	103
10	0.723	0.732	0.139	0.139	5674	5724	132	135
20	0.723	0.734	0.138	0.142	5394	5435	118	114
40	0.729	0.746	0.139	0.140	4831	4445	104	102
60	0.736	0.750	0.140	0.138	4629	4144	102	86
180	0.736	0.763	0.141	0.135	4230	2784	-	-

It can be seen that the DP of hemicelluloses increases in the first 10 minutes and decreased with time after 20 minutes reaction. The values of the hemicellulose DP compare well with those reported in literature for wood (Sjöström, 1993). The initial increase in hemicellulose DP might be explained by the removal low DP hemicellulose during "peeling" delignification. Subsequently the DP of the residual hemicellulose decreases due to radical attack during phenolic delignification.

7.2.6 pH of Waste Liquors

Since the CSTR is continuously fed with a NaOH solution and operates differentially, the outlet NaOH concentration is essentially the same as the inlet NaOH concentration. The pH in the batch reactor decreases continuously because of consumption of NaOH by the pulp and reaction products. The pHs of the waste liquors of the CSTR and batch reactor are shown in Table 7.4. As expected, the CSTR waste liquors have all the same pH. The pH decreases continuously in the batch reactor. Compared to the CSTR, the pH after 20 minutes of reaction in the batch reactor is 1 unit lower than that of CSTR (12.3 versus 13.3), indicating that the alkalinity is only 10% of that in the CSTR.

Table 7.4 pH of the Water Liquors from Batch Reactor CSTR Reactors

Reaction Time (min)	Batch Reactor	CSTR
0	-	13.3
10	12.4	13.3
20	12.3	13.3
40	12.2	13.3
60	12.1	13.3
180	10.7	13.3

7.3 Conclusion

At short reaction times, the kappa number and intrinsic viscosity development in the CSTR agrees with those obtained in the batch reactor at the same operating conditions. At longer reaction times, the CSTR derived kappa numbers and intrinsic viscosities are lower than the corresponding batch reactor data because the CSTR operates at constant NaOH concentration while the NaOH concentration decreases continuously in the batch reactor. The constant high NaOH concentration leads to increased delignification and cellulose degradation. When the pulp is exposed to a constant high NaOH concentration for a longer time, there is an additional contribution to cellulose degradation when compared to batch reactor derived pulp of the same kappa number. Alkaline hydrolysis of cellulose may be responsible for this contribution. The amount of reducing ends in oxygen delignified pulp from both the batch reactor and CSTR reactor decreases initially, followed by a gradual increase at larger reaction times. The initial decrease may be explained by "peeling" and/or oxidation of the carbohydrates. The subsequent increase in amount of reducing ends is likely caused by attack of radicals formed during oxygen delignification.

CHAPTER 8

PROPERTIES OF OXYGEN DELIGNIFIED PULPS FROM THE CSTR

As described in the previous chapter, a differential CSTR is better suited to study the oxygen delignification mechanism and kinetics because the data do not contain the effect of changing caustic concentration and it directly provides the rate of delignification. The purpose of this chapter is to discuss the properties of the pulp samples obtained from the CSTR.

8.1 Effect of Different Operating Conditions on Selectivity

To study the effect of operating conditions on oxygen delignification selectivity, experiments were performed at various oxygen pressures, temperatures and caustic concentrations. The standard reaction conditions are 90°C, 3.3g/l NaOH, 75psig oxygen pressure and 60 minutes. A series of experiments were performed whereby one variable was changed at 4 to 5 different levels while all other variables were kept at the standard condition.

Table 8.1 shows the intrinsic viscosity and kappa number of pulps at different pressures, different temperatures and different caustic concentrations. The temperature and caustic concentration have a large effect on the extent of delignification. Also, a high NaOH concentration leads to a low intrinsic viscosity.

Table 8.1 Viscosity and Kappa Number of Pulps at Different Operating Conditions

(Other conditions if not specified: 90°C, 3.3g/l NaOH, 75psig O_2 and 60 minutes)

Pressure (psig)	**Viscosity (ml/g)**	**Kappa**	**Temp (°C)**	**Viscosity (ml/g)**	**Kappa**	**NaOH (g/l)**	**Viscosity (ml/g)**	**Kappa**
35	884	14.4	**80**	865	14.9	**1.1**	970	16.3
55	847	13.1	**90**	828	12.5	**3.3**	828	12.5
75	828	12.5	**100**	753	10.8	**5.5**	765	10.9
95	800	11.0	**110**	582	6.7	**7.7**	693	9.4
			115	523	5.5	**20**	584	8.1
						50	383	5.1

8.1.1 Effect of Different Oxygen Pressures on Selectivity

It is important to quantify the effect of operating variables on the lignin-cellulose degradation selectivity. The selectivity is calculated as $\frac{K_0 - K_t}{\frac{1}{DP_t} - \frac{1}{DP_0}}$. The DP of cellulose is simply calculated using intrinsic viscosity DP= $(1.65 \times \eta)^{1.1111}$. Figure 8.1 shows the selectivity of the final pulp samples obtained at different oxygen pressures. Figure 8.1 shows that the selectivity does not change much with oxygen pressure. The selectivity is almost the same at 75 psig and 95 psig, which is the normal industrial operating range.

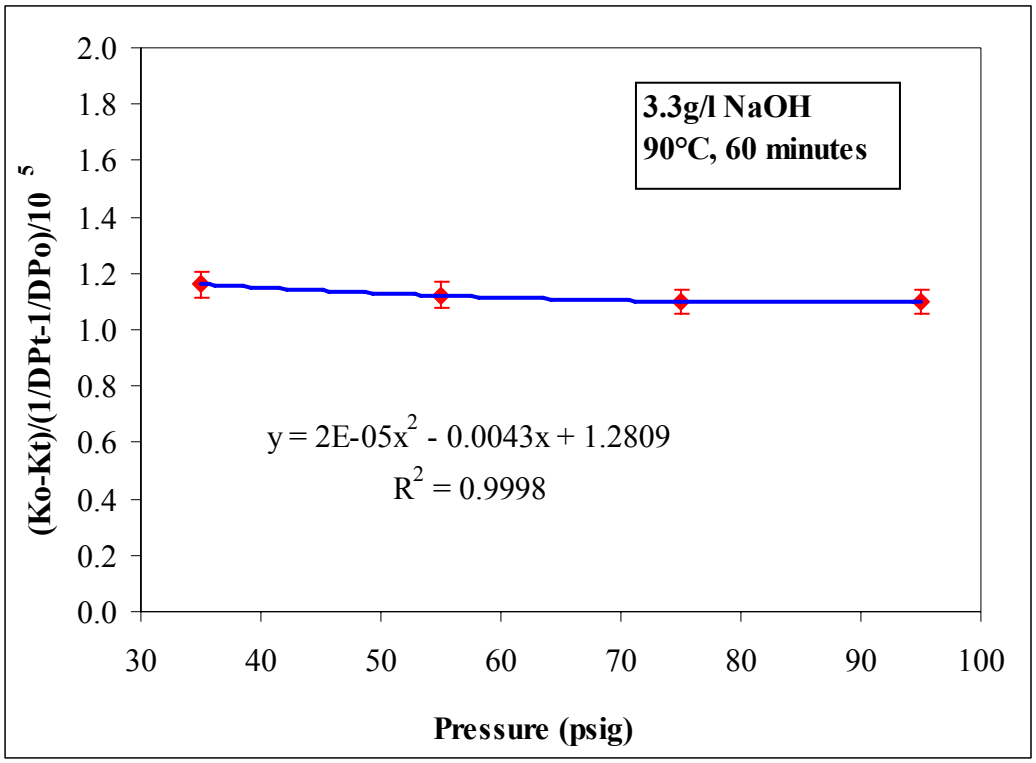

Figure 8.1 Selectivity vs. Different O2 pressures in CSTR

8.1.2 Effect of Different Reaction Temperatures on Selectivity

The effect of reaction temperature on the lignin-cellulose degradation selectivity of the final pulp samples is shown in Figure 8.2.

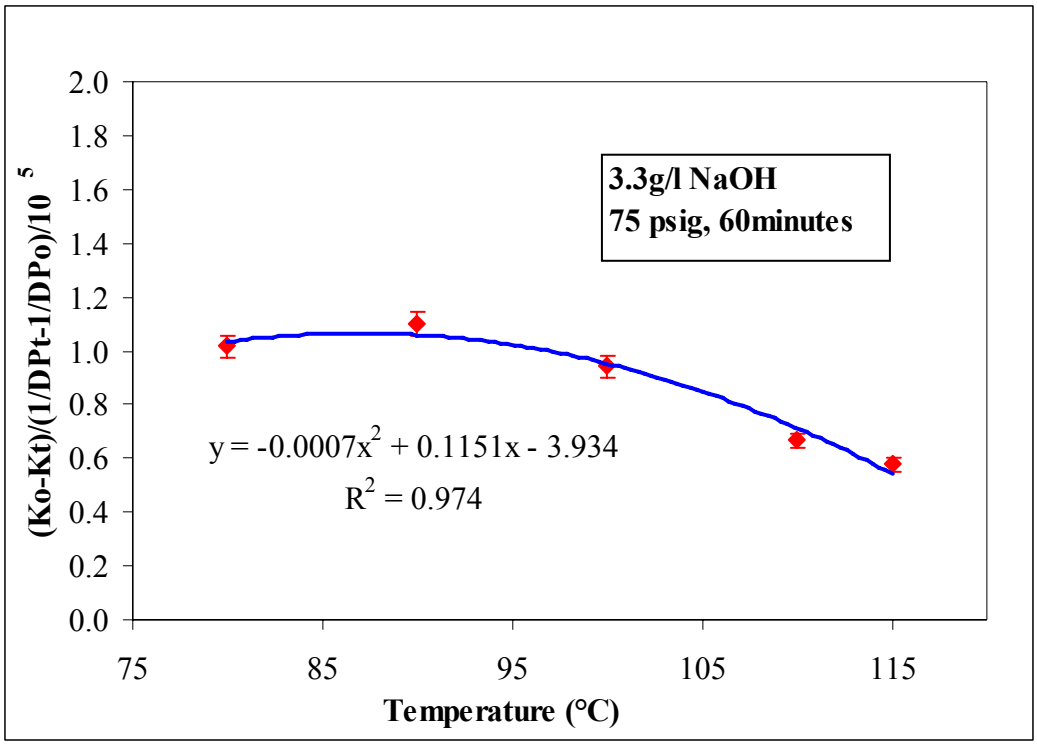

Figure 8.2 Selectivity vs. Different Temperature in CSTR

Figure 8.2 shows that the selectivity does not change significantly from 80 ºC to100 ºC. However, it decreases 30 to 40% when the temperature is higher than 100 ºC. This explains why the pulp and paper industry generally does not operate oxygen delignification above 100 ºC.

8.1.3 Effect of Different Caustic Concentrations on Selectivity

The effect of caustic concentration on the selectivity of the final pulp samples is shown in Figure 8.3.

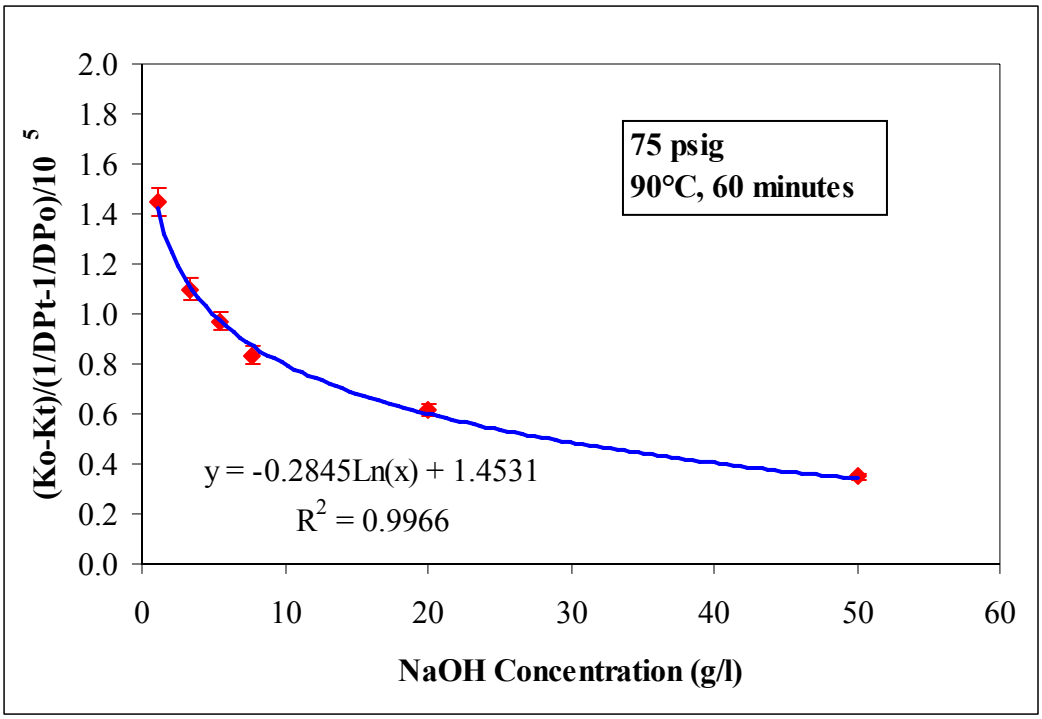

Figure 8.3 Selectivity vs. Different NaOH Concentrations in CSTR

Figure 8.3 shows that the selectivity decreases dramatically with increasing caustic concentration followed by a slower decrease at very high NaOH concentrations. The larger decrease in selectivity occurs over the NaOH concentration range of 1 to 7g/l, i.e. the region of interest for industrial oxygen delignification.

8.1.4 Effect of Reaction Time on Selectivity

The effect of reaction time on selectivity is shown in Figure 8.4. Because part of the kappa number can be removed by alkali without the presence of oxygen, a corrected selectivity can be calculated as $\frac{K_C - K_t}{\frac{1}{DP_t} - \frac{1}{DP_0}}$, where K_c is the kappa number after NaOH extraction without O_2 but at otherwise the same operating conditions. It can be seen that

both the standard and corrected selectivities decrease with reaction time, although the decrease in the corrected selectivity is relatively small. The explanation for the decrease in selectivity is the small contribution of alkaline hydrolysis of cellulose to the viscosity loss in addition to the cellulose degradation by radical species. The cellulose degradation due to alkaline hydrolysis becomes relatively more important at longer reaction times because the delignification rate and thus also the cellulose radical attack decreases with time. The alkaline hydrolysis of cellulose is not important in the batch reactor due to the rapid decrease in alkali concentration with reaction time, and as a result the selectivity in the batch reactor is not a function of reaction time as can be inferred from Figure 7.3 in Chapter 7.2.4.

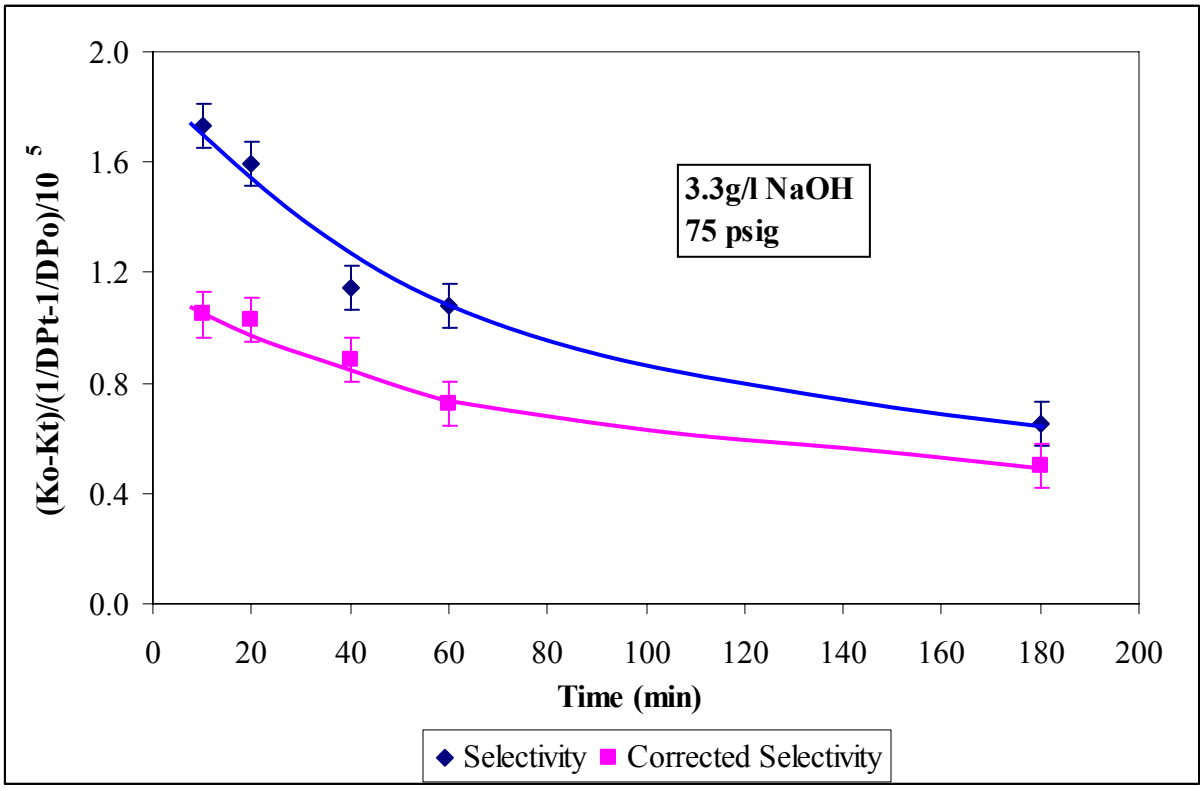

Figure 8.4 Selectivity & Corrected Selectivity vs. Time in CSTR

8.2 Yield of Different Pulps

The yield of the different final pulp samples is shown in Table 8.2. It can be seen that the yield drops with higher oxygen pressure, reaction temperatures, caustic concentrations and reaction time. At an extremely high NaOH concentration of 50g/l, the yield drops to 86.1%.

Table 8.2 Yield of Different Pulps (Other conditions if not specified: 90°C, 3.3g/l NaOH, 75psig O_2,except the 360 minutes experiment was performed at 100°C, 90psig and 7.7g/l NaOH.)

Pressure (psig)	**Yield (%)**	**Temp (°C)**	**Yield (%)**	**NaOH (g/l)**	**Yield (%)**	**Time (min)**	**Yield (%)**
35	96.7	**80**	96.1	1.1	96.6	**0**	100
55	95.9	**90**	95.4	3.3	95.4	**10**	98
75	95.4	**100**	93.9	5.5	94.9	**20**	96.5
95	94.4	**110**	91.3	7.7	94.2	**40**	96.0
		115	90.2	20	92.3	**60**	95.4
				50	86.1	**180**	92.5
						360	84.5

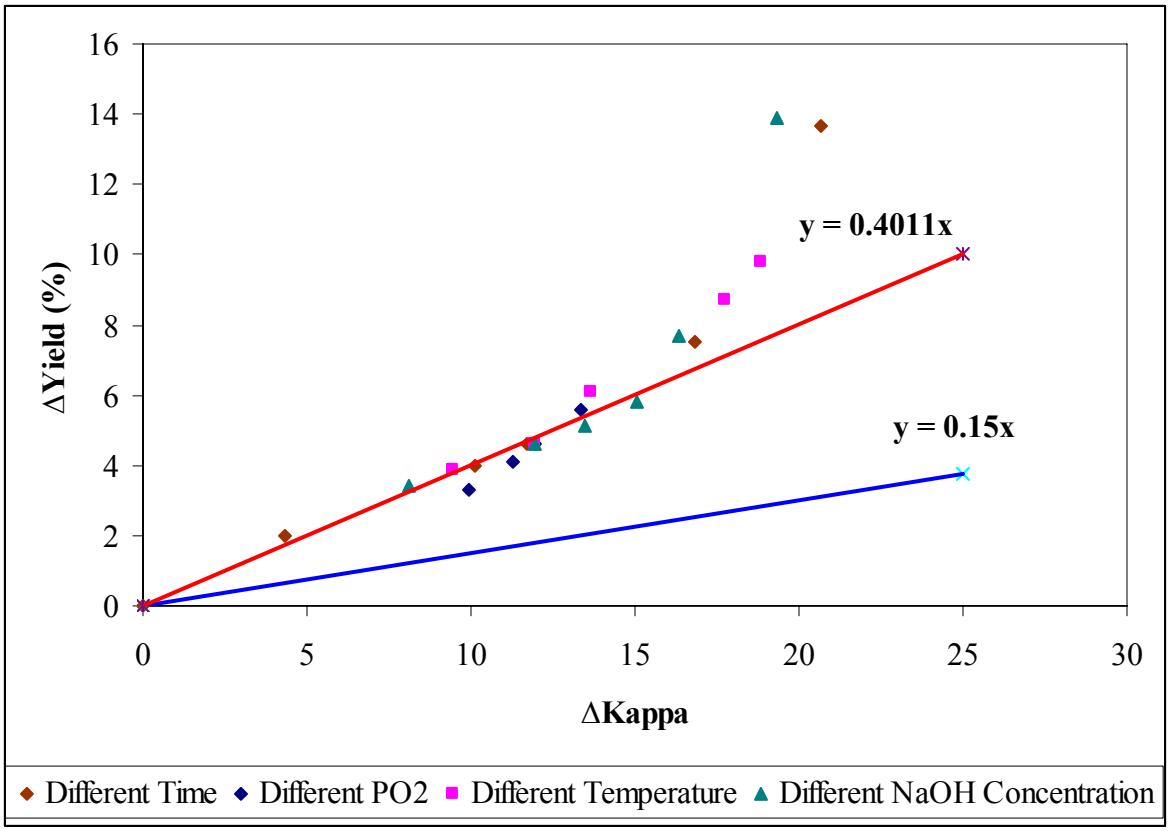

Figure 8.5 ΔYield vs. ΔKappa of Final Pulp Samples

The yield loss, ΔYield, is plotted versus ΔKappa in Figure 8.5 for all the final pulp samples. The yield loss for all the data except those obtained at 110 °C and 115°C and at 20 g/l and 50 g/l NaOH increase proportionally with the kappa number reduction. Thus for conventional oxygen delignification which leads to a decrease in kappa number of up to about 60%, the yield loss may be described by

$$\text{Yield loss (\%)} = 0.40 \times \Delta\text{Kappa} \qquad \text{(Equation 8.1)}$$

The yield loss in addition to that caused by the removal of lignin (Lignin Loss=0.15×ΔKappa) represents carbohydrate loss during oxygen delignification as

$$\text{Carbohydrate loss (\%)} = 0.25 \times \Delta\text{Kappa} \qquad \text{(Equation 8.2)}$$

It can be seen that the contribution of the carbohydrate loss to the yield loss is larger than that of lignin removal. The carbohydrate loss is larger than this linear correlation for the high temperature (110°C and 115°C), high caustic concentration (20 g/l and 50 g/l) and very long time (360minutes) tests. This shows that delignification beyond a kappa number decrease of 60% should be avoided because it leads to an excessive carbohydrate loss.

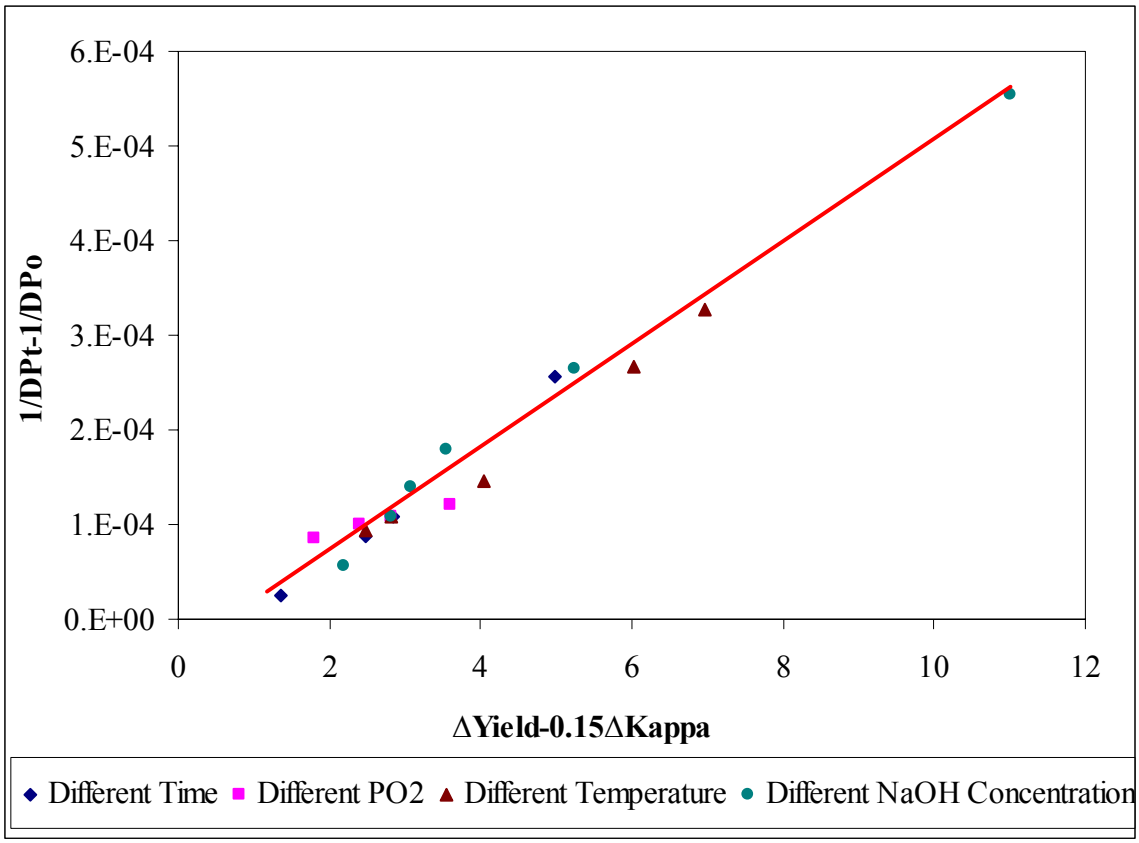

Figure 8.6 (ΔYield-0.15ΔKappa) vs. (1/DPt-1/DP_0) of Final Pulp Samples

Figure 8.6 shows the carbohydrate yield loss (ΔYield-0.15ΔKappa) versus (1/DPt-1/DPo) of all the final pulp samples. The linear relationship indicates the carbohydrate yield loss is related to the cleavage of cellulose independent of operating variables, including the

very high temperature, alkaline concentration and reaction time. In other words, this suggests that carbohydrate loss results after attack by radicals generated from phenolic delignification.

8.3 Hexenuronic Acid (HexA) Content of Different Pulps

Table 8.3 shows the HexA content of the original regular oxygen delignified pulps and those of oxygen delignified pulps in 40-50% ethylene glycol-water mixtures. It can be seen that the HexA content does not change significantly during oxygen delignification regardless of the reaction conditions, except for the very high temperature, caustic concentration and reaction time experiments which show a small decrease. This shows that HexA is not reactive at normal oxygen delignification conditions. However, at severe operating conditions, the pulp experiences a more severe yield loss so that part of the HexA groups may be removed together with the carbohydrates.

Table 8.3 HexA Content of Different Pulp Samples

(Other conditions if not specified: 90°C, 3.3g/l NaOH, 75psig O_2, 60 minutes, except the 360 minutes experiment was performed at 100°C, 90psig and 7.7g/l NaOH)

Pressure (psig)	**HexA (µmol/g)**	**Temp (°C)**	**HexA (µmol/g)**	**NaOH (g/l)**	**HexA (µmol/g)**	**Time (min)**	**HexA (µmol/g)**
35	24.0±1	**80**	23.9±1	1.1	25.7±1	**0**	25.1±1
55	24.1±1	**90**	24.6±1	3.3	24.6±1	**10**	25.6±1
75	24.6±1	**100**	23.5±1	5.5	24.7±1	**20**	25.1±1
95	24.0±1	**110**	22.7±1	7.7	24.5±1	**40**	24.4±1
		115	21.9±1	20	23.3±1	**60**	24.6±1
				50	17.6±1	**180**	24.7±1
						360	20.2±1

In Figure 8.7 the HexA content is plotted versus (ΔYield-0.15ΔKappa) for all the pulp samples. The HexA content is constant when the yield loss due to the carbohydrate

degradation is low. However, the HexA amount is lower when the carbohydrate yield loss is higher than 5%. The results indicate that the HexA content remains essentially unchanged during oxygen delingnification when the operating conditions are within the industrial practice range. However, when the operating conditions are severe, e.g, very high NaOH concentration (50g/l), higher temperature (115°C) or extremely long reaction time (6 hours), the HexA content is lower due to the additional carbohydrate removal.

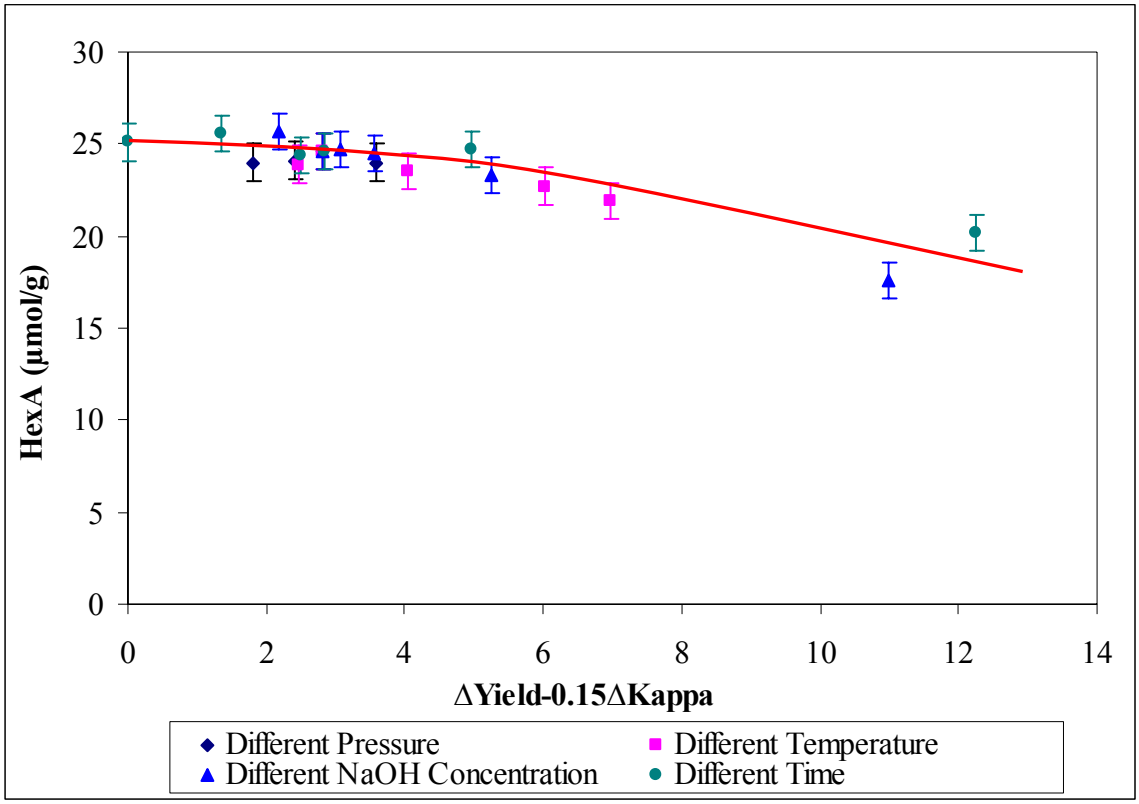

Figure 8.7 HexA Content vs. ΔYield-0.15ΔKappa of all the Pulp Samples

8.4 Klason Lignin and Acid-Soluble Lignin Content of Different Pulps

Table 8.4 shows the klason lignin and acid soluble lignin of all the samples from the CSTR.

Table 8.4 Klason and Acid-Soluble Lignin Content of Different Pulps

(Other conditions if not specified: 90°C, 3.3g/l NaOH, 75psig O_2; except the 360 minutes experiments was performed with 100°C, 90psig and 7.7g/l NaOH)

Pressure (psig)	**Klason Lignin(%)**	**Acid Soluble(%)**	**Temp (°C)**	**Klason Lignin(%)**	**Acid Soluble(%)**
35	2.13	0.42	**80**	2.40	0.42
55	2.01	0.43	**90**	1.97	0.36
75	1.97	0.36	**100**	1.44	0.44
95	1.81	0.47	**110**	0.82	0.44
			115	0.71	0.44
NaOH (g/l)	**Klason Lignin(%)**	**Acid Soluble(%)**	**Time (min)**	**Klason Lignin(%)**	**Acid Soluble(%)**
1.1	2.68	0.42	**0**	3.89	0.36
3.3	1.97	0.36	**10**	3.50	0.36
5.5	1.68	0.45	**20**	2.92	0.38
7.7	1.32	0.46	**40**	2.78	0.39
20	0.88	0.44	**60**	2.02	0.39
50	0.56	0.39	**180**	1.19	0.42
			360	0.31	0.34

The klason lignin content decreases with increased delignification. However, the acid soluble lignin content of all the sample is around 0.4% based on the oven-dried sample weight.

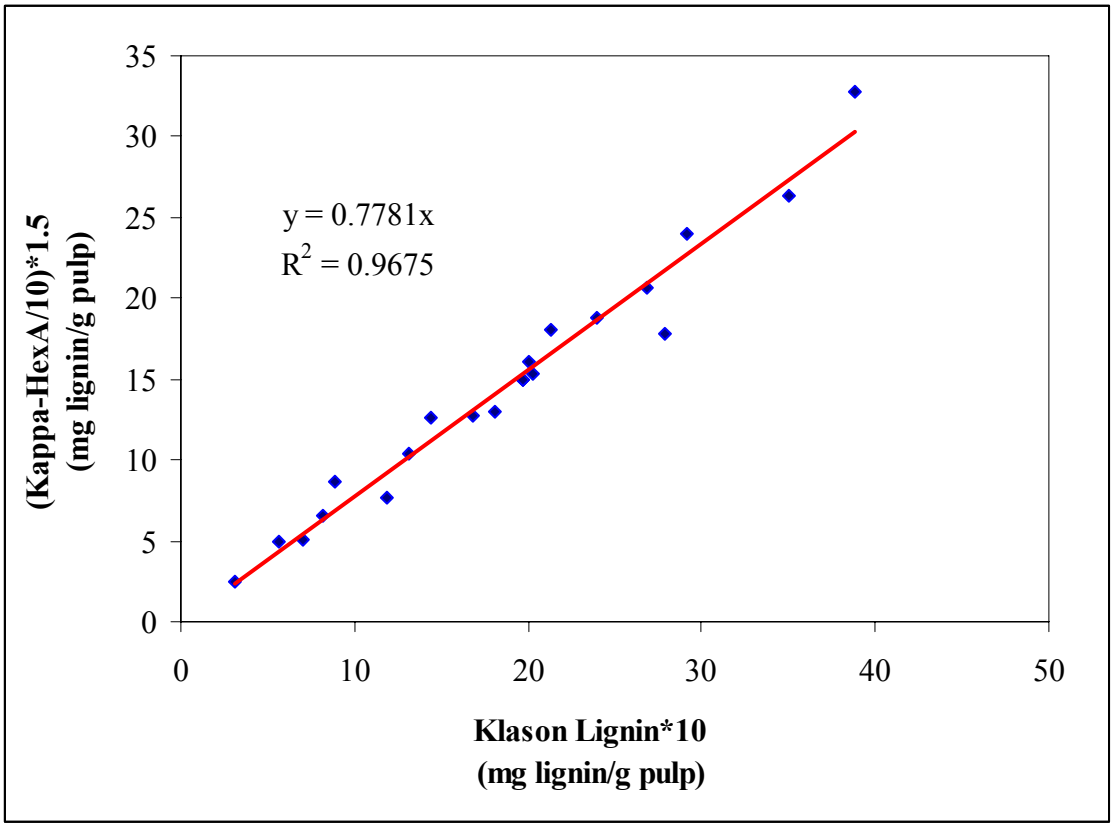

Figure 8.8 (Kappa-HexA/10)×1.5 vs. (Klason Lignin)×10

Figure 8.8 shows (Kappa-HexA/10)×1.5 versus (Klason Lignin)×10 both expressed in mg lignin/g pulp. It can be seen that the klason lignin is direct proportional to the lignin content calculated from the kappa number corrected for the HexA content. It should be noted that the klason lignin is tested based on the weight of lignin in 200 mg pulps which explains the larger experimental error in the data. The slope of the correlation indicates that klason lignin represents 78% of the lignin calculated from the kappa number corrected for the HexA content. The remaining 22% are most likely non-lignin based oxidizable structures. The accuracy of the kappa number method for predicting the lignin content in the pulps is questioned because some oxidizable structures formed during cooking contribute to the kappa number. These were indentified by Li and Gellerstedt (Li and Gellerstedt, 1999) as Ox-Dem kappa which is the kappa number of $HgAc_2$-$NaBH_4$

pretreated pulps. Their work also shows that the Ox-Dem kappa number is about 77%~80% of the conventional kappa number for kraft pulps.

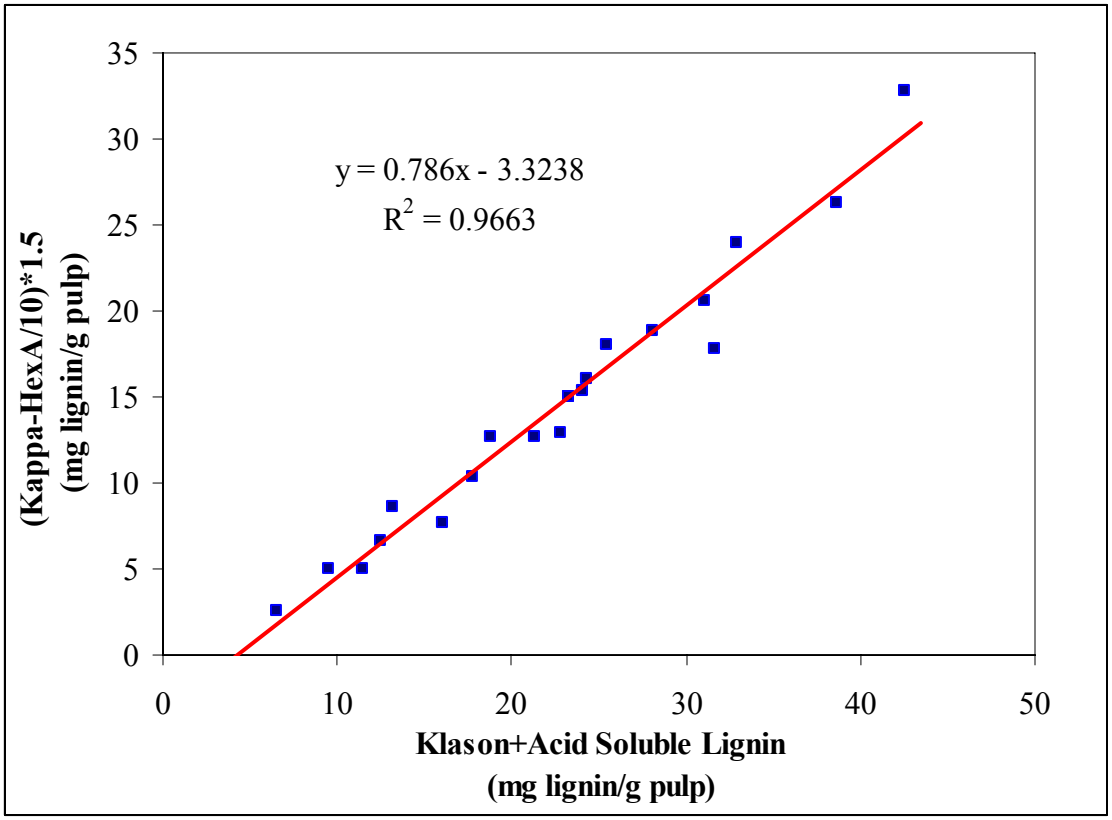

Figure 8.9 (Kappa-HexA/10)×1.5 vs. (Klason+Acid-Soluble Lignin)×10

In Figure 8.9, the theoretical lignin content (Kappa-HexA/10)×1.5 is plotted against measured lignin content (Klason+Acid-Soluble Lignin)×10. The fact that the linear correlation is shifted to the right with the same slope as in Figure 8.8 indicates that UV lignin may actually not be lignin derived, but is carbohydrate based material which dissolves in acid and absorbs UV light at 205 nm.

8.5 Conclusion

The results of this chapter show the effect of operating conditions on oxygen delignification. The selectivity decreases significantly at higher NaOH concentrations and when the reaction temperature is 110°C and higher. The influence of oxygen pressure on the selectivity is very small. The carbohydrate yield loss is proportional to the change in kappa number up to a kappa reduction of 60%. At higher percentages of kappa removal, obtained under more severe conditions such as high NaOH concentration, high temperature or long reaction times, the carbohydrate yield loss increases much faster than the kappa reduction. Thus the present data suggest that oxygen delignification should be limited to about 60% kappa reduction.

The carbohydrate loss is most likely due to peeling following random attack by radicals formed by phenolic delignification. The HexA groups in the pulps are not removed during oxygen delignification except under severe reaction conditions when they are removed together with the carbohydrates. Klason lignin represents 78% of the HexA corrected kappa number. The remaining 22% are most likely non-lignin based oxidisable structures identified earlier by Li and Gellerstedt (1999).

CHAPTER 9

KINETICS OF OXYGEN DELIGNIFICATION

The purpose of this chapter is to find the proper mathematical model to represent the kinetic data of oxygen delignification obtained from the batch and CSTR reactors. The appropriate kinetic equation may be used for engineering purposes such as oxygen delignification tower design and industrial operation. The kinetics describe the change in kappa number and intrinsic viscosity in terms of reaction conditions such as temperature, pressure and caustic concentration, etc. The relative change of the pulp viscosity and kappa number, i.e. the selectivity, will also be considered. In this chapter, two delignification kinetic models are presented; the power law model which is based on the integral approach to analyze kinetic data, and the simple first order delignification rate equation which is based on the differential approach suited for the CSTR technique. Several kinetics studies have shown that the reaction order in residual kappa number of the oxygen delignification rate was significantly larger than one. The mechanistic explanation for the high reaction order has been reported (Agarwal et al, 1998) to be the wide range of reactivities of the different residual lignin moieties present in pulp as proposed by Schoon (Schoon, 1982).

9.1 Kinetic Modeling Using the Integral Method (Power Law Model)

The kinetics of oxygen delignification is usually presented by a power law equation which includes the influence of process variables such as reaction temperature, oxygen pressure and caustic concentration (Iribarne and Schroeder, 1997):

$$r_L = -\frac{dK}{dt} = k[OH^-]^m[P_{O2}]^n K^q \qquad \text{(Equation 9.1)}$$

In equation (9.1), K is the Kappa number; $[OH^-]$ is the caustic concentration and $[P_{O2}]$ is the absolute oxygen pressure. The constants m, n, and q are obtained by fitting the experimental data. The reaction rate coefficient *k* depends on the temperature and is given by the Arrhenius equation:

$$k = A\exp(-\frac{E_A}{RT}) \qquad \text{(Equation 9.2)}$$

In equation (9.2), E_A is the activation energy, R is the gas constant, T is the absolute temperature and A is the frequency factor.

Figure 9.1 shows the experimental pulp kappa numbers obtained in the CSTR and batch reactors at 90ºC, 3.3g/l NaOH or 3% NaOH charge and 75psig O_2 pressure. It also shows that both sets of data obtained are well presented by the power law equation (9.1). As described in chapter 3, equation (9.1) may be integrated when the term $k[OH^-]^m[P_{O2}]^n$ is constant, giving

$$K(t) = \left[\left(\frac{1}{K_0^{q-1}}\right) + k_q\,(q-1)t\right]^{-\left(\frac{1}{(q-1)}\right)} \quad q \neq 1 \text{ (see equation 3.11)}$$

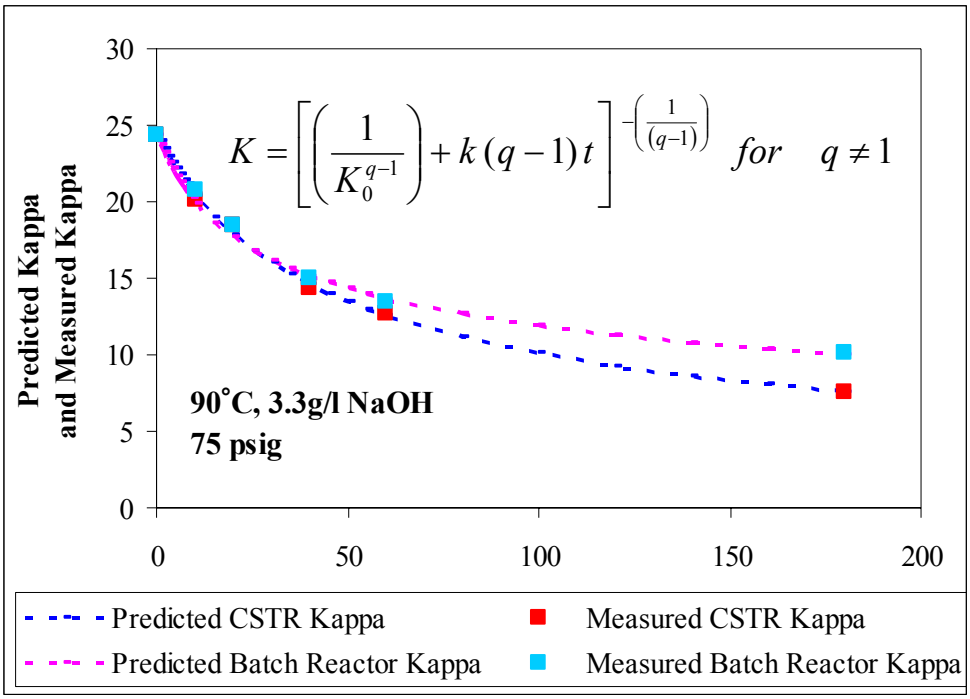

Figure 9.1 Kappa Number Model and Experimental Data of CSTR and Batch Reactor

Table 9.1 summarizes the power law model parameters for delignification in the CSTR and batch reactors calculated from equation (9.1). The reaction order for lignin is higher in the batch reactor in order to describe a larger decrease in delignification rate at lower kappa numbers. However, in both cases the reaction order is significantly larger than one. Because the caustic concentration remains constant in the CSTR, the order obtained in the CSTR gives the correct reaction order for the kappa number on the delignification rate. In another word, the lignin reaction order obtained in the batch reactor is too high because it ignores the effect of the decreasing caustic concentration with time.

Table 9.1 Summary of Batch Reactor and CSTR Kappa Number Power law Model

90˚C, 3.3g/l NaOH, 75 psig, (0,10, 20, 40, 60 and 180min)		
Parameter	**Reaction Order q**	**Reaction Constant k (min^{-1})**
CSTR	2.70	9.03×10^{-5}
Batch	4.25	8.92×10^{-7}

9.2 Cellulose Degradation

The cleavage of cellulose was modeled by Iribarne and Schroeder (1997) as the increase in number-average moles of cellulose per gram of pulp (m_n). Similarly one can describe the cellulose degradation by the number of cellulose chain scissions during oxygen delignification. Violette and van Heiningen (2003) calculate the number of cellulose chain scissions from the average degree of depolymerization of cellulose (DP) in the pulp at time t=0 and time t=t, as $1/DP_t$-$1/DP_0$. DP can be obtained from the intrinsic viscosity [η] by equation (9.3) (van Heiningen et al, 2003):

$$DP = \left(\frac{1.65[\eta] - 116H}{G} \right)^{1.111} \qquad \text{(Equation 9.3)}$$

where [η] is the intrinsic viscosity of the pulp in cm^3/g, and G and H are the mass fractions of cellulose and hemicellulose in the pulp. This formula considers the actual weight of cellulose rather than the pulp weight being responsible for the viscosity, and makes a correction for the small contribution of the hemicelluloses to the pulp intrinsic viscosity.

The number of moles of cellulose per gram of pulp, m_n, can be calculated by equation (9.4) (Iribane and Schroeder, 1997) as:

$$m_n = \frac{1}{162DP_n + 18} \cong \frac{1}{162DP_n} \left(\frac{Moles}{Gram\ Pulp} \right) \qquad \text{(Equation 9.4)}$$

The content of cellulose (G) and hemicellulose (H) in the pulp was measured by high pressure anion exchange chromatography (HPAEC) on double hydrolysed pulp samples (Davis, 1998). The results for the pulp samples in the CSTR and batch reactor are listed in Table 7.2 and Table 7.3. Based on these results the cellulose degradation was modeled

by two contributions: one due to radicals produced by phenolic delignification, and the other due to alkaline hydrolysis. The model can be described as equation (9.5):

$$\frac{dm_n}{dt} = -k_c \frac{dK}{dt} + k_h\left[OH^-\right] \qquad \text{(Equation 9.5)}$$

where k_c is the rate constant for radical attack, and k_h is the alkaline hydrolysis rate constant. [OH^-] is the alkali concentration in g/L.

Integration of equation (9.5) gives:

$$m_n = m_0 + k_c(K - K_0) + k_h[OH^-]t \qquad \text{(Equation 9.6)}$$

Since NaOH is rapidly consumed during the initial phase of oxygen delignification in the batch reactor, the influence of the term $k_h[OH^-]t$ was neglected for t ≥ 20 minutes. This allows the calculation of k_c by fitting the data for the batch reactor at t ≥ 20 minutes as 3.60×10^{-8} (moles/g pulp·kappa). Using this value for the analysis of the CSTR data gives a value for k_h of 1.07×10^{-9} (liter·mol cellulose/g pulp·g NaOH·minute). These values provide a good fit of the cellulose degradation in the CSTR as can be seen in Figure 9.2. The good fit of the batch reactor data was obtained by setting k_h to zero.

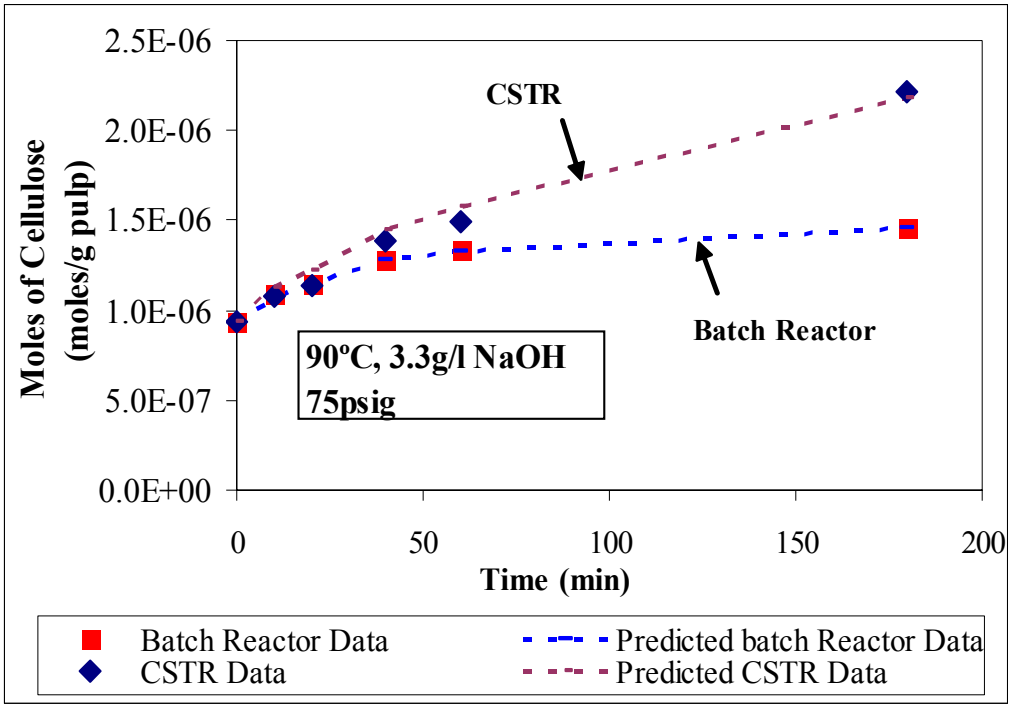

Figure 9.2 Degradation of Cellulose in CSTR and Batch Reactors; Experimental and Predicted Data

9.3 Alternative Modeling Approach of Oxygen Delignification based on CSTR Data

The rate of delignification is directly calculated from the lignin concentration in the effluent of the CSTR using equations (5.3) and (5.5). The delignification rate decreases with time because the residual lignin content of the pulp in the Berty basket decreases with time. Another advantage of the CSTR set-up is that the amount of lignin removed from the pulp can be calculated at any time. This allows the calculation of the residual lignin content in the pulp as well as the delignification rate at each time. The delignification rates are plotted versus residual lignin content for the experiments performed at different temperatures (80ºC, 90ºC, 100ºC and 110ºC), pressures (35psig, 55psig, 75psig and 95psig) and alkali concentrations (1.1g/l, 3.3g/l, 5.5g/l, 7.7g/l 20g/l and 50g/l) in Figure 9.3, 9.4 and 9.5. The residual lignin content in the pulps was

calculated by equation (9.7) which also corrects for the contribution of HexA on the initial kappa number. A constant value of 24μmol/g is taken for HexA because it has been shown in chapter 8 that the hexenuronic acid content in pulp is unchanged during conventional oxygen delignification.

$$\text{Residual Lignin}\left(\frac{\text{mg}}{\text{g Pulp}}\right) = \frac{\left(K_0 - \frac{HexA}{10}\right) \times 1.5 - \phi_v \int_0^{t+t_d} C_L(t)dt + V_r C_L(t+t_d)}{m_P}$$

(Equation 9.7)

where HexA is hexenuronic acid content of pulp (μmol/g pulp)

Ko is the initial kappa number

Φ_v is the liquid flow rate (ml/min)

$C_L(t)$ is the dissolved lignin concentration (mg lignin/ml)

V_r is the reactor volume (ml)

m_p is the pulp weight (o.d pulp)

Figure 9.3 shows the delignification rate vs. residual lignin amount at different oxygen pressures. It can be seen that the delignification rate decreases approximately linearly with the residual lignin content in the pulp. Higher oxygen pressures result in higher delignification rates at the same amount of residual lignin. The rate differences are large in the beginning of the reaction, but become smaller with the reaction time. This result supports industrial practice of two-stage oxygen delignification with the first short stage at high oxygen pressure and the second longer stage at lower oxygen pressure.

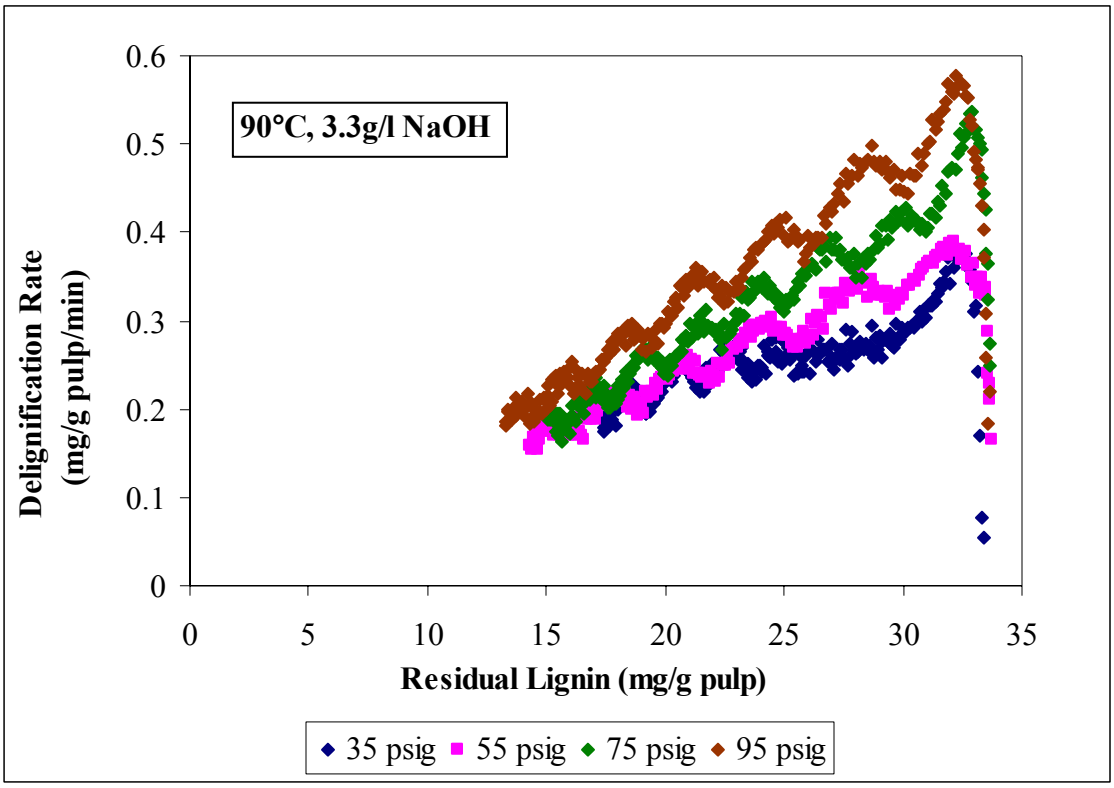

Figure 9.3 Delignification Rate vs. Residual Lignin at Different O_2 Pressures

Figure 9.4 shows the effect of reaction temperature on the delignification rate vs. residual lignin amount in the pulps. The delignification rate at the two highest temperatures (110°C and 115°C) show less of a linear behavior with the residual lignin content than those obtained at 100°C and lower temperatures. The delignification rate increases significantly with temperature especially above 100 ºC. This supports industrial two stage delignification to obtain a larger decrease in kappa number by increasing the temperature in the longer second stage when the residual lignin content in the pulp is low. The experiment at the highest temperature of 115°C predicts almost complete removal of lignin at the end of the experiment (t=60 minutes). This final pulp is predicted to have a kappa number mostly made up of hexenuronic acid groups.

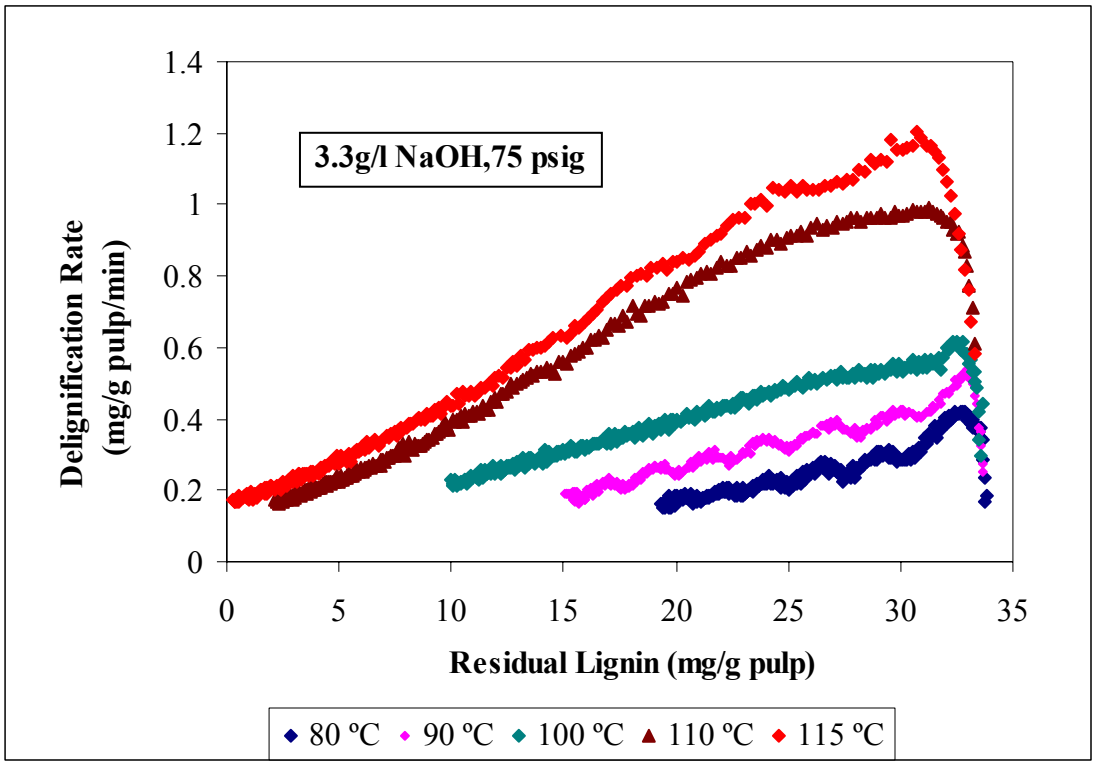

Figure 9.4 Delignification Rate vs. Residual Lignin at Different Temperatures

Figure 9.5 shows the delignification rate vs. residual lignin amount at different caustic concentrations. Higher caustic concentrations give higher delignification rates at the same amount of residual lignin in the pulp samples. Again a fairly linear relationship is seen between the delignification rate and residual lignin content. The increase in delignification rate is largest at the lower alkali levels. This supports industrial practice of avoiding high alkali charges which only modestly improve the delignification rate but are detrimental to the pulp quality.

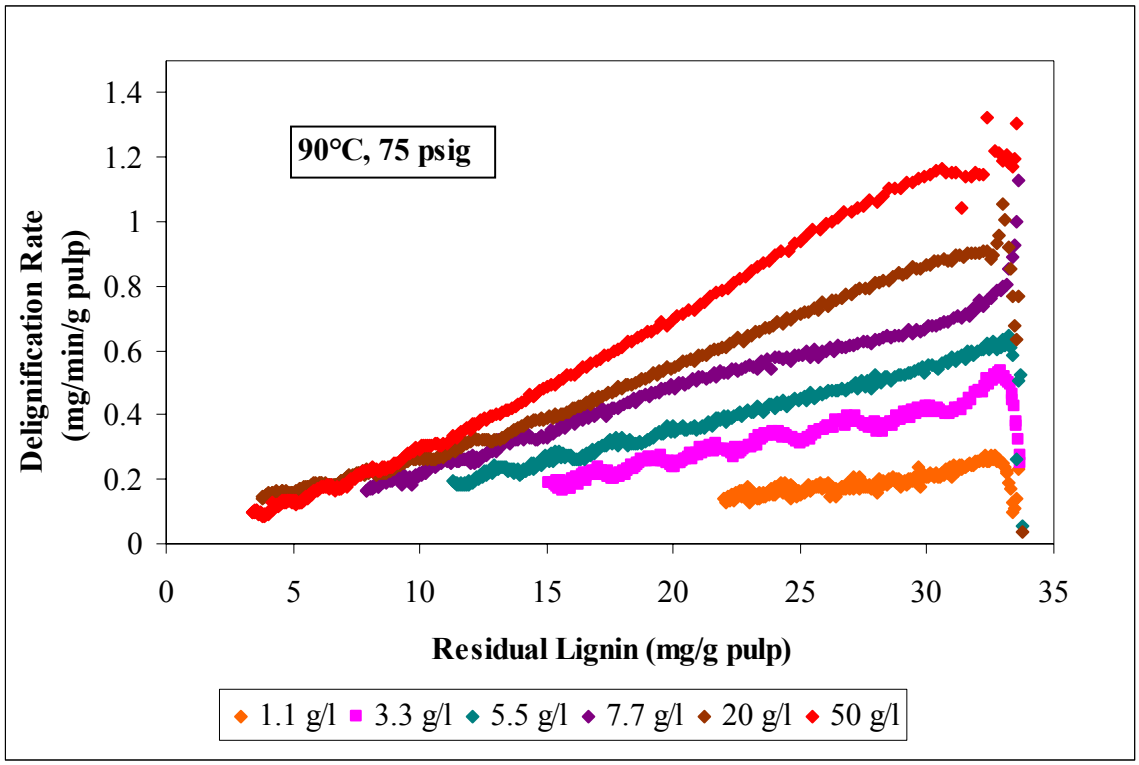

Figure 9.5 Delignification Rate vs. Residual Lignin at Different NaOH Concentration

9.4 Reaction Order in HexA-free Residual Lignin Content

Figures 9.3, 9.4 and 9.5 generally show a linear decrease in delignification rate with residual lignin content if the first few minutes of reaction are ignored when water in the CSTR is replaced by the oxygenated caustic solution. Therefore, a first order reaction in HexA-free residual lignin was considered for modeling the delignification kinetics. To provide more support for this approach, oxygen experiments were performed with three pulps each with a different initial kappa number. One pulp is the standard softwood pulp used in this study with kappa number of 24.4 and two pulps obtained by oxygen delignification of this standard pulp in the batch reactor for 20 and 60 minutes at 90°C, 75 psig and a NaOH charge of 3%. The pulp properties are shown in Table 9.2.

Table 9.2 Kappa Number and Intrinsic Viscosity of Batch Reactor Samples

Batch Reactor (90˚C, 3% NaOH, 75 psig)		
Batch O_2 Delig. Time (min)	**Kappa Number**	**Intrinsic Viscosity (g/ml)**
Original	24.4	1089
20	18.5	1011
60	13.5	898

Figure 9.6 shows the delignification rate versus HexA-free residual lignin for these three pulps.

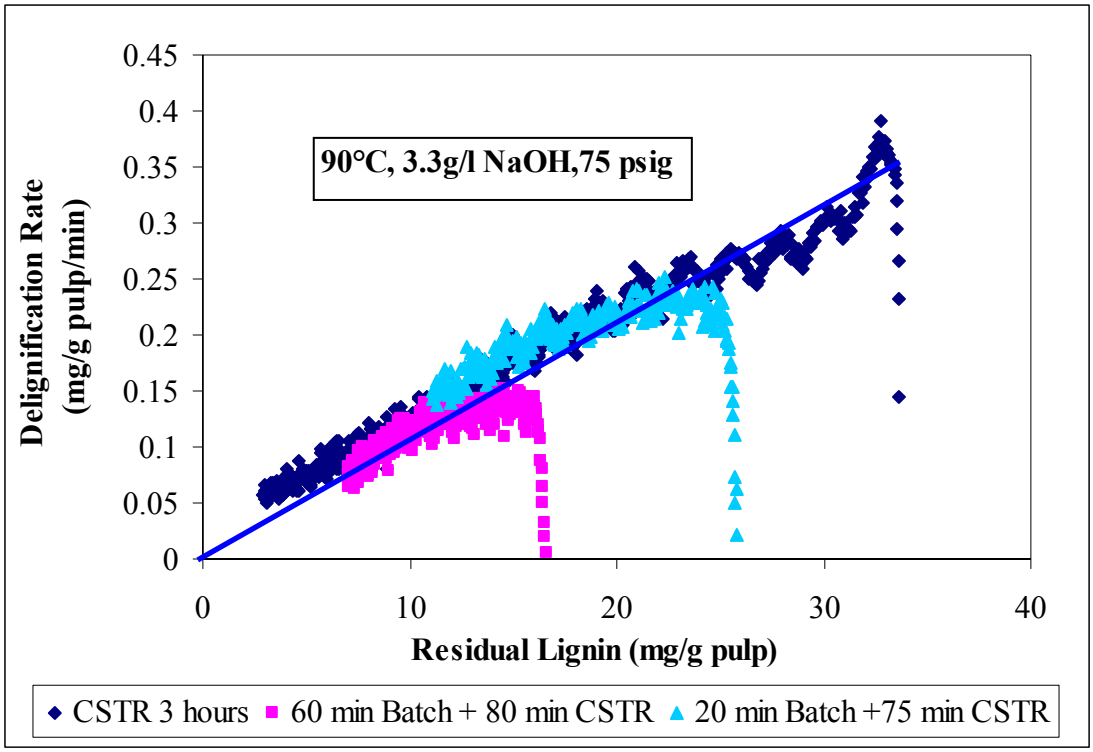

Figure 9.6 Delignification Rate vs. Residual Lignin Amount for Three Experiments ((1) 3 hours experiment in CSTR; (2) 60 minutes batch reactor + 80 minutes CSTR; (3) 20 minutes batch reactor + 75 minutes CSTR)

Figure 9.6 confirms that the oxygen delignification reaction can be described as a first order reaction in HexA-free residual lignin in the pulp. In addition, the finding that the batch reactor oxygen delignified pulp samples follow the same delignification rate curve as the original pulp implies that lignin condensation reactions are insignificant during oxygen delignification in the batch reactor where the pulp is exposed to high dissolved lignin concentrations at the end of the process.

9.5 First Order Reaction Rate Constant, K_L

The slopes of straight line fits through the data in Figures 9.3, 9.4 and 9.5 are listed in Table 9.3 as the first order rate constants. The real oxygen pressure is also included in Table 9.3. It is calculated by subtracting the saturated steam pressure at the different temperatures from the total pressure.

Table 9.3 Rate Constants of Different Experiments

Temperature (°C)	Total Pressure (psig)	Oxygen Pressure (psia)	NaOH (g/liter)	Rate Constant (1/min)
81	75	82.8	3.3	0.0097
91	75	79.5	3.3	0.0134
100	75	75.0	3.3	0.0187
112	75	68.9	3.3	0.0366
117	75	65.2	3.3	0.0423
90	35	39.5	3.3	0.0102
90	55	59.5	3.3	0.0115
93	95	99.5	3.3	0.0154
89	75	79.5	1.1	0.0068
93	75	79.5	5.5	0.0176
93	75	79.5	7.7	0.0232
90	75	79.5	20	0.0273
89	75	79.5	50	0.0353

The first order reaction rate constant in Table 9.3 includes the effect of temperature, caustic concentration and oxygen pressure. Equation 9.8 shows the relationship between these variables and the first order reaction rate constant as:

$$\ln(k_L) = \ln(A) - \frac{E}{RT} + m\ln\left[OH^-\right] + n\ln\left[P_{O_2}\right] \qquad \text{(Equation 9.8)}$$

9.5.1 Reaction Order in Caustic Concentration

At variable NaOH concentration, but constant temperature T and oxygen pressure P_{O_2}, equation (9.8) simplifies to equation (9.9).

$$\ln(k_L) = C1 + m\ln\left[OH^-\right] \qquad \text{(Equation 9.9)}$$

where C1 is a constant.

The logarithm of the rate constant k_L for the experiments with variable $[OH^-]$ at 90°C and 79.5 psia oxygen pressure (75 psig total pressure) is plotted versus $[OH^-]$ in Figure 9.7. A linear relationship is obtained for the 6 data points. The slope yields a reaction order in caustic concentration of 0.423.

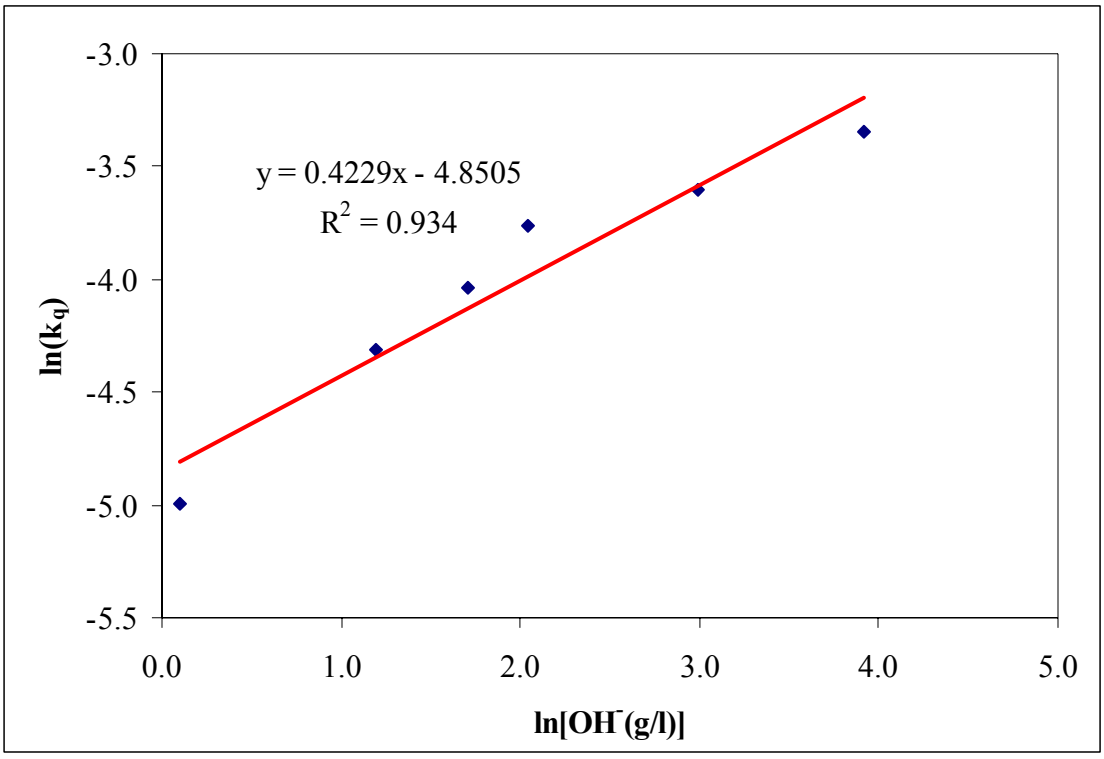

Figure 9.7 ln(kq) vs. ln[OH-] at 90ºC and 75 psig Total Pressure

9.5.2 Reaction Order in Oxygen Pressure

At variable oxygen pressure P_{O_2}, but constant temperature and NaOH concentration equation (9.7) becomes equation (9.10).

$$\ln(k_L) = C2 + n \ln\left[P_{O_2}\right] \qquad \text{(Equation 9.10)}$$

where C2 is a constant.

The $\ln(k_L)$ of the experiments at 90°C and 3.3g/l NaOH are plotted versus the natural logarithm of the real O_2 pressure in Figure 9.8. Again a linear behavior is obtained in agreement with equation 9.10.

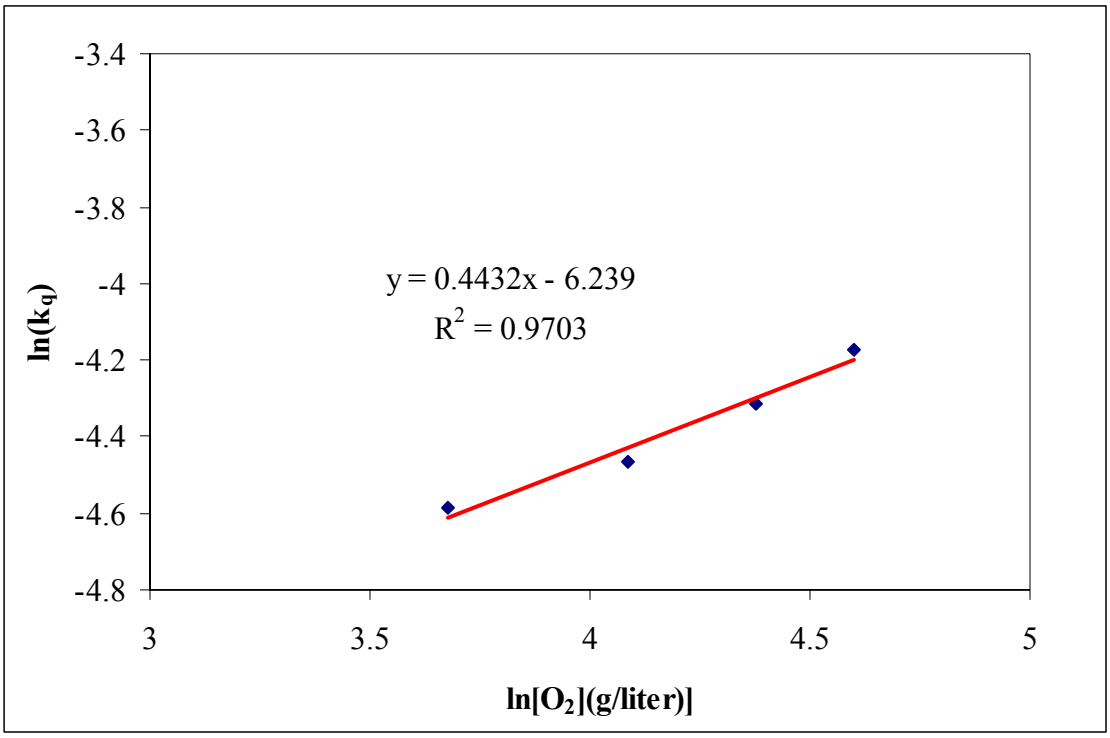

Figure 9.8 ln(kq) vs. ln[P_{O2}] at 90ºC and 3.3 g/l NaOH

From the slope of the linear correlation, one obtains 0.443 as reaction order in real oxygen pressure.

9.5.3 Activation Energy

At variable temperature and real oxygen pressure P_{O_2} but constant NaOH concentration, equation (9.8) reduces to equation (9.11).

$$\ln(k_L) - 0.443 \cdot \ln(P_{O2}) = C3 - \frac{E}{RT} \qquad \text{(Equation 9.11)}$$

where C3 is a constant. In equation (9.11), it is assumed that the reaction oder in P_{O2} is 0.443 found at 90°C is also valid at other temperatures.

Equation (9.11) shows that when $\ln(k_L)$-0.443$\ln(P_{O2})$ is plotted versus 1/T, a straight line is obtained when the kinetics are described by a power law equation. This is indeed the

case as can be seen in Figure 9.9. The slope is equal to –E/R, so activation energy is E = 6382.3×8.314 = 5.31×10^4 J/mol. Since the temperature controller can keep the temperature within ±2°C, this activation energy implies that temperature change of 2°C result in a 10% change in delignification rate.

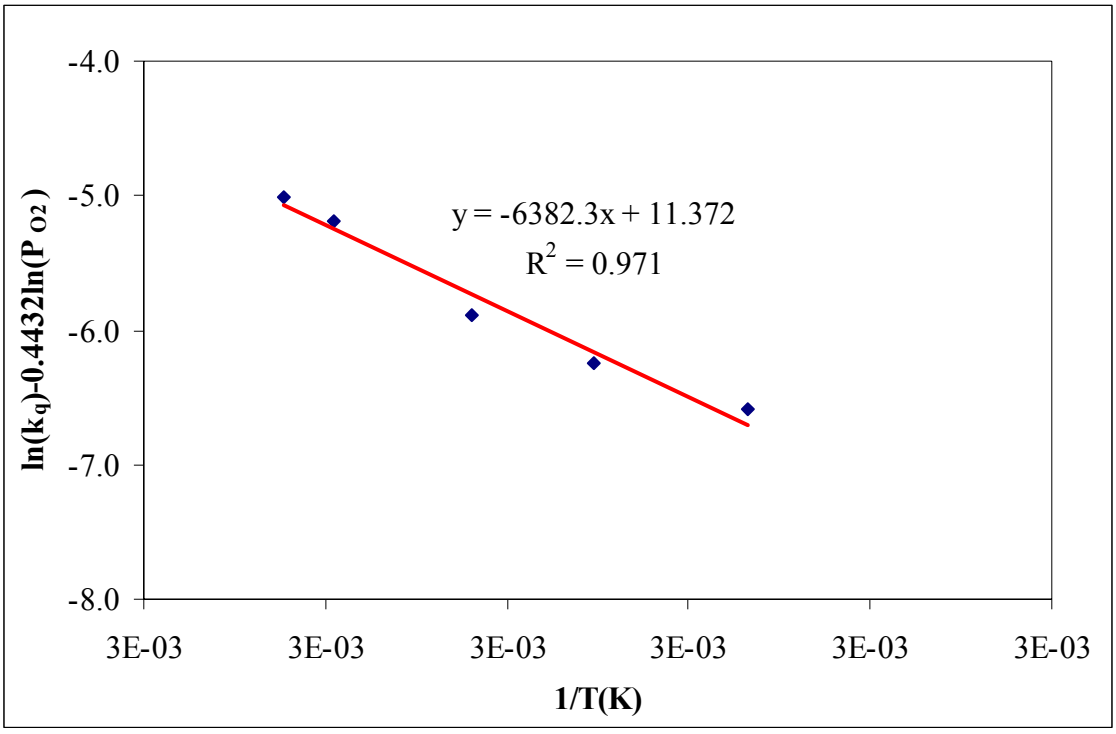

Figure 9.9 ln(kq)-0.443ln(P_{O2}) vs. 1/T at 3.3 g/l NaOH and 75 psig O_2

By inserting the values of m,n and E in equation (9.8), the frequency factor A is calculated by obtaining the best fit for the plot of ln(k_L)(with k_L listed in Table 9.3) versus $-\frac{E}{RT}+m\cdot\ln\left[OH^-\right]+n\cdot\ln\left[P_{O2}\right]$.

Figure 9.10 shows the plot of ln(k_L) versus $-\frac{E}{RT}+m\cdot\ln\left[OH^-\right]+n\cdot\ln\left[P_{O2}\right]$ for all experiments listed in Table 9.3.

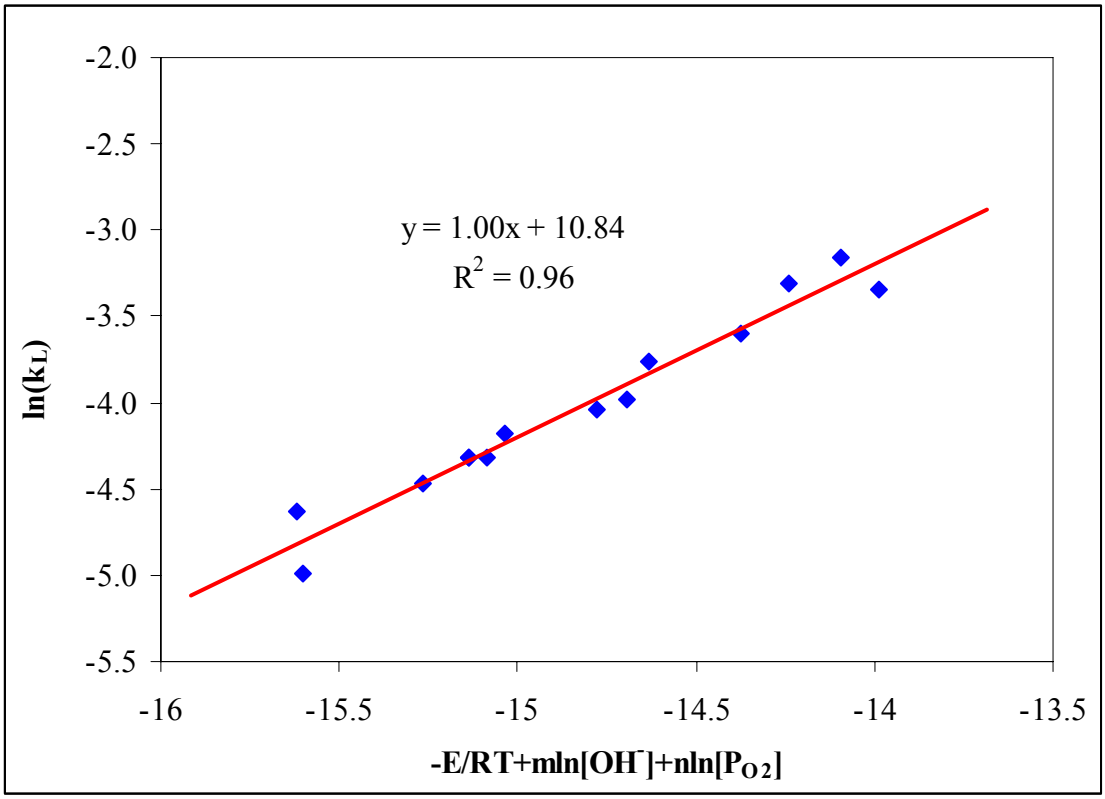

Figure 9.10 $\ln(k_L)$ versus $-\frac{E}{RT}+m\cdot\ln[OH^-]+n\cdot\ln[P_{O2}]$

From the good straight line fit in Figure 9.10, it gives that

$$A = e^{10.84} = 5\times10^4 \ \ \text{min}^{-1}(\text{g/l})^{-m}(\text{psia})^{-n}$$

Thus the expression for the delignification rate becomes:

$$r = 5\times10^4 e^{-\frac{5.31\times10^4}{R\times T}}[OH^-]^{0.423}[P_{O2}]^{0..443}L_C \qquad \text{(Equation 9.12)}$$

where r = delignification rate (mg/g pulp/min)$=-\frac{dL_C}{dt}$

T = reaction temperature (K)

$[OH^-]$ = sodium hydroxide concentration (g/l of NaOH)

$[P_{O_2}]$= real oxygen pressure (psia)

L_c = residual lignin amount in pulp corrected for hexA content (mg/g pulp)

9.6 Model Verification

The predictions obtained with equation (9.12) are shown in Figures 9.11, 9.12 and 9.13. It can be seen that the predictions are quite good except for the highest temperatures of 110ºC and 115ºC, where equation (9.12) slightly underpredicts the rate of delignification especially at low residual lignin content. This can not be explained by a change in the solubility of oxygen in caustic with temperature because Figure 10.2 in chapter 10 shows that the Henry coefficient for oxygen dissolution in water or caustic is virtually unaffected over the temperature range 80°C to 115°C.

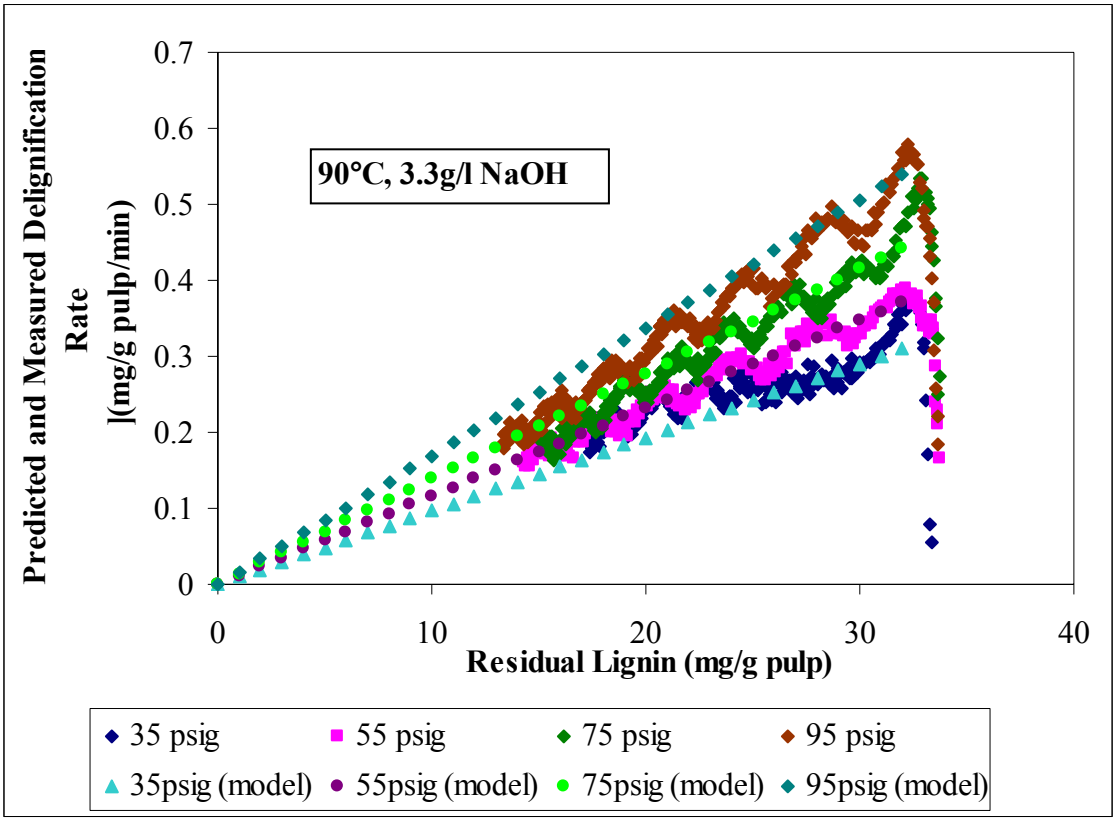

Figure 9.11 Delignification Rate vs. Residual Lignin at Different Total Pressures

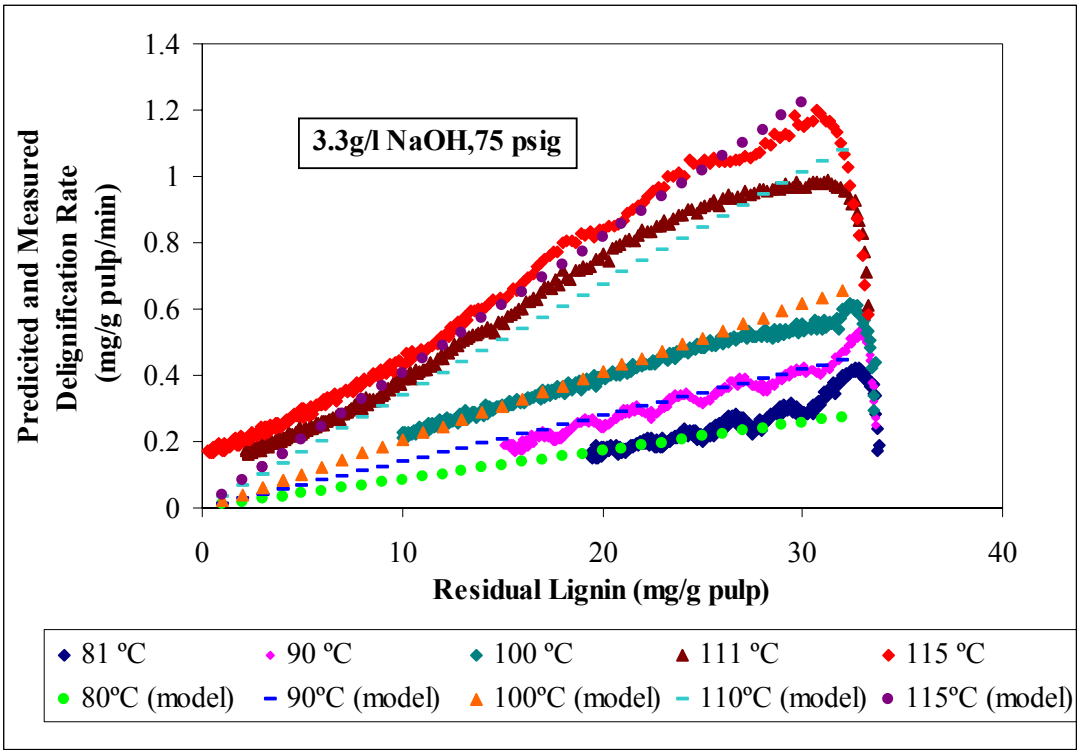

Figure 9.12 Delignification Rate vs. Residual Lignin at Different Temperatures

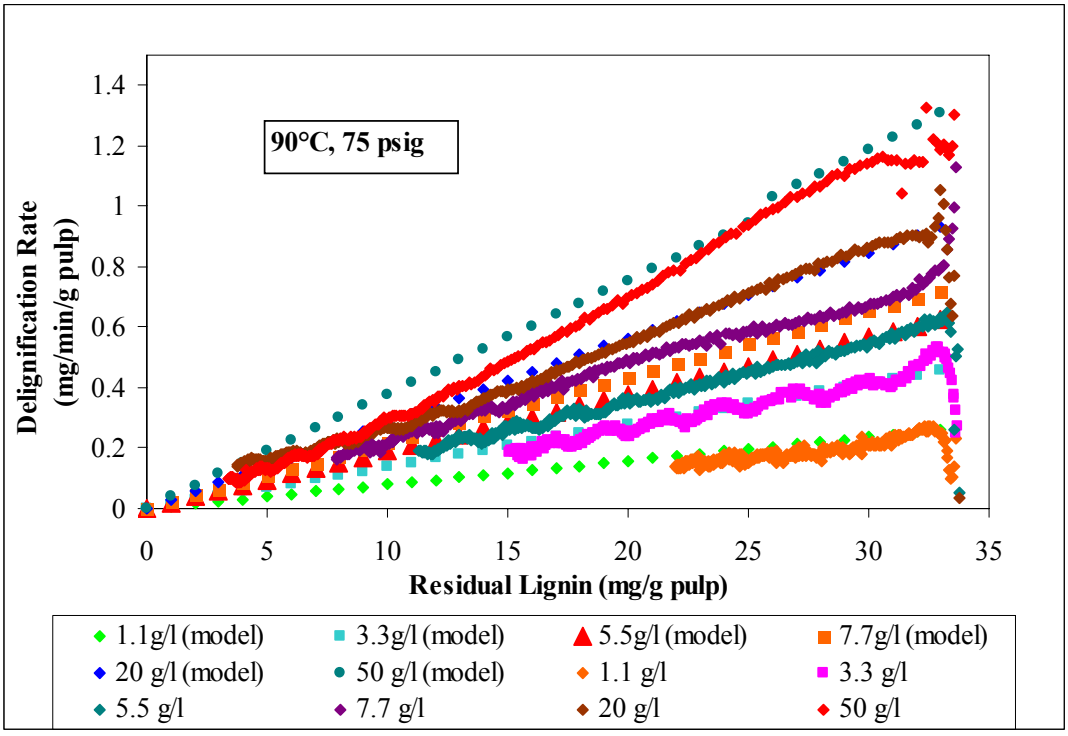

Figure 9.13 Delignification Rate vs.Lignin Amount at Different NaOH Concentrations

9.7 Confirmation of First Order Reaction in Residual Lignin Content

The differential CSTR data showed that the delignification kinetics are well represented by first order in residual lignin calculated as the kappa number minus the permanganate consumption by the hexenuronic acids in pulp. This suggests that the integral approach for the CSTR delignification data should also follow a first order in residual lignin content corrected for the presence of hexenuronic acids. Therefore, the CSTR data in Figure 9.1 was reanalyzed and plotted as $\ln(\frac{L_{C0}}{Lct})$ versus reaction time in Figure 9.13. $\frac{L_{C0}}{Lct}$ is calculated as $\frac{(Kappa_{initial} - HexA/10)}{(Kappa_{time} - HexA/10)}$ The linear behavior in Figure 9.14 confirms that the delignification rate is first order in L_c as was found using the differential approach.

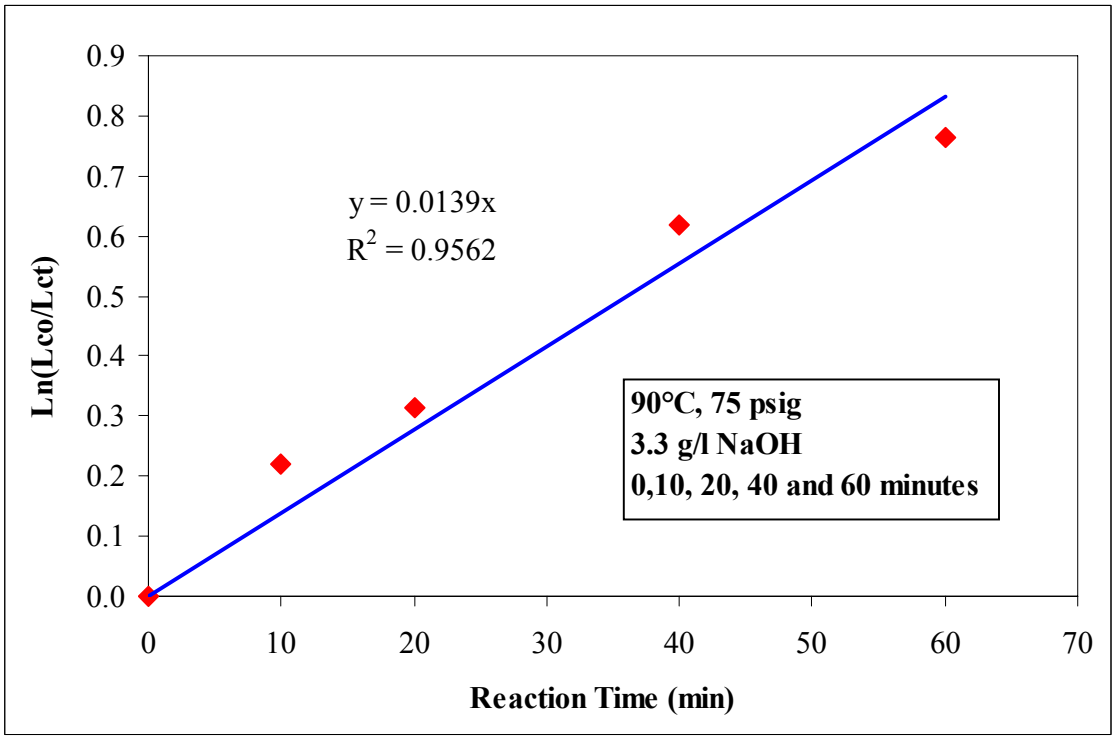

Figure 9.14 $\ln(\frac{L_{C0}}{Lct})$ vs. reaction time for CSTR data

9.8 Conclusion

The rate of delignification is first order in HexA-free residual lignin content of the pulp. Similarly the reaction orders in hydroxide concentration and oxygen pressure are 0.423 and 0.443 respectively. The activation energy of 53.1 kJ/mol is in agreement with a reaction controlled process. It is proposed that the cellulose degradation during oxygen delignification can be described by two contributions: one due to radicals produced by phenolic delignification, and a much smaller contribution due to alkaline hydrolysis. The present kinetic data obtained in the CSTR support two stage oxygen delignification practice of a short higher pressure, lower temperature first stage followed by a longer lower pressure, higher temperature second stage.

CHAPTER 10

MECHANISM OF OXYGEN DELIGNIFICATION

10.1 Introduction

The validity of a kinetic equation is strengthened when it can be derived from a mechanism of elementary reactions. In the previous chapter, we have shown that oxygen delignification is described by a rate equation with reaction orders in L_c, P_{O2} and $[OH^-]$ of 1.0, 0.44 and 0.42 respectively. The first order in L_c suggests that all residual lignin has the same reactivity, in contrast with the earlier proposal of Schoon (1982) and the general consensus that lignin is rather heterogeneous in chemical composition. The objective of this chapter is to provide a mechanistic explanation for the first order dependence on residual lignin content of the delignification rate and for the broken orders in P_{O2} and $[OH^-]$.

10.2 Derivation of Rate Expression

It is well accepted that the first step involving oxygen delignification is the dissociation of phenolic groups in lignin. This first step may be described as equation (10.1).

$$HL^* \leftrightarrow L^{*-} + H^+ \qquad \text{(Equation 10.1)}$$

where HL* represents active lignin sites which can deprotonate to form the anion $L^{*\,-}$ Subsequent abstraction of an electron by oxygen forms a superoxide anion radical and a lignin radical $L^{*\,\cdot}$ as shown in equation (10.2)

$$L^{*-} + O_2 \rightarrow L^{*} \cdot + O_2 \cdot^- \qquad \text{(Equation 10.2)}$$

Assuming that equation (10.2) is the rate determining reaction, the rate expression can be written as equation 10.3:

$$-\frac{dL_C}{dt} = k\left[L*^-\right]\cdot\left[O_2\right]_{ads} \qquad \text{(Equation 10.3)}$$

where $[L*^-]$ is the reactive lignin site concentration

$[O_2]_{ads}$ is the adsorbed oxygen concentration on the reactive lignin sites

The equilibrium constant K_{HL*} of reaction (10.1) is:

$$K_{HL^*} = \frac{\left[L*^-\right]\left[H^+\right]}{\left[HL^*\right]} \qquad \text{(Equation 10.4)}$$

When the total number of active lignin sites is defined as $HL^*_{total} = L^{*-} + HL^*$, it follows that,

$$K_{HL^*} = \frac{\left[L*^-\right]\left[H^+\right]}{\left[HL*_{total}\right]-\left[L*^-\right]} \qquad \text{(Equation 10.5)}$$

Rearranging equation (10.5) gives equation (10.6)

$$\left[L*^-\right] = \frac{K_{HL^*}\left[HL^*_{total}\right]}{\left[H^+\right]+K_{HL*}} \qquad \text{(Equation 10.6)}$$

Since $K_{water} = [H^+]\times[OH^-]$, we can rewrite equation (10.6) as

$$\left[L*^-\right] = \frac{K_{HL^*}\left[HL^*_{total}\right]}{\frac{K_{water}}{\left[OH^-\right]}+K_{HL*}} = \frac{K_{HL^*}\left[HL^*_{total}\right]\left[OH^-\right]}{K_{water}+K_{HL*}\left[OH^-\right]} \qquad \text{(Equation 10.7)}$$

Inserting equation (10.7) in equation (10.3) gives

$$-\frac{dL_C}{dt} = k\frac{K_{HL^*}\left[HL^*_{total}\right]\left[OH^-\right]\left[O_2\right]_{ads}}{K_{water}+K_{HL*}\left[OH^-\right]} \qquad \text{(Equation 10.8)}$$

If it is now assumed that the active sites are uniformly distributed throughout the residual lignin L_c, then $[HL^*_{total}] = C \cdot L_c$, where C is a proportionality constant. Thus, equation (10.8) becomes

$$-\frac{dL_C}{dt} = K_C \frac{[OH^-][O_2]_{ads}}{K_{water} + K_{HL^*}[OH^-]} Lc \qquad \text{(Equation 10.9)}$$

where the constant $K_c = k \cdot K_{HL^*} \cdot [HL^*_{total}] \cdot C$

Equation (10.9) indicates that the rate of delignification is first order in residual lignin Lc. with the reaction constant of $K_C \frac{[OH^-][O_2]_{ads}}{K_{water} + K_{HL^*}[OH^-]}$. Thus, the reaction rate constant (slope of the experimental curve) listed in Table 10.3 is equal to

$$slope = K_C \frac{[OH^-] \cdot [O_2]_{ads}}{K_{water} + K_{HL} \cdot [OH^-]} \qquad \text{(Equation 10.10)}$$

Equation (10.10) indicates that when $[OH^-]$ is very high, the reaction order in $[OH^-]$ approaches zero; on the other hand, when the $[OH^-]$ is close to zero, the reaction order in $[OH^-]$ becomes first order. By taking the inverse of equation (10.10), we obtain

$$\frac{1}{slope} = \frac{K_{HL^*}}{K_C[O_2]_{ads}} + \frac{K_{water}}{K_C[O_2]_{ads}} \cdot \frac{1}{[OH^-]} \qquad \text{(Equation 10.11)}$$

The terms $\frac{K_{HL^*}}{K_C[O_2]_{ads}}$ and $\frac{K_{water}}{K_C[O_2]_{ads}}$ are constants when the temperature and oxygen pressure are kept constant. Thus, by plotting 1/slope versus $1/[OH^-]$ at constant temperature and oxygen pressure, but variable $[OH^-]$ concentrations, a linear relationship should obtained.

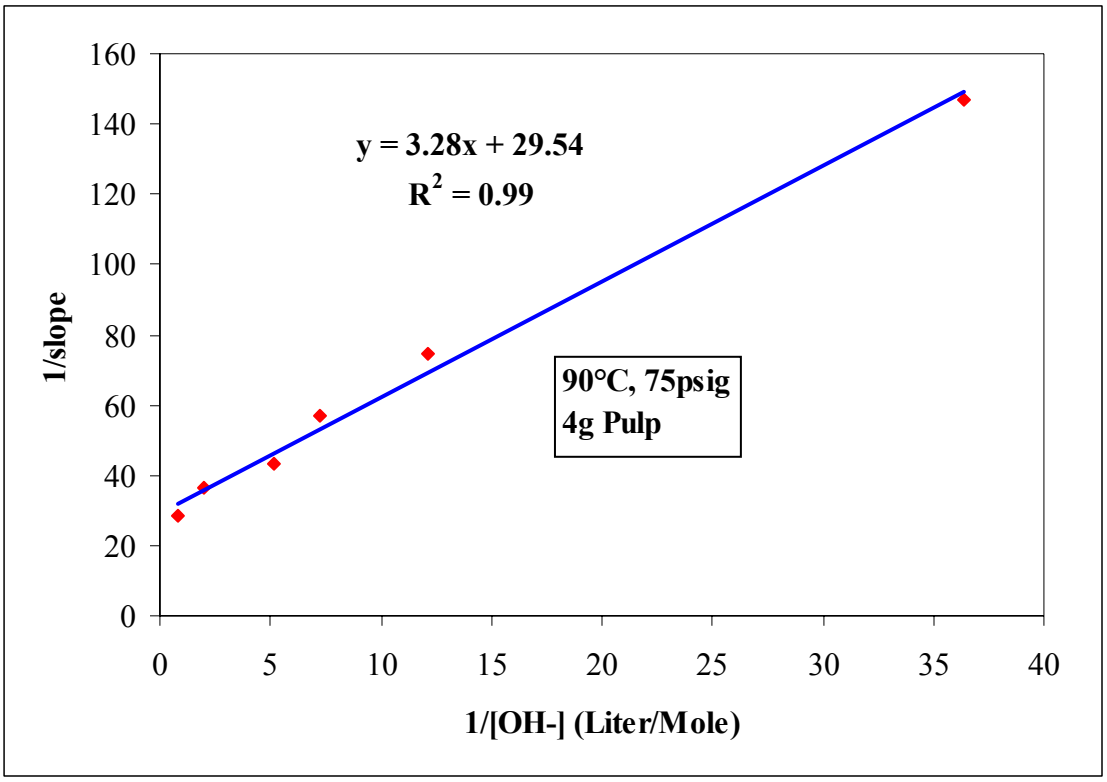

Figure 10.1 1/slope vs. 1/[OH^-]

From Figure 10.1, one obtains that $\frac{K_{HL^*}}{K_C[O_2]_{ads}} = 29.54$ and $\frac{K_{water}}{K_C[O_2]_{ads}} = 3.28$ or $K^*_{HL} = 9.01 \cdot K_{water}$.

Table 10.1 lists the pKa of water, -log(K_{water}), at different temperatures (Reeves, 1972). Using the relationship $K^*_{HL} = 9.01 \cdot K_{water}$, the corresponding pKa of the active lignin sites are calculated at different temperatures. The results in Table 10.1 show that the pKa of the active lignin sites is one unit lower than that of water, i.e, at 25°C the pKa is 13 and at 90°C it is 11.5. These values for pKa of the active lignin sites are in agreement with the fact that oxygen delignification is performed at an initial NaOH concentration of about 0.1mol/liter.

Table 10.1 Temperature Effect of lignin pKa values

T (°C)	pKw	pKa of Active Lignin
0	14.94	13.99
10	14.53	13.58
20	14.17	13.21
25	14.00	13.04
30	13.83	12.88
40	13.54	12.58
50	13.26	12.31
60	13.07	12.12
70	12.84	11.88
80	12.61	11.66
90	12.40	11.45
100	12.29	11.34
110	12.01	11.06
115	11.92	10.97

In order to include the effect of oxygen pressure in equation (10.8), a relationship must be derived between $[O_2]_{ads}$ and P_{O2}. This is done using the following assumptions:

(1) The adsorbed oxygen concentration, $[O_2]_{ads}$, obeys a Langmuir type adsorption isotherm;

(2) The total number of adsorption sites is constant;

(3) The adsorption/desorption equilibrium can be described by equation (10.12). The adsorption and desorption of oxygen from the active lignin sites is much faster than the actual delignification reaction, i.e. $[O_2]_{ads}$ is at quasi-equilibrium.

$$HL^{*-} + O_{2\,dis} \leftrightarrow O_{2\,ads} \qquad \text{(Equation 10.12)}$$

where O_{2dis} is oxygen dissolved in the caustic solution.

At quasi-equilibrium, the adsorption rate, $r_a = k_a [\mathrm{HL}^{*-}][\mathrm{O}_2]_{dis}$ is equal to the desorption rate, $r_d = k_d [\mathrm{O}_2]_{ads}$.

Since the total number of active sites is constant, i.e. $[HL^{*-}]+[O_2]_{ads} = C_t$, it may be derived that

$$[O_2]_{ads} = \frac{K_e C_t [O_2]_{dis}}{1 + K_e [O_2]_{dis}} \qquad \text{(Equation 10.13)}$$

$$\text{where} \quad K_e = \frac{k_a}{k_d}$$

Equation 10.13 shows that when $[O_2]_{dis}$ is very large, the reaction is zero order in dissolved oxygen concentration, while it is first order in dissolved oxygen concentration at very low oxygen concentration.

The dissolved oxygen concentration may be obtained from Figure 10.2.

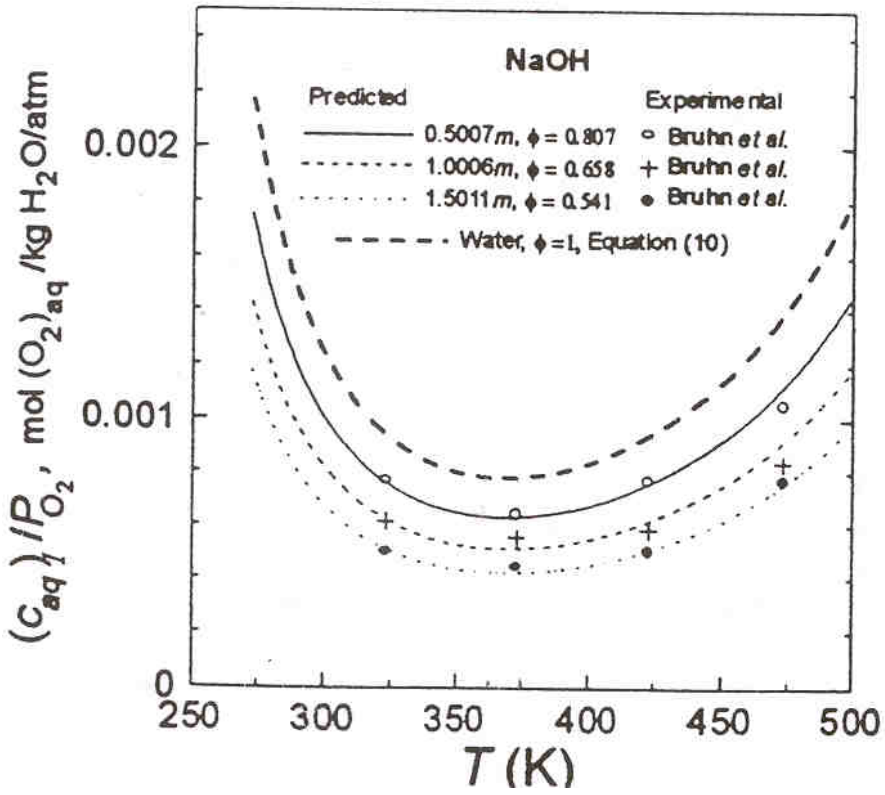

Figure 10.2 Dissolved Oxygen Concentration Prediction (Tromans, 1998)

Figure 10.2 shows the Henry coefficient of dissolved oxygen in alkaline solutions at different concentrations and different temperatures. It can be seen that the saturated dissolved oxygen concentration decreases with increasing caustic concentration. For the present experiments, the caustic concentration is generally significantly smaller than 0.5 molar (20g/l), i.e. the Henry coefficient is close to that of water. Figure 10.3 also shows that the Henry coefficient is almost independent of temperature over the range of the present experiments from 353 to 388K. Thus the saturated oxygen concentration at normal alkali concentrations can be calculated using equation

$$[O_2]_{dis} = 4.4 \times 10^{-5} \times P_{O2} \qquad \text{(Equation 10.14)}$$

where $[O_2]_{dis}$ expressed in mol/l and P_{O2} in psia.

Table 10.2 shows the saturated oxygen concentration at different oxygen partial pressures for the present experiments performed at 90°C. P_{H2O} is the saturated steam pressure at 90°C.

Table 10.2 Oxygen Concentrations at Different Partial Pressures at 90°C.

P_{total} (psig)	**P_{O2} (=P_{total}+14.7-P_{H2O}) at 363K, (psia)**	**O_2 Concentration (mol/l)**
35	39.5	0.001748
55	59.5	0.002632
75	79.5	0.003517
95	99.5	0.004401

Inserting equation (10.13) into equation (10.8) gives

$$-\frac{dL_C}{dt} = k \cdot K_{HL*} C \cdot K_e C_t \frac{[OH^-]}{K_{water} + K_{HL*}[OH^-]} \cdot \frac{[O_2]_{dis}}{1 + K_e [O_2]_{dis}} \cdot L_C \qquad \text{(Equation 10.15)}$$

Using the linear relationship between P_{O2} and $[O_2]_{dis}$, equation (10.15) can be rewritten as

$$-\frac{dL_C}{dt} = C_1 \frac{[OH^-]}{K_{water} + K_{HL*}[OH^-]} \cdot \frac{P_{O2}}{1 + K_e P_{O2}} \cdot L_C \qquad \text{(Equation 10.16)}$$

$$\text{where } C_1 = k \cdot K_{HL*} C \cdot K_e C_t$$

At constant temperature and $[OH^-]$, equation (10.16) can be simplified to

$$-\frac{dL_C}{dt} = C_2 \frac{P_{O2}}{1 + K_e P_{O2}} \cdot L_C \qquad \text{(Equation 10.17)}$$

where C_2 is a constant.

For the four conditions listed in Table 10.2, the slope of plots of $-\frac{dL_C}{dt}$ versus L_c for these experiments may be used to calculate K_e using equation (10.18)

$$slope = C_2 \frac{P_{O2}}{1 + K_e P_{O2}} \text{ or } \frac{1}{slope} = \frac{K_e}{C_2} + \frac{1}{C_2 P_{O2}} \qquad \text{(Equation 10.18)}$$

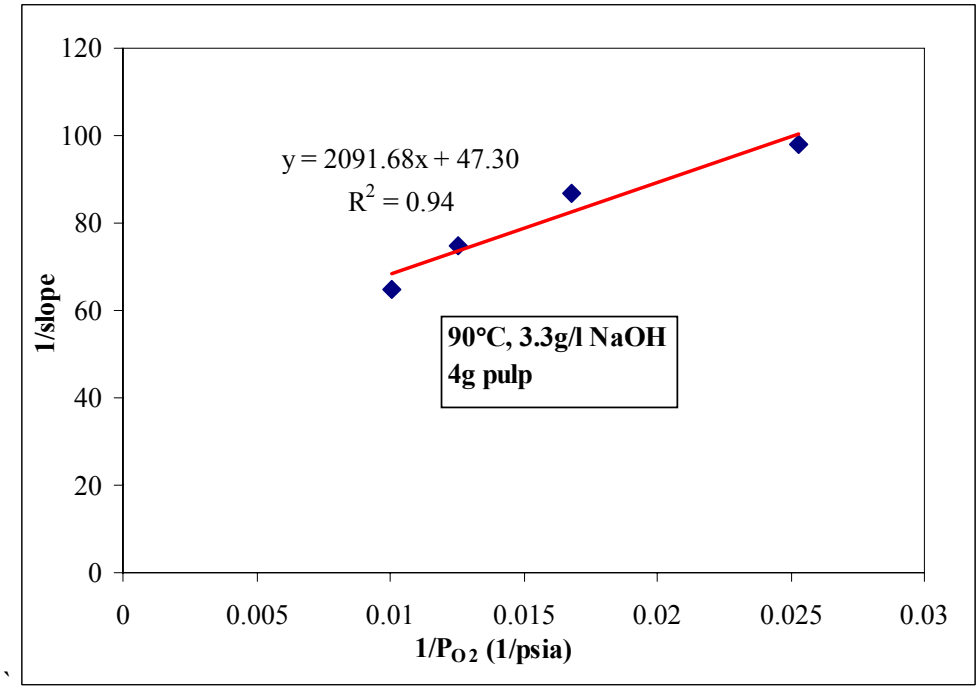

Figure 10.3 1/slope vs. $1/P_{O2}$

It can be seen from Figure 10.3 that a relative straight line behavior is obtained when plotting 1/slope versus $1/P_{O2}$. This supports the assumption that $[O_2]_{ads}$ is governed by a Langmuir-type adsorption. The value of K_e obtained from Figure 10.3 is

$$K_e = 47.30/2091.68 = 2.26\times10^{-2} \quad (1/\text{psia})$$

Finally the constant C_1 in equation (10.16) must be calculated using all the CSTR experiments performed at 90°C. Shown in Table 10.3 are the values of C_1 for all the 90°C experiments.

Table 10.3 Values of C1 for all the 90°C experiments in CSTR

Temperature (°C)	**Pressure (psig)**	**NaOH (g/liter)**	**NaOH (mol/liter)**	**Partial P_{O2} (psia)**	**Slope of Curve**	**Value of C_1**	**Calcu. K_L (1/min)**
90	35	3.3	0.083	39.5	0.0102	1.15E-03	0.0105
90	55	3.3	0.083	59.5	0.0115	1.06E-03	0.0128
91	75	3.3	0.083	79.5	0.0134	1.11E-03	0.0143
93	95	3.3	0.083	99.5	0.0154	1.18E-03	0.0154
89	75	1.1	0.028	79.5	0.0068	1.20E-03	0.0067
93	75	5.5	0.138	79.5	0.0176	1.12E-03	0.0186
93	75	7.7	0.193	79.5	0.0232	1.29E-03	0.0213
90	75	20	0.50	79.5	0.0273	1.17E-03	0.0275
89	75	50	1.25	79.5	0.0353	1.35E-03	0.0308

Based on Table 10.3, the average value of C_1 is 1.18×10^{-3} with standard derivation of 0.09×10^{-3}. Thus, the final oxygen delignification kinetic equation at 90°C is

$$-\frac{dL_C}{dt} = 1.18\times10^{-3}\,\frac{[OH^-]}{0.111+[OH^-]}\cdot\frac{P_{O2}}{1+2.26\times10^{-2}P_{O2}}\cdot L_C \qquad \text{(Equation 10.19)}$$

with $\frac{dL_C}{dt}$ expressed in mg lignin/g pulp/min, $[OH^-]$ in mol/L and P_{O2} in psia.

Based on equation (10.19), a first order reaction rate constant K_L can be defined as

$$K_L = 1.18\times10^{-3}\frac{[OH^-]}{0.111+[OH^-]}\cdot\frac{P_{O2}}{1+2.26\times10^{-2}P_{O2}} \qquad \text{(Equation 10.20)}$$

Figure 10.4 shows the comparison of the measured reaction rate constant (slope of the experimental curve) listed in Table 10.3) and predicted reaction rate constant (K_L). The correlation shows that the prediction of the rate constant is good. However, the slope of the linear relationship is 1.04, which indicates that the predicted K_L is a slightly lower than the measured reaction rate constant. The explanation of this phenomenon is some of the experiments were performed at 1~3 degrees higher than desired temperatures which increases the rate constant.

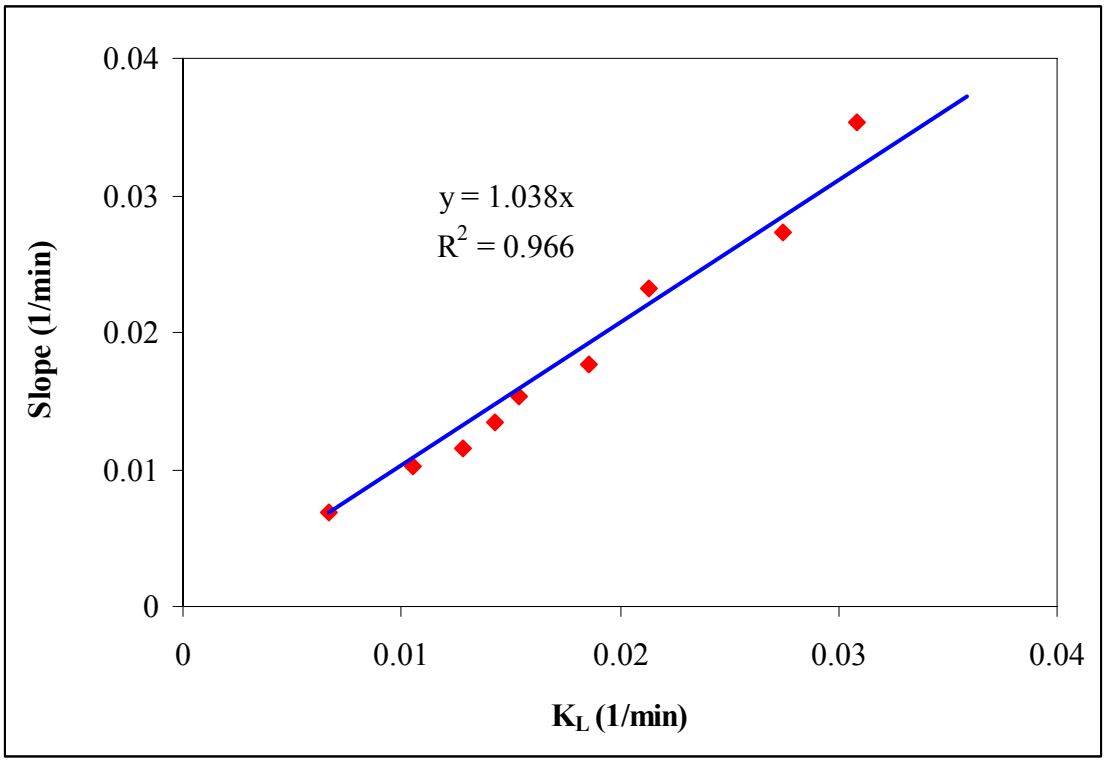

Figure 10.4 Slope vs. Predicted Reaction Rate Constant K_L

Integration of equation (10.19) at constant $[OH^-]$ and P_{O2} gives equation (10.21)

$$L_{ct} = L_{c0} \cdot e^{-K_L \cdot t} \qquad \text{(Equation 10.21)}$$

For the experiments listed in Table 10.3, the final kappa number, K_t, can be calculated as

$$K_t = (K_0 - \frac{HexA}{10}) \cdot e^{-K_L \cdot t} + \frac{HexA}{10} \qquad \text{(Equation 10.22)}$$

where K_0 is the original kappa number

K_L is the model predicted reaction rate constant

HexA is the hexenuronic acid content of the pulp (μmol/g)

The predicted kappa number using equation (10.22) is compared with the measured kappa number in Table 10.4.

Table 10.4 Predicted Kappa and Measured Kappa for all 90°C Experiments

Temperature (°C)	**temp (K)**	**Pressure (psig)**	**NaOH (g/liter)**	**Predicted Kappa from Eq. (10.22)**	**Measured Kappa**
90	363	35	3.3	14.5	14.4
90	363	55	3.3	13.0	13.1
91	363	75	3.3	12.0	12.5
93	363	95	3.3	11.4	11.0
89	363	75	1.1	17.6	16.3
93	363	75	5.5	9.9	10.9
93	363	75	7.7	8.8	9.4
90	363	75	20	5.8	8.1
89	363	75	50	4.7	5.1

The data in Table 10.4 shows that the predicted kappa numbers using equation (10.22) are close to the measured kappa numbers for most experiments. However, the predicted kappa numbers are lower than the measured kappa numbers at high caustic concentrations. Part of the explanation may be that the dissolved oxygen concentration at

higher NaOH concentration is lower (see Figure 10.2) while this was not taken into account in Equation (10.19). Figure 10.2 shows the Henry coefficient of oxygen at 1.25 molar NaOH or a concentration of 50g/l is about 30% lower than that of 0.08 molar NaOH or 3.3g/l solutions. The overestimated dissolved oxygen concentration leads to lower kappa number prediction. The slightly lower HexA content of the pulps obtained after severe oxygen delignification will not have a significant effect on the predicted kappa number (< 0.5 kappa unit).

Figure 10.5 shows the measured kappa versus predicted kappa using equation (10.22). The relative good linear correlation suggests that the predicted kappa numbers are close to experimental data.

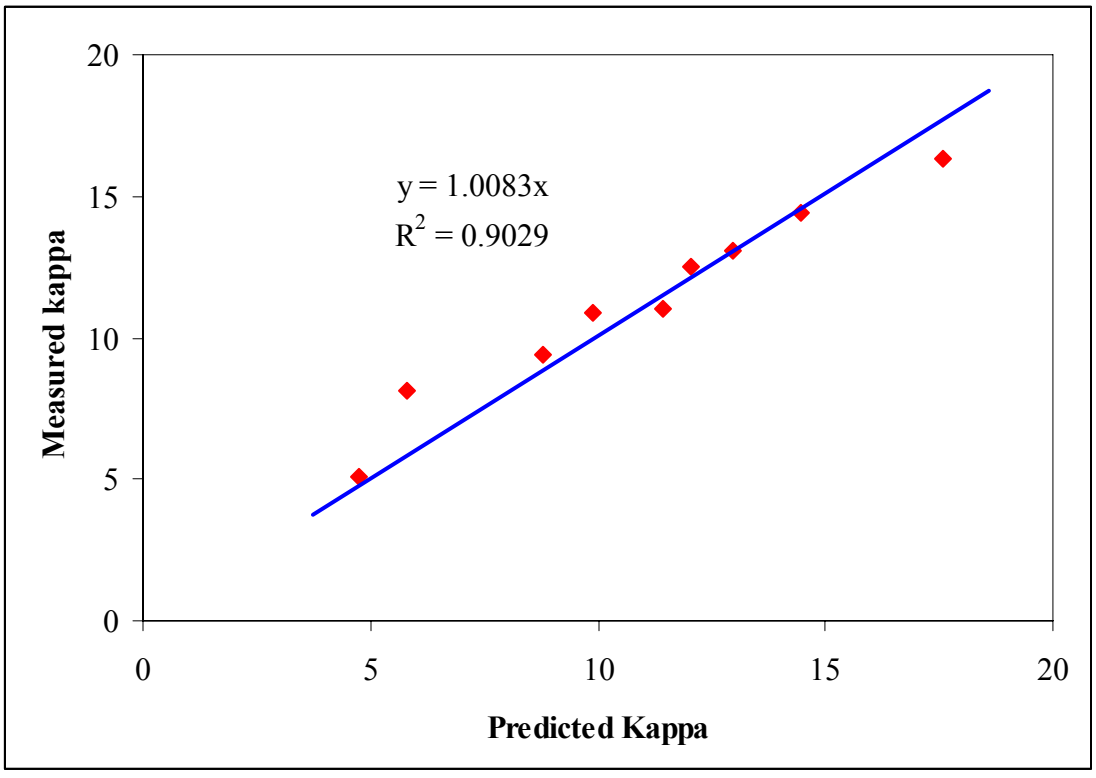

Figure 10.5 Slope vs. Predicted Reaction Rate Constant K_L

10.3 Phenolic Hydroxyl Group Content of Pulp and Waste Liquor Samples

The phenolic group content of isolated residual lignin for different oxygen delignified pulps was determined to verify the proposed mechanism. The phenolic group content of the liquor samples taken at different times was also measured by double beam UV. The phenolic group content of pulp samples and liquor samples are listed in Table 10.5 and Table 10.6 respectively. The phenolic group content of residual lignin expressed in mmol/g lignin and as a fraction of C9 monomer units, and the phenolic group content of the pulp sample expressed in mmol/g pulp are calculated using equations (10.23), (10.24) and (10.25) respectively.

$$\left[\text{Ph - OH}^{-}\right] = \frac{0.25 \times \left[A_{300}(\text{Alk}) - A_{300}(\text{Neu})\right] + 0.107\left[A_{350}(\text{Alk}) - A_{350}(\text{Neu})\right]}{\text{Lignin Concentration(g/liter)}} \quad \left(\frac{\text{mmol}}{\text{g Lignin}}\right)$$

(Equation 10.23)

$$\text{Phenolic Fraction} = \left[\text{Ph} - \text{OH}^{-}\right] \times \frac{185g}{mol} \times \frac{1mole}{1000mmoles} \qquad \text{(Equation 10.24)}$$

$$\text{Ph - OH in Pulp} = \left[\text{Ph} - \text{OH}^{-}\right] \times \left[\text{Klason Lignin}\right] \quad \left(\frac{\text{mmol}}{\text{g pulp}}\right) \qquad \text{(Equation 10.25)}$$

$$\text{Ph - OH in Liquor} = \left[\text{Ph} - \text{OH}^{-}\right] \times \left[\text{Dissolved Lignin}\right] \times \text{Flow Rate} \times \Delta\text{Time} \quad \left(\frac{\text{mmol}}{\text{g pulp}}\right)$$

(Equation 20.26)

Table 10.5 Phenolic Group Content of Residual Lignin in Different Pulps

Reaction Time (min)	Ph-OH in Pulp (mmol/g lignin)	Ph-OH Fraction	Klason Lignin (mg/g pulp)	Ph-OH in Pulp (mmol/g pulp)
0	2.23	0.41	38.9	0.0867
10	2.10	0.39	35.0	0.0736
20	1.80	0.33	29.2	0.0525
40	1.61	0.30	27.8	0.0447
60	1.44	0.27	20.2	0.0291
180	1.19	0.22	11.9	0.0141

Table 10.5 shows that the original residual lignin has 2.23 mmol phenolic group/g lignin and that after 3 hours oxygen delignification at 90°C, 75psig and 3.3g/l, the phenolic group content decreases by almost of a factor 2. The phenolic fraction of lignin in the original pulp of 0.41 and of 0.27 after 60 minutes agrees with values reported in literature (Rööst et al, 2003).

The phenolic group content and phenolic group fraction of the dissolved lignin of the effluent samples as well as the total amount of phenolic groups removed with the liquor in mmol/g pulp calculated using equation (10.26) at different times are shown in Table 10.6.

Table 10.6 Phenolic Group Content of Dissolved Lignin in Waste Liquor Samples at Different Times

Reaction Time (min)	**Ph-OH from Pulp (mmol/g lignin)**	**Ph-OH Group Fraction**	**Total Amount of Ph-OH Removed with Liquor (mmol/g pulp)**
5	2.01	0.37	0.0021
7	3.38	0.62	0.0087
12	2.15	0.40	0.0164
20	1.42	0.26	0.0246
30	1.34	0.25	0.0325
40	1.27	0.23	0.0397
50	1.03	0.19	0.0450
60	1.39	0.26	0.0501

It can be seen that the phenolic group content of the dissolved lignin in the liquor samples increases from an initial value of about 2.3 mmol/g lignin at the beginning of the reaction to a maximum of 5 mmol/g lignin and then decreases to about 2.5 mmol/g lignin at 60 minutes. The phenolic fraction of the dissolved lignin in the effluent approaches almost 1.0 at 20 minutes of reaction. This implies that the dissolved lignin is mostly monomeric or dimeric in character.

Figure 10.6 shows the total amount of phenolic groups removed with the liquor and the total amount of phenolic group remaining in the pulp at different reaction times. The sum of the total amount of phenolic groups remaining in the pulp and removed with the liquor at different times is also shown.

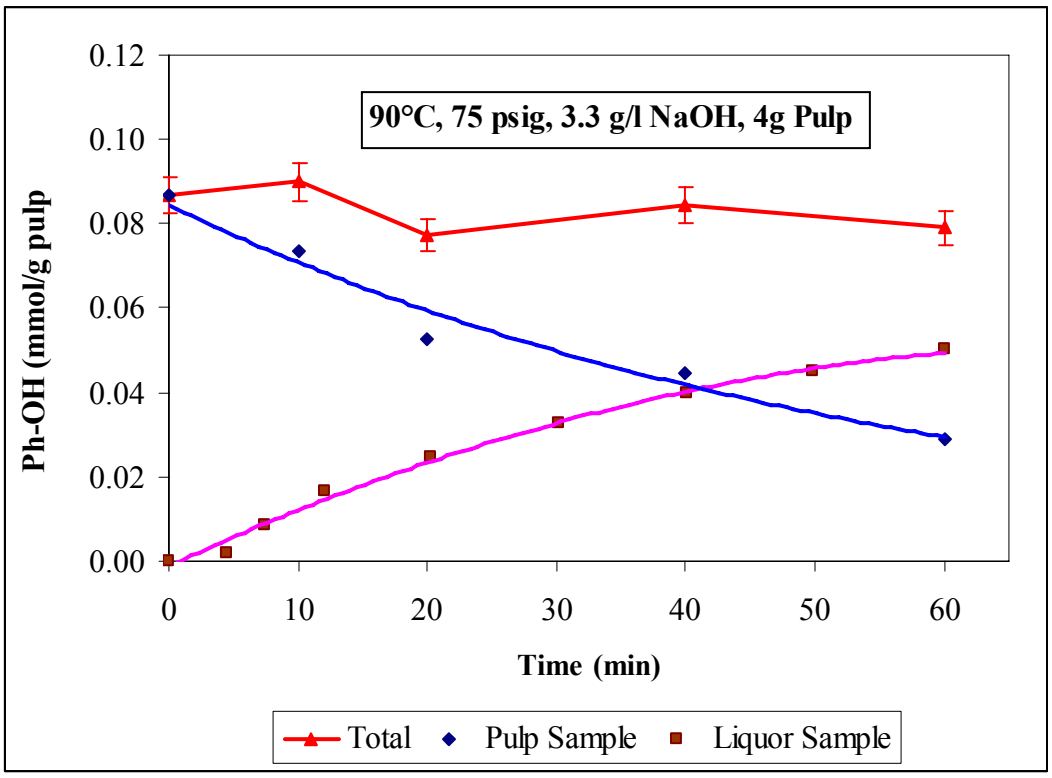

Figure 10.6 Phenolic Group Content of Liquor and Pulp Samples at Different Reaction Times

Figure 10.7 shows that the reduction in the amount of phenolic groups in the pulp is nearly equal to the amount of phenolic groups removed with the liquor during the same reaction time since the sum of phenolic groups does not change significantly. This implies that aromatic ring opening is not a significant delignification reaction in oxygen delignification, and that cleavage of lignin unit linkages which lead to the formation of new phenolic groups is also not important.

10.4 Nature of the Lignin Active Sites

Table 10.1 shows that the pKa value of the active lignin sites is 11.5 at 90°C. This compares to pKa values for industrial lignins ranging from 10.5 to 11.5 at 25°C(Lindberg, 1959; Woerner and McCarthy, 1987) and for phenolic lignin model compounds ranging from 6.2 to 11.3 at 25°C (Ragnar et al, 2000). The effect of temperature on the pKa values of guaiacyl and syringyl derived phenols and lignin sample have not been reported in literature. The present calculated pKa value of 13 at 25°C is 2 units higher than that normally reported for phenolic lignin. The implication is that the active lignin site is not the phenolic group, but another less acidic site which also must be uniformly distributed throughout the residual lignin to satisfy the first order in lignin rate behavior.

Hou-min Chang et al reported some possible reactions of lignin model compounds with oxygen at alkaline conditions (1980). Figure 10.7 shows the process of ionization of lignin models and cyclohexadienone hydroperoxide which is formed by attack of oxygen at alkaline conditions modified from Hou-min Chang's paper (1980).

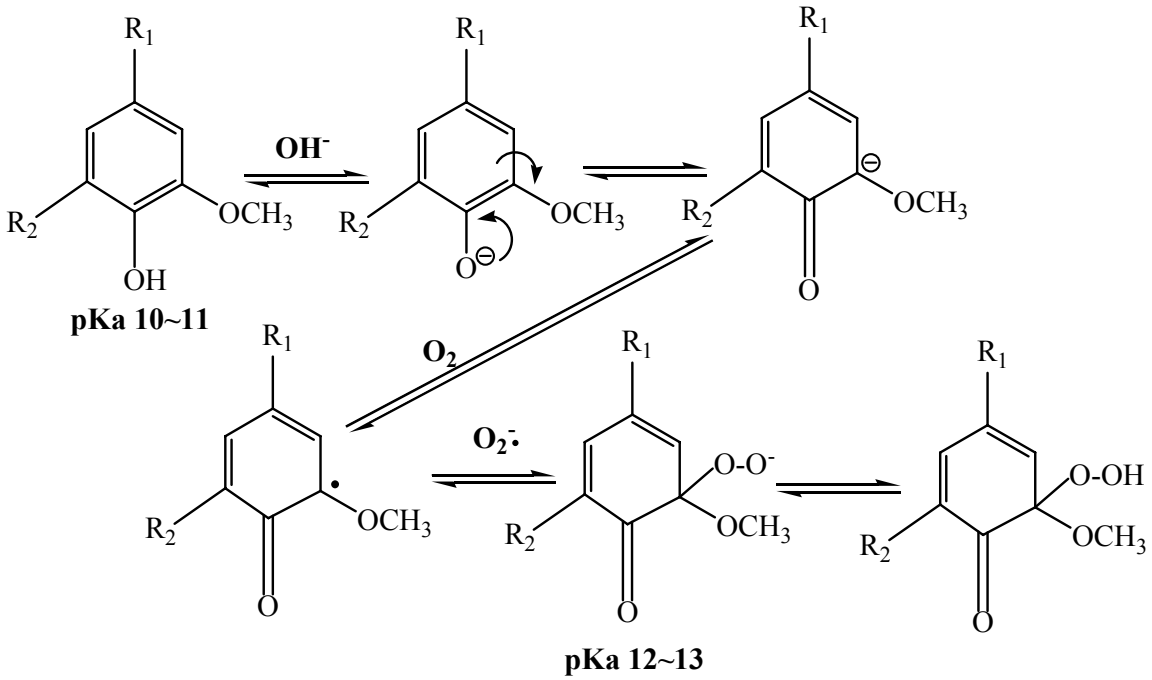

Figure 10.7 Ionization of Lignin Models and Cyclohexadienone Hydroperoxides Formed by Attack of Oxygen (Adopted from Chang, et al 1980)

Because oxygen is a biradical, a singlet state can be formed from triplet state by either reversing the spin on one of the unpaired electrons or by reduction. It can be seen in Figure 10.7 that a hydroperoxide anion is formed by reaction of superoxide radical anion with the phenolate radical. It is interesting to note that the cyclohexadienone hydroperoxide exhibits a pKa of 12~13 (Chang et al, 1980). Margaret et al (2003) used computational methodology to calculate the enthalpies of reactions for the ligninw models. Their results suggest that the reaction pathway in Figure 10.7 is reasonable.

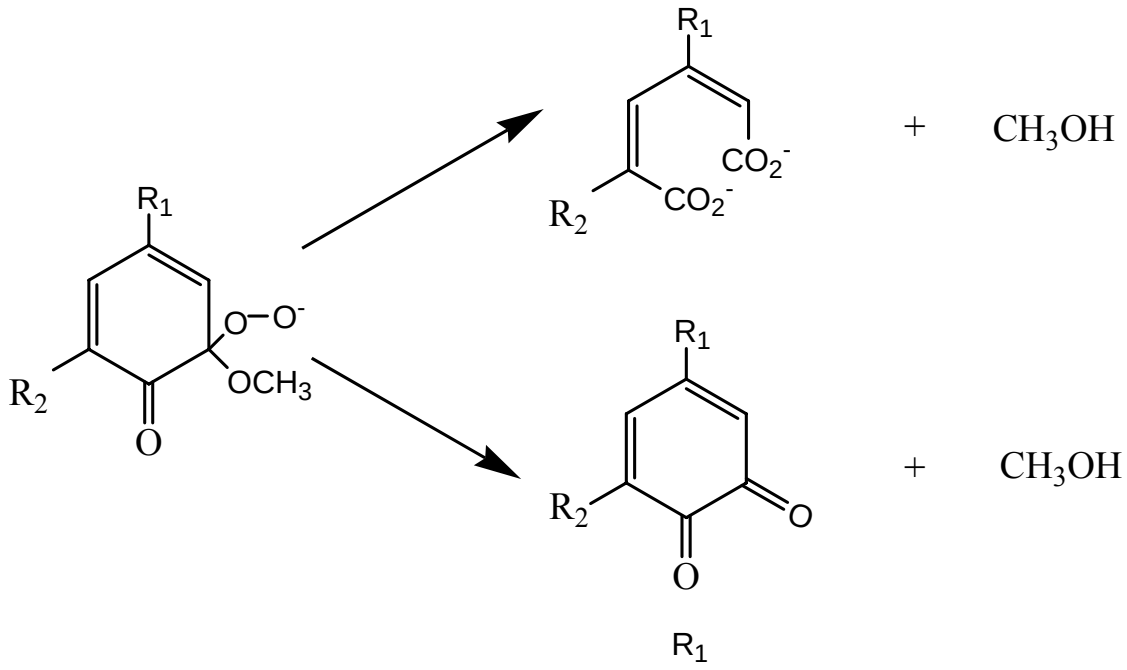

Figure 10.8 Homolytic and Heterolytic Fragmentation of Para-cyclohexadienone Hydroperoxides (Adopted from Chang et al, 1980)

Figure 10.8 shows the further fragmentation of the cyclohexadienone hydroperoxide as proposed by Chang et al (1980). It can be seen that the hydroperoxide anion forms either a muconic acid structure and methanol or an orthoquinone structure and methanol. Since the hydroperoxide anion is the dominant species at pH>12~13, the present kinetics suggests that the carbon at the 3 position of the lignin aromatic ring is the active site for adsorption of oxygen. Subsequently the adsorbed oxygen undergoes an electrophilic reaction with the 3 carbon to form the hydroperoxide anion. This reaction determines the overall rate of oxygen delignification. Further support for this hypothesis is that methoxyl groups are present in almost all residual softwood lignin monomer units, thus satisfying the uniform reactivity required for first order delignification kinetics.

10.5 Relationship of Delignification rate and Methanol Formation Rate

Figure 10.8 shows that the fragmentation of the hydroperoxide active sites leads to equimolar formation of methanol. Table 10.7 shows the methanol concentration in effluent samples collected at reaction time 4, 7. 12, 20, 30, 40, 50 and 60 minutes for different oxygen delignification experiments. The methanol formation rate was calculated from the data in Table 10.7 using equation (5.5).

Table 10.7 Methanol Concentrations of the Liquor Samples of Different Experiments

Sample	**Other operating conditions are 90C, 3.3g/l and 75 psig if not specified.**										
Flow Rate (ml/min)	**Methanol (ppm) measured by GC-HS**										
	59.8	**75.1**	**66.9**	**68.8**	**77.8**	**66.4**	**68.4**	**70.4**	**75.8**	**63.8**	**71.2**
Time (min)	**1.1g/l**	**3.3 g/l**	**5.5 g/l**	**7.7 g/l**	**80°C**	**100°C**	**110°C**	**115°C**	**35 psig**	**55 psig**	**95 psig**
4	2.5	3.2	3.2	3.8	2.8	2.5	4.0	4.8	2.5	2.9	3.1
7	3.5	3.4	3.6	4.0	2.9	3.8	5.5	6.6	2.7	3.1	3.2
12	3.5	4.0	3.8	3.9	2.9	4.6	6.6	7.0	2.7	3.4	3.5
20	2.8	3.9	3.6	3.6	2.9	4.3	6.7	5.8	2.5	3.2	3.4
30	2.4	3.5	3.1	2.9	2.8	3.9	4.7	4.3	2.3	2.9	3.1
40	2.1	2.9	2.4	2.5	2.5	3.6	3.8	3.8	2.1	2.4	2.8
50	2.1	2.5	2.4	2.3	2.0	3.2	3.2	3.4	2.0	2.3	2.3
60	2.0	2.3	2.3	2.0	1.7	2.9	2.9	3.1	2.0	2.1	2.0

The dissolved lignin concentrations of the same samples in Table 10.7 are listed in Table 10.8. The delignification rate is calculated from these data using equation (5.5)

Table 10.8 Dissolved Lignin Concentrations of the Liquor Samples of Different Experiments at Different Times

Sample	**Other operating conditions are 90C, 3.3g/l and 75 psig if not specified.**										
Flow Rate	**Dissolved Lignin (mg/liter) measured by UV-VIS at 280nm using Indulin AT as Calibration Standard**										
(ml/min)	**59.8**	**75.1**	**66.9**	**68.8**	**77.8**	**66.4**	**68.4**	**70.4**	**75.8**	**63.8**	**71.2**
Time (min)	**1.1g/l**	**3.3 g/l**	**5.5 g/l**	**7.7 g/l**	**80°C**	**100°C**	**110°C**	**115°C**	**35 psig**	**55 psig**	**95 psig**
4	12.24	11.91	18.52	23.52	8.45	9.91	24.34	30.24	15.44	12.20	11.63
7	13.63	18.69	26.34	30.96	13.56	22.18	38.78	46.41	15.99	19.78	20.68
12	13.52	19.72	28.80	32.29	15.44	27.85	48.05	54.16	14.20	21.78	23.22
20	11.27	17.95	26.15	28.48	12.43	27.61	45.15	46.60	12.15	20.49	21.71
30	10.05	15.87	20.97	22.37	10.45	23.36	31.14	28.81	11.09	17.65	17.63
40	9.33	12.95	17.06	16.09	9.35	18.94	19.22	18.01	11.14	14.83	14.27
50	8.66	10.58	13.29	11.84	7.20	15.42	12.53	11.99	10.18	12.58	11.14
60	7.84	8.46	10.47	8.19	6.20	12.38	8.87	8.48	8.50	10.57	8.92

Shown in Figure 10.9 is the $\frac{\text{Methanol Formation Rate}/32}{\text{Delignification Rate}/185}$ versus time for the 90°C, 75 psig total pressure experiments performed at different NaOH concentrations. It can be seen that the $\frac{\text{Methanol Formation Rate}/32}{\text{Delignification Rate}/185}$ molar ratio increases from an initial value of about 0.6 to about 0.8 at 30 minutes. Then the ratio increases further at the higher NaOH concentrations.

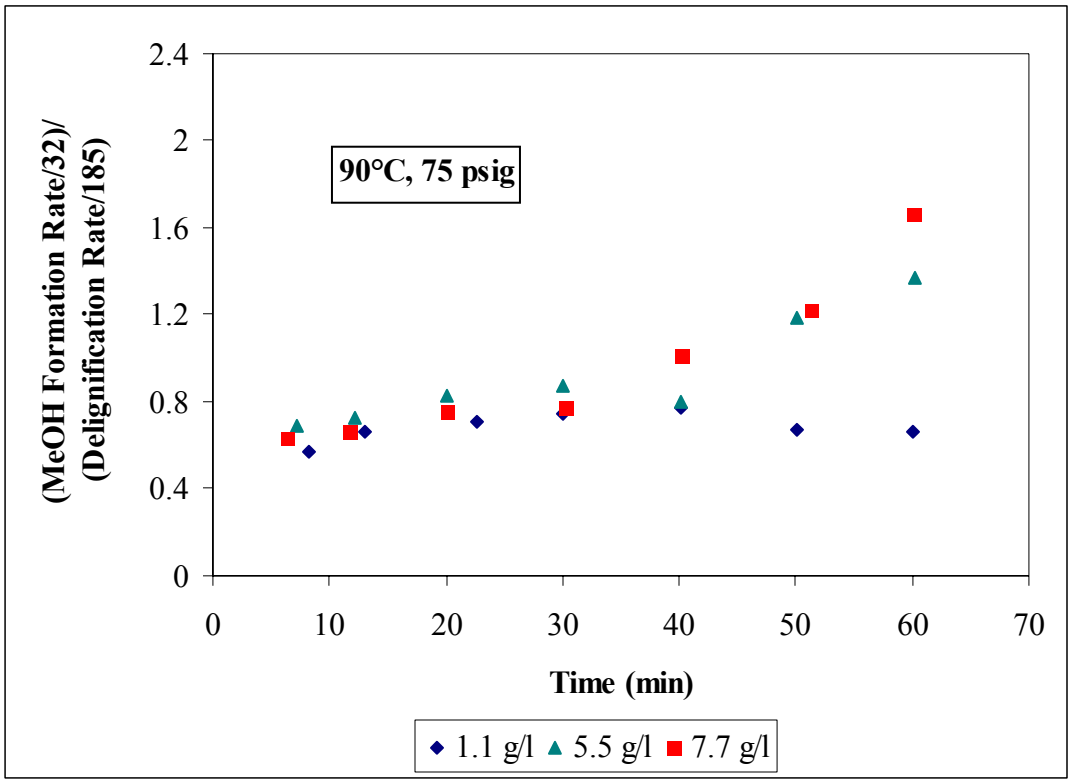

Figure 10.9 $\frac{\text{Methanol Formation Rate}/32}{\text{Delignification Rate}/185}$ versus time of at different [NaOH]

Figure 10.10 shows the ratio $\frac{\text{Methanol Formation Rate}/32}{\text{Delignification Rate}/185}$ versus time of the liquor samples at different total pressures. It can be seen that the ratio is mostly about 0.9±0.2 which supports that methanol is released essentially quantitatively from lignin monomer units when they are solubilized during oxygen delignification.

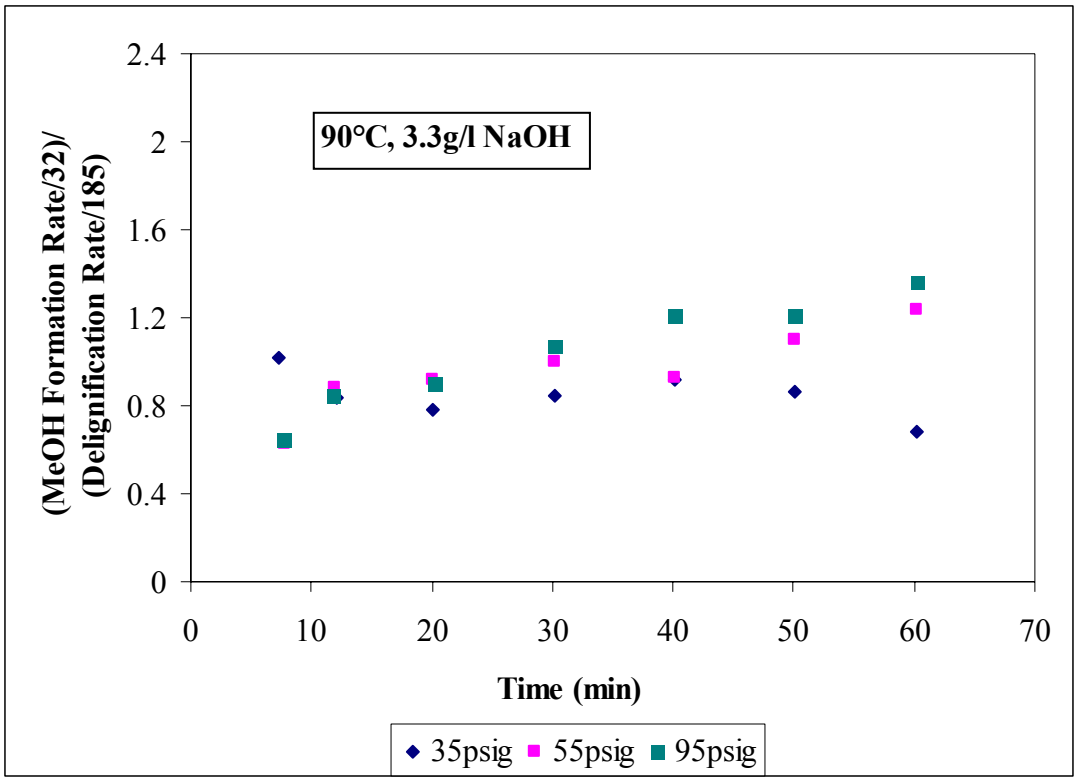

Figure 10.10 $\frac{\text{Methanol Formation Rate}/32}{\text{Delignification Rate}/185}$ versus time of at different Total Pressures

Figure 10.11 shows $\frac{\text{Methanol Formation Rate}/32}{\text{Delignification Rate}/185}$ versus time of liquor samples at different temperatures. Again most of the data is around 0.9±0.2. However, the molar ratio increases beyond this range at the highest temperatures from 40 to 60 minutes. The reason for the apparent high degree of demethoxylation rate at the end of high temperature oxygen delignification is not clear at the present time. Perhaps the precision of the methanol concentration data is low at the present low concentrations.

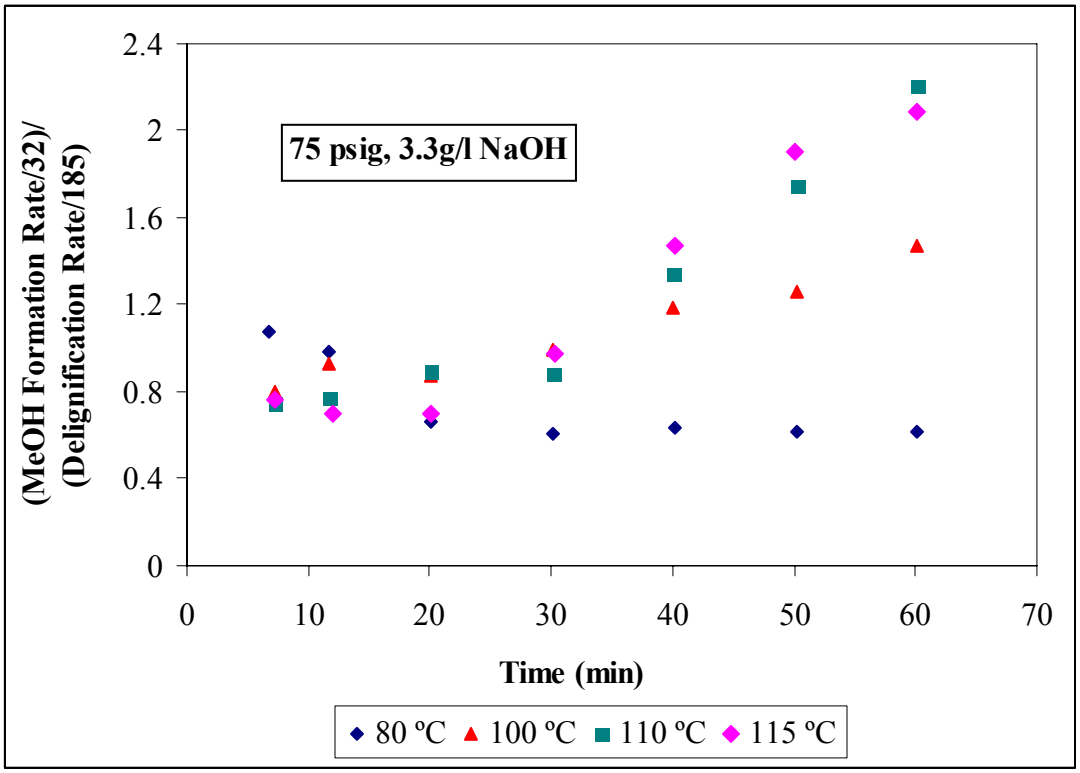

Figure 10.11 $\frac{\text{Methanol Formation Rate}/32}{\text{Delignification Rate}/185}$ versus time of at different Temperatures

10.6 Effect of Ethylene Glycol Caustic Solution

In Table10.9, the properties of pulps obtained in caustic and ethylene glycol-water fed CSTR experiments are shown.

Table 10.9 Pulp Properties of Regular and Ethylene Glycol Treated Samples in CSTR

(Operating Conditions: 90°C, 3.3g/l NaOH, 75psig O_2)

Sample	Kappa	Intrinsic Viscosity (ml/g)	Ph-OH (mmol/g)	Yield (%)	HexA (µmol/g)	Klason Lignin (%)	Acid Soluble Lignin(%)
Original	24.4	1189	2.23±0.1	100	25.1±1	3.89	0.36
40% glycol (60min)	16.1	1071	1.39±0.1	96.7	24.0±1	2.25	0.57
CSTR (60 min)	12.7	828	1.44±0.1	95.4	24.6±1	2.02	0.39
50% glycol (200min)	10.1	980	1.34±0.1	94.3	24.6±1	-	-
CSTR (180 min)	7.6	592	1.19±0.1	92.5	24.7±1	1.19	0.42

With ethylene glycol-water as feed, the pulp samples have significant higher viscosities and kappa numbers compared to the regular oxygen delignified pulps at the same operating conditions. The lower cellulose degradation rate in ethylene glycol-water is expected because the hydroxyl radicals are scavenged by ethylene glycol and thus lead to a reduced viscosity drop. The lower delignification rate in ethylene glycol may be due to the 30% lower solubility of oxygen in ethylene-water mixtures compared to pure water (Hideki Yamamoto et al, 1994). The phenolic group content of the isolated lignin in the ethylene glycol oxygen delignified pulps is very close to that of the corresponding regular oxygen delignified pulp. This indicates that hydroxylation of aromatic lignin by hydroxyl radicals is not significant during regular oxygen delignification.

In Figure 10.12 the selectivity of ethylene glycol-water treated and regular oxygen delignified pulps are compared. The ethylene glycol experiments were performed at two ethylene glycol:water volume ratios (40:60 and 50:50) for 60 and 200 minutes. It is clear that the ethylene glycol-water treated pulps have a selectivity more than double that of the regular experiments. Also, the selectivity of the ethylene glycol-water oxygen delignified pulps does not decrease much with reaction time.

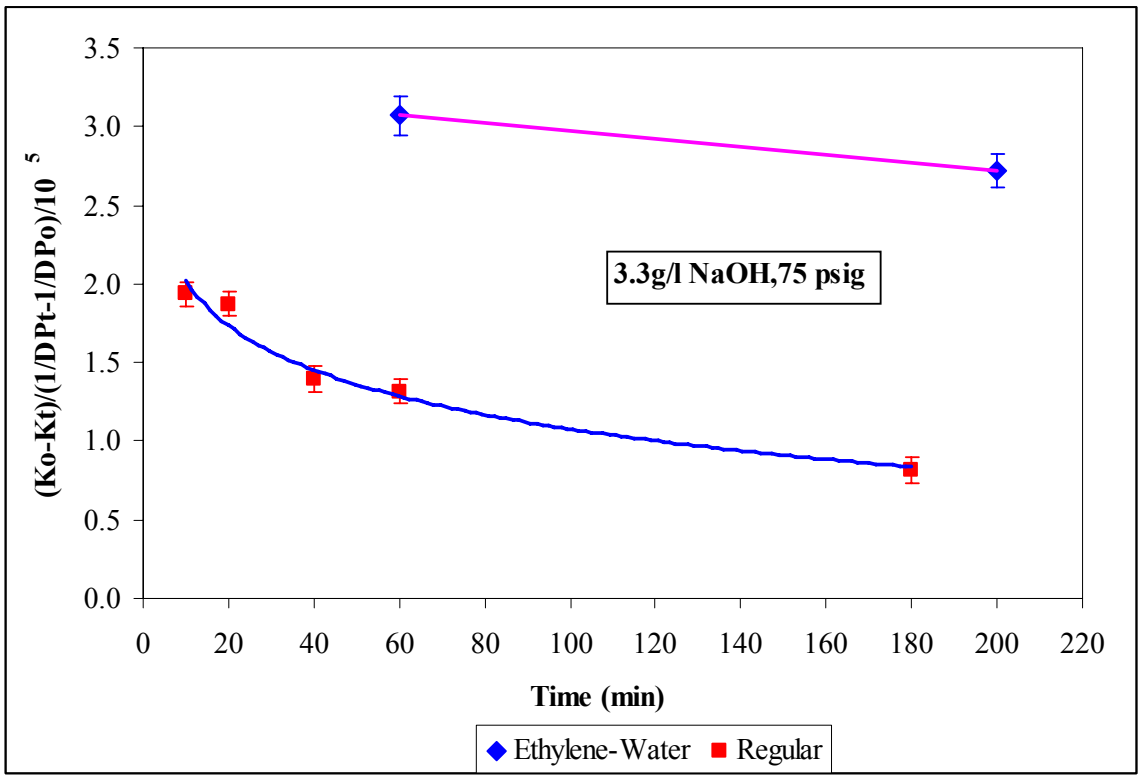

Figure 10.12 Selectivity Comparison of Ethylene Glycol and Regular Experiments

In Figure 10.13, the delignification rate vs. reaction time is shown when using an ethylene-glycol-caustic solution mixture for oxygen delignification. It shows that the rate of delignification in 50% ethylene glycol is lower than that of the control experiment using a regular aqueous NaOH solution. As discussed in earlier, the low rate may be explained by the lower dissolved oxygen concentration in the ethylene-water mixture (Yamamoto and Tokunaga, 1994). By extrapolating the first order delignification behavior to zero delignification rate, the ethylene glycol pulp still has about 5mg lignin/g pulp residual lignin which is around 15% of the total lignin. This may be explained by almost complete scavenging of the hydroxyl radical by ethylene glycol. The absence of hydroxyl radicals in the ethylene glycol-caustic mixture leads to the elimination of

degradation of the carbohydrate based kappa. Therefore, the radicals may be important during oxygen delignification for the removal of carbohydrate based kappa condtribution.

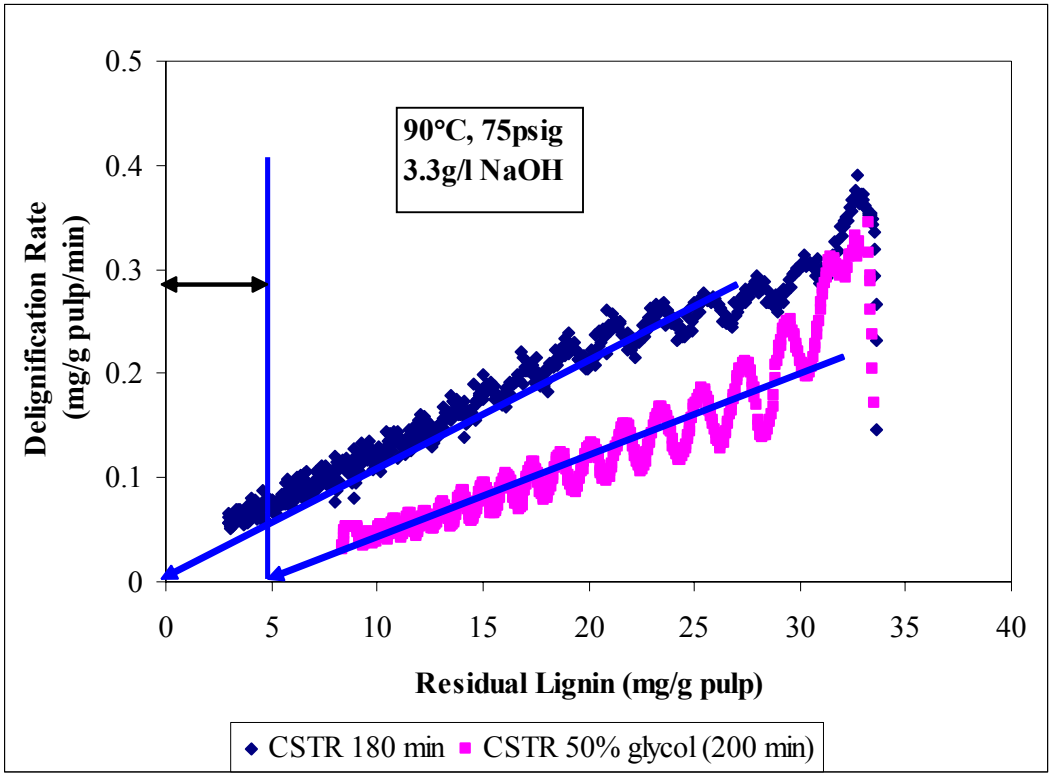

Figure 10.13 Delignification Rate vs. Residual Amount of 50% Ethylene Glycol (200min) Sample and Reference Sample (180min)

10.7 Peeling Delignification

It has been proposed (Backa et al, 2004) that so-called "peeling delignification" may occur when the hemicelluloses are subject to the "peeling reaction". Lignin attached to these "peeled" hemicelluloses by covalent bonds will then also be removed from the pulp. Since hemicelluloses with reducing ends may be present in the unbleached pulp, and oxygen is not needed for the peeling reaction, peeling delignification may possible occur preferentially at the start of oxygen delignification. However, it is commonly thought that

during kraft pulping, most of the remaining reducing ends are stabilized against peeling by conversion to metasaccharinic acid (Sjostrom, 1977). Therefore the existence of reducing ends to in brown stock is questionable. However as was repeatedly shown in earlier chapters, the original kraft pulp and the oxygen delignified pulps contained significant amount of reducing ends as measured by the dinitrosalicylic acid assay (Chapter 4). To further investigate peeling delignification, the pulp was treated in the CSTR with a hot, oxygen-free alkaline solution or with hot oxygenated water.

10.7.1 Effect of Alkali Extraction under Nitrogen in the CSTR

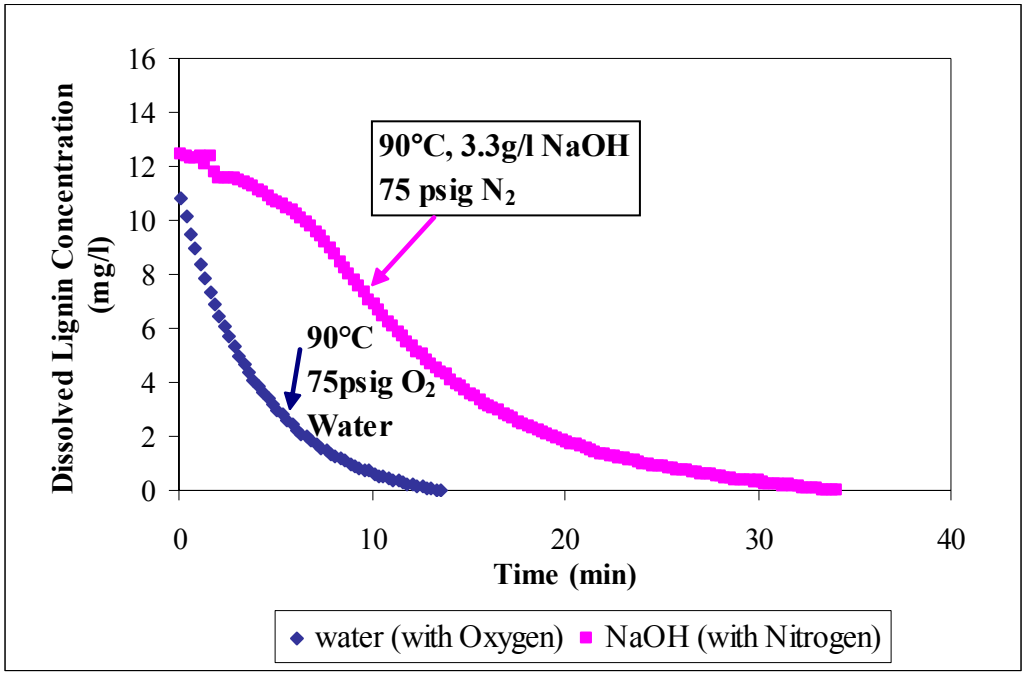

Figure 10.14 Dissolved Lignin Concentration vs. Reaction Time for water (with O_2) and NaOH (with N_2) in CSTR

Figure 10.14 shows the dissolved lignin concentration vs. time when the CSTR is fed with pure water under an atmosphere of oxygen, or fed by a caustic solution saturated

with nitrogen. The hot water with oxygen experiment shows a rapid decrease in lignin concentration. However, the experiment with caustic under nitrogen shows a different behavior, and a much larger lignin removal.

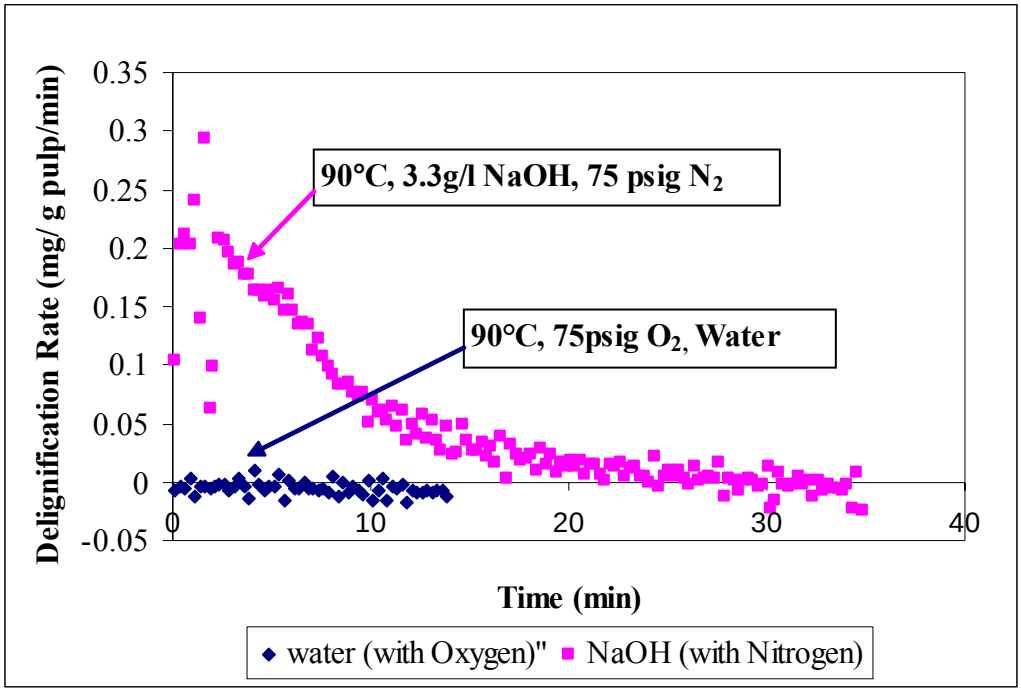

Figure 10.15 Delignification Rate vs. Reaction Time for water (with O_2) and NaOH (with N_2) in CSTR

Figure 10.15 shows the delignification rate vs. reaction time using equation 5.5 applied to the data in Figure 10.14. For hot water with oxygen extraction, the delignification rate is essentially zero all the time, showing that the behavior shown in Figure 10.14 is just that of displacing lignin dissolved in the water in the CSTR during reactor heat-up. Thus this lignin is removed from the pulp simply by leaching. On the contrary, the caustic with nitrogen extraction experiment shows a relatively high initial delignification rate which then decreases to zero after about 20 minutes. This lignin removal may be caused by "peeling delignification". The number of reducing ends in the original pulp is 8.2

mmol/Kg pulp. The reducing ends content in the NaOH extracted pulp under nitrogen is 5.31 mmol/Kg pulp. This shows that the delignification is accompanied by a decrease in reducing ends content in agreement with the concept of peeling delignification. However, it also shows that the content of reducing ends is not reduced to zero. The explanation for this may be that the measured reducing ends also include other moieties which are not carbohydrate reducing ends.

Table 10.10 Pulp Properties of alkali and Hot Water Extraction

Sample	Viscosity (ml/g)	Kappa Number	Methanol in filtrate(ppm)	Reducing ends (mmol/Kg Pulp)	Ph-OH (mmol/glignin)
Original	1189	24.39	-	8.2	2.23±0.1
Hotwater+O_2 (70 min)	1103	22.24	Trace	10.2	2.29±0.1
NaOH+N_2 (70 min)	1096	20.52	at 7 min: 2.3	5.3	2.87±0.1

Table 10.10 shows the intrinsic viscosity and kappa number of hot water+O_2 and NaOH+N_2 extracted pulp samples, the methanol concentration in the effluent, and the phenolic hydroxyl group content of the residual lignin of the pulps isolated according to the procedure described in Chapter 4.5. It can be seen that the viscosity drop is similar for the two extracted pulps. The hot water extraction reduces the kappa number by about 2 units, while alkali extraction leads to a reduction of 4 kappa units. The larger kappa number reduction with the caustic treatment may be explained by peeling delignification. The phenolic group content in the isolated residual lignin shows an interesting behavior. When the experiment was done with oxygen and hot water solution, the phenolic group content remains the same as that in the original kraft pulp. However, the phenolic group content in the pulp exposed to the NaOH solution under N_2 is higher than that of the kraft pulp. Because the liquor samples of this experiment also contained a small amount of

methanol, this suggests that lignin methoxyl groups are subject to alkaline hydrolysis and form methanol and new phenolic groups. This implies that demethoxylation is accompanying "peeling delignification".

10.7.2 Effect of $NaBH_4$ Pretreatment of the Original Pulp

Another experiment was performed to study "peeling delignification". In this case, the original pulp was pretreated with $NaBH_4$ to stabilize the carbohydrates against alkaline peeling reactions.

Table 10.11 Results of $NaBH_4$ Pretreated and Control Experiments

(90C, 3.3g/l NaOH and 75 psig)

Pulp sample	***Kappa***	***ΔKappa***	***UV Lignin as Kappa***	***Reducing Ends (mmol/Kg Pulp)***
Original kraft pulp	24.4	-	-	8.2
$NaBH_4$ Reduced pulp	22.5	1.9	1.2	3.8
Control Pulp after 60 O_2	12.8	13.2	-	9.5
NaBH4 Pulp after 60min O_2	13.5	9	-	7.8

The results in Table 10.11 show that the borohydride pretreatment of the original kraft pulp leads to a decrease in kappa number of 1.9 units. However, standard UV analysis of the dissolved components after reduction showed that the calculated concentration correspond to a change in kappa number only 1.2 kappa units. This indicates that reduction reactions occurring in the carbohydrate part of the kappa number also took place during the pretreatment. Li and Gellerstedt (1998) showed that degraded structures of polysaccharide origin such as ketoglutaric acids and aldehydic structures contribute significantly to the kappa number of pulp. In Figure 10.16, the delignification rates vs. reaction time for the $NaBH_4$ pretreated and control pulps are shown.

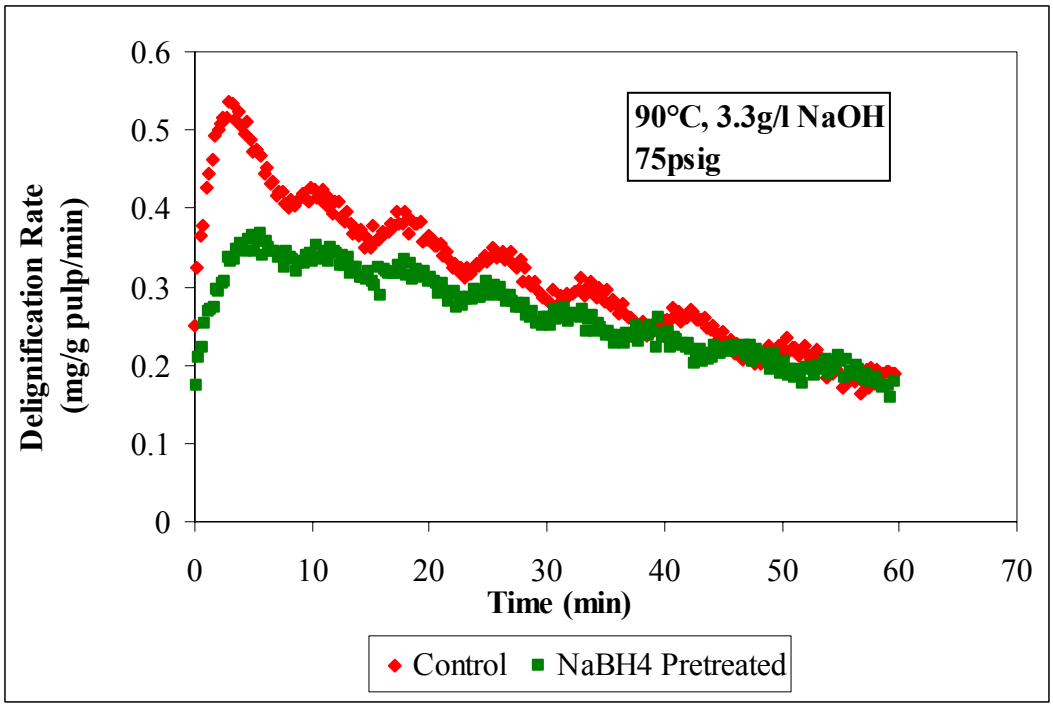

Figure 10.16 Delignification Rate vs. Time for Control and $NaBH_4$ Pretreated Pulps

It is clear that the $NaBH_4$ pretreated pulp has a significant lower delignification rate than the control kraft pulp, especially in the beginning of the reaction. This is confirmed by the significant lower kappa number reduction of 9 units compared to 13.2 for the control (see Table 10.11). Since the reduction of kraft pulp by $NaBH_4$ pretreatment does not change the known oxygen delignification reactions occurring in the lignin skeleton, other non-lignin related reactions may explain the observed difference. Thus, considering the existence of lignin carbohydrate bonds, it is likely that the stabilization of reducing ends against peeling after $NaBH_4$ reduction leads to elimination of peeling delignification and thus to a concomitant lower rate of lignin removal. Because the $NaBH_4$ pretreated pulp has a lower kappa number than the control pulp, the delignification rate was also compared at the same residual lignin content calculated as the residual kappa number minus HexA content.

Figure 10.17 shows the delignification rate vs. residual lignin content for the control and $NaBH_4$ pretreated pulps.

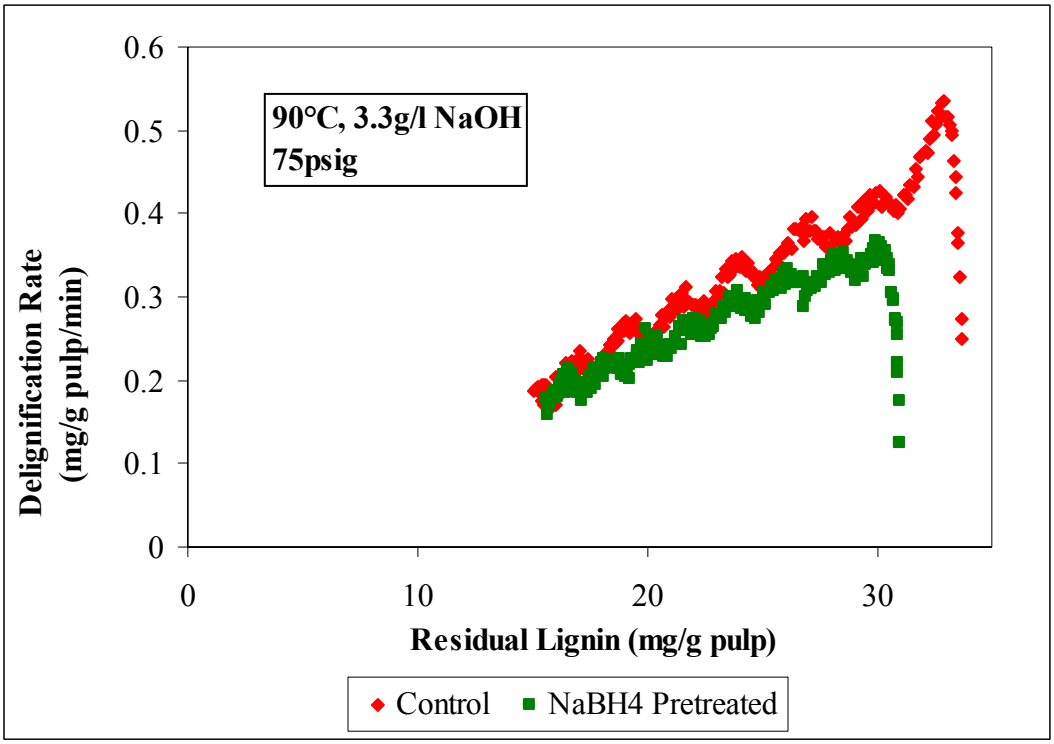

Figure 10.17 Delignification Rate vs. Residual Lignin Content for Control and $NaBH_4$ Pretreated Pulps

It shows that the borohydride reduced pulp has a slightly lower delignification rate than the control at the beginning of the reaction. This confirms that the stabilization of carbohydrates against peeling reactions reduces the delignification rate. Thus based on the oxygen delignification results with the $NaBH_4$ pretreated pulp and those of hot NaOH extraction without the presence of oxygen, it appears that peeling delignification contributes to the overall lignin removal during initial phase of oxygen bleaching. However, the impact of peeling delignification on the overall kappa number reduction and kinetics of delignification is relatively small. In the present CSTR set-up, the extra

delignification by this mechanism compensates for the loss of delignification due to the start-up transient of the CSTR.

10.8 Conclusion

The mechanism of oxygen delignification is complex because it consists of two major delignification pathways and at least four groups of chemical constituents must be considered. The major delignification pathway is the so-called phenolic delignification and a smaller contribution comes from “peeling” delignification. The chemical groups important for phenolic delignification are residual aromatic lignin, carbohydrate-based oxidizable structures and hexenuronic acids. Hemicellulose polymers with a reducing end and covalently bonded lignin structures are important for peeling delignification.

The phenolic delignification kinetics are first order in HexA corrected residual lignin (includes carbohydrate-based oxidizable structures). The kinetics also follows a langmuir-type behavior for adsorption of oxygen on the active aromatic lignin sites. Based on the influence of the NaOH concentration on the kinetics, it is proposed that the active site is the 3 carbon of the aromatic ring where oxygen reacts to form a hydroperoxide with a pKa of approximately 13 at room temperature. The kinetics of phenolic delignification can be described by assuming that the reaction between the adsorbed oxygen and the 3 carbon of the aromatic ring is the rate determining step. The almost uniform presence of aromatic methoxyl groups in residual lignin further supports the first order in lignin kinetics. Further decomposition of the formed hydroperoxide leads to delignification and methanol formation. The dissolved lignin consists mostly of monomeric or dimeric aromatic structures. Aromatic ring opening is unimportant during

phenolic delignification. It is likely that the carbohydrate-based oxidizable structures are degraded simultaneously by radical species generated during phenolic delignification. The HexA structures are non-reactive during oxygen delignification. Peeling delignification only provides a relatively small contribution to the kappa number reduction during the initial phase of oxygen delignification.

CHAPTER 11

CONCLUSIONS AND RECOMMENDATIONS FOR FUTURE WORK

11.1 Uniqueness of Experimental Approach

Pulp oxygen delignification experiments were performed in a batch reactor and differential CSTR reactor. Both reactors give reproducible experimental results. The uniqueness of this study is the kinetic data obtained from the differential operated CSTR which allows direct determination of the rate of oxygen delignification. The data obtained from the differential reactor system were of a pure chemical nature because the kinetics were independent of pulp mass, degree of mixing and feed flow rate.

11.2 Kinetics of Oxygen Delignification

Knowledge of the correct kinetic equation for oxygen delignification may benefit laboratory study and industrial practice. Although there are many kinetic equations reported in literature, some new insights have come from the present kinetics using the differential CSTR reactor:

- The rate of oxygen delignification can be described as a first order reaction in HexA-free residual lignin content of the pulp.
- The delignification reaction orders in hydroxide concentration and oxygen pressure of 0.42 and 0.44 respectively over the present experimental range are the result of the pKa of and Langmuir-type adsorption on the lignin active sites.
- At 90°C an alternative mechanistic delignification rate equation is $-\frac{dL_C}{dt} = 1.18\times10^{-3}\frac{\left[OH^-\right]}{0.111+\left[OH^-\right]}\cdot\frac{P_{O2}}{1+2.26\times10^{-2}P_{O2}}\cdot L_C$ (Equation 10.19). This

equation shows that the reaction orders in hydroxide concentration and oxygen pressure range from one to zero when these variables are increased from very low values to very high values.

- The delignification activation energy of 53 kJ/mol is in agreement with a reaction controlled process.
- The carbohydrate degradation during oxygen delignification can be described by two contributions: one due to radicals produced by phenolic delignification, and a much smaller contribution due to alkaline hydrolysis.

11.3 Mechanism of Phenolic Delignification

A modified mechanism of oxygen delignification is proposed based on interpretation of the kinetics as the result of the rate determining reaction between adsorbed oxygen and an active lignin site. More specifically, the first order kinetics in residual lignin content of the pulp suggests that the lignin active site is uniformly distributed throughout the lignin and has the same reactivity during the entire oxygen delignification process. In addition, the high pKa value of the active lignin sites does not support the conventional mechanism which considers the phenolic group with a much lower pKa value as the initial reaction site. Rather it is proposed that the 3 carbon in the aromatic ring with attached methoxyl group forms the lignin active site for oxygen adsorption. Subsequently the oxygen reacts to form a hydroperoxide with a pKa value similar to that derived for the present delignification kinetics. The uniform presence of the aromatic methoxyl groups in residual lignin further support the first order in lignin kinetics. Further decomposition of the formed hydroperoxide leads to delignification and mostly monomeric and dimeric aromatic structures. Aromatic ring opening is unimportant during phenolic delignification.

11.4 Peeling Delignification

Peeling delignification occurs during oxygen delignification by peeling of hemicelluloses which have lignin covalently bonded to them. Peeling delignification only provides a relatively small contribution to the kappa number reduction during the initial phase of oxygen delignification.

11.5 Recommendations for Future Work

The present study was performed with unbleached softwood kraft pulp with kappa number of 24.4. To understand the kinetics of oxygen delignification better, it is recommended to do experiments with other pulps. Especially it is recommended to

- study the influence of different initial kappa numbers, pulp types (kraft, sulfite and organosolv et al) and species (hardwood and softwood) to verify whether these pulps still follow first order kinetics during oxygen delignification;
- study the effect of different additives in the solution such as glycol, sodium gluconate, etc);
- study the detailed kinetics and mechanism of the pulp viscosity development during oxygen delignification.

REFERENCES

Agarwal S. B., Genco J.M., Cole B.J.W., Miller W., "Kinetics of Oxygen Delignification", TAPPI Pulping Conference, 351-364 (1998)

Akim, L., J. Colodette, and D. Argyropoulos, "Factors Limiting Oxygen Delignification of Kraft Pulp", Canadian Journal of Chemistry, 79(2),201-210 (2001)

Backa, S., C. Gustavsson, M. E. Lindstrom and M. Ragnar, "On the Nature of Residual Lignin", Cellulose Chemistry and Technology, 38, 5-6, 321-331 (2004)

Berry R., Jiang, Z.H., Faubert M., Van Lierop B., Sacciadis G., "Recommendations from Computer Modelling for Improving Single Stage Oxygen Delignification Systems", PAPTAC 88th Annual Meeting, B151-B161 (2002)

Camilla Roost, Martin Lawoko and Goran Gellerstdedt, "Structural Changes in Residual Kraft Pulp Lignins. Effect of Kappa Number and Degree of Oxygen Delignification", Nordic Pulp and Paper Res, J. 18:4, 397-401 (2003)

Chai, X. S., Q, Luo and J. Y. Zhu, "Analysis of Nonvolatile Species in a Complex Matrix by Deadspace Gas Chromatography", Journal of Chromatography A, 909, 249-257 (2001)

Da Silva Perez, D. and A.R.P. van Heiningen, "Determination of Cellulose Degree of Polymerization in Chemical Pulps by Viscosimetry", 7th European Workshop on Lignocellulosics and Pulp (EWLP) Conference, Turku, Finland 393-396 (2002)

Edwards L. and S-E. Nordberg, "Alkaline Delignification Kinetics, a General Model Applied to Oxygen Bleaching and Kraft Pulping", TAPPI, 56(11), 108-111 (1973)

Eero Sjostrom, Raimo Alen, "Analytical Methods in Wood Chemistry, Pulping and Papermaking", Springer-Verlag Berlin Heidelberg, Printed in Germany (1999)

Evans J.E., Venkatesh V., Gratzl J.S., Chang H-M, "The Kinetics of Low Consistency Oxygen Delignification, Kraft and Soda Anthraquinone Pulps", TAPPI, 62(6), 37-39 (1979)

Evans J.E.W., "Use of Oxygen in Pulping Softwoods and Hardwoods Proves Successful", Pulp Pap., 53(5), 142-143, 152 (1979)

Evans R. and Wallis A.F., "Cellulose Molecular Weights Determined by Viscosity", Journal pf Applied Polymer Science, 37, 2331-2336 (1989)

Fengel Wegener, Wood Chemistry, Ultrastructure, Reactions, Walter de Gruyter & Co., Berlin, New York (1984)

Fu, S. and L.A. Lucia, "Investigation of the Chemical Basis for Inefficient Lignin Removal in Softwood Kraft Pulp during Oxygen Delignification", Industiral and Engineering Chemistry Research, 42:19, 4269-4276 (2003)

Fujimoto, A., "Covalent Association between Lignin and Cellulose as a Major Lignin and Polysaccharide Linkage", 10th ISWPC, 48-51 (1998)

Gellerstedt, G. and E. L. Lindfors, "On the Structure and Reactivity of Residual Lignin in Kraft Fibers", International Pulp Bleaching Conference (IPBC), Stockholm, Sweden, 78-88 (1991)

Gierer, J. and F. Imsgard, "The Reaction of Lignin with Oxygen and Hydrogen Peroxide in Alkaline Media", Svensk Papperstidning, 80(16), 510-518 (1977)

Goring, D.A.I. and Timell, T.E., "Molecular Weight of Native Celulose", Tappi (45), 454-460 (1962)

Guay D. F., Cole B. J., Fort R.C. Jr., Hausman M.C., Genco J.M., T.J. Elder, and K.R. Overly, Mechanisms of Oxidative Degradation of Carbohydrates during Oxygen Delignification. II. Reaction of Photochemically Generated Hydroxyl Radicals with Methyl β-Cellobioside, Journal of Wood Chemistry and Technology, 21(1), 67-79 (2001)

Guolin Tong, Tokoyama, Yuji Matsumoto, Gyosuke Meshitsuka, Li Zhongzheng, "How Lignin Oxidation is Related to the Delignification During Oxygen Delignification", 2003 ISWPC, Madison (2003)

Gustavsson, C., Sjostrom, K., and W. Wafa Aldajani, "Influence of Cooking Conditions on the Bleachability and Chemical Structure of Kraft Pulps", Nordic Pulp and Paper Research Journal 14(1), 71-81 (1999)

Hasan Hameel, Kosef Gratzl, D.Y. Prasad and Sreeran Chivukula, "Extended Delignification with AQ/Polysulfide", TAPPI Processing, Pulping Conference, 781-785 (1994)

Heiningen A.V. and Violette S., "Selectivity Improvement during Oxygen delignification by Adsorption of a Sugar-based Polymer", Journal of Pulp and Paper Science, 29(2), 48-53 (2003)

Hideki Yamamoto and Junji Tokunaga, "Solubilities of Nitrogen and Oxygen in 1, 2-Ethanediol+Water at 298.15K and 101.33 kPa, J. Chem. Eng. Data, (39), 544-547 (1994)

Hou-min Chang and Josef S. Gratzl, "Ring Cleavage Reactions of Lignin Models with Oxygen and Alkali", In Chemistry of Delignification with Oxygen, Ozone and Peroxide, Uni Pub. Co. Ltd (1980)

Hsu C. L., Heish, J.S., "Reaction Kinetics in Oxygen Bleaching", AICHE, J., 34(1), 116-122 (1988)

Hsu C. L., Hsieh J.S., "Gas- Liquid Mass Transfer and Pressure Drop in Pulp Bed with Flexible Fibers as Solid Supports", AICHE Journal, 32(10), 1710-1715 (1986)

Irabarne J., Schroder L.R., "High-Pressure Oxygen Delignification of Kraft Pulps", TAPPI Journal, 80(10), 241-250 (1997)

Jiang, Z.H., Audet, A., Sullivan, J. Van Lierop B. and Berry R., "A New Method for Quantifying Hexenuronic Acid Groups in Chemical Pulps", Journal of Pulp and Paper Science, Vol. 27 No. 3 March (2001)

Jiebing Li and Goran Gellerstedt, "Oxymercuration-Demercuration-Kappa Number: a more accurate estimation of lignin content of pulp", Fifth European Workshop on Lignocellulosics and Pulp, Aveiro, Portugal, 281-284 (1998)

Jiebing, Li, "Towards an Accurate Determination of Lignin in Chemical Pulps", PhD Thesis, Royal Institute of Technology (1999)

Johansson, E. and S. Ljunggren, "The Kinetics of Lignin Reaction during Oxygen Delignification, Part 4. The Reactivates of Different Lignin Model Compounds and the Influence of Metal Ions on the Rate of Degradation", Journal of Wood Chemistry and Technology, 14(4), 507-525 (1994)

Kovasin K., Uusitalo P., Viilo M., Dimensioning of Oxygen Delignification Reactors, International Oxygen Delignification Conference, 223-230 (1987)

Lawoko, M., Berggren, R., Berthold, F., Henriksson, G., Gellerstedt, G., "Changes in the Lignin-Carbohydrate Complex in Softwood Kraft Pulp during Kraft and Oxygen Delignification", Holzforschung, 58(6), 603-610 (2004)

Lawoko M. , Henriksson G. and Gellerstedt G, "Structural Differences between the Lignin-Carbohydrate Complexes Present in Wood and in Chemical Pulps", Biomacromolecules. Nov-Dec; 6(6):3467-3673, (2005)

Lindgren C.T. and Lindstrom M.E., "The Kinetics of Residual Delignification and Factors affecting the Amount of Residual Lignin during Kraft Pulping", Journal of Pulp and Paper Science, 22 (8), J290 (1996)

Ljunggren, S and Johansson E., "The Kinetics of Lignin Reactions during Oxygen Bleaching", Nordic Pulp and Paper Research Journal, J.5:3, 148-154 (1990)

Margaret C. Hausman, Thomas R. Elder and Raymond C. Fort Jr., "How Do Phenoxyl Radicals Form During Oxygen Delignification?" 12th International Symposium on Wood and Chemistry (ISWPC), Madison, WI, USA (2003)

Martin Ragnar, On the Importance of Radical Formation in Ozone Bleaching, PhD Dissertation, KTH, Sweden (2000)

McDonough T.J, "The Technology of Chemical Pulp Bleaching-Oxygen Delignification", Pulp Bleaching-Principles and Practice, edited by Dence C.W., Reeve D. W., TAPPI Press, 868 (1996)

McDonough, T., "Oxygen Delignification, in Pulp Bleaching, Principle and Practices", Tappi Press: Atlanta. 213-239 (1996)

Michaud, J.P, "A Citizen's Guide to Understanding and Monitoring Lakes and Streams", Publ. #94-149, Washington State Department of Ecology, Publications Office, Olympia, WA, USA (360) 407-7472 (1991)

Miller G.G. and Raleigh J.A, "Action of Some Hydroxyl Radical Scavengers on Radiation-Induced Haemolysis, International Journal of Radiation Biology, Volume 43, 411-419 (1983)

Miller, G.L., Use of Dinitrosalicylic Acid Reagent for Determination of Reducing Sugar, Analytical Chemistry, **31,** 426 (1959)

Moe, S. T. and A. J. Ragauskas, "Oxygen Delignification of High-Yield Kraft Pulp. Part 1. Structural Properties of Residual Lignins", Holzforschung, 53(4), 416-422 (1999)

Myers M.R., Edwards L.L., "Development and Verification of a Predictive Oxygen Delignification Model for Hardwood and Softwood Kraft Pulp", TAPPI Journal, 72(9), 215-219 (1989)

Ni, N., "A Fundamental Study of Chlorine Dioxide Bleaching of Kraft Pulp", Ph.D thesis, McGill University, Montreal, Canada (1992)

Olm L., Teder A., "The Kinetics of Oxygen Bleaching", TAPPI Journal, 62(12), 43-46 (1979)

Perrin D.D., Boyd Dempsey, E.P. Serjeant, "pKa Prediction for Organic Acids and Bases", Book, Chapman and Hall Ltd (1981)

Ragnar, M. and K. Ala-Kaila, "On the Demand for Oxygen in Oxygen Delignification of Chemical Pulp", Das Papier, (8), 53-56 (2004)

Reid, D.W., J. Ayton, and T. Mullen, CPPA, "Oxygen Delignification Survey", Pulp and Paper Canada, 99(11, 43-47 (1998)

Rewatkar V. B., Bennington C.P.J., "Gas-Liquid Mass Transfer in Pulp Retention Towers", TAPPI International Pulp Bleaching Conference, Portand, OR (2002)

Salmela M., Alen R., Ala-Kaila K., "Fate of Oxygen in Industrial Oxygen- Alkali Delignification of Softwood Kraft Pulp", Nordic Pulp and Paper Research Journal, 19(1), 97-104 (2004)

Sjöström, E., Wood Chemistry, Fundamentals and Applications, Academic Press, New York, (1993)

Standard Test Method for Intrinsic Viscosity of Cellulose, Standard D1795-62, ASTM, West Conshohochen, PA, USA (1985)

Tappi 1997 Kraft Pulping Short Course, (4) (1997)

Teder A. and L. Olm, "Extended Delignification by Combination of Modified Kraft Pulp and Oxygen Bleaching", Paperi ja Puu, 63 (4a), 315-326 (1981)

Thompson N.S, Corbett H. M., "The Effect of Oxygen Consumptions during Bleaching on the Properties of Southern Pine Kraft Pulp", Tappi, 59(3), 78-80 (1976)

Tromans D., "Oxygen Solubility Modeling in Inorganic Solutions: Concentration, Temperature and Pressure Effects", Hydrometallurgy, (50), 279-296, (1998)

Van Tran, A., "Effect of pH on Oxygen Delignification of Hardwood Kraft Pulp", Paperi ja Puu 83(5), 405-410 (2001)

Vuorenvirta K., Fuhrmann A., Gullichsen J., "Effect of Black Liquor Carryover on Selectivity of Oxygen Delignification", Pulp and Paper Canada, 102(3), 50-52 (2001)

Wagberg, L., Annergren, G.O., "Physicochemical Characterization of Papermaking Fibers, in the fundamentals of Papermaking Materials: Transaction of the 11th Fundamental Research Symposium, Pira International. 1-82 (1997)

Woerner D.L. and McCarthy J.L.; Ultrafiltration and Light Scattering Evidence for Association of Kraft Lignins in Aqueous Solutions, 4th International Symposium on Wood and Pulping Chemistry, 71-76, Paris, France (1987)

Zou, Haixuan "Effect of Kraft Pulping on Oxygen Delignification", PhD Thesis, University of Maine (2002)

APPENDIX A

SAMPLE CACULATION PROCEDURE FOR POWER LAW MODEL

A.1 Power Law Model for Kappa Number

$$-\frac{dK}{dt} = k_q K^q \qquad \text{(Equation A.1)}$$

$$k = A\exp(-E_A / RT)(OH^-)^m (P_{O_2})^n \qquad \text{(Equation A.2)}$$

$$\frac{\left(\frac{1}{K^{q-1}}\right)-\left(\frac{1}{K_0^{q-1}}\right)}{(q-1)} = k_q \ t \quad for \quad q \neq 1 \qquad \text{(Equation A.3)}$$

$$y = k_q \times t = \frac{\left(\frac{1}{K^{q-1}}\right)-\left(\frac{1}{K_0^{q-1}}\right)}{(q-1)} \qquad \text{(Equation A.4)}$$

where K is Kappa Number (unitless)

t is time (min)

k_q is reaction rate constant (unitless)

q is reaction order

E_A = activation energy (J/gmol)

R = gas constant (8.314J/gmol K)

T = temperature (K)

OH^- = initial sodium hydroxide concentration (g/L)

P_{O2} = oxygen pressure (psig)

m = parameter showing alkali dependence (unitless)

n = parameter showing oxygen pressure dependence (unitless)

k_q = reciprocal time units (min^{-1})

A_q = frequency factor (min^{-1}) $(g/l)^{-m}$ $(psig)^{-n}$

Equation $y = k \times t$ is a linear line cross zero point with slope of k. From equation A.4, $\frac{\left(\frac{1}{K^{q-1}}\right)-\left(\frac{1}{K_0^{q-1}}\right)}{(q-1)}$ vs. time t is a linear line with slope of k when q is certain constant (Figure A.1). A trial and error method is used to get the best reaction order q. With every assumed value of q, $\frac{\left(\frac{1}{K^{q-1}}\right)-\left(\frac{1}{K_0^{q-1}}\right)}{(q-1)}$ vs. time t is plotted and the regression coefficient R^2 is obtained. At the maximum R^2, q is considered the best value. Figure A.1 shows how to find the best q from best R^2 value.

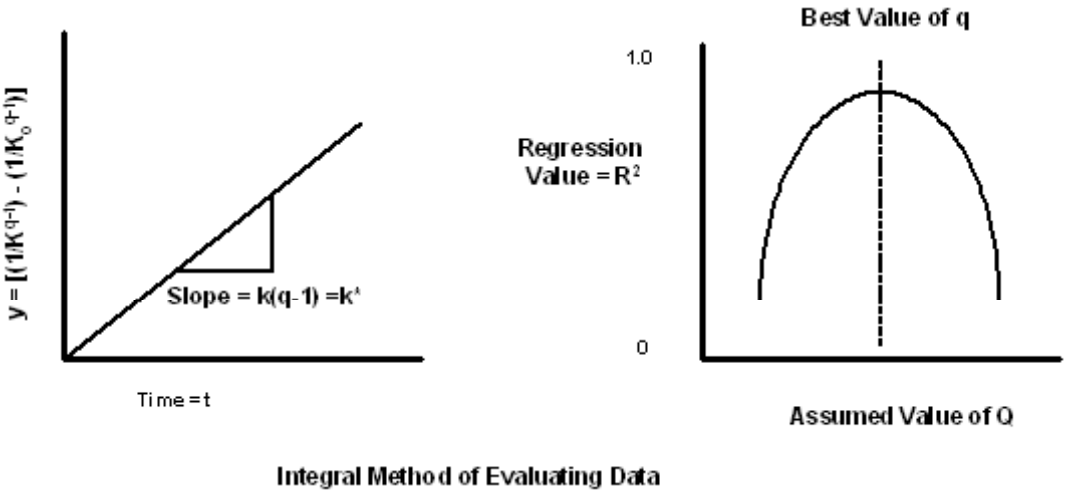

Figure A.1 Integral Method of Evaluating Data of Oxygen Delignification

A.2 Model of CSTR Kappa Numbers

Table A.1 shows the values for q and k estimated from integral method.

Table A.1 Values for q and k Estimated from Integral Method

Reaction Time (min)	Kappa Number	$(1/K^{(1-q)}-1/K_0^{(1-q)})/(q-1)$
0	24.4	0.000E+00
10	20.1	1.009E-03
20	18.5	1.552E-03
40	14.3	3.824E-03
60	12.7	5.246E-03
180	7.6	1.629E-02

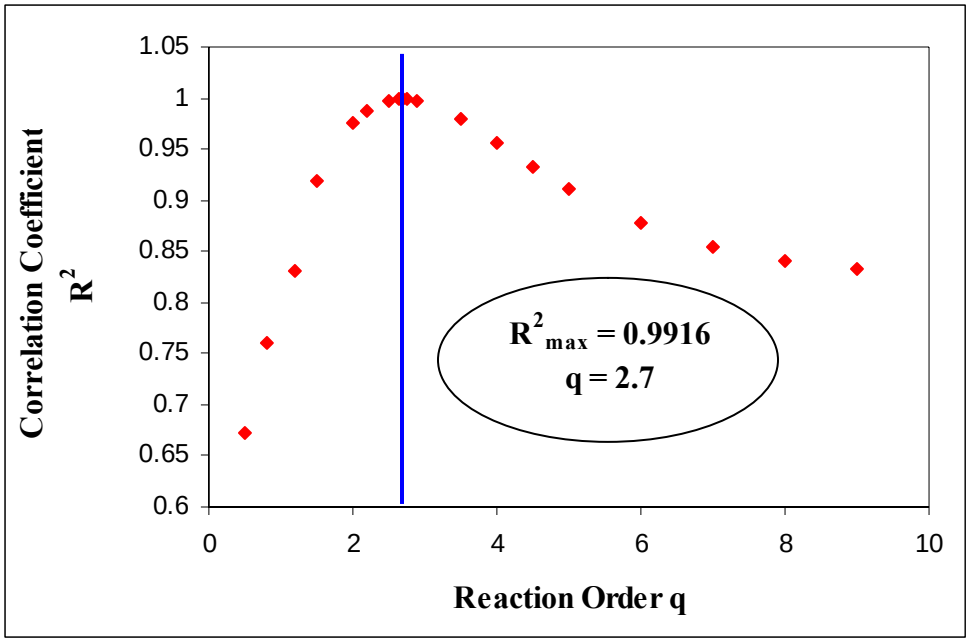

Figure A.2 Method to Find the Best Reactor Order q for CSTR

Figure A.2 shows correlation coefficient R^2 vs. different reaction order q for CSTR data. CSTR data have the best reaction order of 2.7 when the correlation coefficient R^2 is 0.9916.

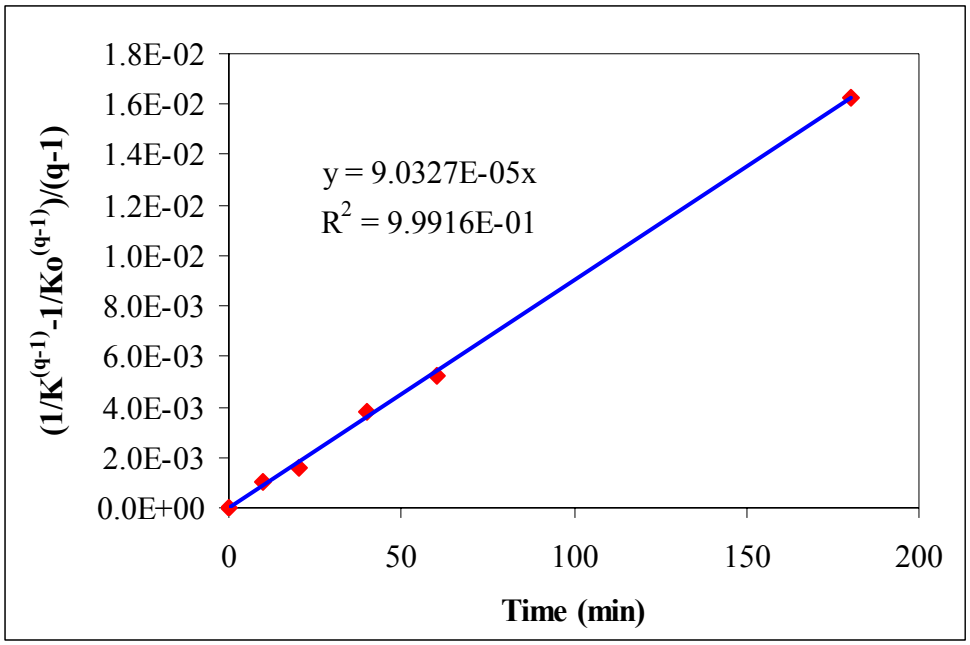

Figure A.3 Method to Estimate Reaction Constant k of Best Reaction Order q = 2.7

In Figure A.3, $\frac{\left(\frac{1}{K^{q-1}}\right)-\left(\frac{1}{K_0^{q-1}}\right)}{(q-1)}$ (when reaction order is 2.7) vs. time is shown. The slope of the curve is 9.033×10^{-5} which is the value of reaction constant. Therefore, at the reaction condition of 90ºC, 75psig oxygen pressure and 3% NaOH charge, the kappa number model of CSTR is

$$K=\left[\left(\frac{1}{K_0^{1.7}}\right)+1.536\times10^{-4}\times t\right]^{-\frac{1}{1.7}}$$

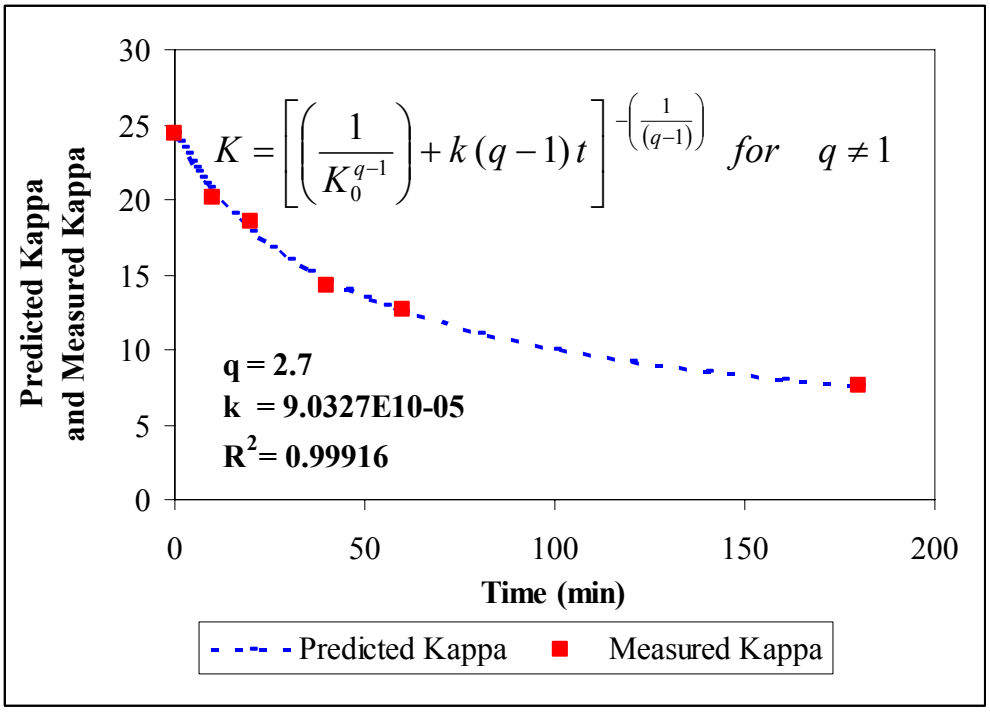

Figure A.4 Predicted Kappa and Measured Kappa vs. Reaction Time in CSTR

In Figure A.4, Predicted kappa calculated from the kappa model and measured kappa number are plotted vs. reaction time. It is obvious that the predicted kappa numbers are almost the same with the measured kappa number.

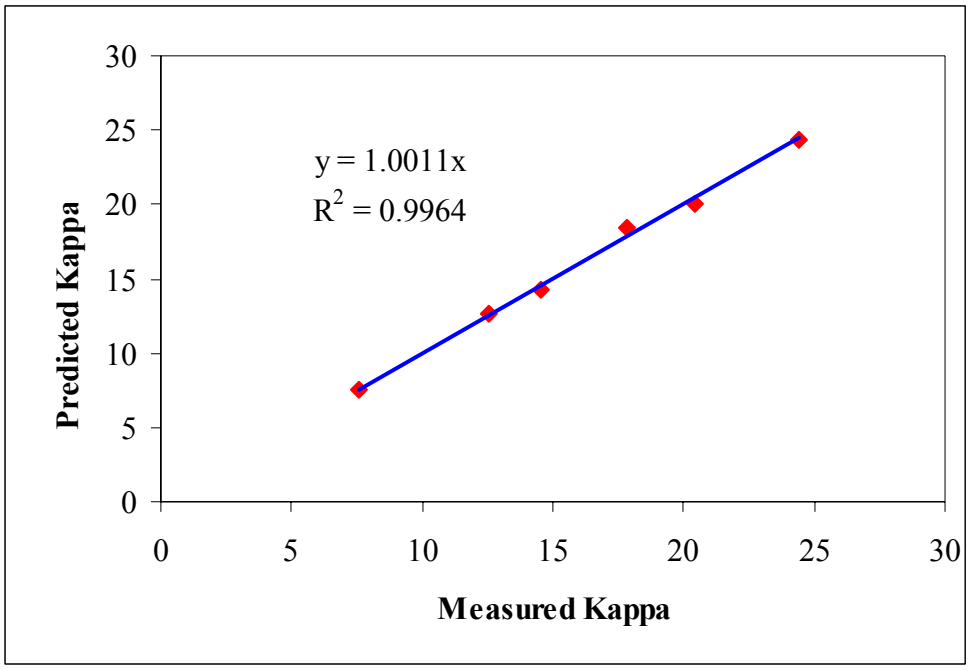

Figure A.5 Predicted Kappa Number vs. Measured Kappa Number in CSTR

In Figure A.5, the relationship of predicted kappa and measured kappa is shown. The linear line is y=1.0011x with R^2 of 0.996 which means the predicted kappa numbers are very close to the experimental data.

APPENDIX B

SPECIAL EQUIPMENT USD IN THIS PROJECT

B.1 Control Tower of the Berty Reactor

Figure B.1 Control Tower

The CT-2000/3000 control tower is designed to be used primarily in a laboratory environment. The Control Tower is a complete reactor control system; configured & tested to control a high pressure, stirred laboratory reactor. The technical specifications are:

Supply Voltages: 115/240 VAC +/-10%

Supply Frequencies: 50 to 60 Hz

Instrument Power Circuit Breaker: 115 Vac, 2.5 Amp, 50/60 Hz

Mixer Power Circuit Breaker: 250 Vac, 10 Amp, 50/60 Hz

Armature Fuse (motor): [1 to 8] Amp

Heater Power Circuit Breaker: 250 VAC, 15 Amps, 50/60 Hz

External Power Junction Box (Optional): 250 VAC, 35 Amps, 50/60 Hz

Operating Temperature: 0 to 55°C with 12 inches of open air space on all sides of the controller

Relative Humidity: 5 to 90% non condensing

The Autoclave TowerView software makes it is easy and quick to access the data from Autoclave Engineer's Control Tower Series. It is capable of communicating with up to four towers and each tower is capable of containing four controllers. The main functions of this application include:

- Monitoring the process variable, process variable setpoint and the PID output percentage from a computer workstation

- Storing the process variable from each controller in data log files
- Providing a real-time trend for each process variable
- Logging events and alarms in event log files
- Generating custom reports from stored process variable values
- Ability to alter various parameters in the controller from the computer terminal.

B.2 Berty Stationary Basket Catalyst Testing Reactor

- 3-inch (76.2mm) inside diameter with a 4×4 mesh, 0.062 inch (1.5mm) wire and a nominal opening size of 0.187 inch (4.75 mm) basket; when the experiment is done, PTFE fine mesh is used to prevent the pulp fines go through the basket
- Go up to 5800 psig (400 bar) and 650ºF (343ºC)
- basket volume is 100 cm^3 and the free volume is 280 cm^3

B.3 HP8453 UV-VIS Spectrophotometer and Flow Cell

- Fast Scanning Diode Array UV-VIS Spec.
- Wavelength range is 190-1100 nm
- Slit width 1 nm
- Both continuous and batch measurement

Figure B.2 HP8453 UV-VIS

- 13×2mm &13×1mm SiO_2 windows and 3mm path length
- Max. pressure is 660 psi

Figure B.3 Flow Cell

B.4 Experimental Setup in University of Maine

Figure B.4 Differential CSTR in University of Maine

B.5 FLR-1000 Liquid Flow Measurement

Operating Temperature: 0~50 ºC

Maximum Operating Pressure: 100 ºC

Flow Rate: 20~200 ml/min

Figure B.5 Liquid Flow Meter

APPENDIX C

VISSIM PROGRAM FOR REACTOR AND DEAD VOLUME

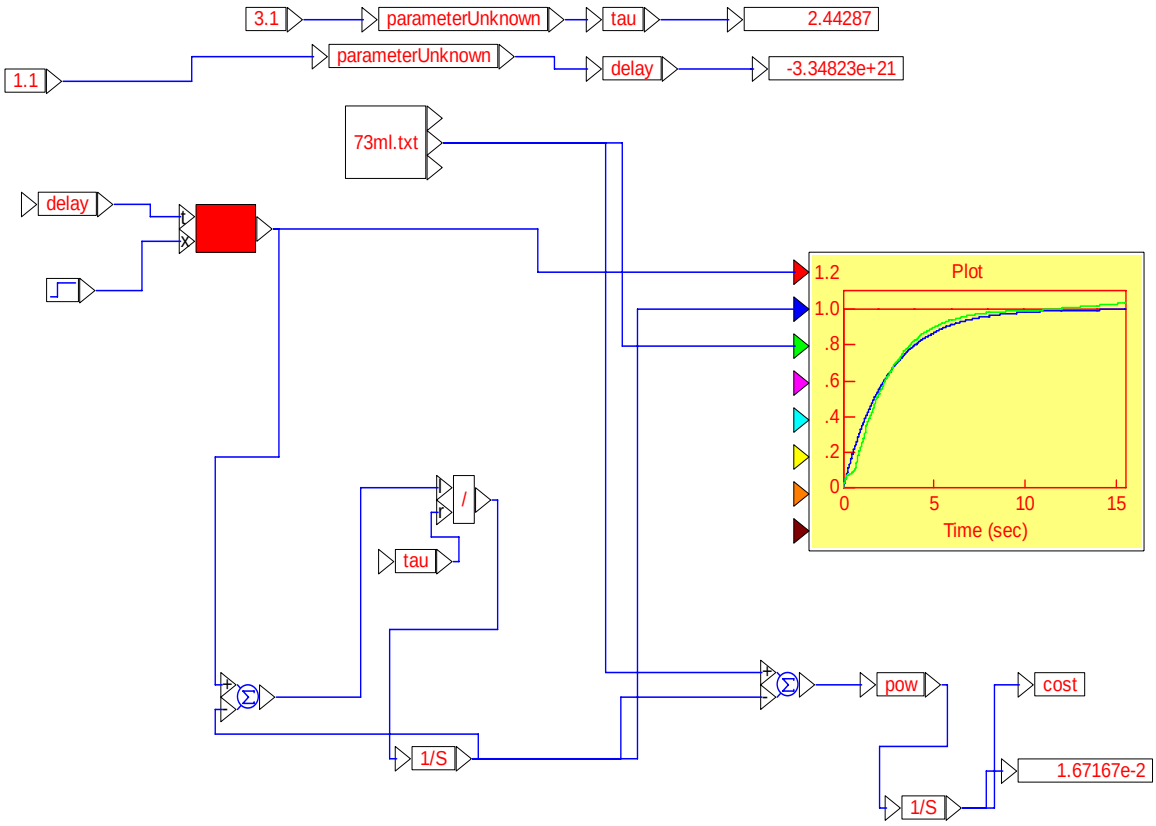

Figure C.1 VisSim Program to Calculate Reactor Volume and Dead Volume

APPENDIX D

PULP SAMPLE APPEARANCE FROM CSTR

D.1 Pulp Samples at Different NaOH Concentration

Figure D.1 Pulp Samples of Different NaOH Concentrations

D.2 Pulp Samples at Different Temperatures

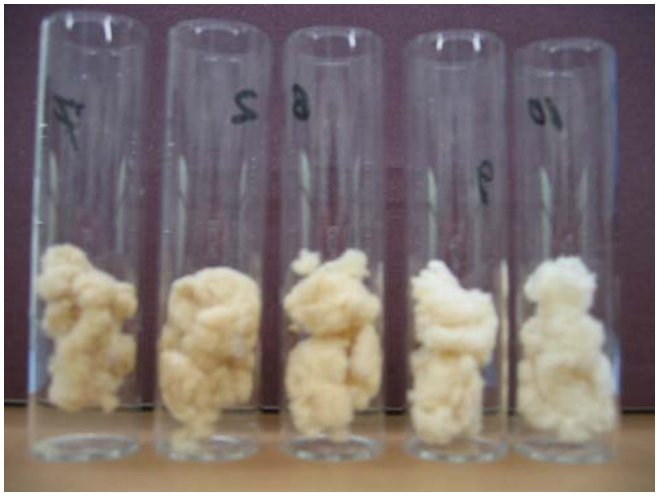

Figure D.2 Pulp Samples of Different Reaction Tempeartures

D.3 Pulp Samples at Different Pressures

Figure D.3 Pulp Samples of Different Total Pressures

D.4 Pulp Samples at Different Reaction Times

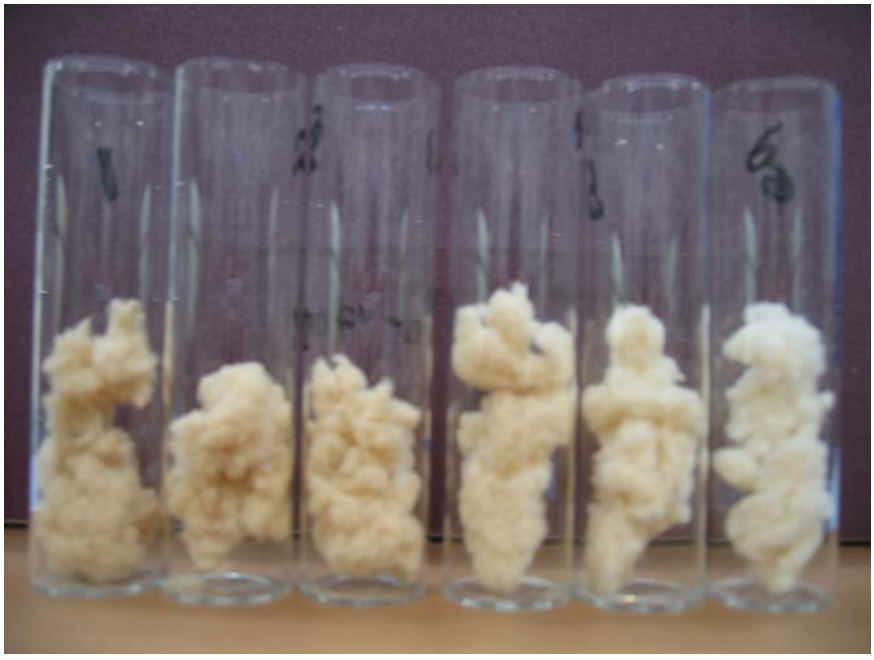

Figure D.4 Pulp Samples of Different Reaction Times

APPENDIX E

TOTAL ORGANIC CARBON (TOC) IN THE LIQUOR SAMPLES

E.1 TOC Formation Rate vs. Time at Different Operating Conditions

Eight liquor samples were collected at 4, 7. 12, 20, 30, 40, 50 and 60 minutes for several experiments and the TOC concentration was measured using a Shimadzu TOC-5000. Table E.1 shows the TOC concentrations of the liquor samples and the flow rate of the experiments at different operating conditions.

Table E.1 TOC Concentrations of the Liquor Samples of Different Experiments

Sample	Other operating conditions are 90C, 3.3g/l and 75 psig if not specified.										
Flow Rate (ml/min)	TOC (ppm) measured Shimadzu TOC-5000										
	59.8	75.1	66.9	68.8	77.8	66.4	68.4	70.4	75.8	63.8	71.2
Time (min)	1.1g/l	3.3 g/l	5.5 g/l	7.7 g/l	80°C	100°C	110°C	115°C	35 psig	55 psig	95 psig
4	13.51	14.19	15.42	17.32	12.43	15.96	25.59	26.54	12.43	11.21	14.23
7	13.68	18.32	19.19	19.80	13.66	23.82	37.16	34.33	11.97	14.93	20.06
12	12.78	17.19	19.17	19.73	14.35	25.85	43.55	38.48	9.42	14.43	19.91
20	9.19	14.53	16.98	17.36	11.86	25.67	44.32	34.50	9.10	14.53	17.63
30	8.93	14.52	16.22	15.29	8.17	22.66	35.59	29.43	9.70	13.24	15.27
40	8.52	14.03	14.08	12.64	9.07	18.43	25.66	25.64	8.09	10.95	14.35
50	7.88	11.49	10.81	12.70	7.98	18.22	22.50	24.23	8.12	9.99	11.18
60	8.69	10.33	10.40	12.00	8.06	16.07	20.56	22.77	7.48	8.25	11.46

The TOC formation rate in the liquor samples was calculated using equation (5.5).

Figure E.1 shows the trend of TOC formation rate vs. reaction at different O_2 Pressures. The TOC rate generally increases with increasing oxygen pressure. However, 75 psig and 95 psig oxygen pressure give almost the same TOC formation rates.

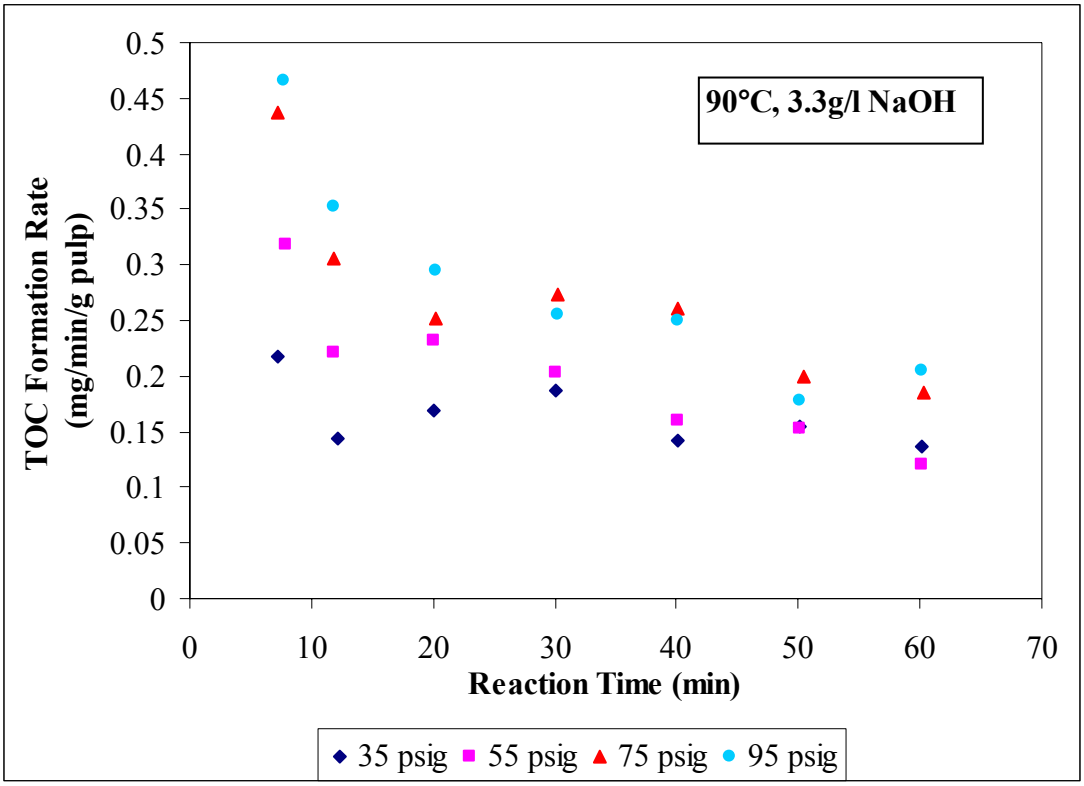

Figure E.1 TOC Formation Rate vs. Time at Different O_2 Pressures

The TOC formation rate vs. reaction time at different reaction temperatures is shown In Figure E.2, it is obvious that the higher temperature generates higher TOC formation rates.

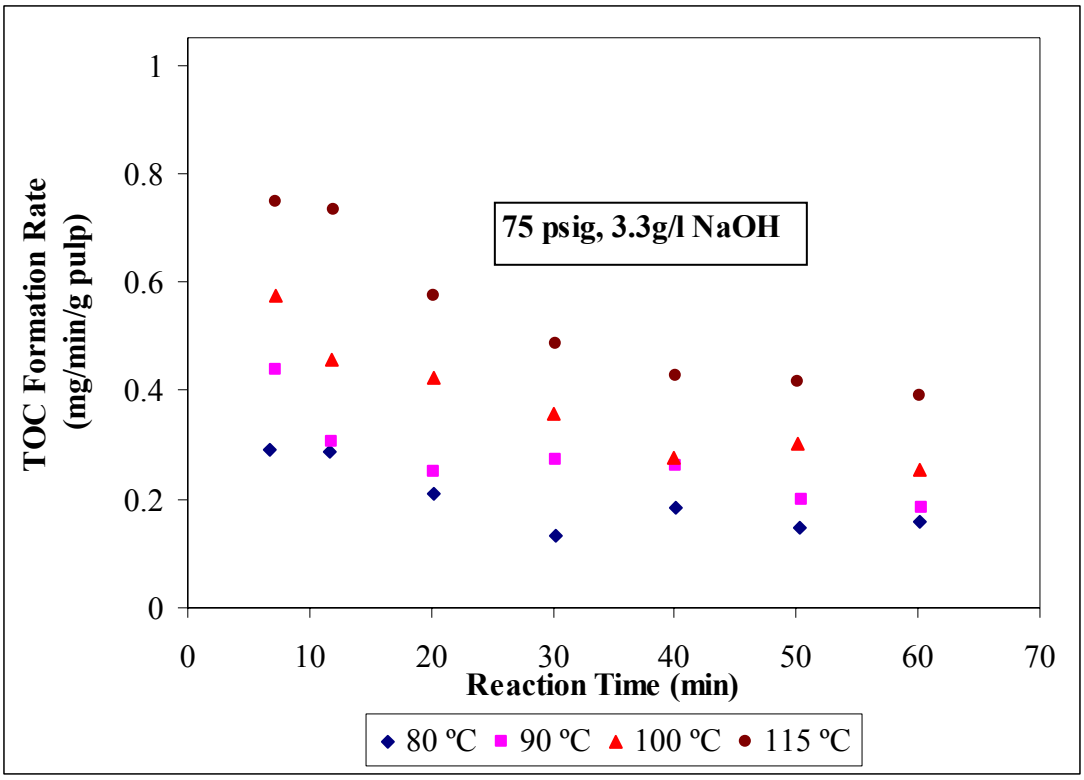

Figure E.2 TOC Formation Rate vs. Time at Different Reaction Temperatures

Figure E.3 shows the TOC formation rate vs. reaction time at different caustic concentrations. At 1.1g/liter NaOH concentration, the TOC formation rate is sigficantly lower than at the three higher NaOH concentrations. At 3.3g/l, 5.5g/l and 7.7g/l NaOH concentrations, there is not a clear difference between the TOC formation rates.

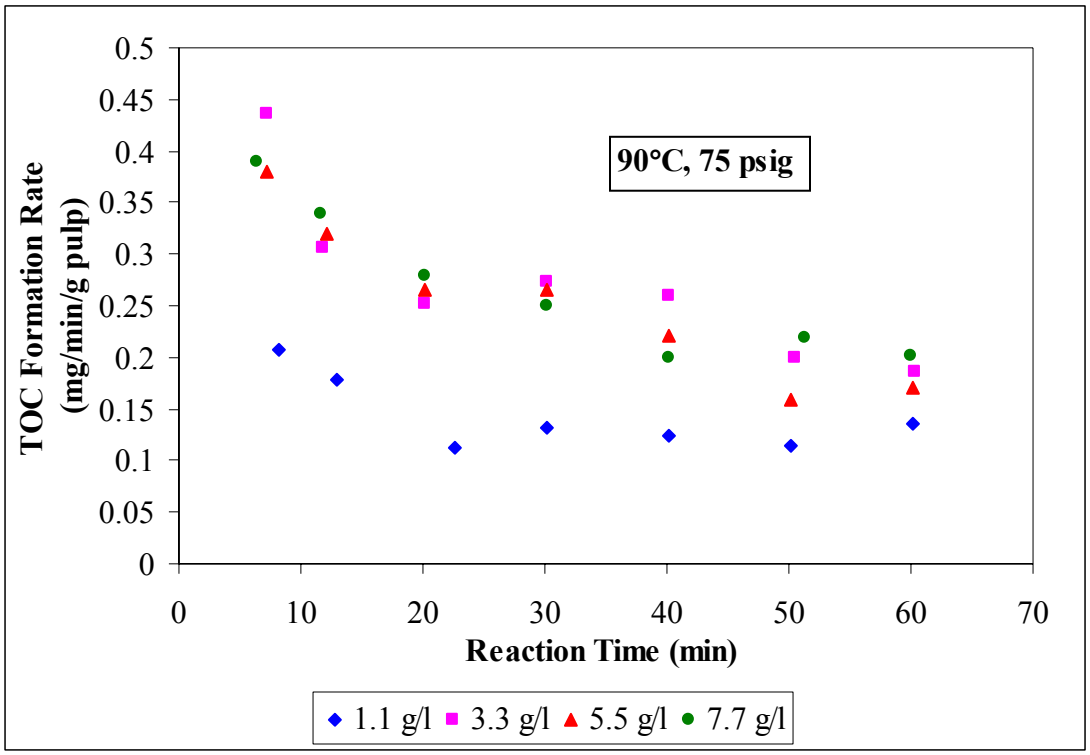

Figure E.3 TOC Formation Rate vs. Time at Different NaOH Concentrations

BIOGRAPHY OF THE AUTHOR

Yun Ji was born in Henan Province, China. She has studied in four different countries. She received her Bachelor of Engineering degree in China in 1999. She then received a scholarship from the Government of Finland to study for the Master of Science degree at the Asian Institute of Technology (AIT), Thailand. As part of this program, she participated in an extended internship in Finland in 2002. She was then accepted for study at the University of Maine and initiated work on her Ph.D under the direction of Professor Adriaan R. P. Van Heiningen in 2002.

Yun Ji is a candidate for Doctor of Philosophy degree in Chemical and Biological Engineering from The University of Maine in May, 2007.